

The Effect of Temperature on Liquid Product Composition
from the Fast Pyrolysis of Cellulose

Donald S. Scott, J. Piskorz, A. Grinshpun and R.G. Graham

Department of Chemical Engineering
University of Waterloo
Waterloo, Ontario, Canada N2L 3G1

Introduction

In recent years, a good deal of attention has been focused on the thermal conversion of biomass to gases and liquids, and in particular, on the products obtainable from short time, high temperature pyrolysis of wood and other lignocellulosics. This flash pyrolysis is usually carried out at or near atmospheric pressures, while hydrolypyrolysis commonly employs hydrogen pressures to 20 MPa.

Residence times of only a few seconds or less with reaction at high temperatures requires a reactor configuration capable of very high heating rates. Two of the most appropriate designs are the entrained flow reactor, and the fluidized bed reactor. Many flash pyrolysis studies have employed one or the other of these reactor types.

In general, two approaches to flash pyrolysis of biomass have been used by various workers. One approach has the objective of producing a maximum yield of a desirable gas, which in atmospheric pressure non-catalytic pyrolysis processes is usually ethylene, or other olefins. Examples of processes for this purpose, such as "ultrapyrolysis" (10)(17), "ablative pyrolysis" (7), the flash pyrolysis process described by Antal (2) and the fluidized bed process of Kuester (14) have been studied in recent years for the production of olefins. These processes are characterized by high temperatures $>650^{\circ}\text{C}$ and residence times of 1 second or less.

A second approach to flash pyrolysis has been described by Scott and Piskorz (19)(20) and Scott et al. (21). In these publications the development has been outlined of an atmospheric pressure flash pyrolysis process utilizing a fluidized bed of solid as heat carrier. The process studied has as a primary objective the determination of conditions for maximum yield of liquids from biomass, particularly forest materials. Results indicated that at apparent vapor residence times of about 0.5 seconds, organic liquid yields of 60%-70% on a moisture free basis could be obtained from hardwoods such as aspen-poplar and maple. Lower but still high yields of organic liquids (40%-60%) could be obtained from agricultural wastes such as wheat straw, corn stover and bagasse.

More recently, Knight et al. (11) have described the operation of an entrained flow reactor for the production of liquids. A somewhat different upflow entrained pyrolyzer for the production of liquids from wood has been described by Beaumont (5). Kosstrin (12) has also used a fluidized bed for thermal conversion of biomass to liquid. In general, processes for the attainment of high liquid yields operate at much lower temperatures, commonly 450°-550°C than do processes to yield gaseous products, but at about the same vapor residence times of about 500 ms.

In rapid pyrolysis processes, the rate of heat transfer is all-important. Ideally, in such a process, the time required for a biomass particle to reach about 95% of the reaction temperature would be much less than the particle residence time itself. The residence times normally quoted in thermal pyrolysis studies are usually mean gas residence times, that is, the net empty reactor volume divided by the volumetric flow rate, usually taken at reactor inlet conditions. Particle residence times are not as precisely known, and will vary with the reactor configuration and type. Measurement of mean particle residence times has not been done in the majority of fast pyrolysis process studies. However, Berruti (6) measured these residence times in a fluidized sand bed for 1 mm wood particles, and found that these varied from 2 to 6 s depending on the gas residence time (400 to 800 ms). Recently, Solomon et al. (22) reported measurements of the velocity of fine coal particles in a downward flow entrained reactor and found these were only about 40% of the gas velocity over most of the reaction period. Therefore, although the residence time of particles is generally not known very precisely in fast pyrolysis processes, it will likely be from 2 to 10 times the apparent gas residence time for most of the applicable reactors, that is, for entrained flow, fluid bed, spouted bed or cyclonic reactors. It is likely, therefore, that given a reactor capable of high heat flux, and particles of appropriate size with the "normal" gas residence time of about 500 ms, the heat-up time may not be a large fraction of the total particle residence time.

It is likely that each process will have its limits such that inadequate heat transfer causes marked changes in the distribution of the pyrolysis products. However, within these limits (which may not differ very much for different reactors capable of high heat transfer rates), the product distribution at a given gas residence time might be expected to be a function of the final reaction temperature only, especially if particles are smaller than about 1 mm and are reasonably dry. The principal criterion for this to be true is that the heat-up time for the particle should be considerably less than the time spent near reaction temperature, possibly only 20% of the total particle reaction time. As a result, the kinetic rate of reaction will probably be the rate limiting process. An equivalent criterion due to Lidén (16) would be to require that a particle reach decomposition temperature e.g. 450°C before any significant weight loss is observed.

Experimental

For this work, two completely different pyrolysis reactors were used, operated by two different research groups. The "ultraprolysis" entrained flow reactor was developed by workers at the University of Western Ontario, and was capable of operation to 1000°C with gas residence times of 50 ms to 900 ms (10). The second reactor was the fluidized bed pyrolysis unit developed at the University of Waterloo for thermal conversion of biomass to liquids (20). It operated up to 750°C with gas residence times of 300 to 1500 ms. Typical operating ranges for the two reactors are summarized in Table 1. Detailed descriptions of the respective apparatus and procedures are given in the two articles cited.

Table I Range of Experimental Parameters

	Ultraprolysis	Fluid Bed
Temperature, °C	700-1000	400-750
Reactor Residence Time (Gas), ms	50-900	300-1500
Maximum Feed Rate, kg/hr	1.0	3.0
Estimated Heating Rates, °C/s	10^4 - 10^5	10^4 - 10^5
Pressure, atm abs.	1.0	1.0
Reaction Atmosphere	N ₂	N ₂ or Product Gas

In all tests reported here, only one feed material was used, Avicel PH-102 microcrystalline cellulose. Both groups of experimenters used samples from the same lot, which at time of use had moisture content from 2.9-4.0%, with ash <0.1%, and C 44.24, H 6.16, O 49.6. Particle size range was -250 +40 µm with a mean particle diameter of 100 µm.

Results

The pyrolysis experiments in the fluid bed were all carried out at gas residence times of 450-550 ms. In this range, yields of liquid, gas and char show only a small variation with time. Pyrolysis in the transport reactor over the reaction time span of 350-900 ms, showed that the yields of liquid, char and gas became nearly independent of residence time in the reactor. Accordingly, yields from the transport reactor in this asymptotic range at 500 ms were compared to data from the fluidized bed pyrolyzer. All data were reported as percent by weight of the moisture free feed of total liquids (including water of reaction), gas and

char. Yields were normalized to 100% by correcting the liquid yield. In all experiments, material balances were generally $\pm 5\%$ or better, and the major errors were considered to reside in losses of the most volatile liquids during liquid recovery, and inaccuracies in the water balance. Also, methanol was normally used as the solvent for recovery of tars from lines and condensers, which means that methanol yields could not be determined.

The results of pyrolysis experiments with Avicel cellulose are shown in Figures 1-4 with all data presented on a dry feed basis. Figure 1 shows that over the temperature range of 450°C-900°C the yields of gas, char and liquids from two different reactors, operated by two different research groups, are in very close agreement. Figures 2 and 3 show the variation in CO and CO₂ yields with temperature over the same range. Again, agreement of the two sets of results is very good. Yields of hydrocarbon gases are shown in Figure 4, and the good agreement of data from the two reactors is again evident for both CH₄ yield and C₂H₄ + C₂H₂ yield.

Liquid products from the pyrolysis tests were obtained over a temperature range of 375°-700°C. These liquids were analyzed for specific chemical components using methods described elsewhere (18). Results for nine of the more significant components obtained in a water extract of the tars are shown in Figures 5-8. All of these results were obtained using the fluid bed pyrolysis system of the University of Waterloo. It is apparent that at a constant reaction time, well defined and fairly narrow optimal temperature ranges exist corresponding to the maximum yields for each component.

Discussion

In order to determine if the criterion of the ratio of heat-up time to time at reaction temperature is $\ll 1.0$, it is necessary to estimate heat transfer rates in the reactors and for the particles used. If the ideas of Kothari and Antal (13) are accepted, the time required for the centre of a particle to approach 500°C would represent the heat-up time. Lede (15) comes to similar conclusions for pyrolysis at high heat fluxes, but sets the decomposition temperature at 466°C for wood. The most extreme case, that is, the longest heat-up time in the present work, would be for the largest particles at the lowest reactor temperatures. The center point temperature was calculated for 600 μm and 100 μm particles for the heating conditions of a fluidized bed (16), for a reactor temperature of 500°C with feed at 20°C. The time required for the particle mid-point temperature to reach 450°C was found to be 618 ms for the 600 μm particle and 62 ms for the 100 μm particle. Inasmuch as the solid particle residence times for the larger particles were from 2 to 6 seconds in the fluidized bed, and for smaller particles in the transport reactor were at least 500 ms, the criterion of ratio of heat-up time/available reaction time $\ll 1$ is well satisfied for all the work reported here.

Another approach was taken by Lidén (16) to estimate the importance of the heat-up period. On the basis of low temperature pyrolysis results reported in the literature, and the results obtained in our laboratory, it was assumed that if the particle temperature reached at least 450°C before more than 10% of the wood decomposed (as measured by a rate-of-weight loss kinetic expression) then excessive char production would be avoided, and the condition for high tar yields would be met, since tar decomposition would be minimized by the rapid volatilization and removal of tar components. Assuming a first order weight loss expression, this heat-up time criterion can be expressed as

$$\ln \left[\frac{1}{0.9} \right] \geq \int_0^{t_c} k [T(t)] dt \quad (1)$$

where t_c is the time required for the particle centre to reach 450°C and $T(t)$ are the set of functions describing the particle centre temperature as a function of time after introduction of feed into the reactor. The value of the first order rate constant, k , used should be one which is applicable for the rate of weight loss of the biomass species used. For the purposes of evaluating the above criterion, the kinetic parameters for the rate expression describing the total decomposition of wood as given by Thurner and Mann (23) were used, that is

$$k = 2.468 (10^6) \exp - 106.5/RT \quad s^{-1} \quad (2)$$

where the activation energy is given in kJ/mole.

Numerical integration of the right hand side of equation (1) for hardwood particles in a fluidized bed reactor at 500°C shows that for all particle sizes less than 2 mm diameter the criterion will be satisfied. It follows that for all the data presented here for the two reactors, the particles were heated throughout to at least 450°C, even at the lowest reaction temperatures, before any appreciable weight loss occurred from them. Under these conditions, then, the product distribution from either reactor for the same gas residence times could be expected to be a function of reactor temperature only, even though biomass solids were well mixed in one reactor, and in plug flow in the other.

Recently, Lidén (16) and Diebold (8) using different reactor configurations have presented very similar kinetic models for the secondary decomposition of primary pyrolysis tars from biomass. The kinetic steps for which rate constants were evaluated are proposed to be parallel initial first order decompositions, one yielding volatile liquids, while the other yields char and gas, with respective rate constants k_1 and k_2 . The ratio of k_1/k_2 in both models was assumed to be a constant with respect to temperature and to represent a theoretical maximum (ultimate) liquid (or tar) yield. The volatile organics were then assumed to decompose by another first order process to lower molecular

weight products, because experimental results for short time pyrolysis suggest that little secondary char is formed in this step (see Figure 1). Experimental results also suggest that the primary decomposition step is largely completed before significant loss of tar yield occurs, as evidenced by a nearly minimum char yield at the maximum liquid yield, as well as low gas yields at this point. As tar yield decreases due to secondary decomposition reactions, gas yield increases proportionally. It becomes possible, then, to neglect the rate of the tar forming step and to express the change of tar yield due to secondary reactions by a simplified kinetic expression, given by both Lidén (16) and Diebold (8) as

$$x = \frac{x_0 [1 - \exp(-k_3 \theta)]}{k_3 \theta} \quad (3)$$

where x is the fractional tar yield, x_0 is the theoretical "ultimate" tar yield, k_3 is the first order constant for the tar decomposition step and θ is the reaction time for the vapor phase. The values used for the reaction parameters for tar decomposition were

Lidén $k_3 = 3.1 \times 10^6 \exp(-107500/RT) \text{ s}^{-1}$ $x_0 = 0.703$

Diebold $k_3 = 1.551 \times 10^5 \exp(-87634/RT) \text{ s}^{-1}$ $x_0 = 0.78$ or 0.76

Lidén's parameters are based on experimental data from hardwood (poplar) pyrolysis in a fluidized bed, while Diebold's values are obtained from measurements of the ablative pyrolysis of softwood followed by thermal cracking of the pyrolysis vapors.

Equation (3) was applied to the results from the pyrolysis of Avicel cellulose with prediction as shown in Figure 9. In applying equation (3) to these results, the ultimate yield, x_0 , was assumed to be 100%, although the low temperature results suggest a value slightly less than this might be more appropriate. Similarly, the yield of water was neglected, although it ranges from 2%-5%. The predicted tar yields as shown in Figure 9 are in remarkably good agreement with experiment, considering the assumptions of the model, and the fact that parameters derived from wood pyrolysis are being used to predict yields from the pyrolysis of a microcrystalline cellulose. Further, no effort was made to optimize values of the parameters with the experimental data, but only to use the values of Lidén or Diebold.

In summary, equation (3) appears to give a reasonable description of the complex cracking reactions in which biomass pyrolysis tars are converted to gaseous products, at least over the temperature range of about 500°-900°C, and for short vapor phase reaction times.

The yields of individual components shown in Figures 5-8 suggest strongly that a series of sequential decomposition steps is occurring. However, it is not clear from these results what

the precursor for any particular compound may be, or what system of parallel or sequential reactions can satisfactorily explain the nature of the variation of yield with temperature. More extensive analyses of these data are now underway.

Acknowledgement

The authors wish to extend their thanks to the National Research Council of Canada for the financial support of this work.

Literature Cited

- 1 Antal, M.J., Jr. *Advances in Solar Energy* 1983, 1, 61-112
- 2 Antal, M.J., Jr. *Ind. Eng. Chem. Prod. Res. Dev.* 1983, 22, 366-376
- 3 Antal, M.J., Jr. *Advances in Solar Energy* 1985, 3, 175-255
- 4 Antal, M.J., Jr. *Fuel* 1985, 64, 1483-1486
- 5 Beaumont, O. *Ind. Eng. Chem. Process Des. Dev.* 1984, 23, 637-641
- 6 Berruti, F. "Measuring and Modelling Lateral Solids Mixing and Residence Times in a Fluidized Bed Reactor" Ph.D. Thesis, Dept. of Chemical Engineering, University of Waterloo, December, 1985
- 7 Diebold, J. *Proc. Specialists Workshop on Fast Pyrolysis of Biomass, SERI/CP622-1096, 1980, 237-252*
- 8 Diebold, J. "The Cracking Kinetics of Depolymerized Biomass Vapors in a Continuous Tubular Reactor" MSc Thesis, Dept. of Chemical and Petroleum Refining Engineering, Colorado School of Mines, Golden, Colo. 1985
- 9 Funazukuri, T.; Hudgins, R.R.; Silveston, P.L. *Ind. Eng. Chem. Process Des. Dev.* 1986, 25, 172-181
- 10 Graham, R.G.; Bergouganou, M.A.; Overend, R.P. *J. Anal. Appl. Pyrol.* 1984, 7,
- 11 Knight, J.A.; Gorton, C.W.; Stevens, D.J. *BioEnergy* 84, H. Egneus and A. Ellegard (eds) Elsevier Appl. Sc. Publ., London, 1985, 9-14
- 12 Kosstrin, H. *Proc Specialists Workshop on Fast Pyrolysis of Biomass, SERI/CP 622-1096, 1980, 105-121*
- 13 Kothari, V.; Antal, M.J. Jr. *Fuel* 1985, 64, 1487-1494
- 14 Kuester, J.L. *BioEnergy* 84, H. Egneus and A. Ellegard (eds), Elsevier Appl. Sc. Publ., London, 1985, 48-55
- 15 Lede, J.; Panagopoulos, J.; Huai Zhi Li; Villiermaux, J. *Fuel* 1985, 64, 1514-1520

- 16 Lidén, A.G. "A Kinetic and Heat Transfer Modelling Study of Wood Pyrolysis in a Fluidized Bed" MASC Thesis, Dept. of Chemical Engineering, University of Waterloo, 1985
- 17 Mok, L.K.; Graham, R.G.; Overend, R.P.; Freel, B.A.; Bergouganou, M.A. BioEnergy 84, H. Egneus and A. Ellegard (eds), Elsevier Appl. Sc. Publ., London, 1985, 23-30
- 18 Piskorz, J.; Radlein, D.; Scott, D.S. J. Anal. Appl. Pyrol. 1986 9, 121-137
- 19 Scott, D.S.; Piskorz, J. Can. J. Chem. Eng. 1982, 60, 666-674
- 20 Scott, D.S.; Piskorz, J. Can. J. Chem. Eng. 1984, 62, 405-412
- 21 Scott, D.S.; Piskorz, J.; Radlein, D. Ind. Eng. Chem. Process Des. Dev. 1985, 24, 581-588
- 22 Solomon, P.R.; Serio, M.A.; Carangelo, R.M.; Markham, J.R. Fuel 1986, 65, 182-194
- 23 Thurner, F.; Mann, U. Ind. Eng. Chem. Process Des. Dev. 1981, 20, 482-488

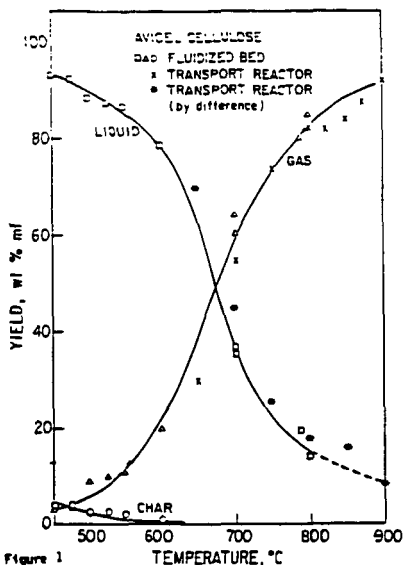


Figure 1 Product Yields from Avicel Cellulose for Two Reactors

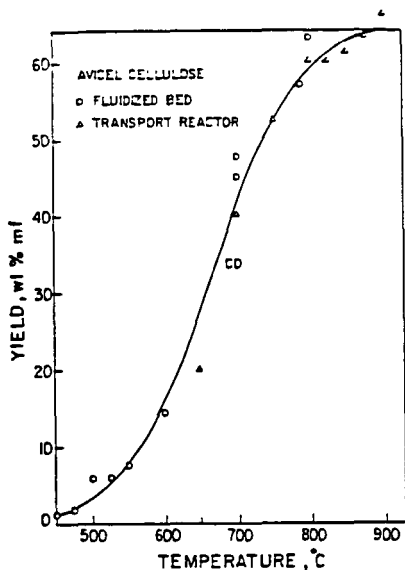


Figure 2 Yield of CD from Avicel Cellulose

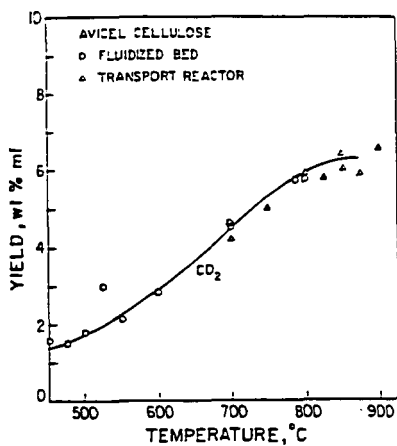


Figure 3 Yield of CO₂ from Avicel Cellulose

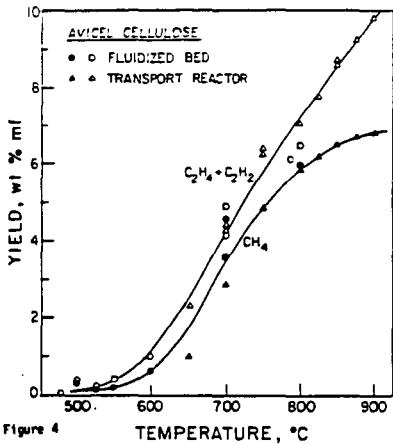


Figure 4 Yield of Hydrocarbon Gases from Avicel Cellulose

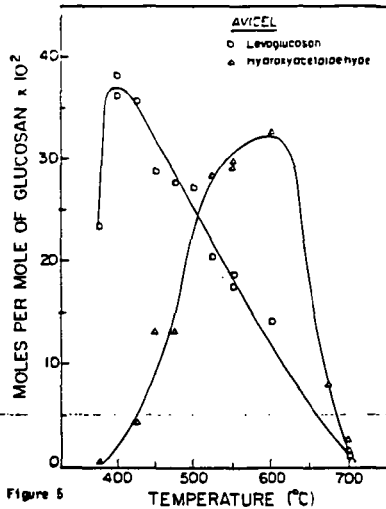


Figure 5 Yields of Levoglucosan and Hydroxyacetaldehyde, 800 ms, Fluidized Bed

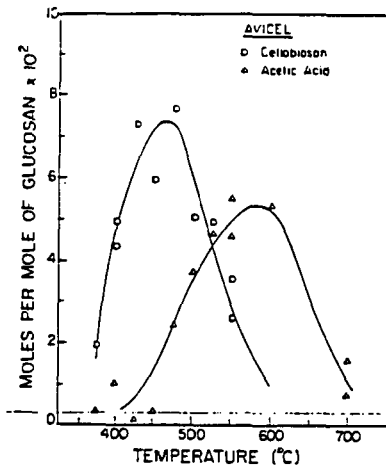


Figure 6 Yields of Celllobiosan and Acetic Acid, 500 ms, Fluidized Bed

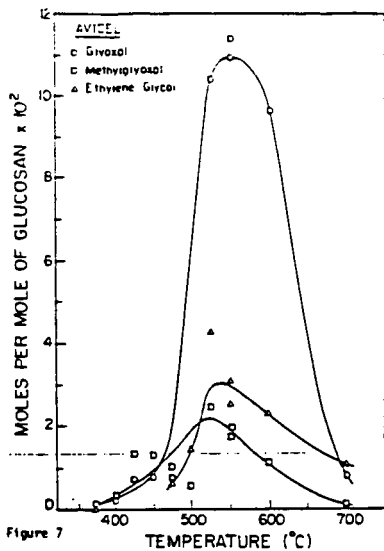


Figure 7 Yields of Glyoxal, Methylglyoxal and Ethylene Glycol, 500 ms, Fluidized Bed

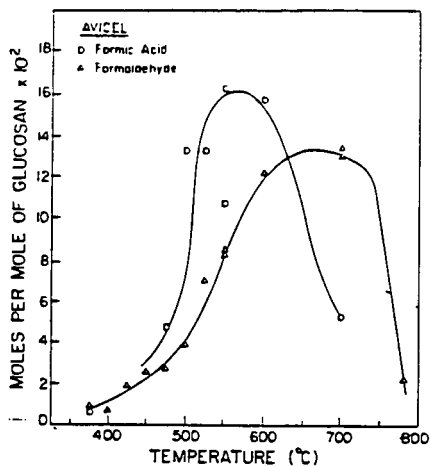


Figure 8 Yields of Formic Acid and Formaldehyde, 500 ms, Fluidized Bed

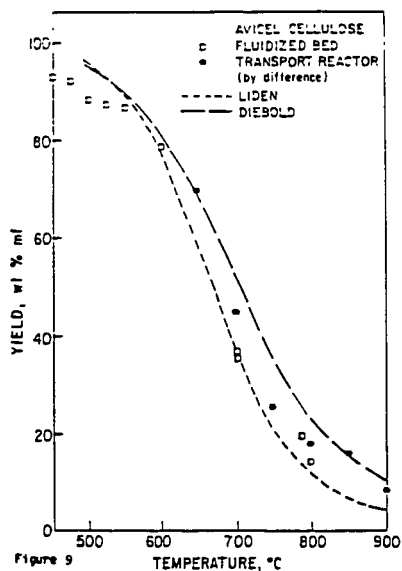


Figure 9 Prediction of Total Liquid Yields from Avicel Cellulose

PRELIMINARY ENGINEERING DATA FOR SCALE UP
OF A BIOMASS VACUUM PYROLYSIS REACTOR

Richard Lemieux**, Christian Roy*,***, Bruno de Caumia* and Daniel Blanchette*.

* Université Laval
Chemical Engineering Department
Pavillon Adrien-Pouliot
SAINTE-FOY (Québec)
G1K 7P4

** Université de Sherbrooke
Chemical Engineering Department
SHERBROOKE (Québec)
J1K 2R1

*** Assistant Professor at Université Laval and
Adjunct Professor at Université de Sherbrooke

INTRODUCTION

The thermal decomposition of wood into charcoal and tar is an old process. One example of the existing technology for wood carbonization is the Lambiotte process. The ATOCHEM plant located in Premery, France, is based on the principle of external gas circulation and is a completely continuous process (1). The heating gas moves upward in the retort and constantly releases its heat into the wood, which is moving downward. The annual wood charcoal production of this plant is nowadays 20 000 t. The charcoal finds its use in the barbecue and the iron industries. Another example is the Brazilian beehive kiln for charcoal production in a batch mode. In Brazil, charcoal is mainly sold to the iron, the cement and the barbecue industries. In 1986, the total annual production of wood charcoal in Brazil was 7.5×10^6 t (2).

The recovery of by-products is important for the economy of both processes. The French recover high-value chemicals such as food aromas from the pyrolygneous liquors (3). The Brazilians market the wood tar by-product as a bunker fuel oil (4). However, further studies are still needed and are being conducted by the industry in order to make a greater and a better use of the tar and oil fraction.

Laboratory (5) and Process Development Unit (6,7) studies originally conducted at the Université de Sherbrooke, and now conducted jointly with the private industry at the Université Laval, have led to the conclusion that thermal decomposition under reduced pressure is an attractive approach for the conversion of biomass into chemical and fuel products. This approach is characterized by low pressure and short residence time of the vapor products in the reactor. When compared with conventional, atmospheric pressure carbonization, vacuum pyrolysis has the potential to significantly enhance the yields of organic liquid products with respect to solid and gaseous products. The pyrolytic oils obtained from this process can be deoxygenated into transportation fuels (8) and sugars (9) upon further upgrading. Specialty as well as rare chemicals can also be extracted from the oil product (10).

This paper discusses the preliminary engineering data leading to the construction of a vacuum pyrolysis pilot plant for the conversion of wood into oils, chemicals and charcoal.

EXPERIMENTAL

A schematic of the Process Development Unit (P.D.U.) used in this study is shown on Figure 1. The reactor is a multiple-hearth furnace 2 m high and 0.7 m diameter, with six hearths. Heat transfer is provided through heating elements.

At the onset of an experiment wood chips are poured batchwise in a hopper that sits on top of the reactor. The hopper is equipped with a feeding device and is hermetically sealed. For the experiments reported, 6 to 16 kg of wood chips with a granulometry 1/4" to 1/2" Tyler Sieves were fed at a constant rate of 0.8 to 4 kg h⁻¹.

A mechanical vacuum pump removed the organic vapor and gas products from the reactor through a series of outlet manifolds set along the reactor cylinder. Each outlet was connected to a heat exchanger where the vapors were condensed and recovered as liquid into individual glass receivers. Cold tap water circulating on the shell side of the exchangers was used as cooling medium. The vapors from the heat exchange units were collected in a train of receivers that served as a secondary condensing unit. The first receiver was immersed in a bath of a water-ethylene glycol mixture. Receivers 2 and 3 were immersed in baths of dry ice-acetone. Receiver 4 was filled with glass wool at room temperature.

Pressure in the system was lower than 80 mm Hg (absolute) under steady-state conditions. The noncondensable gas was continuously pumped into a 500 L vessel that was set under vacuum at the beginning of the run.

The solid residue was directed toward the bottom of the reactor. The residual charcoal was received in a metallic jar installed on a load cell.

At time zero of the run, wood chips were fed in the preheated reactor. The heating plate temperatures increased from top to bottom of the reactor. A typical temperature profile was 200 °C to 450 °C. The radial temperature gradient for any heating plate was lower than 5 °C during any single run.

The P.D.U. was attached to a central microprocessor that permitted simultaneous data acquisition and control of some 75 operating parameters (64 are recorded and 11 are controlled). Air leakage through the system was lower than 1.3×10^{-3} atm L s⁻¹.

The experiments conducted on the P.D.U. were performed with Populus deltoides. The 8-year-old fast-growing poplar clone D-38 was planted in Brockville, Ontario. The sample was essentially all sapwood with no bark. It was shipped to our laboratories in the form of chips by Forintek Canada Corp., Ottawa. Its elemental composition was determined to be 48.2% C, 6.4% H, 45.3% O, 0.09% N, and 0.05% S. Its gross heating value was 4660 kcal kg⁻¹ with an average ash content of 0.6%. Moisture of the air-dry feedstock was determined to be 5.9%.

RESULTS AND DISCUSSION

Yields and mass balance

Results for the operation of the multiple-hearth furnace at varying final thermal decomposition temperature and reactor pressure are presented in Table 1 of the paper. Oil, pyrolytic water, charcoal and gas yields are

presented along with the mass balance calculation for each run. Table 1 indicates that the largest amount of oil is obtained at the lowest pressure and the higher temperature conditions. The oil yield in particular drops sharply with even a slight increase in pressure. Table 1 also indicates that a reactor temperature in the range of 425 - 450 °C is optimum to get the maximum yield of oil from wood. Table 2 summarizes the data obtained for the gas phase composition for the different runs.

Separation of water from the organic liquid phase

One objective of the vacuum pyrolysis process is to produce large quantities of liquid fuels and chemicals from wood. However during the process the liquid organic product is mixed with water (moisture and pyrolytic water). Since extraction of chemicals or further processing of pyrolytic oils mixed with water is difficult and expensive, it is highly desirable to separate the bulk of the aqueous phase from the organic liquid phase.

The separation of water and the organics was achieved during this study by using a series of shell and tube heat exchangers with cool to warm water circulating in the shell section. This series of heat exchangers served as a primary condensing stage for the recovery of the liquid organic fraction. Water was primarily recovered in the series of traps that followed (see Figure 1). The relative proportion of water and oil in both condensing sections is shown in Table 3 of the paper. Table 3 indicates that the lower the pressure, the better the separation between oil and water (see runs C019 and C025). On the other hand at similar operating pressure, the lower the cooling temperature, the more efficient the recovery of oil in the primary condensing section (see runs C023 and C025).

Oil refining

Further fractionation of the wood oil product is necessary if the objective is to either recover pure chemical compounds, or upgrade or process specific chemical group components. Results which are reported by Renaud *et al* (8) and Pakdel *et al* (10) show that the multiple-hearth reactor can be operated in a mode that enables the separation and recovery of selected fractions of liquid fuels and chemicals.

Heat requirement for the pyrolysis reaction

Another engineering parameter to be considered when designing a full scale pyrolysis plant is the amount of energy required for the pyrolysis of each mass unit of wood fed to the reactor. Such value has been empirically determined using the P.D.U. described in this paper, and the detailed procedure has been published elsewhere (11). The determination was based on the difference of electric energy consumed before of after wood was fed to the reactor (heat loss to the atmosphere), and that of the electric energy required for maintaining the multiple-hearth furnace at predetermined set-point temperature with wood chips flowing through the reactor. It was concluded that the heat required for vacuum pyrolysis of aspen wood is about 134 kcal kg⁻¹ of anhydrous wood. Overall, the reaction is slightly endothermic.

Heat required for cooling the organic vapors

The amount of heat removed when cooling the organic vapor products at the primary condensing stage was also experimentally determined (see Figure 1). The heat exchange (Q_w) between the cooling medium (water) and the hot vapor products was calculated using the Equation 1.

$$\text{Equation 1)} \quad Q_w = mC_p (T_{w,in} - T_{w,out})$$

where m is the water flowrate, C_p is the heat capacity for water and $T_{w,in}$ and $T_{w,out}$ is the water temperature at the inlet and the outlet of the heat exchanger, respectively. After taking into account the heat loss to the atmosphere, the overall heat exchanged while cooling the gas and vapor product to 50 °C was found to be 112 kcal kg⁻¹ of air-dry wood.

The experimental set-up simultaneously enabled the calculation of the overall heat-transfer coefficient U for the heat exchangers. The data were plugged in Equation 2.

$$\text{Equation 2)} \quad Q_w = UA (\Delta T)$$

where A is the transfer area and (ΔT) is the temperature driving force. The calculations led to the conclusion that U values vary between 7 and 13 kcal h⁻¹ m⁻² °C⁻¹ according to the position of the heat exchanger attached to the multiple-hearth furnace (11).

Determination of standard heat of reaction

The equipment used enabled us to determine the standard heat of reaction for pyrolysis of air-dry wood chips. For matter of convenience the standard state for wood considered as "a pure substance" was 323 K (50 °C) and 12 mm Hg. The standard heat of reaction was calculated using the Equation 3.

$$\text{Equation 3)} \quad \Delta H^\circ_{323} = \Delta H^\circ_t - \Delta H^\circ_r - \Delta H^\circ_p$$

where ΔH°_r is the total enthalpy change for the reactants from temperature T to 323 K.

ΔH°_p is the total enthalpy change for the products from 323 K to temperature T

ΔH°_t is the enthalpy change for the three-step process including the enthalpy change during the isothermal reaction at 323 K.

Figure 2 illustrates how each term in Equation 3 was empirically determined during run CO23. ΔH°_r and ΔH°_p in Equation 3 were calculated using an average heat capacity of 0.5 cal g⁻¹ °C⁻¹ for wood and 0.246 cal g⁻¹ °C⁻¹ for wood charcoal. The value for ΔH°_{323} in Equation 3 was found to be 22 kcal kg⁻¹, which confirms that the reaction is slightly endothermic. Although this value has limiting practical use, it should be viewed as an attempt to improve our theoretical knowledge of thermodynamics of wood pyrolysis.

Calculation of thermal efficiency of the reactor system

The thermal efficiency of the system defined as the ratio of useful energy provided by the vacuum pyrolysis reactor, to the energy supplied to it during a specific period of operations, has been determined for the same experiment CO23. The calorific values of the end-products represented the following percentages of the heating value of the initial feedstock: wood

charcoal 36%, wood oil 41% and gas, 5%. Using these data together with values from Figure 2 enabled us to determine that the thermal efficiency was 82%. For this calculation the mechanical pump electric energy requirement was not considered and the reactor was assumed to be perfectly insulated.

Heat transfer phenomena in the reactor

In the pyrolysis reactor, heat can be transferred by conduction, by radiation and by convection. Heat transfer by convection is negligible due to the low pressure conditions in the reactor. Both conduction and radiation play a significant role during pyrolysis and the latter factor is increasingly important at higher temperature levels (12).

The overall heat-transfer coefficient was estimated using the general relation $Q = UA (\Delta T)$. For the multiple-hearth furnace used, the actual heat transfer area used was estimated to be approximately 30% of the total available surface (6 heating plates), since the wood chips moving bed didn't cover the entire section. The transfer area was estimated to be 0.4 m^2 . The temperature driving force was calculated to be $62 \text{ }^\circ\text{C}$ (logarithmic mean), with $25 \text{ }^\circ\text{C}$ and $437 \text{ }^\circ\text{C}$ for the temperature of incoming raw material and the exiting charcoal, respectively, and $200 \text{ }^\circ\text{C}$ and $450 \text{ }^\circ\text{C}$ for the temperature of the top and the bottom heating plate, respectively. With Q_w equal to 150 kcal kg^{-1} (air-dry wood), the overall heat-transfer coefficient was found to be equal to $22 \text{ kcal h}^{-1} \text{ m}^{-2} \text{ }^\circ\text{C}^{-1}$.

CONCLUSION

A multiple-hearth reactor has been successfully tested for the production of high yields of liquid fuels and chemicals. The reactor enabled the separation and recovery of water on the one hand and oil fractions or the other hand. Oil yields reached about 50% by weight of the air-dry feedstock.

Heat required for the pyrolysis of wood is slightly endothermic and was determined to be 134 kcal kg^{-1} (on an anhydrous basis). The standard heat of reaction at 323 K and 12 mm Hg was found to be approximately 22 kcal kg^{-1} of air-dry wood. The thermal efficiency of the process is high, in the range of 82%. The overall heat transfer coefficient in the reactor is about $22 \text{ kcal h}^{-1} \text{ m}^{-2} \text{ }^\circ\text{C}^{-1}$ which is in range with the existing commercial multiple-hearth furnaces. Preliminary theoretical calculations indicate that a significant reduction of the heat surface area of the reactor can be achieved by operating the reactor at a higher temperature zone in order to enhance the radiative effect.

ACKNOWLEDGMENTS

This study was supported by Energy, Mines and Resources Canada (Ottawa) and Petro-Sun International Inc., (Longueuil, P.Q.).

REFERENCES

- 1- H.F.J. Wenzl. The Chemical Technology of Wood. Academic Press. 1970. p. 285.
- 2- Rodrigues de Almeida, M. Texto apresentado no Curso "Siderurgia para nao Siderurgistas" Estudos Sobre o Redutor: Carvao Vegetal-Carvoejamento. Comissao Técnica de Ensino - COENS, Associação Brasileira de Metais - ABM, Sao Paulo 27 a 31 de Outubro de 1986. July 1986.

- 3- Findeling, O. Société Usines Lambiotte, Premery, France. Private communication. June 1985.
- 4- Rodrigues de Almeida, M. Acesita Energética, Belo Horizonte, Brazil. Private communication. September 1986.
- 5- Roy, C., B. de Caumia, D. Brouillard and H. Ménard. The Pyrolysis under Vacuum of Aspen Poplar. Fundamentals of Thermochemical Biomass Conversion: An International Conference. R.P. Overend, T.A. Milne and L.K. Mudge, Eds. Elsevier Applied Science Publishers, New York. 1984. (237-256).
- 6- Roy, C., B. de Caumia, D. Blanchette, R. Lemieux and S. Kaliaguine. Development of a Biomass Vacuum Pyrolysis Process for the Production of Liquid Fuels and Chemicals. Energy from Biomass and Wastes IX, IGT Symposium. Lake Buena Vista, Florida. January 28 - February 1, 1985. (1085-1106).
- 7- Roy, C., R. Lemieux, B. de Caumia and H. Pakdel. Vacuum Pyrolysis of Biomass in a Multiple-Hearth Furnace. Biotechnology and Bioengineering. Symp. No. 15. 107-113 (1985).
- 8- Renaud, M., J.-L. Grandmaison, C. Roy and S. Kaliaguine. Conversion of Vacuum Pyrolytic Oils from Populus deltoides over H-ZSM-5. Production, Analysis and Upgrading of Pyrolysis Oils from Biomass, ACS Symposium. Denver, Co. April 5-10, 1987.
- 9- Roy, C., J.P. Larouche and B. de Caumia. Hydrolysis of Pyrolytic Liquors Derived from Wood. In preparation.
- 10- Pakdel, H., and C. Roy. Chemical Characterization of Wood Oils Obtained in a Process Development Vacuum Pyrolysis Unit. Production, Analysis and Upgrading of Pyrolysis Oils from Biomass, ACS Symposium. Denver, Co. April 5-10, 1987.
- 11- Lemieux, R. Development of a Multiple-Hearth Furnace for Vacuum Pyrolysis of Biomass. M.Sc.A. Thesis. Université de Sherbrooke, Québec. In preparation. (In French).
- 12- Labrecque, B. Study of the Thermal Radiation during Vacuum Pyrolysis of Scrap Tires. M.Sc.A. Thesis. Université de Sherbrooke, Québec. In preparation. (In French).

FIGURE 1 - SCHEMATIC OF THE VACUIN PYROLYSIS PROCESS DEVELOPMENT UNIT

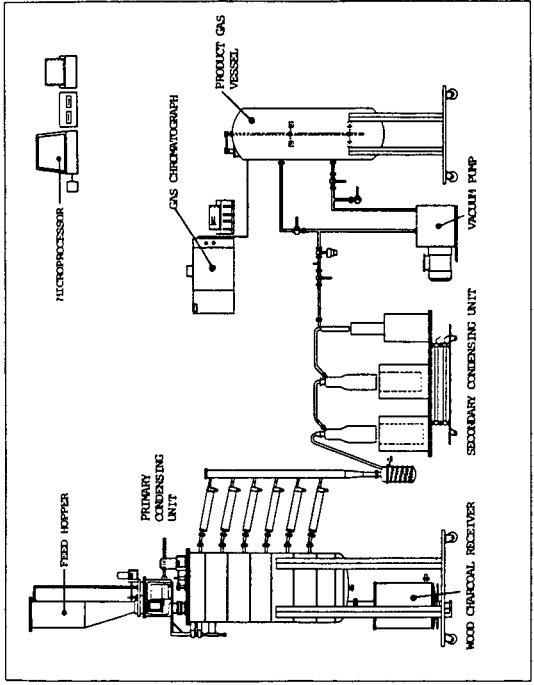


FIGURE 2 - MASS AND ENERGY BALANCES AROUND THE PYROLYSIS REACTOR

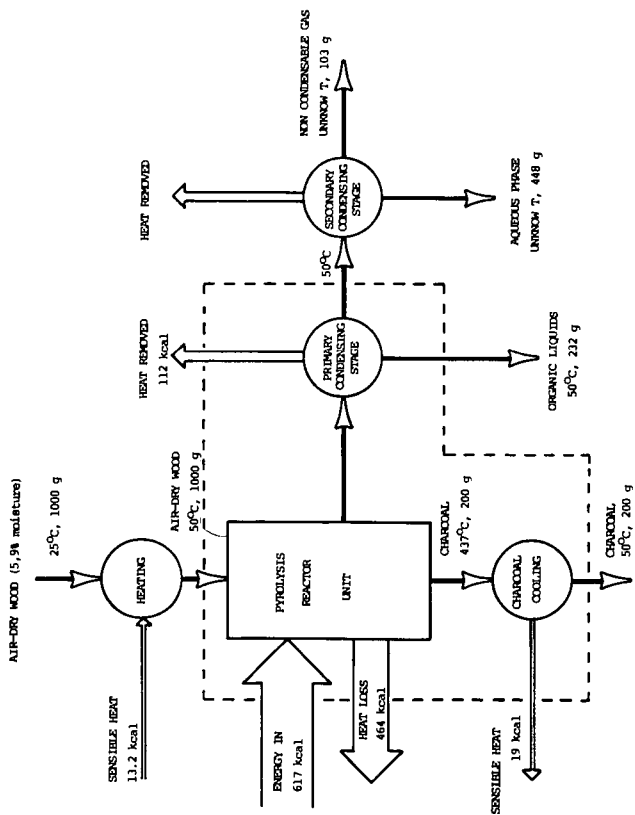


TABLE 1 - YIELDS AND MASS BALANCE FOR VACUUM PYROLYSIS OF WOOD IN A P.D.U.

RUN #	FINAL TEMPERATURE (°C)	REACTOR PRESSURE (mm Hg)	WOOD FEEDSTOCK (kg)	YIELDS (% wt. wood organic basis)				MASS BALANCE CLOSURE
				OIL	WATER	CHARCOAL	GAS	
0010	425	12	5.98	46.4	18.2	24.2	11.2	96.7
0012	363	18	5.99	41.6	14.9	33.0	10.5	97.5
0014	450	25	6.03	45.8	17.0	25.6	11.6	96.1
0015	425	14	6.00	50.1	15.2	25.0	9.7	96.3
0019	465	80	3.39	39.7	21.6	24.7	14.0	96.7
0023	450	12	15.43	50.9	16.5	21.3	11.3	98.3
0024	450	30	18.30	47.4	16.9	25.5	10.2	97.9
0025	450	10	15.99	50.0	15.6	23.0	11.4	98.6

TABLE 2 - GAS PHASE COMPOSITION DURING VACUUM PYROLYSIS OF WOOD IN A P.D.U.

RUN #	FINAL TEMPERATURE (°C)	REACTOR PRESSURE (mm Hg)	TOTAL GAS YIELD (% wt. wood organic basis)	GAS COMPOSITION (% wt)					OTHERS*	CO/CO ₂
				CO ₂	CO	CH ₄	H ₂	C ₂ -C ₆ HYDROCARBONS		
0010	425	12	11.2	59.2	33.6	2.4	0.9	1.5	2.4	0.57
0012	363	18	10.5	60.4	34.9	0.9	0.1	0.9	2.8	0.57
0014	450	25	11.6	65.7	28.1	1.4	1.0	1.6	2.2	0.43
0015	425	14	9.7	63.8	30.5	1.5	0.8	1.3	2.1	0.48
0019	465	80	14.0	60.0	31.4	3.3	0.7	2.8	1.8	0.52
0023	450	12	11.3	60.7	31.6	2.7	0.0	1.4	3.6	0.52
0024	450	30	10.2	63.5	29.8	2.6	0.7	1.5	1.9	0.47
0025	450	10	11.4	64.6	30.3	1.9	0.4	1.0	1.8	0.47

* Others gases were among the followings : methanol, ethanol, acetone and acetaldehyde.

TABLE 3 - SEPARATION OF WATER AND PYROLYTIC OIL DURING CONDENSATION

RUN #	REACTOR PRESSURE	FINAL TEMPERATURE	COOLING TEMPERATURE (°C)	PRIMARY CONDENSING UNIT		SECONDARY CONDENSING UNIT		TOTAL LIQUIDS (kg)
	(mm Hg)	(°C)		OIL (%)	WATER (%)	OIL (%)	WATER (%)	
0019	80	465	11-28	52.2	19.2	7.4	21.2	2.06
0023	12	450	50-55	32.2	1.5	36.7	29.6	10.45
0024	30	450	30-35	39.8	1.6	27.2	31.4	11.85
0025	10	450	15-20	47.8	3.4	27.2	21.6	10.53

Production of Primary Pyrolysis Oils in a Vortex Reactor

James Diebold and John Scahill

Chemical Conversion Research Branch
Solar Energy Research Institute
1617 Cole Blvd., Golden, Colorado 80401

ABSTRACT

A vortex tube has certain advantages as a chemical reactor, especially if the reactions are endothermic, the reaction pathways are temperature dependent, and the products are temperature sensitive. With low temperature differences, the vortex reactor can transmit enormous heat fluxes to a process stream containing entrained solids. This reactor has nearly plug flow and is ideally suited for the production of pyrolysis oils from biomass at low pressures and residence times to produce about 10 wt % char, 13% water, 7% gas, and 70% oxygenated primary oil vapors based on mass balances. This product distribution was verified by carbon, hydrogen, and oxygen elemental balances. The oil production appears to form by fragmenting all of the major constituents of the biomass.

INTRODUCTION

The pyrolysis of biomass follows a complex set of different chemical pathways, which have thus far not been well established. However, several global pathways have been established, which explain most of the observed phenomena. As shown in Figure 1, the first reaction in fast pyrolysis of biomass is the depolymerization of the lignocellulose macropolymers to form viscous primary oil precursors. These precursors are formed with almost no by-products, and consequently their elemental composition is very similar to the original biomass. With low heating rates, much of the primary oil precursors can repolymerize to thermally stable polymers through the elimination of mostly water to eventually form the material known as char. Physical evidence for a liquid or plastic phase intermediate in the formation of char is the physical shrinkage of the macrodimensions of wood, which takes place during charring (1) in a manner analogous to heat shrinkable polyethylene tubing. If the heating of the biomass proceeds very quickly to temperatures above 450°C, most of the primary oil precursors can crack and vaporize before they form char. In the vapor state, the primary oil molecules are quite dilute, which slows possible second-order polymerization reactions. This dilution allows any unstable primary oil vapors to be converted by first-order reactions to more stable compounds, which can be collected from a reactor designed to have a short gaseous residence time followed by rapid quenching. Thermal stability is relative, however, and these stabilized primary oil vapors readily crack to gases following a global first-order reaction (2). The cracking of the primary oil vapors proceeds with a 10% loss in 36 ms at 700°C and extrapolated 10% losses in 6 ms at 900°C and 591 ms at 500°C.

Obviously, the lower the temperature of the primary vapors in the reactor, the greater the yield of primary vapors which can survive passing through the reactor to the quench zone. Minimizing the time required to travel from the vapor formation zone in the reactor to a lower temperature quench zone also helps to maximize the primary oil vapor yields. The ideal reactor would thus provide large heat fluxes preferentially to the pyrolyzing biomass particle, while not overheating the surface of the particle to cause cracking of the primary vapors to gases as the vapors escape the surface of the particle. The ideal reactor would allow the vapors to be immediately swept away by a colder carrier gas stream out of the reactor to a cold quench zone in order to preserve as much of the vapors as possible. The residence

time of the biomass particles in the ideal reactor must be long enough to ensure complete pyrolysis, but the accumulation of dead char in the reactor is undesirable. It would also be advantageous if the reactor could selectively remove dead char and recycle partially pyrolyzed particles.

The use of thermal radiation for fast pyrolysis has been explored, as this approach preferentially heats the solid with potentially high heat fluxes. However, heating the particle with a high temperature heat source can drive the surface temperature of the particle too high and some vapor cracking would be expected. The use of hot flue gases or hot solids as a heat transfer medium requires that they be at very high temperatures to lessen the amount of the medium which must be generated or recycled; flue gases or hot sand at 900° to 1000°C have been used for fast pyrolysis, but tend to produce higher yields of noncondensable gases from cracking the primary pyrolysis oil vapors to gases as described above. The ideal reactor for the pyrolysis of biomass to primary oils would achieve high heat transfer rates through the use of a mechanism which has an inherently high heat-transfer coefficient, rather than through the use of a high-temperature source. Such a heat transfer mechanism is attained by the conduction of heat from a moderately hot reactor wall directly to the biomass particle.

It can be readily demonstrated that when a stainless steel wire at 500° to 900°C is contacted with a monolithic piece of biomass, the biomass surface is ablatively pyrolyzed and converted to a liquid which allows passage of the wire and to vapors which condense to form smoke. If the stored energy in the wire is transferred to the biomass by sliding the wire across the biomass, pyrolysis rates over 3 cm/sec are observed (3). This method of heat transfer has been studied by pushing a wooden rod into a heated, stainless steel disk, and the pyrolysis rate has been found to be proportional to the pressure exerted and to the temperature difference, where the biomass surface was calculated to be pyrolyzing at 466°C. Heat transfer coefficients as high as 8 W/cm² were reported, which is over 300 times higher than for thermal radiation from a wall at 900°C having an emissivity of one (4).

Although a reactor can be designed to push wooden rods into a hot surface for research purposes (4, 5), most practical biomass feedstocks are expected to be in the form of sawdust or chips. A modified entrained-bed reactor was selected in which the entrained particles enter the reactor tangentially so that centrifugal forces push the feedstock particles onto the externally heated cylindrical wall. Drag forces induced on the particle by the entraining gas stream serve to keep the particles moving on the wall. Since the particles are on or very nearly on the wall, they tend to intercept preferentially the heat, which is conducted through the reactor wall. With nonreacting solid particles in a heat exchanger made from a cyclone separator, the total heat transferred to the process stream was relatively independent of the solids' content at carrier-to-solids (C/S) mass ratios as low as one, whereas with more solids, the heat transferred increased dramatically. The temperature rise in the gas stream was as little as half of that seen in the solids at these low C/S ratios. The heat transfer coefficient from the wall to a solids-free gas was found to follow traditional convective heat transfer relationships, but to be 1.8 times higher in the cyclone than in a straight tube for the same entering tube diameter and entering gas velocities (6). A reported property of a cyclone is that above an entering Reynold's number of 3000, the cyclone has plug flow (7). The cyclone is an interesting reactor concept for the pyrolysis of biomass, as reported in the literature (7, 8). However, the reactor of interest in this paper is a vortex tube, which has many similarities to a cyclone separator.

Vortex tubes have a tangential entrance into one end of a cylindrical tube and an exit at the other end of the tube. If a second exit is added near the tangential

entrance, but in an axial location, a Ranque-Hilsch tube is created which can be fed warm gas in the tangential entrance and produce cold gas coming out of the near axial exit and hot gas out of the far exit. The vortex tube is commercially used for reliable refrigeration where the cost of the compressed gas is of no concern. Research into the aerodynamics of the vortex tube revealed that in the Ranque-Hilsch tube there was an outer vortex which exited the hot end and an inner vortex which exited the cold end. If the cold end was not open, the vortex tube was reported to have a third concentric vortex, which flowed toward the hot end (9). The pitch of the vortex near the cylindrical wall was reported to be about 1.2 times the diameter of the vortex tube. This results in a coarse helical path of the gases near the wall, as measured by pitot tubes (9, 10). This coarse helical path on the wall also exists for the more conventional cyclone separator (11). The effect of the coarse path is that entrained solids, which are centrifuged to the wall, follow the same coarse path through the reactor. This has two deleterious effects: only a narrow path of the cylindrical wall would be used for heat transfer; and the residence time of the solid particles is only a fraction of what it would be with a tighter helical path.

The vortex tube reactor which we developed is shown in Figure 2 and has some unique features, which were found necessary to achieve the desired reactor performance in the fast pyrolysis of biomass. The carrier gas is pressurized to between 75 and 150 psia, depending upon the desired flow rate, and passes through a supersonic nozzle. Biomass in the form of minus 3-mm sawdust is metered into, and is entrained by, the supersonic carrier gas stream. Cold-flow studies with 4000-frames-per-second movie coverage established that this entrainment method results in rapid acceleration of the sawdust particles to velocities over 125 m/s. The cold-flow studies also verified that the entrained particles were following the reported coarse path of the gas flow near the wall. This coarse helical path appeared to be independent of the entrance angle, the entrance duct shape, and the flow rate of the carrier gas (12). The pitch angle of the solids flow in the conical section of a conventional cyclone was observed to be about one-fifth that in the cylindrical section (11), but the cylindrical vortex tube has more heat-transfer surface area per unit length. To force the entrained particles into a tight helical path, the 316 SS cylindrical vortex tube wall was machined to leave a 3-mm high and 3-mm wide raised helical rib. High-speed movies taken of the cold-flow system verified that the raised rib forced the solids to take the desired tight helical path (13). A tracer gas experiment, following the progress of propane pyrolysis, verified that this reactor design was essentially plug flow, with the inner vortices contributing a very small amount of internal recycling (14).

Initial operation with this vortex tube as a reactor for the fast pyrolysis of biomass was with heating the reactor wall to relatively high temperatures of 800°C or so. At that time, the goal was to crack the primary vapors to gases, rather than the preservation of the primary oils. Under these conditions, the sawdust had ample time to pyrolyze, as well as the char having time to partially gasify to produce char yields of only about 5%. However, as the vortex reactor wall became hotter, the tendency increased to accumulate a layer of secondary tar and char on the wall. By reducing the wall temperature to 625°C, the buildup of an insulating char-tar layer became negligible, but the rate of pyrolysis of the sawdust particles was so low that about 30% of the feed could be recovered in the char cyclone as scorched feed. A tangential exit was then added to the vortex tube reactor to allow the unreacted feed and large char particles to be recycled to the entrance of the reactor. The carrier gas nozzle acts as an ejector to create the pressure differential to drive the recycle loop. The recycle stream blows the sawdust off the feeder screws to positively entrain the feed to the carrier gas ejector.

The temperature at the exit of the insulated, but unheated, recycle loop is typically 400° to 450°C. The carrier gas is preheated to between 600° and 700°C prior to expansion through the ejector nozzle. With these conditions, the temperature of the pyrolysis stream is 480° to 520°C, as it exits the vortex reactor system. About 10% of the feed is converted to char, which is recycled with the scorched feed until it is attrited to less than 50 micrometers in size. The vortex reactor system acts as a particle size classifier, and the char fines are entrained out of the vortex system to be removed by a cyclone separator having a higher collection efficiency. The fine char has a volatile content of 15% to 20% and burns readily, especially when hot. The bulk density of the fine char is between 0.18 and 0.24 g/mL, depending upon whether it was freshly poured or has been allowed to settle (the bulk density of the sawdust feedstock was 0.24 g/mL). The empirical formula for this volatile char is $\text{CH}_{0.53}\text{O}_{0.12}$, and it has a heating value (HHV) of 33 kJ/g (14,000 Btu/lb). A microscopic examination of the char fines shows that the particles have the appearance of broken thin-walled tubes; i.e., charred and broken cell walls.

As noted above, the primary vapors are cracking significantly even at 500°C and a residence time of half a second. If the recycle loop of the vortex reactor is removed, the yield of permanent gases is about 3%, based on the reacted feed. The initial gases, which are formed under these conditions, are extraordinarily rich in carbon dioxide and are associated with the formation of char. With the recycle loop open, some of the primary pyrolysis vapors are recycled along with the carrier gas, unreacted solids, and large char. The additional time, which the recycled primary vapors spend in the vortex reactor leads to a small loss in the yield of primary vapors and a higher yield of noncondensable gases of about 7%. The composition of the gases shifts considerably from the initial gases formed to that associated with a small loss of primary vapors. An even greater shift in the gas composition occurs with more extensive cracking of the primary vapors to produce an asymptotic gas composition as the primary vapors near extinction, which is low in carbon dioxide, as shown in Table 1.

The experimental determination of the feed consumed, the char yield, and the noncondensable gas yields are relatively straightforward. However, the primary vapor and water yields have proven difficult to measure directly due to the formation of aerosols. These aerosols escape high-pressure sprays, cyclonic separators, and impingement or inertial collection techniques. The use of condensable steam as the carrier gas makes the water yield very sensitive to small measurement errors in the steam carrier gas flow. The use of noncondensable gases as the carrier tends to strip the volatile organics and the water of pyrolysis from the condensate. These considerations have led to the use of a noncondensable carrier gas, nitrogen, and to the determination of the water formed during pyrolysis and the primary oil yield by difference. By analyzing the recovered condensate for water, the yield of water may be determined. These techniques led to the conclusion that yields of about 70% primary vapors were achieved, based on taking the difference between the sawdust fed and the measured gas flow and char collected, correcting for the water content of the condensates. After elemental compositions were obtained for the feed and the collected products, an elemental balance was computed which verified the high primary vapor yields of 69 to 77 wt %, as shown in Table 2, based on the yield of recovered char (2).

The primary pyrolysis oils, which have been recovered from the vortex reactor, are highly oxygenated and have nearly the same elemental composition as the biomass feedstock. The oils have a dark brown color and are acidic with a pH between two and three. The heating value (HHV) of the dry oils is 20 to 22 kJ/g (8700 to 9500 Btu/lb). The oils can absorb up to about 25% water before forming two

phases. The viscosity of the oils was 1300 cp at 30°C, and the density was 1.3 g/mL (15). Although the primary vapors have a low molecular weight as determined by the FJMBMS (16), they rapidly polymerize upon physical condensation to form high-molecular-weight compounds in the oils (17). Attempts to slowly distill the oils led to the rapid polymerization of the oils boiling above 100°C (15). The oils have significant chemical activity, which suggests their potential use in low-cost adhesives, coatings, and plastics.

The concept of supplying heat through the wall of a vortex reactor to drive endothermic processes is in its early development. The scale-up potential of this concept depends upon the angular momentum of the swirling carrier gases to keep the entrained feed particles moving on the wall. The heat flux delivered to tubular pyrolysis reactors typically ranges between 5 and 15 W/cm² (20,000 to 50,000 Btu/hr-ft²). Reported data for vortex tubes indicates that with diameters larger than 2.5 cm most of the angular momentum is retained even after traveling a tube length equivalent to 20 tube diameters. The major momentum losses are due to the frictional contact of the solids and the gases with the vortex-tube wall. With larger vortex tubes needed for scale-up, the angular momentum of the process stream will increase more than the frictional losses. The heat transferred to the reactor will scale by the product of the diameter AND the length. These considerations have led to calculations which suggest that a vortex reactor with a 250 TPD capacity would have a diameter of only about 0.5 m and a length of 9 to 12 m. The fabrication technique would most likely be by the welding up of a spirally wrapped tube to form the raised, helical rib.

CONCLUSIONS

For the fast pyrolysis of biomass, a vortex reactor has significant advantages for the production of primary pyrolysis vapors, including: high heat transfer coefficients which allow the use of moderately low temperatures of the vortex reactor walls to supply the endothermic heat of pyrolysis; separation of the partially pyrolyzed feed particles from the char; the ability to recycle the partially pyrolyzed feed; the ability to accept a wide spectrum of particle sizes in the feed; short gaseous residence times; nearly plug flow; and preferential heating of the solid feed over the vapor stream, to preserve the primary vapors. Primary pyrolysis vapor yields in the 70% range have been calculated by mass balances and verified by elemental balances, although physical collection of these vapors has proven to be elusive due to the formation of persistent aerosols and due to the volatility of the vapors in the carrier gas (methods to recover these vapors more completely with practical means are under development).

ACKNOWLEDGEMENTS

The financial support for the development of the vortex reactor and the catalytic conversion of the primary vapors to high-octane gasoline has been provided by the Biofuels and Municipal Waste Technology Division of DOE (FTP 646) with Mr. Simon Friedrich as the DOE program manager and Dr. Don J. Stevens of PNL as the technical monitor. The physical recovery of the primary oils for use as chemicals and adhesives is being developed through the financial support of the Office of Industrial Programs of DOE with Mr. Al Schroeder as the DOE program manager (FTP 587).

REFERENCES

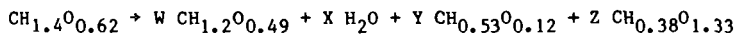
- (1) McGuinness, E. A., Jr.; Harlow, C. A.; and Beall, F. C. (1967), Scanning Electron Microscopy (Part VII), 543-526.

Table 1. Pyrolysis Gas Composition at Various Cracking Severities (mol %)

	Vortex Exit Gases w/o Recycle (Run 34)	Vortex Exit Gases w/Recycle (Run 58)	Severely Cracked Vapor Gases (Run 58)
H ₂	3.4	8.3	17.8
CO	46.2	49.2	52.2
CO ₂	43.1	27.6	7.5
CH ₄	4.6	8.9	12.0
C ₂ H ₂	--	0.1	1.1
C ₂ H ₄	1.3	2.4	5.9
C ₂ H ₆	0.3	0.7	0.6
C ₃ H ₈	0.1	0.1	--
C ₃ H ₆	0.4	0.8	0.8
C ₄ H ₈	0.3	0.3	0.6
C ₅ +	0.5	1.4	1.4
wt % yield of gases	~4	~6	65%

Table 2. Elemental Balance for Fast Pyrolysis to Primary Vapors

Feed → Primary Vapors + Water + Char + Gas



Exp. Char Yield	Calculated Product Values, Wt %		
	Primary Vapors	Water	Prompt Gas
7.5	76.8	11.7	4.0
10.5	73.1	12.8	4.1
12.7	69.0	14.0	4.3

- (2) Diebold, J. P. (1985), Thesis T-3007, Colorado School of Mines, Golden, CO 80401.
- (3) Diebold, J. P. (1980), Proceedings of Specialists Workshop on Fast Pyrolysis of Biomass, Copper Mountain, Colorado, October 19-22. Solar Energy Research Institute, Golden, CO 80401. SERI/CP-622-1096.
- (4) Lede, J.; Panagopoulos, J.; Li, H. Z.; Vettermaux, J. (1985), FUEL, 64, 1514-1520.
- (5) Reed, T. B. (1987), ACS Symposium on Production, Analysis, and Upgrading of Pyrolysis Oils from Biomass, Denver, CO, April 5-10.
- (6) Szekely, J., and Carr, R. (1966), Chem. Eng. Sci., 21, 1119-1132.
- (7) Lede, J.; Verzaro, F.; Antoine, B.; and Villermaux, J. (1980), Proceedings of Specialists Workshop on Fast Pyrolysis of Biomass, loc. cit., pp. 327-346.
- (8) Diebold, J. P.; Benham, C. B.; Smith, G. D. (1976), Monograph on Alternate Fuel Resources, AIAA Monograph Series, Volume 20, 322-325.
- (9) Hartnett, J. P., and Eckert, E. R. G. (1957), Trans. ASME, May, 751-758.
- (10) Scheller, W., and Brown, G. (1957), Ind. Eng. Chem., 49, No. 6, 1013-1016.
- (11) ter Linden, A. (1949), Inst. Mech. Eng. J., 160, 233-251.
- (12) Diebold, J. P., and Scahill, J. W. (1981), Proceedings of the 13th Biomass Thermocontractor's Meeting, Arlington, VA. October 27-29, CONF-8110115. PNL-SA-10093, 332-365.
- (13) Diebold, J. P., and Scahill, J. W. (1983), Proceedings of the 15th Biomass Thermocontractors Meeting, Atlanta, GA, March 16-17, CONF-830323, PNL-SA-11306, pp. 300-357.
- (14) Diebold, J. P., and Scahill, J. W. (1984), AIChE Winter National Meeting, Atlanta, GA, March 11-14, paper 31d.
- (15) Elliott, D. C. (1985), "Analysis and Comparison of Biomass Pyrolysis/Gasification Condensates - An Interim Report," Pacific Northwest Laboratory, Richland, WA 99352. PNL-5555/VC-61a.
- (16) Evans, R. J. (1985), Appendix C in "Entrained-Flow, Fast Pyrolysis of Biomass, Annual Report, 1 October 1983 - 30 November 1984," by J. P. Diebold and J. W. Scahill, Solar Energy Research Institute, Golden, CO. SERI/PR-234-2665.
- (17) Johnson, D. K., and Chum, H. L. (1987), ACS Symposium on Production, Analysis, and Upgrading of Pyrolysis Oils from Biomass, Denver, CO, August 5-10.

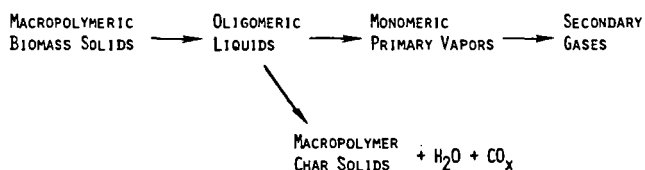


FIGURE 1. GLOBAL REACTIONS IN FAST PYROLYSIS

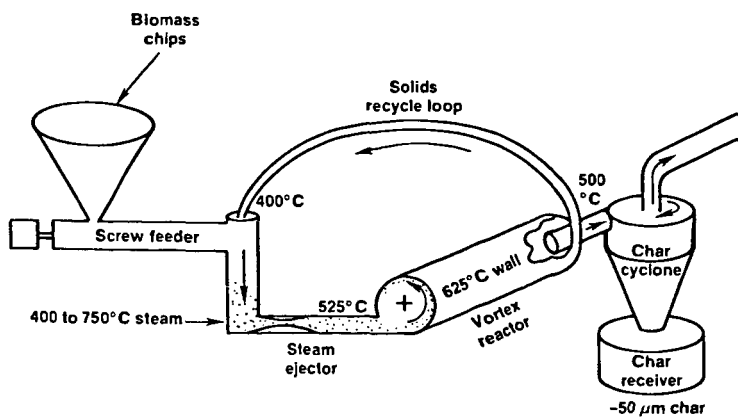


FIGURE 2. VORTEX REACTOR SCHEMATIC

FAST PYROLYSIS OF PRE-TREATED WOOD AND CELLULOSE

D. St.A.G. Radlein, J. Piskorz, A. Grinshpun and D.S.Scott

Department of Chemical Engineering
University of Waterloo
Waterloo, Ontario, Canada N2L 3G1

Introduction

Over the last several years, the Waterloo Fast Pyrolysis Process (WFPP) has been developed to maximize yields of liquids by the rapid thermal decomposition of lignocellulosic biomass. The process operates at atmospheric pressure and the reaction is carried out in a fluidized bed of sand as a heat transfer medium. Optimal conditions for woody biomass are 450°-550°C and about 0.5 seconds gas residence time. The nature of the fluidizing gas has little influence on yields.

Liquid yields from wood at optimal conditions are 70%-80% of the dry feed, with the organic liquid yields being 60%-65% of the dry wood fed. A description of the process and the yields obtained with various types of biomass has been published previously by the authors (1)(2). Extensive identification and quantification of many of the individual compounds present in these pyrolytic oils have also been reported (3)(4)(5).

Shortly before his death, Shafizadeh suggested (6) that pre-treatment of the wood by a mild acid hydrolysis to remove hemicelluloses followed by pyrolysis of the wood would allow a higher yield of fermentable sugars to be obtained, because the pentoses could be recovered from the acid hydrolysate and added to the anhydrosugars customarily formed in wood pyrolysis oils. However, this argument overlooked the fact that very low yields of anhydrosugars are normally obtained from wood except under slow heating at low temperatures (and perhaps vacuum) conditions. Certainly, yields of anhydrosugars and glucose from the rapid pyrolysis of wood in the WFPP are usually less than 5%. However, it was decided in this work, for other reasons, to investigate the effect on pyrolysis yields, and on the composition of the liquid product, of a mild pre-hydrolysis to remove part or most of the pentoses while leaving the cellulose content unaffected. The results of preliminary work are reported here.

Experimental

Samples of a standard poplar wood and of commercial cellulose products (IEA hybrid poplar, SS-144 chromatographic celluloses and Avicel pH 102 microcrystalline cellulose) were used as test materials. Properties of these feeds are given in Table 1.

Pyrolysis of raw and treated wood or cellulose was carried out at standardized conditions for all runs (500°C, 0.46 seconds gas residence time, N₂, -590 µm particle size) using the bench

scale fluidized bed apparatus which has been described elsewhere (1). Methods of analysis of tar, gas, char and water yields has also been described previously (2).

Wood or cellulose was hydrolyzed in a batch reactor at 90°C using sulfuric acid concentrations of 1%, 3% and 5% with reaction times of 6 or 19 hours and liquid to solid weight ratios of 4:1 or 12:1. A summary of reaction conditions is given in Table 1. Hydrolysis conditions were selected to give a high degree of conversion of the glucuronoxylan, which is the principal component of hardwood hemicellulose, to xylose, while leaving the cellulose unaffected. After treatment, the sample was filtered, washed to a pH of 6.3 and dried at room temperature.

Analysis of acid hydrolysate and of the water extract of the pyrolysis oils was done by HPLC (Aminex HPX-87H column at 65°C, eluent 0.07 N H₃PO₄, eluent flow rate 0.32 x 2.25 ml/min).

Results

Table 2 shows the amount of xylan removed during the various acid treatments. The calculated percent removal is based on an assumed value of 20.5% by weight of pentosans in the IEA poplar (7). The total weight loss from the wood exceeded the equivalent amount of xylose recovered, because of the hydrolysis of some lignin and some minor hemicellulose constituents. The results of Table 2 suggest that at even the mildest hydrolysis conditions (1% H₂SO₄ at 90°C for 19 hours at a 4:1 liquid to solid ratio) most of the readily hydrolyzable xylan has been converted to xylose. Changing the liquid to solid ratio at constant acid strength had little effect, indicating the relative completeness of the initial hydrolysis reactions of hemicellulose. Also shown in Table 2 are the blank run carried out using hot water only, as well as the conditions for the acid treatment of the commercial celluloses used.

The results of the pyrolysis runs for the untreated and treated poplar wood are given in Table 3. The two runs in which most of the xylan was removed by acid hydrolysis gave a 78%-80% yield of organic liquid, and a greatly reduced yield of water. The char and gas yields were also reduced to about one half the value of that for the untreated wood. Table 4 gives the analyses of the organic liquid fraction produced in the pyrolysis runs shown in Table 3. The most notable feature is the sharp increase in levoglucosan and in total sugar content of the oils from the acid hydrolyzed wood, while a sharply reduced yield of hydroxyacetaldehyde occurred simultaneously. A marked decrease in the amounts of acid produced from treated wood is also apparent.

Similar results are shown in Table 5 for a commercial low ash cellulose (SS144) which gave high yields of hydroxyacetaldehyde from pyrolysis at 500°C, and much less levoglucosan. After a mild hydrolysis, levoglucosan yield was sharply increased, and that of hydroxyacetaldehyde decreased. A large increase in

cellobiosan yield was also observed for both this cellulose and for the treated wood.

Results for the pyrolysis of untreated and for acid washed Avicel PH-102 are also given in Table 5. Again, a large increase in levoglucosan yield and an almost zero yield of hydroxyacetaldehyde result from acid washing. The yields of acids and of other minor constituents is also sharply decreased for the acid washed Avicel, although cellobiosan yield increases.

The hydrolysate liquors from wood were analyzed for Ca, Mg, Na and K contents, which were compared to those found from analysis of the ash from the untreated wood. Essentially all these cations were removed in the acid treating step.

Discussion

The reason for the great increase in levoglucosan and the parallel decrease in hydroxyacetaldehyde yield following acid treatment is not clear from these results. It is tempting to say that the change in product distribution is due to the removal of inorganic cations during the acid treating process, since it is known that these cations can catalyze the decomposition of cellulose and its degradation products. However, the low ash content SS144 cellulose also showed this remarkable increase in levoglucosan yield. Also a comparison of results for the untreated and the acid washed Avicel PH102 microcrystalline cellulose (average ash content 40 ppm) also shows an increase in levoglucosan yield from 27.0%-38.4% of the feed when pyrolyzed at 500°C while hydroxyacetaldehyde and cellobiosan decreased from 8.6%-0.43% and 10.1%-5.6% respectively.

While there is little doubt that the content of inorganic cations affects the product distribution, it appears that it is not the only effect, and the morphology and degree of hydrogen bonding in the cellulose must also influence the composition of the pyrolytic liquids.

Apparently, the xylan content of wood is a primary source of much of the gas and char formed in fast pyrolysis, as well as being a major contributor to the acid content of the pyrolytic oils.

When the results of Tables 3 and 4 are recalculated on the basis of cellulose content, then it is found that fast pyrolysis of the acid treated wood can convert 75% of the cellulose to sugars - largely anhydrosugars, with 15% reducing sugars and 15% disaccharides. When the pentose content of the acid hydrolysate is added to this, a high conversion of the wood to sugars is obtained, with about 80% of the holocellulose content yielding sugars of various kinds. Fast pyrolysis of acid treated wood may well be an economical route for the production of fermentable sugars, as Professor Shafizadeh suggested.

References

- 1 D.S. Scott and J. Piskorz, *Can. J. Chem. Eng.*, 60, 666-674, (1982)
- 2 D.S. Scott, J. Piskorz and D. Radlein, *Ind. Eng. Chem. Proc. Des. Devel.*, 24, 581-588, (1985)
- 3 J. Piskorz and D.S. Scott, *Symp. on Production, Analysis and Upgrading of Pyrolysis Oils from Biomass*, ACS Meeting, Denver, April 5-10, (1987)
- 4 D. Radlein, A. Grinshpun, J. Piskorz and D.S. Scott, "On the Presence of Anhydro-Oligosaccharides in the Sirups from the Fast Pyrolysis of Cellulose", *J. Anal. Appl. Pyrolysis*, accepted for publication, October, (1986)
- 5 D. Radlein, J. Piskorz and D.S. Scott, "Lignin Derived Oils from the Fast Pyrolysis of Biomass", *J. Anal. Appl. Pyrolysis*, accepted for publication, July, (1986)
- 6 F. Shafizadeh and T.T. Stevenson, *J. Appl. Polymer Sc.*, 27, 4577-4585, (1982)
- 7 D.C. Elliott, "Analysis and Upgrading of Biomass Liquefaction Products" IEA Co-operative Project, Biomass Liquefaction Test Facility, Final Report, Vol. 4, Dec. 1983 (PNWL Battelle)

Table 1
Properties of Feed Materials

Source	Cellulose		Poplar Wood
	Avicel pH 102	Schleicher & Schuell #144 TLC Cellulose Powder	Clean Wood Only Ontario MNR Clone D-38
Moisture, wt%	2.9	4.0	4.6
Ash, % mf	< 0.01%	0.062	0.46
Elemental Analysis, %			
C	44.3	44.4	49.45
H	6.16	6.17	6.05
O	49.5	49.4	44.4
N	Tr	Tr	0.07
Cellulose (Typical) %	> 99	> 95	42.3
Hemi Cellulose (Typical) %	--	--	31.0
Lignin (Typical) %	--	--	16-22

Table 2
Hydrolysis Conditions for Wood and Cellulose

Run No.	Residue After Hydrolysis grams*	Acid Conc.	Time hrs.	Temp °C	Liquid; Solid	Xylose Conc.	% of Xylan Removed
A-1 (Wood)	106	5%	6	90	4:1	3.24%	67%
A-3 (Wood)	101.2	1%	19	90	4:1	2.5%	51%
A-4 (Wood)	-150	None	5.5	90	4:1	Tr	Tr
A-5 (SS-144)	-150	5%	5.5	90	4:1	Tr	--
A-6 (Avicel)	-150	5%	5.5	90	4:1	N11	--

* Initial amount in all tests was 150 grams

Table 3
Pyrolysis of Raw and Treated Wood
Overall Product Yields

Feed	PP 59	A-2	A-4	A-3	A-1
	Poplar Wood Pilot Plant	Poplar Wood bench Unit	Wood Hot H ₂ O ext.	Wood Very Mild Hyd.	Wood Mild Hyd.
Feed Rate, gm/hr	3,390	29.6	33.4	16.2	21.9
Temp °C	504	497	504	503	501
Vapor Res. Time, s	0.48	0.46	0.46	0.46	0.45
Particle Size, μ m	-1000	-590	-590	-590	-590
Moisture, %	4.6	3.3	7.0	0.83	16.5
Cellulose, %	49.1	49.1	50.0	63.4	62.8
Yields, % Wood mf					
Organic Liquid	66.2	65.8	69.8	78.3	79.6
Water	10.8	12.2	7.6	5.0	0.9
Char	11.8	7.7	9.3	6.0	6.7
Gas	11.0	10.8	12.3	7.7	6.4
	<u>99.8</u>	<u>96.5</u>	<u>99.3</u>	<u>97.0</u>	<u>93.6</u>

Table 4
Pyrolysis of Raw and Treated Wood
Analysis of Organic Liquids

	PP 59	A-2	A-4	A-3	A-1
Yields of					
Tar Components					
% of Feed					
Oligosaccharides		0.7	2.58	3.80	1.19
Cellobiosan		1.3	3.18	10.08	5.68
Glucose		0.4	1.0	1.67	1.89
Fructose		1.31	2.35	4.00	3.89
Glyoxal		2.18	3.68	4.10	0.11
1,6 Anh. Glucofuranose		2.43	4.12	3.08	4.50
Levoglucoosan	<1	3.04	5.17	15.7	30.42
Hydroxycetaldehyde	8.86	10.03	12.61	5.35	0.37
Formic Acid		3.09	3.42	2.54	1.42
Acetic Acid	4.33	5.43	5.20	1.46	0.17
Ethylene Glycol		1.05	0.78	0.43	-
Acetol	2.93	1.40	1.20	0.06	0.06
Methylglyoxal		0.65	1.28	0.41	0.38
Formaldehyde		1.16	1.78	0.72	0.8
Aromatics (lignin)	↓ by G.C.	16.2	-	16.0	19.0
Totals		51.5	-	71.4	69.9
% of Pyrolysis Oil		78.3	-	91.2	87.8
Sugars		9.2	18.4	38.3	47.6

Table 5
Pyrolytic Products from Celluloses

Run Source	SS-12 Commercial SS 144	A-5 Treated SS 144	6 Avicel pH-102	A-6 Treated Avicel
Temp °C	500	502	500	503
Yields, % mf of feed				
Organic liquid	72.5	83.5	87.1	86.3
Water	10.8	6.1	3.1	?
Char	5.4	1.3	2.5	5.7
Gas	7.8	3.9	8.9	3.3
Hydroxyacetaldehyde	15.3	6.2	8.6	0.43
Levoglucofan	7.0	31.8	26.9	38.41
Cellobiosan	4.0	11.5	10.1	5.6
Glucose	1.0	1.8	2.1	2.0
Fructose	2.0	3.0	4.7	2.7
Glyoxal	3.5	5.5	6.5	2.1
Methylglyoxal	0.8	1.3	0.23	0.30
Formic Acid	5.5	1.9	3.8	1.5
Acetic Acid	4.9	0.1	1.4	0.03
Ethyleneglycol	1.7	0.02	0.56	0.00
Formaldehyde	1.2	0.94	0.72	0.24
Acetol	2.2	0.12	0.04	0.02
Anhydroglucofuranose		5.5		7.0
Oligosaccharides		5.3		
% of Oil Quantified		89.6		

EARLY PRODUCTS OF PYROLYSIS OF WOOD

William F. DeGroot, Wei-Ping Pan, M. Dalilur Rahman, Geoffrey N. Richards

Wood Chemistry Laboratory, University of Montana, Missoula, Montana 59812 USA

INTRODUCTION

We are studying the first stages in pyrolysis of wood and other cellulosic materials as part of a study of the chemistry of smoldering or low-temperature combustion. In the latter processes both oxidative and non-oxidative pyrolysis occur. This paper describes an investigation of the first volatile products of pyrolysis of wood and we believe that many of the conclusions regarding the first pyrolysis reactions at low temperatures are applicable also to higher temperature treatments of wood such as are utilized in liquifaction processes. Our aim was primarily to determine the relative rates and modes of pyrolysis of the three major constituents of wood (viz. cellulose, hemicelluloses and lignin) from their chemically intact situation in whole wood. We believe that interactions of these substances and of their degradation products during pyrolysis make this approach necessary and may invalidate some aspects of earlier studies of pyrolysis of isolated wood fractions.

METHODS

Our major technique has been the coupling of a thermogravimetric analysis system (TG) with a Fourier transform infrared spectrometer. The coupling is by a heated 1 m. teflon tube from the TG to an infrared gas cell. All of the results were obtained with cottonwood sapwood (*Populus trichocarpa*) which had been ground to pass an 80 mesh sieve. All pyrolyses were carried out in flowing nitrogen, the time lag between the thermal balance and the gas cell was 1 min, and heating was either isothermal at 250°C or at 3°/min. from 100° to 500°. In the isothermal runs for periods up to 2 hrs. the whole infrared spectrum could be accounted for by the absorption bands of the 6 components shown in Table 1. The system was therefore calibrated for these compounds by heating the pure liquid in a loosely covered pan on the thermal balance at an appropriate temperature and relating the rate of weight loss to the infrared spectrum. Where a wavenumber range is shown in Table 1, the absorbance was integrated between these values and where a single wavenumber is given, the height of that Q branch was used. These values bore a linear relationship to the rate of weight loss for an individual compound, and the resultant calculated response factors were used to calculate the rates of production of each product from heated wood samples. For carbon dioxide the calibration was based on air versus a pure nitrogen blank and the carbon monoxide calibration was then deduced from a standard mixture of the two oxides in nitrogen.

The effects of cations on the pyrolyses were investigated with wood which had been washed with acid to remove all metal ions and with samples in which the indigenous cations had been replaced entirely with either potassium or calcium ions. These ion exchange processes caused no other chemical change in the wood. E.g. the content of L-arabinofuranose units (which comprise one of the most acid-labile groups in wood) was unchanged.

Total absolute glucose contents of the wood samples were determined by acid hydrolysis, reduction, acetylation and gas chromatography using i-inositol as internal standard (1). Uronic acids were determined on a aliquot portion of the hydrolyzates (2) and vanillin and syringaldehyde from lignin were generated by nitrobenzene oxidation (3) and determined by gas chromatography of trimethylsilyl ethers. The glucan components of the heated wood samples were very resistant to hydrolysis with 72% sulfuric acid and it was necessary to "reactivate" with water before hydrolysis.

RESULTS AND DISCUSSION

Figure 1 shows that the cations have a major influence on the rate of pyrolysis of wood. The results confirm earlier studies (4) and show that of the two major cations present in wood, potassium is dominant in catalysis of pyrolysis, whereas calcium tends to stabilize the wood towards pyrolysis. The low temperature inflection in the DTG curves at 250-300° has often been assumed to be associated with hemicellulose and/or lignin degradation and since the cations occur predominantly in the hemicelluloses (5) we have studied pyrolysis in this region in some detail by isothermal pyrolysis at 250°. Figure 2 shows the weight loss under such conditions and the rates of weight loss for original wood and for potassium-exchanged wood were indistinguishable. The weight loss curves for acid-washed and for calcium-exchanged wood were also indistinguishable, but corresponded to a much lower rate of pyrolysis.

The rates of formation of the volatile products determined by infrared spectroscopy are shown in Figure 3 for the original wood. Similar results are also available for the ion-exchanged woods. Table 2 shows the proportion of total weight loss in the wood sample that can be accounted for by the infrared analysis. The 40% of unaccounted weight loss represents material which condensed before reaching the infrared cell. This is likely to consist of a mixture of larger molecules containing two or more carbon atoms. It is evident that carbon dioxide and methanol are the first products of pyrolysis at 250°, very closely followed by water, which is the major product on either a weight or molar basis. Formic acid is produced steadily over a relatively long period, while acetic acid production peaks much later than the carbon dioxide, methanol and water. The changes in glycose, uronic acid, vanillin and syringaldehyde content are shown in Table 3. We conclude that the methanol is formed predominantly by pyrolysis of lignin with syringyl units pyrolysing rather more rapidly than guaiacyl. The amount of methanol released is much greater than could be accounted for by the 4-O-methylglucuronic acid units of the hemicelluloses. Evidently however, some units or regions of the lignin are especially labile; only about half of the available methanol is released in 1 hr. at 250°, possibly in two stages, and the remainder requires higher temperatures (see below). The carbon dioxide is evidently derived predominantly from decarboxylation of uronic acids which decrease rapidly in the solid residue and the molar yield of carbon dioxide corresponds approximately with the uronic acid content of the wood. Since the glucan content of the wood is virtually unchanged in 50 min. at 250°, it appears that cellulose survives this treatment, although it is quite likely that some chain scission will occur and perhaps some transglucosylation. The acetic acid is almost certainly released by pyrolysis of the acetyl ester groups from the xylan and its yield is approximately that anticipated from the acetyl content of the wood.

The water, which is the major product, must be formed predominantly from the hemicelluloses. Some water will obviously be formed from the uronic acid and arabinose units which decompose rapidly, but water must also be derived from xylose units which show some decrease. Since we would anticipate that the β -1,4-xylan chain should have a thermal stability similar to cellulose and since glucose does not decrease, it seems probable that some of the xylose units may be subject to rapid elimination reactions yielding water, particularly in the regions of the hemicellulose molecules in which uronic acids are decomposing. The pyrolysis of acetyl ester groups might also be associated with decomposition of the attached xylose units.

The mechanism of formic acid formation is not known. It could be derived from either hemicelluloses or lignin, although by analogy with its formation from polysaccharides by alkali degradation, the former seem more likely.

The influences of cations on yields of carbon dioxide, carbon monoxide (formed above 250°), methanol and formic acid during pyrolysis at temperatures up to 400° are shown in Figures 4-7. The yields of water and acetic acid were much less

sensitive to cation variation and are not shown. Figure 4 shows that the potassium ions favor increased formation of carbon dioxide and lower the temperature of peak production compared with the acid-washed or calcium forms. The total yield of carbon dioxide is much greater than could be explained by decarboxylation of uronic acids alone. The mechanism of formation of this carbon dioxide is not known. Since the bulk of the carbon dioxide is formed above 300° it must be derived at least partly from cellulose. Carbon monoxide was not significantly formed at 250°, but was produced in similar molar amount to carbon dioxide at higher temperatures, peaking at about 350° (Figure 7). It seems probable that this product also is largely produced from cellulose.

The formation of methanol (Figure 5) shows a distinct second peak at about 300° for original and for potassium-exchanged wood. Presumably the methanol evolved above 320° is catalyzed by potassium and derived by pyrolysis reactions from the more resistant lignin which survives pyrolysis at lower temperatures. Formic acid (Figure 6) evidently forms at higher temperatures by potassium catalyzed pyrolysis reactions from cellulose. The same acid is a major product of alkaline degradation of cellulose in absence of air and it is probable that the greater effectiveness of potassium compared with calcium in catalyzing formation of formic acid (and perhaps methanol) is associated with the greater basicity of the former.

REFERENCES

1. E.g., M.J. Neilson and G.N. Richards, Carbohydr. Res. 104 (1982) 121-138.
2. N. Blumenkrantz and G. Asboe-Hansen, Anal. Biochem., 54 (1973) 484-489.
3. B. Leopold and I.L. Malmstrom, Acta Chem. Scand., 6 (1952) 49-55.
4. W.F. DeGroot and F. Shafizadeh, J. Anal. Appl. Pyrol., 6 (1984) 217-232.
5. W.F. DeGroot, Carbohydr. Res., 142 (1985) 172-178.

Table 1. Infrared absorbances used to quantify the first volatile products from pyrolysis of wood and conditions used for calibration.

Compound	Wavenumbers (cm ⁻¹)	Temperature (°C)	Rate of Weight Loss (µg/min)
CO ₂	2240 - 2400	--	
CO	2020 - 2240	--	
CH ₃ COOH	1140 - 1230	23, 30	16, 32
H ₂ O	1653	23, 30	17, 61
HCOOH	1105	23, 26	12.6, 30.0
CH ₃ OH	1032	23, 30	42.6, 137

Table 2. Yield of volatile products by infrared detection as percentage of total weight loss; cottonwood at 250°C in nitrogen.

	<u>% of Total Weight Loss</u>			
Methanol	3.5	3.7	3.8	4.4
Formic acid	5.0	6.4	8.2	7.0
Acetic acid	7.5	15.5	19.0	23.0
Carbon dioxide	10.5	9.2	12.0	13.2
Water	<u>21.5</u>	<u>18.3</u>	<u>16.0</u>	<u>13.2</u>
Total	47.5%	53.1%	59.0%	60.8%
Time at 250°	11 min	23 min	40 min	58 min
Total weight loss	5.5%	8.0%	11.0%	12.5%

Table 3. Analyses of cottonwood after heating at 250°C under nitrogen.

<u>Analysis (% dry weight)</u>	<u>Original Dry Wood</u>	<u>250°/N₂/50 min.</u>
<u>(Anhydroglycoses)</u>		
Rhamnose	0.2	0
Arabinose	0.5	trace
Xylose	15.8	12.3
Mannose	3.0	2.4
Glucose	51.3	51.3
Uronic acid	4.9	1.7
Total Carbohydrate	75.7	67.7
Vanillin	2.7	1.8
Syringaldehyde	5.7	2.2
Weight loss	0	11.9%

FIG. 1
DTG
Cottonwood, N₂, 3°/min.

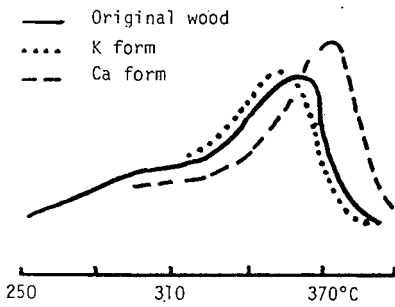
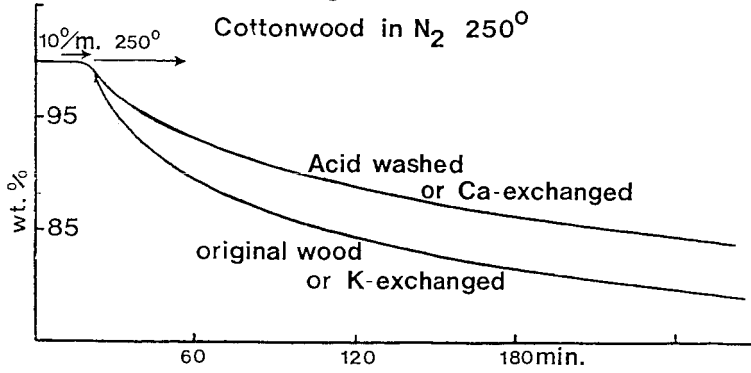
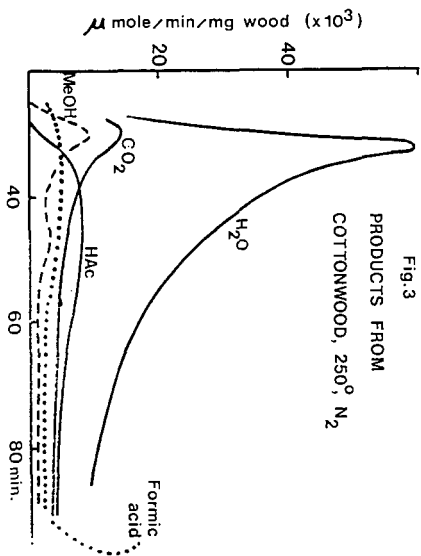
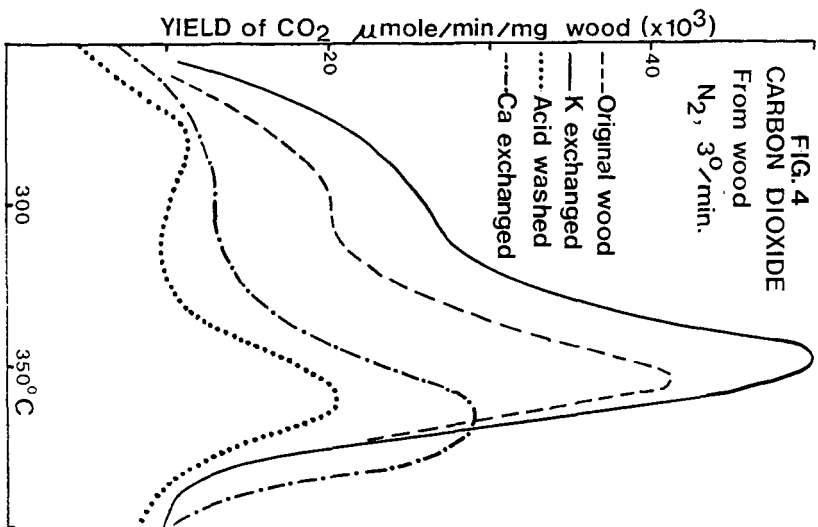
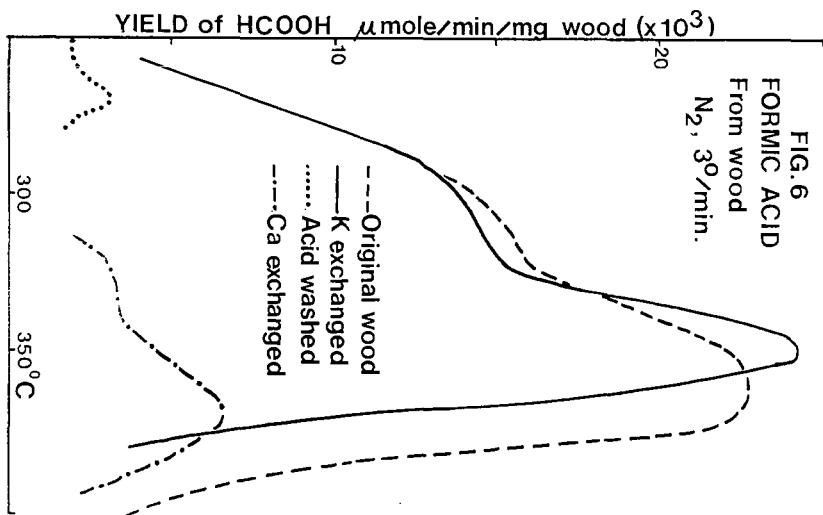
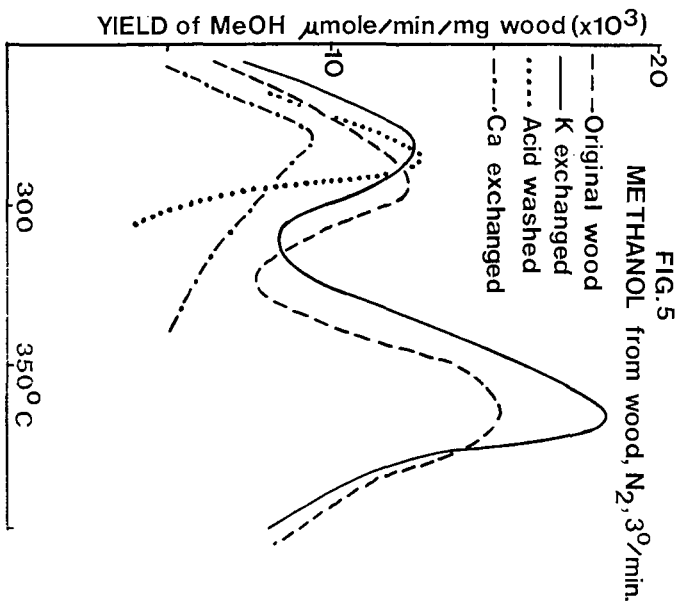
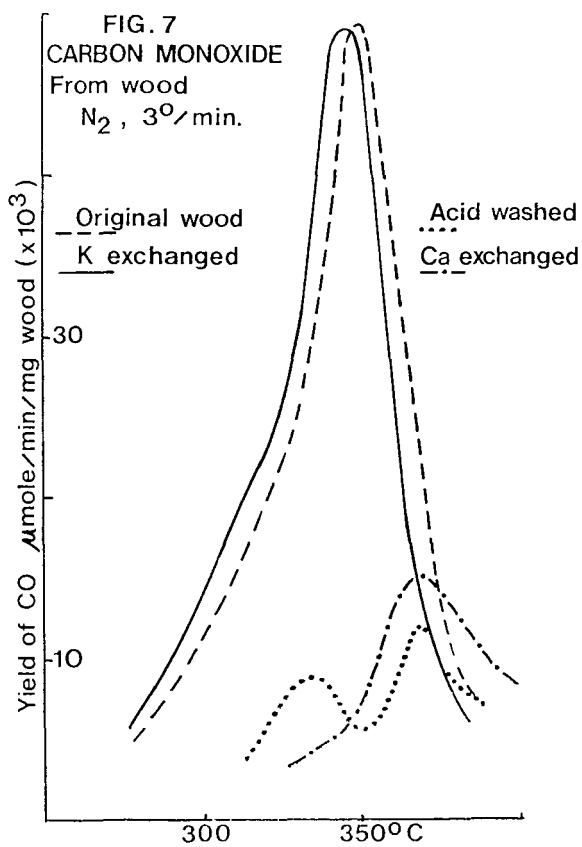


Fig. 2









Conditions that Favor Tar Production from Pyrolysis of Large, Moist Wood Particles

Marcia Kelbon, Scott Bousman, and Barbara Krieger-Brockett

Dept. of Chemical Engineering, BF-10
University of Washington
Seattle, WA 98195

Abstract

The production of pyrolytic oils from biomass will be greatly facilitated if large, and perhaps moist, particles can be used directly as a feedstock. This paper describes experiments to quantify product evolution rates, as well as spatial and temporal temperature distributions, during pyrolysis of large wood particles. The experiments have been performed using well-defined, reactor-independent conditions which will aid in identifying favorable conditions for tar production from large particles. The experiments reveal that an optimum moisture content can facilitate tar production. The reacted fraction that is tar is greater for intermediate moisture contents, particle sizes, and heating rates, and the optimum tar production conditions for moist feed change with both heating intensity and particle size.

INTRODUCTION

The economics of making pyrolytic oils from biomass will be improved if large, and perhaps moist, particles can be used directly as a feedstock. This is a result of the high cost of size reduction and drying of fibrous and often green biomass. However, the pyrolysis of realistically sized particles (about 1 x 1 x .5 cm or greater) is complicated by the lack of uniform temperature profiles within the particle, and the synergistic effects that external heating intensity, moisture, and particle size have in altering the intraparticle temperature histories. Nevertheless, both present and planned industrial biomass converters employ large particles, sometimes using them in fluidized beds which are less sensitive to feed size distributions (1).

Selectively producing a particular pyrolysis fraction such as tar, or specific components in any fraction, is difficult. The majority of studies to date have used finely ground (< 100 μm diameter) wood samples in which heat transfer rates are rapid enough to cause a uniform particle temperature, and mass transfer is fast enough to minimize secondary reactions. For these particles, pyrolysis with a high heating rate to moderately high temperatures generally favors tar formation, if the tar can be quickly removed from the reaction zone. However, reducing fibrous materials to such a small size is costly. Pyrolysis feeds are likely to be wood chips used routinely in the forest products industry. In wood chip pyrolysis, the particle interior heats slowly and secondary reactions of tar are significant.

The scope of this preprint is limited to the presentation and discussion of experimental conditions of practical importance that maximize tar from pyrolysis of large wood particles. By design, results are as independent of reactor type to the greatest possible, and reveal the effects of heat and mass transport that are critical to conversion of the large, poorly conducting porous particles. Since typical feeds are heterogeneous, the entity appropriate for chemical engineering studies is the single particle. The findings are then applicable to all reactors in which the chosen experimental conditions prevail. The study of reacting single particles has proven extremely successful in the development of catalytic reactors (2) and coal pyrolysis (3,4,5).

Since reaction temperature is not an independent variable for large pyrolyzing particles, special attention must be given to choosing experimental conditions for the 0.5 cm to 1.5 cm thick

particles studied. Heating intensity can be made precise by controlling the applied heat flux at the particle surface or imposing a surface temperature, and measuring the particle thermal properties (6). One dimensional heating has been used experimentally (7,8) and typifies the type of heat transfer experienced by most wood chips owing to the large aspect ratios they usually have (9). The lowest heating intensity studied, $2 \text{ cal/cm}^2\text{-s}$, barely chars thick samples (or causes smoldering combustion if oxygen is present). The highest, $6 \text{ cal/cm}^2\text{-s}$, is found in furnaces or high temperature reactors designed for maximum heating of particles. Biomass moisture varies with species and age as well as from region to region. Typical moisture contents (dry basis) found for feed piles in the Pacific Northwest range from 10% to 110%, thus the choices for the experiments reported here. A more complete discussion of practical conditions appears elsewhere (10). Also, simultaneous variations in two or three experimental conditions were systematically investigated in order to determine if pyrolysis tar yields, as well as other reaction products, were dependent on process condition combinations in a non-additive, or multiplicative way (11).

EXPERIMENTAL

Apparatus - A description and diagram of the single particle pyrolysis reactor appears in Chan, et al. (12) but a brief presentation is given for completeness. A wood cylinder was placed in a glass sleeve and reactor assembly. An arc lamp provided radiative, spatially uniform, 1-D axial heating as verified by absolute calibration of the heat flux (6,13, 14). The heating period was the same for all experiments, 12 min, sufficiently short to enable the study of active devolatilization in the thinnest of these particles. Thermocouples at 2, 4, and 6 cm from the heated face automatically measured the devolatilization front progress. An infrared pyrometer, mounted off-axis from the arc lamp beam, measured the surface temperature of the pellet. The glass housing and baffle allowed the front face of the pellet to be uniformly irradiated and prevented volatiles from condensing on the window. The large helium carrier gas flowrate quenched the volatiles and swept them without significant backmixing or reaction (6) to the analysis system. The helium pressure on the unheated face was slightly elevated to ensure volatiles flow toward the heated face for maximum recovery. It has been verified (7) that during devolatilization of a large particle, nearly of the volatiles flow toward the heated surface owing to the decreased porosity behind the reaction front. A cold trap (packed with glass wool and at -40 C) immediately downstream from the reactor condensed tars and water from the volatiles. Permanent gases were sampled near the cold trap exit at preselected times during the experiment using two automated gas sampling valves, thus providing information on evolution rates of gaseous products. All volatiles were later analyzed by gas chromatography.

Sample Preparation - The wood pellets were all cut, with great attention to grain direction, from uniform sections of the same lodge pole pine tree provided by Weyerhaeuser Co. (Corvallis Mill). The cylinders were oven-dried at 90 C for at least three weeks. Moisture was quantitatively added using a microsyringe and balance, and allowed to come to a uniform distribution as described by Kelbon (13).

Gas Analysis - Permanent gases, operationally defined as all components passing through the -40 C cold trap, were collected in 30 stainless steel sample loops of known volume. Immediately after the experiment, samples were automatically injected into a Perkin-Elmer Sigma 2 Gas Chromatograph using a Supelco 100/120 mesh Carbosieve S column $1/8 \text{ in.}$ diameter and 5 ft. long. The peaks were integrated and identified by a Perkin-Elmer Sigma 15 Chromatography Data Station. Both a thermal conductivity detector and a flame ionization detector were used as described in Bousman (14).

Tar Analysis - The tar is comprised of two parts, that which was trapped and that which was washed from the reactor, though the latter is often a small amount. The tar trap sample was analyzed for water and low molecular weight tar compounds by gas chromatography using a Supelco 80/100 mesh Porapak Q column $1/8 \text{ in.}$ diameter and 1.5 ft. long. After the low molecular weight tar analysis, the trap tar and reactor tar samples were treated with approximately 2 g of MgSO_4 to remove water and then filtered. A known quantity of p-bromophenol was added to each sample as an internal standard. Each sample was concentrated in order to remove THF while minimizing the loss of the other compounds. The resulting high molecular weight tar liquid was analyzed by gas chromatography using either a J and W Scientific DBWAX or Carbowax 20M fused silica capillary column 0.25 mm ID, 30 m long with a Perkin-Elmer splitting injection port. The major peaks which appeared in the

majority of the samples are numbered and presented in this paper as simplified, composite chromatograms.

Char Analysis - The char was weighed and a qualitative chemical analysis of some char samples was performed using a Fourier Transform Infrared Spectrometer (FTIRS) with preparation as described in Bousman (14). The surface area of the char was also characterized using CO₂ adsorption.

Experimental Design - The experimental conditions were picked according to a type of factorial experimental design which facilitates identification of optima and empirical models of the class given in Eq. 1 (11,15):

$$y_k = b_0 + \sum b_i x_i + \sum \sum b_{ij} x_i x_j, \quad \text{for } i \leq j, \quad (1)$$

where

y_k is the k-th product yield of interest,

x_i, x_j are the independent variables (process controllables) and

b_0, b_i and b_{ij} are least square parameter estimates obtained from multiple regression.

When variables combine to affect the reaction process in a non-additive way, as when the last term of Eq. 1 is large, non-linear dependence of yields on the process controllables is demonstrated. Plots of Eq. 1 are presented in subsequent figures as trend lines.

RESULTS AND DISCUSSION

The range of intraparticle temperatures measured throughout pyrolysis at a constant heat flux of 4 cal/cm²-s for a particle initially at 60% moisture (Fig. 1) corresponds to those found in other studies for both small (16-18) and large (19) particles. As can be seen when moisture is added, the temperature rises in the first ~30 sec to a plateau at 100 C until the water has locally evaporated, and then the temperature rises to the same level as found in dry wood particles, although at a somewhat later time. The surface temperature is of some qualitative value but once volatiles are produced, the infrared pyrometer cannot accurately "see" the surface and the measured temperature is artificially low. Note that reaction in zones near the surface experience quite high heating rates, which should favor tar production early in the devolatilization of a large particle.

In this preprint, overall yields are reported as graphs rather than tables, and correspond to time-integrated pyrolysis or devolatilization products from a large wood particle heated under constant applied heat flux at the surface. The yields are expressed as weight fractions of that which reacted in the 12 min pyrolysis duration. Fractional yields are an important measure of selectivity and are useful for downstream separation process considerations. The appropriate measure of experimental reproducibility and accuracy is the standard error calculated from replicate runs. This is given as an uncertainty. However, because of the inherent difficulty in recovering all products, especially tars, the mass balances do not always add to 100%. Thus, another measure of error is the discrepancy in the mass balance. For these experiments, the average mass balance closure was 80%, with a standard deviation of 11%.

In Fig. 2 the weight fraction water-free tar produced from the fixed duration pyrolysis of dry wood particles of several thicknesses is presented. The symbols, when there are two at the same heat flux, represent tar yield for 2 different particle densities. It can be seen that a 0.3 g/cc density change has little effect on tar yield. The trend lines result from regression of all the data to a single set of parameters for Eq. 1. The average prediction error as approximated by the standard error of the residuals is 2%, and the standard deviation of replicate runs is the same. In Fig. 2, the synergy, or interaction of particle size and heat flux can be clearly seen. The reduction in tar for an increase in heating rate, as characterized by the slope of the trend lines at any point, increases as the particle thickness increases. The thickest particle pyrolyzed at the lowest heat flux produces over 65% tar, and it decreases to 20% at the maximum intensity investigated. This is consistent with the extensive tar cracking that likely occurs near the particle surface char zone where high temperatures prevail

for severe heating. Note that all dry particles heated at the intermediate heat flux result in approximately 25%-35% tar.

The pyrolytic tar produced from a wet wood particle is presented in Fig. 3 as a function of both initial moisture content (abscissa) and heating intensity for the thickest particle size used in this study, 1.5 cm. The prediction error and the experimental error in the measured tar from wet particle pyrolysis is about 5%. Note that moisture causes the optimum tar conditions to occur at 4 cal/cm²-s, rather than the 2 cal/cm²-s for dry particles, consistent with the lower particle temperature expected when water is present. Overall, the level of tar produced is considerably higher, 50-70%, than for dry wood particles. Hydrogen is measured in the gases, as well.

In Fig. 4, a composition profile of some components of both tar and gas is presented. Changes in this profile simply highlight changes in composition as process conditions change. The ordinate is the weight fraction of the reacted portion of the 1 cm particle data used in this figure. Thus all components plotted are each less than 2% of the moist wood particle that was pyrolyzed. The error as estimated from replicated determinations is about 0.5%. The high molecular weight species composition appears to vary little as particle temperature is manipulated by changing both moisture and heating intensity of the pyrolysis. However, the low molecular weight tar compounds are in greater concentration for mild intensity heating (2 cal/cm²-s) than for a greater heating rate which appears to favor the hydrocarbon gases and hydrogen. Although the composition differences are nearly within the experimental error, moisture appears to slightly enhance the production of methanol and acetic acid for these experiments (1 cm particle).

CONCLUSIONS

Data has been presented which suggests that moisture can enhance the production of tar from the pyrolysis of large wood particles using conditions that occur in a large scale reactor where the heat flux a particle experiences is quite constant. The most favorable conditions result in about 70% of the reacted biomass becoming tar. If one assumes that the mass balance discrepancy results from tar condensing on reactor surfaces, this is a conservative estimate.

ACKNOWLEDGEMENTS

This work was supported by the National Science Foundation, Grant No. CPE- 8400655. Marcia Kelbon gratefully acknowledges the support of a Weyerhaeuser Fellowship and Scott Bousman acknowledges the fellowship support of Chevron Corp.

REFERENCES

1. Cady, T., personal communication, Weyerhaeuser Corp., Cosmopolis, WA, 1982.
2. Petersen, E.E., *Chemical Reaction Analysis*, Prentice Hall, 1965.
3. Russel, W.A., D.A. Saville, and M.I. Greene, *AIChEJ.* 25, 65 (1979).
4. Srinivas, B. and N.R. Amundson, *AIChE J* 26, 487 (1980).
5. Massaquoi, J.G.M., and J.B. Riggs, *AIChEJ* 29, 975 (1983).
6. Chan, W.C.R., Ph.D. Thesis, Dept. Chem. Engrg., U. Washington, 1983.
7. Lee, C.K., R.F. Chaiken, and J.M. Singer, *16th International Symposium on Combustion*, Combustion Institute, Pittsburgh, PA, 1459 (1976).
8. Ohlemiller, T. K. Kashiwagi, and K. Werner, NBSIR 85-3127, NBS Center for Fire Research, April 1985.
9. Miles, T.R., *Thermochemical Processing of Biomass*, Ed. by A.V. Bridgewater, Butterworths, London, p. 69 (1984).
10. Chan, W.C.R., submitted to *I.E.C. Proc. Des. Dev.*, (1986).
11. Box, G.E.P. and D.W. Behnken, *Technometrics* 2, 455 (1960).
12. Chan, W.C.R., M. Kelbon, B.B. Krieger, *Fuel* 64 1505(1985).
13. Kelbon, M., M.S. Thesis, Dept. Chem. Engrg., U. Washington, 1983.
14. Bousman, W.S., M.S. Thesis, Dept. Chem. Engrg., U. Washington, 1986.
15. Box, G.E.P., J.S. Hunter, W.G. Hunter, *Statistics for Experimenters*, Wiley, 1978.

16. Scott, D.S., J. Piskorz, and D. Radlein, *I.E.C. Proc. Des. Dev.* 24 , 581 (1985).
17. Nunn, T.R. J.B. Howard, J.P. Longwell, and W.A. Peters, *I.E.C. Proc. Des. Dev.* 24 , 836 (1985).
18. Bradbury, A.G.W. F. Sakai, and F. Shafizadeh, *J. Appl. Poly. Sci.* 23, 3271 (1979)
19. Kanury, A.M., *Combustion and Flame* 18 , 75 (1972).

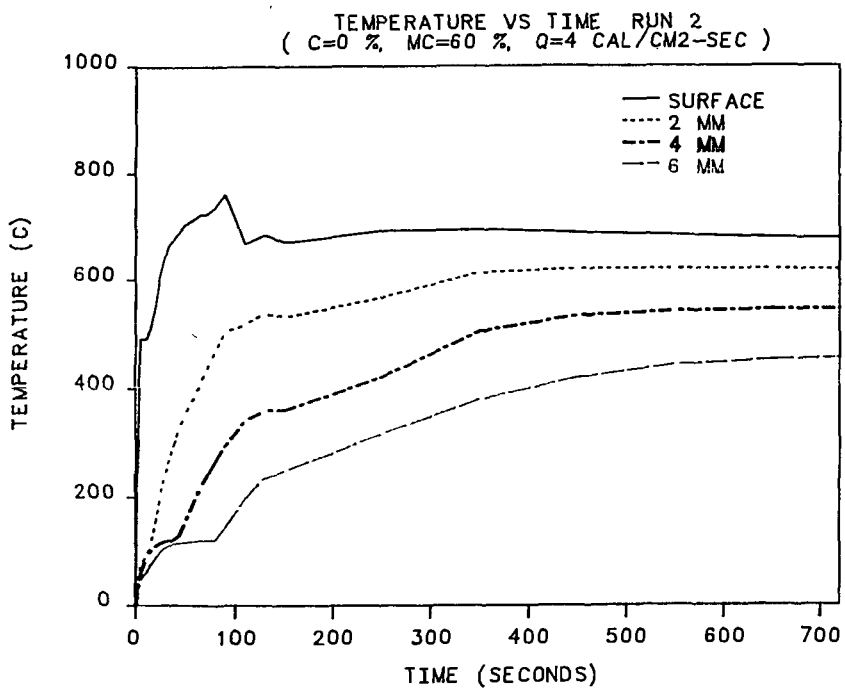


Fig. 1 - Temperature histories at 4 positions in a 1 cm thick wood particle pyrolyzed with an applied heat flux of 4 cal/cm²-s.

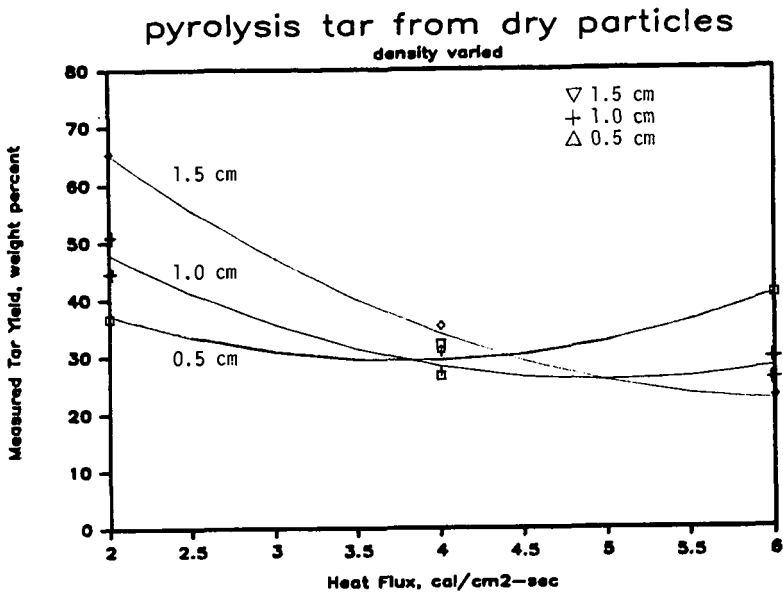


Fig. 2 - Weight fraction tar yield for the pyrolysis of dry wood particles at varying surface heat fluxes for three thicknesses; trend lines are least square fits and symbols are some of the experimental data.

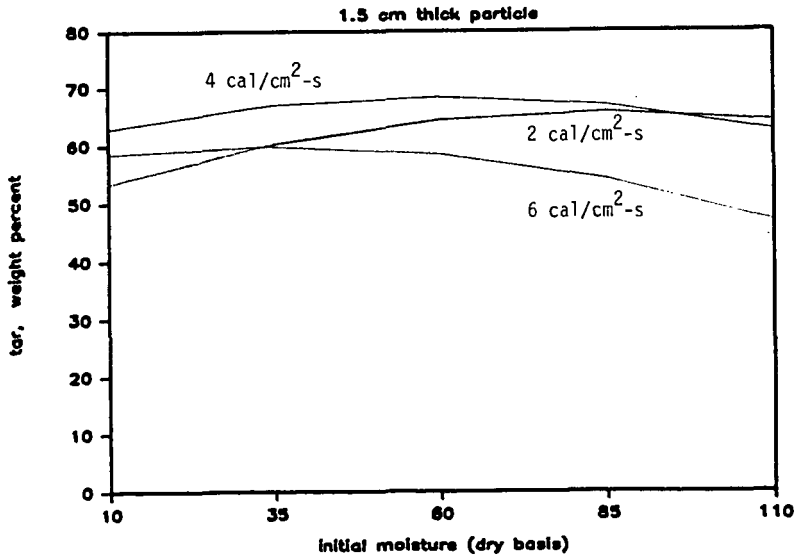
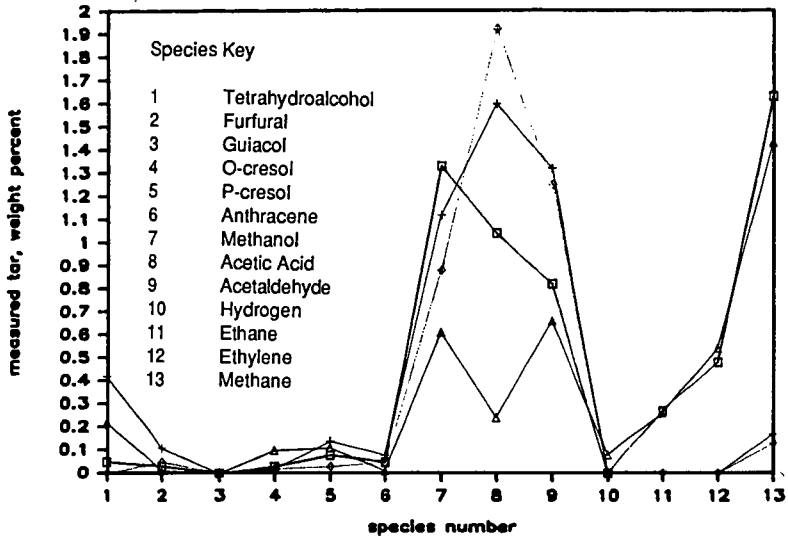


Fig. 3 - Measured weight fraction tar produced from a 1.5 cm thick wood particle as a function of moisture content for 3 different heating rates.

pyrolysis product profile



Symbol Key

- + 110% initial moisture, heated at 2 cal/cm²-s
- ◇ 10% initial moisture, heated at 2 cal/cm²-s
- 110% initial moisture, heated at 6 cal/cm²-s
- △ 10% initial moisture, heated at 6 cal/cm²-s

Fig. 4 - Product composition profile for two moisture content 1 cm thick particles heated at two heating rates.

Effects of Extra-particle Secondary Reactions of Fresh Tars on Liquids Yields in Hardwood Pyrolysis

Michael L. Boroson, Jack B. Howard, John P. Longwell,
and William A. Peters

Department of Chemical Engineering and Energy Laboratory
Massachusetts Institute of Technology
Cambridge, MA 02139

Introduction

Wood pyrolysis involves a complex system of chemical and physical processes. It is not yet possible to identify and model the individual reactions occurring during pyrolysis; however, a simplified model using lumped product groups such as tar, char, and gases can provide insight into the overall process.

Upon heating wood decomposes by an unknown series of bond-breaking reactions. The species formed by this initial step may be sufficiently immobile to preclude rapid escape from the particle. Consequently they may undergo additional bond-breaking reactions to form volatiles or may experience condensation/polymerization reactions to form higher molecular weight products including char. During transport within the particle volatile species may undergo further reactions homogeneously in the gas phase or heterogeneously by reaction with the solid biomass or char. The rate of volatiles mass transport within and away from the particle will influence the extent of these intraparticle secondary reactions. After escaping the particle, the tars and other volatiles may still undergo secondary reactions homogeneously in the vapor phase or heterogeneously on the surface of other biomass or char particles. Depending on reaction conditions intra- and/or extra-particle secondary reactions can exert modest, to virtually controlling influence on product yields and distributions from wood pyrolysis.

There exists a substantial amount of literature on the primary pyrolysis of wood. The literature on homogeneous secondary reaction kinetics of wood pyrolysis tars, however, is limited to only two studies (1,2) and no literature exists on the heterogeneous secondary reactions of tar over fresh wood char. The objective of the present study, therefore, was to obtain improved quantitative understanding of the homogeneous and heterogeneous extra-particle secondary reactions of sweet gum hardwood pyrolysis tar under conditions pertinent to gasification, combustion, and waste incineration. Sweet gum hardwood was chosen for two reasons: (a) this type of wood has commanded interest as an energy crop in the southern United States, and (b) secondary reaction results can be compared to sweet gum hardwood primary pyrolysis results already reported in the literature (3).

Results on homogeneous tar cracking are presented below. Studies of heterogeneous cracking of tar vapors over freshly generated wood char are in progress. Results will be presented.

1. Experimental

Yields of individual primary and secondary pyrolysis products as affected by reaction conditions and physical and chemical characteristics of "primary" (newly formed) and "secondary" (surviving thermal treatment) tar samples, were needed to fulfill the study objectives.

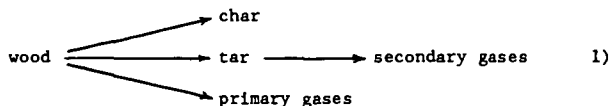
A two-chamber tubular reactor (Fig. 1) developed by Serio (4) for systematic studies of secondary reactions in coal pyrolysis, was adapted for the present measurements. In this apparatus "primary" tar, *i.e.*, tar that has undergone minimal extra-particle secondary reactions, is generated in an upstream reactor (No. 1) by heating a shallow packed bed of biomass, usually at a constant heating rate (typically 12°C/min). This tar and other volatiles are rapidly swept into a second reactor (No. 2) by a continuous flow of carrier gas (helium with an argon tracer). Here the volatiles are subjected to controlled extents of post-pyrolysis thermal treatment at temperatures between 400 to 800°C, pressures from 120 to 250 kPa, homogeneous residence times (V/F) between 0.9 and 2.2 sec, and heterogeneous space times (V_b/F) between 5 and 200 msec.

Four reactor configurations have been employed in the present investigation. In Mode I runs, only the first-stage reactor is used, and freshly evolved wood pyrolysis products spend little time at high reaction severities. Thus they reflect minimal contributions from secondary reactions and are taken as well representative of the tars evolved near the wood surface. In the present work tars so evolved will be defined as "primary" tars. In Mode II runs, only the second-stage reactor is used, and yields and surface characteristics of fresh char as a function of initial wood bed depth are determined. In Mode III runs, the empty second reactor is connected downstream of Reactor 1, preheated, and then maintained isothermal. Homogeneous secondary reactions of wood tar vapors are studied quantitatively by controlling their extent of thermal treatment in this reactor and measuring its effect on product yields, tar loss and tar composition. In Mode IV runs, the second reactor is packed with a mixture of wood and quartz and again connected downstream of Reactor 1. Reactor 2 is first heated to 800°C to generate the fresh char then cooled to the desired reaction temperature prior to heating Reactor 1. Heterogeneous secondary reactions of wood tar vapors are studied by varying the temperature and heterogeneous residence time over the bed of char and quartz.

Product characterization includes quantifying tar and light volatiles yields, and global analysis of tars. A Perkin-Elmer Sigma 2B Gas Chromatograph was used to determine the yields of carbon monoxide, carbon dioxide, methane, acetylene, ethylene, ethane, and C₃ hydrocarbon gases. Size exclusion chromatography (SEC) was used to determine the weight averaged molecular weights of the primary and secondary tars. The equipment is a Waters Associates ALC/GPC 201 SEC system with two μ styragel columns, 500 and 100 Å, in series, and a 405 nm UV detector.

2. Mathematical Modeling

Wood pyrolysis involves a complex set of parallel and series chemical reactions frequently influenced by heat and mass transfer, and tractable models generally must be built upon simplifying assumptions. Our model assumes the following reaction sequence:



and describes each of the above pathways with a single-reaction, first-order rate constant, the parameters for which are determined by curve-fitting product yield data. The kinetic parameters for the formation of char, tar, and primary gases from pyrolysis of the same sweet gum hardwood used in this study have been reported (3). The present modeling focuses on homogeneous cracking of the tar vapor and on the secondary gas formation reactions.

Net cumulative yields of unreacted tar and of individual gaseous products from tar vapor cracking were calculated as the difference between the cumulative amount of each entering (from Mode I runs) and leaving (from Mode III runs) Reactor 2. The data were then fit to the kinetic equation

$$\frac{dV_i}{dt} = k_i(V_i^* - V_i) \quad 2)$$

where V_i is the yield of material i at time t , V_i^* is the ultimate value of V_i at long residence times and high temperatures, and k_i is the global rate coefficient. Thus the rate of tar cracking at any time is modeled as first order in the difference between the ultimate (minimum) yield of tar (wt% of nonreactive tar) and the total amount of tar unconverted at that time. The rate of formation of an individual gaseous product is first order in the difference between the ultimate (maximum) yield of that gas and the amount of that gas generated up to that time. The kinetic parameters for homogeneous tar cracking and individual gaseous product

formation were found by a least squares parameter fitting technique.

3. Results and Discussion

Approximately fifty runs were performed to generate a broad data base on product yields as a function of primary and secondary reactor operating parameters. Good overall material balances and reproducibility were obtained. Selected tars collected from these runs were further characterized by SEC.

3.1 Homogeneous Cracking Product Yields

Product yields were determined for each experiment as described in Section

1.2. Representative yields for primary pyrolysis of wood and for homogeneous secondary tar cracking at 600, 700, and 800°C are shown in Table 1.

Primary pyrolysis products from the first reactor were tar, char, water, carbon dioxide, carbon monoxide, and a trace of methane. More reactive primary products, such as tar, become reactants for secondary reactions, when the thermal treatment reactor (Mode-III) is in place. These secondary reactants, and products arising from their secondary reactions can in turn be identified by observing whether their yield increases, decreases, or remains constant when changing from Mode I to Mode III, or when increasing the Mode III temperature. Tar, for example, is a primary product and a secondary reactant as demonstrated by its high yield from Mode I experiments and its decreasing yield with increasing reaction severity in Mode III experiments. For residence times of about 1 sec. homogeneous tar conversion ranged from 9wt% at 500°C to 30wt% at 600°C and up to 88wt% at 800°C.

Carbon dioxide is both a primary and secondary product, since the yield in Mode I is about half the total CO₂ yield from high severity Mode III runs (800°C, Table 1). Carbon dioxide accounted for about 14% of the tar lost during secondary tar cracking.

Carbon monoxide and methane are evolved in modest quantities from Reactor 1. However, most of the production of these compounds along with acetylene, ethylene, ethane, and hydrogen arises from secondary reactions as evidenced by their substantial yield increases in the Mode-III experiments.

Carbon monoxide was the major product of secondary tar cracking at all temperatures, accounting for about 60-70wt% of the tar cracked. Methane and ethylene accounted for about 10 and 11wt% of the tar cracked, respectively, and the remaining 2-4wt% of the tar was cracked to form acetylene, ethane, and hydrogen. At high tar cracking severities (> 85%) the dry gas composition by volume was 48% CO, 19% H₂, 13% CH₄, 11% CO₂, and 7% C₂H₄, with traces of C₂H₂ and C₂H₆.

Negligible amounts of char were observed in the second stage of the tubular reactor upon completion of experiments on homogeneous cracking of tar vapor. This implies that when char formation is observed in wood pyrolysis other pathways such as liquid phase tar condensation reactions, possibly surface assisted, are responsible. This picture is consistent with the ablative pyrolysis studies of Lede et al. (5) who found that char formation in wood devolatilization can be prevented by rapidly removing prompt pyrolysis tar liquids from wood surfaces at elevated temperature.

3.2 Tar characterization

The tar samples collected after different extents of homogeneous secondary thermal treatment were characterized by size exclusion chromatography (SEC). The weight average molecular weight behavior of tars as a function of conversion is shown in Figure 1. As shown, the average molecular weight of tar surviving secondary cracking is lower than the molecular weight of primary tar (640 gm/mole) entering the cracking reactor. Average molecular weights tend to decrease with increasing conversion; however, the change in average molecular weight over the range of conversion 20-80% is small after a sharp drop in average molecular weight from zero to ten percent conversion. This behavior is consistent with tar cracking occurring by a random scission mechanism.

3.3 Homogeneous Kinetics

Yield data from the tubular packed bed reactor were used to calculate kinetic

parameters as described in Section 2. Resulting best fit kinetic parameters for formation of secondary gases and for the homogeneous cracking of tar are given in Table 2.

The extent of secondary reaction is a function of both temperature and time. The separate effects of temperature and time can be described by a single parameter called "reactor severity," equal to the product of the rate constant at the reactor temperature and the isothermal residence time. Plots of the experimental yield of tar and individual gaseous products as a function of the dimensionless reactor severity (kt) are shown in Figures 2 - 5 together with smooth curves denoting the corresponding model predictions. The model predicts the experimental yields with an error generally less than ten percent.

Homogeneous kinetic results of this study were compared to results found in the literature. Vapor phase cracking of wood pyrolysis tars from an unspecified softwood was studied by Diebold (1) and cracking of tars from both cherry and yellow pine was studied by Mattocks (2). Due to differences in product group definitions as well as modeling techniques and assumptions, our results could not be directly compared to the results of Mattocks.

Diebold's kinetic parameters for the cracking of volatiles to gases ($A = 10^{5.19} \text{ sec}^{-1}$, $E = 87.5 \text{ kJ/mole}$) are comparable to the tar cracking parameters from this study ($A = 10^{4.98} \text{ sec}^{-1}$, $E = 93.3 \text{ kJ/mole}$). Over the common temperature range of experimentation (650 - 800°C) the rate constant of Diebold is only 3 - 3.5 times higher than that found in this work despite the differences in the reactor type and wood producing the primary volatiles. The small discrepancy could be due to effects of wood type, to slight differences in the models, or to Diebold's need to calculate the gas composition entering the isothermal section of his volatiles cracking reactor. In the present work the entering gas composition is measured directly in the Mode I runs.

4. Conclusions and Significance

The experimental results of this study identified and quantified those products generated by primary pyrolysis of wood and those formed by extra-particle secondary cracking of newly-formed wood pyrolysis tar. Tar, char, water, and carbon dioxide are primary products of wood pyrolysis. Additional carbon dioxide, however, is also formed by vapor phase cracking of tar. Carbon monoxide, hydrogen, methane, ethylene, acetylene, and ethane are products of homogeneous secondary cracking of wood tars, although modest amounts of CO, and trace quantities of methane are also observed under conditions chosen to arrest vapor phase tar cracking (Mode I). Carbon monoxide accounts for about 65 wt% of the products when fresh wood tar undergoes vapor phase cracking.

Tars surviving various extents of post pyrolysis secondary thermal cracking were characterized by size exclusion chromatography (SEC). SEC indicates that tars surviving vapor phase cracking are lower in weight-average molecular weight than the uncracked tars. In addition, there was no evidence for tar molecular weight growth among these surviving tars. This result is consistent with the experimental observation of negligible coke production during vapor phase tar cracking.

The experimental yields of the individual gaseous products from homogeneous cracking of wood pyrolysis tar can generally be predicted by global single-reaction first-order kinetic models to within better than ten percent. These first-order kinetic parameters are sufficiently intrinsic to be used in reactor design calculations including predictions of the contributions of extra-particle homogeneous vapor phase tar reactions. These parameters can also be used to estimate the kinetics of intra-particle homogeneous reactions of tar vapor, but further work will be needed to define the validity of this application.

Notation

- A_1 - Arrhenius pre-exponential factor for species 1
- E_1 - apparent Arrhenius activation energy for species 1
- $k_1 = A_1 \exp(-E_1/RT)$ - Arrhenius rate constant
- R - gas constant
- T - absolute temperature

V_1^* - ultimate yield in weight percent of wood of species 1
 V_1 - yield in weight percent of wood of species 1
 V - volume of reactor 2
 V_b - volume of char bed in reactor 2
 F - volumetric gas flow rate at reactor 2 temperature

Acknowledgements

Most of the above work was supported by the National Science Foundation, Division of Chemical and Process Engineering, Renewable Materials Engineering Program, under Grant Nos. CPE-8212308 and CBT-8503664. We also gratefully acknowledge an NSF Fellowship for M. Boroson and financial support by the Edith C. Blum Foundation of New York, NY and the Robert C. Wheeler Foundation of Palo Alto, CA. Drs. M. K. Burka, J. Hsu, L. Mayfield, and O. R. Zaborsky (NSF) have served as technical project officers. Christine Clement and Anne Reeves have made valuable contributions to this work.

Literature Cited

1. Diebold, J. P., "The Cracking Kinetics of Depolymerized Biomass Vapors in a Continuous, Tubular Reactor," M.S. Thesis, Dept. of Chemical and Petroleum-Refining Engineering, Colorado School of Mines, Golden, Colorado (1985).
2. Mattocks, T. W., "Solid and Gas Phase Phenomena in the Pyrolytic Gssification of Wood," M.S. Thesis, Dept. of Mechanical and Aerospace Engineering, Princeton University, Princeton, New Jersey (1981).
3. Nunn, T. R., J. B. Howard, J. P. Longwell, and W. A. Peters, "Product Compositions and Kinetics in the Rapid Pyrolysis of Sweet Gum Hardwood," Ind. Eng. Chem. Process Design Develop., 24, 836-844, (1985).
4. Serio, M. A., "Secondary Reactions of Tar in Coal Pyrolysis," Ph.D. Thesis, Dept. of Chemical Engineering, MIT, Cambridge, Massachusetts (1984).
5. Lede, J., J. Panagopoulos, and J. Villermaux, "Experimental Measurement of Ablation Rate of Wood Pieces, Undergoing Fast Pyrolysis by Contact With a Heated Wall," Am. Chem. Soc. Div. of Fuel Chem. Preprints, 28 (5), 383 (1983).

Table 1. Product Yields (weight % of wood)
 as a Function of Thermal Treatment

	Primary Yields	Secondary Reaction Yields		
		600°C 1.2 s	700°C 1.0 s	800°C 1.0 s
Tar	52.8	36.6	16.6	6.1
Char	18.3	18.1	18.4	17.8
CH ₄	0.4	1.7	3.8	5.5
CO	3.2	14.7	25.7	35.7
CO ₂	6.8	9.7	11.4	13.2
C ₂ H ₂	0.0	0.1	0.5	0.6
C ₂ H ₄	0.0	1.2	3.6	5.4
C ₂ H ₆	0.0	0.1	0.3	0.4
H ₂ O	16.3	17.3	17.0	15.2
H ₂	0.0	0.1	0.6	1.0

Table 2: Kinetics Parameters for Gas Formation and Tar Cracking

	log A (sec ⁻¹)	E (kJ/mole)	v* (wt% of wood)
CH ₄	4.89	94.1	5.83
C ₂ H ₄	5.76	109.3	5.17
C ₂ H ₆	7.52	138.8	0.38
CO ₂	2.55	48.8	13.20
CO	4.66	87.8	36.33
H ₂	6.64	128.4	1.09
TAR	4.98	93.3	5.79

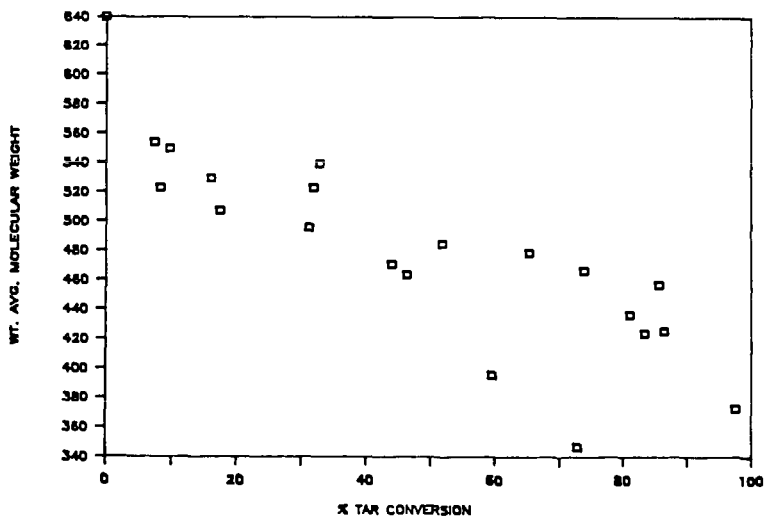


Figure 1: Effect of Vapor Phase Thermal Treatment on Weight Average Molecular Weight of Surviving Tar

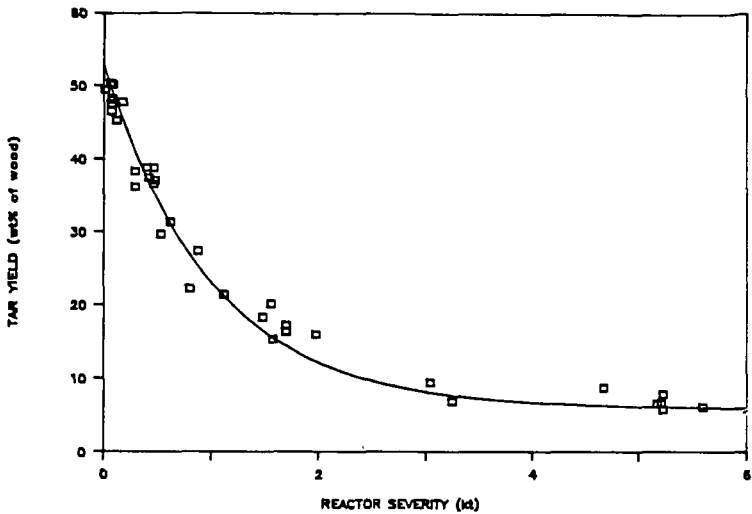


Figure 2: Effect of Reactor Severity on Tar Yield (— model prediction)

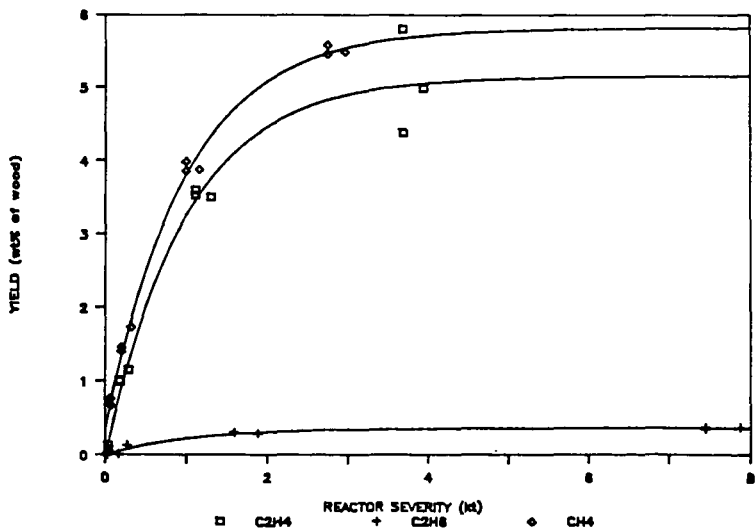


Figure 3: Effect of Reactor Severity on Ethylene, Ethane, and Methane Yields (— model prediction)

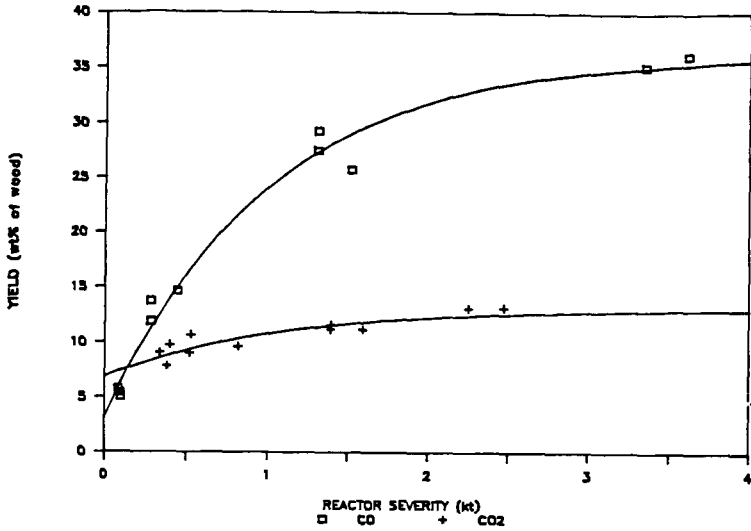


Figure 4: Effect of Reactor Severity on Carbon Monoxide and Carbon Dioxide Yields (— model prediction)

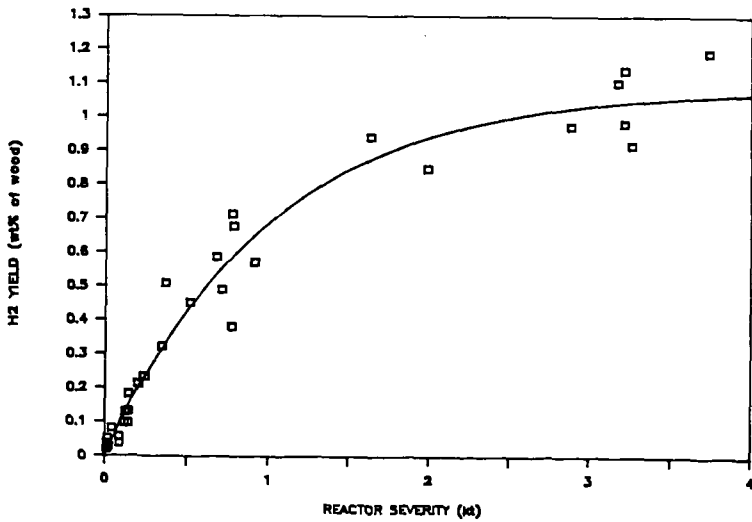


Figure 5: Effect of Reactor Severity on Hydrogen Yield (— model prediction)

FUSION-LIKE BEHAVIOUR OF BIOMASS PYROLYSIS

Jacques LEDE, Huai Zhi LI and Jacques VILLERMAUX

Laboratoire des Sciences du Génie Chimique, CNRS-ENSIC
1, rue Grandville 54042 NANCY (FRANCE)

INTRODUCTION

Considering a thermal reaction of a Solid \rightarrow Fluid type, the apparent rate of reaction can be controlled by chemistry, thermal and mass transfer resistances. If the chemical processes are very fast, and if the fluid products are easily eliminated from the medium, the overall rate of reaction is controlled by heat transfer resistances. This is the case of the ablation regime [1], characterized by a steep temperature gradient at the wood surface and consequently by a thin superficial layer e of reacting solid moving at a constant velocity v towards the cold unreacted parts of the solid.

Suppose now that heat is provided by a surface at T_w . A theoretical increase of the surface temperature T_d of the solid (by increasing T_w) would lead to a subsequent increase of the heat flux demand. Such a demand would be satisfied by an equal external heat flux supply, a condition fulfilled only with large temperature gradients ($T_w - T_d$). The consequence would be a stagnation of T_d , leading to a fusion like behaviour of the reaction.

Wood pyrolysis carried out in conditions of high available heat fluxes and efficient elimination of products occurs in ablation regime with production of very low fractions of char [2,3,4] and could therefore behave as a simple fusion. This paper presents a brief outline of the main ideas and results obtained to this effect and issued from different approaches. More details can be found in related papers [5,6,7,8].

The reaction has been carried out in three different conditions : heating against a hot spinning disk ; against a fixed heated surface ; in a continuous cyclone reactor. In the first two cases, the behaviour of the reaction is compared to that of solids undergoing simple fusion in the same conditions.

SPINNING DISK EXPERIMENTS

The melting of ice, paraffin and "rilsan" (polyamide 11) and the pyrolysis of wood have been carried out by applying under known pressures p , rods of the corresponding solids against a hot spinning stainless steel disk (temperature T_w) [5,6]. In wood experiments, the reaction produces almost exclusively gases and liquids, the solids being mainly ashes deposited on the disk. The liquids produced are rapidly extracted from the wood surface and eliminated by the fast moving disk on which they undergo further decomposition to gases at a rate depending on T_w . The presence of the thin liquid layer acts as a kind of lubricant.

Figure 1 reveals that under comparable values of p , the behaviour of v as a function of v_R is similar, the orders of magnitude of v being the same for the four types of solids. For $v > 2 \text{ m s}^{-1}$, v increases with p following :

$$v = a p^F$$

(1)

a depends on T_w and F on the material. The mean values of F (ice : 0.035 ; paraffin : 0.29 ; "rilisan" : 0.83 ; wood : 1) can be fairly well represented by :

$$F(\text{melting solid}) = \frac{Cp_s(T_f - T_o)}{Cp_s(T_f - T_o) + L} \quad \text{or} \quad F(\text{wood}) = \frac{Cp_s(T_d - T_o)}{Cp_s(T_d - T_o) + \Delta H} \quad (2)$$

F being close to 1 for wood shows that it is probable that ΔH , the enthalpy of pyrolysis, is small with respect to sensible heat in agreement with literature.

The equations of heat flux density balances between the disk and the rod are :

$$\begin{aligned} \text{melting solid} : h(T_w - T_f) &= v\rho_s Cp_s (T_f - T_o) + v\rho_s L \\ \text{wood} : h(T_w - T_d) &= v\rho_s Cp_s (T_d - T_o) + v\rho_s \Delta H \end{aligned} \quad (3)$$

Assuming that the heat transfer coefficient h is the only parameter depending on the pressure ($h = Kp^F$) it can be deduced :

$$\frac{v}{p^F} (\text{melting solid}) = \frac{K}{\rho_s Cp_s (T_f - T_o) + L} \frac{T_w - T_f}{p^F} ; \quad \frac{v}{p^F} (\text{wood}) = \frac{K}{\rho_s Cp_s (T_d - T_o) + \Delta H} \frac{T_w - T_d}{p^F} \quad (4)$$

In agreement with (4), Figure 2 shows that the variations of $\frac{v}{p^F}$ with T_w are linear for the three melting solids and also for wood. The values of T_f calculated from the extrapolation of the straight lines to $v = 0$ are in very good agreement with the known values of melting points (better than 2 % accuracy). The corresponding "fusion temperature" of wood is then calculated close to 739 K.

The values of heat transfer coefficients obtained from the slopes of the straight lines in figure 2 are of the same order of magnitude (around $10^4 \text{ W m}^{-2} \text{ K}^{-1}$) whatever the solid showing that the mechanisms of heat transfer are probably similar for wood and melting solids. For wood, h varies as $h = 0.017 p(\text{W m}^{-2} \text{ K}^{-1}) [5]$. These values reveal very efficient transfers.

FIXED HEATED WALL

The same experiments as before have been made with rods of ice, paraffin and wood pressed against a stationary piece of brass heated at T_w .

An analytic solution has been found for representing the rate of ablative melting of a solid cylinder pressed against a horizontal wall maintained at T_w [7]. In steady state, a liquid layer of constant thickness is formed between the hot surface and the rod, with a radial flow of liquid. The resolution of the equation of liquid flow associated with that of energy balance between the two surfaces allows to derive the following relationship:

$$v = \frac{\rho_l}{\rho_s} \left[\frac{2}{3} \frac{\alpha_l^3}{\mu_l R^2} Pe^3 (Ph) p \right]^{1/4} \quad (5)$$

where Pe is a Peclet number, a function of a phase change number

$$Ph = \frac{Cp_l(T_w - T_f)}{L} \quad \text{as} \quad Pe = \frac{Ph}{1 + Ph^{5/6}/3}$$

The relation (5) shows that v varies as $p^{0.25}$ whatever the type of solid. In reduced form, (5) can be written as follows :

$$v = \frac{2}{3} [Pe^3 P]^{1/4} \quad (6)$$

with
$$v = \frac{\rho_s R}{\rho_l \alpha_l} v \quad \text{and} \quad P = \frac{R^2}{\mu_l \alpha_l} p$$

By plotting V against $\left[\frac{2}{3} Pe^3 P\right]^{1/4}$ one should obtain a straight line of slope one whatever the nature of melting solid and wall temperature.

As in the case of ice and paraffin [7], ablation rate v for wood pyrolysis varies as P^F with a mean value of F (0.29) close to the theoretical one (0.25) (Fig. 3). The figure 4 gathers all the experimental points according to (7). The physical properties used for the calculation of V and P for ice and paraffin are reported in ref. [7,8]. In the case of wood, the factor containing these properties in equation (5) has been fitted to the experimental results (fig. 3) leading to $v = 1.55 \times 10^{-3} (Pe^3 p/p_0)^{1/4} (m s^{-1})$. The fitted constant associated with estimated values for ρ_l (500 kg m^{-3}), Cp_l ($3.65 \text{ kJ.kg}^{-1}\text{K}^{-1}$) and α_l ($0.3 \times 10^{-7} \text{ m}^2 \text{ s}^{-1}$) allows to calculate $\mu_l = 72.5 \times 10^{-3} \text{ Pa.s}$, a reasonable value for the viscosity of a liquid at a melting point of 739 K [7,8].

CYCLONE REACTOR EXPERIMENTS

The continuous fast pyrolysis of wood sawdust has been studied in a Lapple type ($2.8 \times 10^{-2} \text{ m}$ diameter) cyclone reactor heated between 893 and 1330 K [2]. The wood particles carried away by a flow of steam enter tangentially into the cyclone on the inner hot walls of which they move and undergo decomposition. Mass balances show in all the cases, a very low fraction of char (< 4 %) while the gasification yield increases with wall temperature T_W . It appears from figure 5 that the reaction seems to occur only for wall temperatures greater than about 800 K in good agreement with fusion temperature of 739 K. In such a model, the decomposition temperature of particles being roughly constant, the gasification yield increase with T_W would then result from further vaporization and/or decomposition of primary products (mainly liquids) at the wall and/or in the gas phase with an efficiency depending on T_W .

DISCUSSION

All these results obtained in different experimental conditions, show striking similarities between ablative wood pyrolysis and melting of solids. Nevertheless the equivalent fusion temperature of 739 K has been calculated from relation (4) based on the assumption that T_d is constant. Let suppose now that T_d depends on external physical conditions (p , T_W) under the assumption that $\Delta H \ll v \rho_s Cp_s (T_d - T_0)$. The heat flux density balance equation is :

$$h(T_W - T_d) = \rho_s Cp_s v (T_d - T_0) \quad (7)$$

The reaction occurring in ablation condition concerns only a thin external wood layer e inside which the equation of mass balance $ke = v$ associated with $ev = \alpha_s$ [5] leads to a relationship between the ablation velocity and the chemical first order kinetic constant k : $k = v^2/\alpha_s$ and finally to :

$$T_d = \frac{h T_W + T_0 \sqrt{k \lambda_s \rho_s Cp_s}}{h + \sqrt{k \lambda_s \rho_s Cp_s}} \quad (8)$$

Figure 6 shows the variations of T_d with T_W ($\lambda_s = 0.2 \text{ W m}^{-1} \text{ K}^{-1}$; $C_{p_s} = 2800 \text{ J kg}^{-1} \text{ K}^{-1}$; $\rho_s = 700 \text{ kg m}^{-3}$) with h as a parameter. The first order rate constant for the formation of "active cellulose" [9] $k(\text{s}^{-1}) = 2.83 \times 10^{19} \exp -29000/T_d$ has been supposed to fit the present case of wood primary decomposition.

It can be observed that the smaller the values of h , the shortest the domain of wall temperature where $T_d = T_W$ (for the lowest values of h , T_d/T_W becomes less than one as wood begins to decompose). In most of usual experimental devices wood temperature is then very different from source temperature. Consequently, the direct determination of pyrolysis rate laws would have sense only for low wall temperatures ($< 750 \text{ K}$).

Figure 6 shows that T_d varies with T_W and h indicating that strictly speaking, the fusion model is not appropriate. But it can be observed (specially for the low h) that as soon as $T_d/T_W < 1$, T_d increases more and more slowly with T_W and rapidly reaches a roughly constant value. Fusion model seems then to be an excellent first approximation.

The hatched zone reported in figure 6 is bounded by the extreme values of h determined in ref. [5] and by the extreme values of T_W explored. The "fusion temperature" of 739 K appears to be well situated inside the hatched surface. Such a fair agreement shows that the chosen kinetic law is a good approximation for wood decomposition. The "fusion temperature" must then be considered a mean value lying roughly between 660 and 725 K for $T_W = 773 \text{ K}$ and between 700 and 800 K for $T_W = 1173 \text{ K}$.

CONCLUSION

The behaviour of wood rods undergoing ablative pyrolysis by more or less intimate contact with a hot surface has revealed strong similarities with a phase change phenomenon. The principal reasons developed are the followings : quite similar behaviour of wood rods with true melting solids when applied on moving or fixed surfaces : same orders of magnitude of v and h ; same dependance law with applied pressure with a power F showing probable low values of the enthalpy of reaction ; same $p^{0.25}$ dependance of v in the case of fixed surface ; same low of variations of v with wall temperature. Ablative pyrolysis carried out with sawdust in a cyclone reactor proves that no fast reaction occurs for wall temperatures lower than $\sim 800 \text{ K}$.

A consequence of these conclusions is that the accurate direct determination of kinetic rate constant of wood decomposition is a difficult task, likely impossible over wide ranges of temperatures in most of experimental devices (upper limit around about 800 K). Even if such high temperatures could be reached, the system should be designed in such a way that the products of the reaction could also be removed from the reacting surface with high efficiencies. For example, figure 6 shows that $T_d = T_W = 800 \text{ K}$ would be observed for $h = 10^6 \text{ W m}^{-2} \text{ K}^{-1}$. Assuming that the available heat flux is controlled by conduction through the oil layer, such a heat transfer coefficient would be effective for an equivalent layer thickness of $0.1 \mu\text{m}$! (calculation made with a thermal conductivity of $0.1 \text{ W m}^{-1} \text{ K}^{-1}$ for oil). Of course, an efficient removal of these liquids would prevent also the extent of their subsequent decomposition to secondary products and then to reduce the formation of new thermal isolating layers.

All these conclusions are in agreement with the analysis of other authors. Diebold pointed out in 1980 the efficiency of "solid convection" for carrying out the reaction of ablative pyrolysis of biomass (demonstration of

"sawing" biomass [4]. The same author stated also recently that cellulose passes probably through a liquid or plastic unstable state ("active cellulose") during pyrolysis before further decomposition [14] in agreement with Antal who points out the strong analogies observed between cellulose pyrolysis at high heating rates and phase change phenomena [10,11] with an upper limit at which pyrolysis occurs of 773 K. Evidence of such an upper limit is explained by a competition between heat demand from biomass and available external heat flux [12]. The same author [12] notices also the difficulty and indeed impossibility of achieving conditions whereby pyrolysis kinetics could be studied at very high temperatures. Finally, it must be reminded that in 1980, Reed [13] proposed a model for estimating the enthalpy of flash pyrolysis of wood based on several steps : heating of biomass up to a reaction temperature of 773 K, followed by a depolymerisation to form a solid which subsequently melts, melted matter being afterwards able to vaporize, following the temperature.

NOMENCLATURE

a	Constant ($m s^{-1} Pa^{-F}$)
Cp	Specific heat capacity ($J kg^{-1} K^{-1}$)
e	Thickness of reacting wood layer (m)
F	Exponent
h	Heat transfer coefficient ($W m^{-2} K^{-1}$)
H	Specific enthalpy ($J kg^{-1}$)
K	Constant ($W m^{-2} K^{-1} Pa^{-F}$)
k	First order kinetic constant (s^{-1})
L	Heat of fusion ($J kg^{-1}$)
p	Pressure (Pa)
p _o	Atmospheric pressure (Pa)
P	Reduced pressure
Pe	Peclet number
Ph	Phase change number
R	Radius of the solid cylinder (m)
T _d	Wood surface temperature (K)
T _f	Fusion temperature of a melting solid (K)
T _o	Ambient temperature (K)
T _w	Wall temperature (K)
v	Ablation velocity of the solid cylinder ($m s^{-1}$)
X	Gasification yield
V	Reduced velocity
α	Thermal diffusivity ($m^2 s^{-1}$)
λ	Thermal conductivity ($W m^{-1} s^{-1}$)
μ	Viscosity (Pa s)
ρ	Density ($kg m^{-3}$)

Subscripts :

s	solid cylinder
ℓ	liquid layer

REFERENCES

1. J. VILLERMAUX, B. ANTOINE, J. LEDE and F. SOULIGNAC. Chem. Eng. Sci. 41 (1986), 151
2. J. LEDE, F. VERZARO, B. ANTOINE and J. VILLERMAUX. Chem. Eng. Process, 20 (1986), 309
3. J. LEDE, F. VERZARO, B. ANTOINE and J. VILLERMAUX. Proceedings of Specialists Workshop on Fast Pyrolysis of Biomass, Copper Mountain Co, October 1980, p. 327

4. J.P. DIEBOLD, As Ref. 3, p. 237
5. J. LEDE, J. PANAGOPOULOS, H.Z. LI and J. VILLERMAUX. Fuel, 64 (1985), 1514
6. J. LEDE, H.Z. LI, J. VILLERMAUX and H. MARTIN. J. Anal. Appl. Pyrolysis, in press.
7. H. MARTIN, J. LEDE, H.Z. LI, J. VILLERMAUX, C. MOYNE and A. DEGIOVANNI. Int. J. Heat Mass Transfer, 29 (1986), 1407
8. H.Z. LI. Pyrolyse éclair de baguettes de bois. Modèle de fusion. DEA, (INPL, Nancy)(1984)
9. A.G.W. BRADBURY, Y. SAKAI and F. SHAFIZADEH. J. Appl. Polym. Sci., 23 (1979), 3271
10. V. KOTHARI and M.J. ANTAL. Fuel, 64 (1985), 1487
11. M.J. ANTAL. Fuel, 64 (1985), 1483
12. M.J. ANTAL. Biomass Pyrolysis. A review of the literature. Part 2 : Ligno-cellulose Pyrolysis. In Advances in Solar Energy, Plenum Press, New York vol. 2 (1985)
13. T.B. REED, J.P. DIEBOLD and R. DESROSIERS, As Ref. 3, p. 7
14. J.P. DIEBOLD. Thesis, T-3007, Colorado School of Mines, Golden, Co USA 80401 (1985)

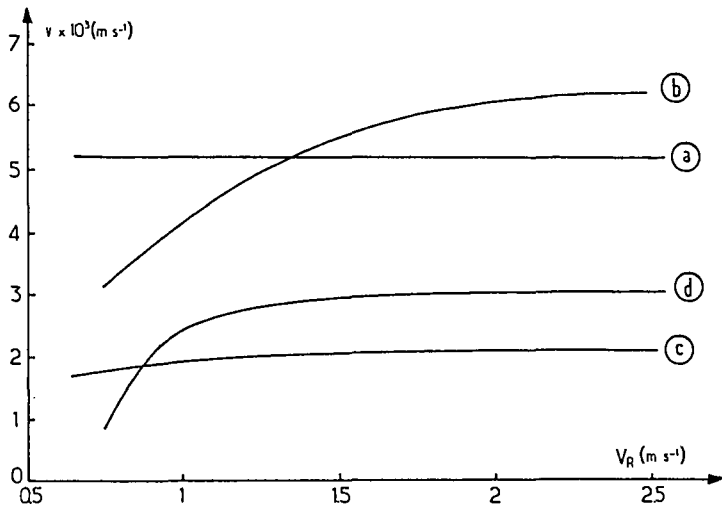


Fig. 1. Experimental variations of ablation velocities v with disk velocity V_R for four kinds of solids : a(ice, $T_W = 348 \text{ K}$, $p = 2 \times 10^5 \text{ Pa}$), b("rilsan", $T_W = 723 \text{ K}$, $p = 3,45 \times 10^5 \text{ Pa}$), c(paraffin, $T_W = 373 \text{ K}$, $p = 3,45 \times 10^5 \text{ Pa}$), and d (wood, $T_W = 1073 \text{ K}$, $p = 3,7 \times 10^5 \text{ Pa}$) (From [8]).

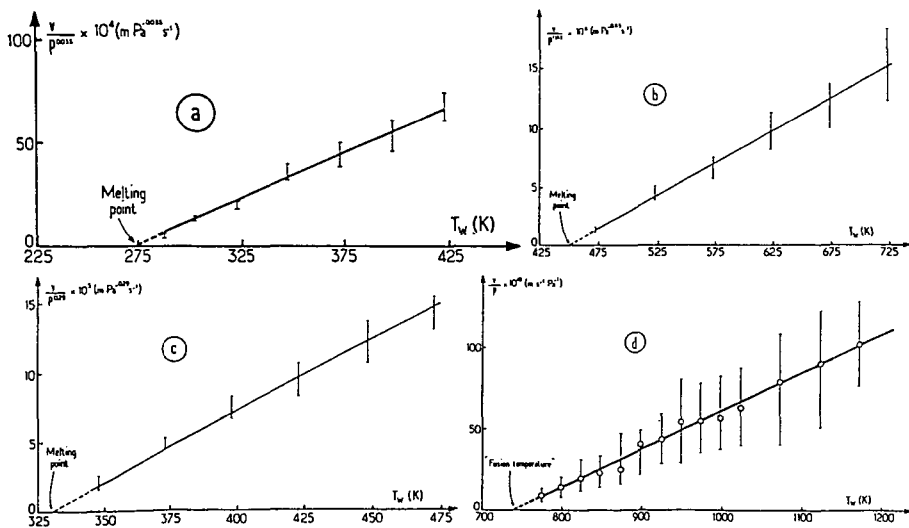


Fig. 2. Experimental variations of v/p^F with disk temperature T_W for : a(ice), b("rilsan"), c(paraffin) and d(wood) (From [8]).

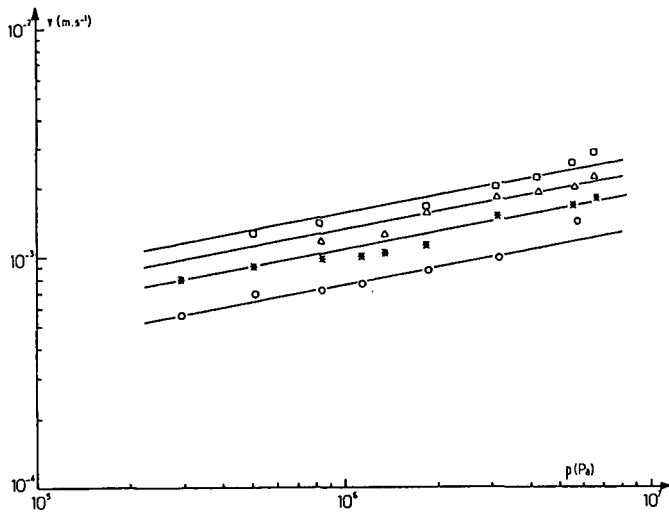


Fig. 3. Ablative pyrolysis rate of wood v as a function of applied pressure p for different wall temperatures - \circ : 823 K ; $*$: 873 K ; Δ : 923 K ; \square : 973 K

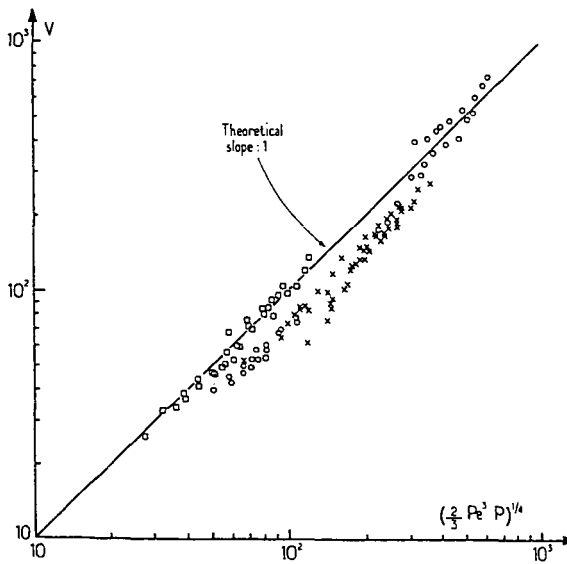


Fig. 4. Dimensionless representation of reduced velocity V as a function of reduced pressure P for three kinds of solids - \circ : paraffin ; x : ice ; \square : wood ...

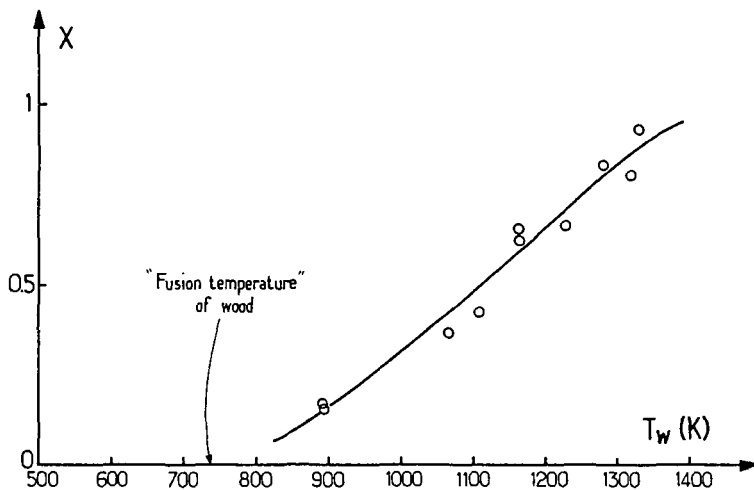


Fig. 5. Variation of the gasification yield X as a function of wall temperature T_w in the fast pyrolysis of wood sawdust in a cyclone reactor : comparison with the "fusion temperature" of 739 K.

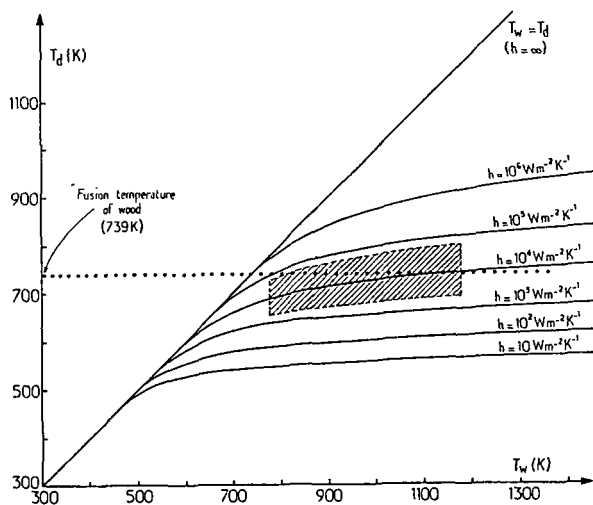


Fig. 6. Theoretical variations of wood surface temperature T_d as a function of heat source temperature T_w for different values of the external heat transfer coefficient. The hatched surface corresponds to the experimental domain ($776 \leq T_w(K) \leq 1176$ and $10^3 < h(W m^{-2} K^{-1}) < 6 \times 10^4$).

HEAT FLUX REQUIREMENTS FOR FAST PYROLYSIS AND A NEW METHOD FOR GENERATING BIOMASS VAPOR

Thomas B. Reed & Craig D. Cowdery
Colorado School of Mines, Golden CO 80401

ABSTRACT

The term "fast pyrolysis" has been used to describe a pyrolysis regime in which vapor production is enhanced and char minimized by rapid heating. It has been found in the last decade that high yields of primary pyrolysis oil can be achieved using fast pyrolysis. More recently it has been found that the pyrolysis vapors can be converted to high grade fuels using a catalyst. This makes fast pyrolysis of biomass desirable for synthetic fuel manufacture.

We present here results derived from the Diebold Integrated Kinetic Model (DKM) that predict the time, the temperature, and the products of pyrolysis and the heat for pyrolysis of cellulose as a function of heating rates between 0.01 and 10⁵°C/min. This range covers very slow pyrolysis requiring days to fast pyrolysis occurring in fractions of a second. The predictions are in good qualitative agreement with experimental measurements.

We then compare the heat flux required for slow and fast pyrolysis for particles with that which can be obtained with practical heating devices. The comparison shows that convective and radiative heat transfer is adequate for fast pyrolysis of small particles, but not for large particles, due to conduction to the interior. We derive the heat flow requirements for large bodies, the time for onset of pyrolysis, and the depth of heat penetration in that time. We compare the heat flux from various practical devices with those observed in "contact pyrolysis" experiments of Diebold and Lede on large particles. The comparison shows that higher heat flux methods are required for fast pyrolysis of larger particles.

We have designed a "heat flux concentrator", based on the experiments of Diebold and Lede to generate wood vapors for upgrading to gasoline-like liquids. A rotating birch dowel is fed into a heated copper block. Vapors emerge from the bottom and are condensed and collected, or passed over a catalyst to establish optimum conversion conditions. The pyrolysis rates and results of catalytic conversion in these experiments will be described.

INTRODUCTION

Pyrolysis of biomass is a very old and complex process producing variable quantities of charcoal, pyrolysis liquids and gases from biomass, peat or coals (1). Pyrolysis was the principle source of chemicals in Western society for about a century and could gain become a major source, particularly if the products can be tailored to modern needs through better understanding of the pyrolysis process or improved upgrading of the products.

The relative amounts of charcoal, liquid and gas obtained from pyrolysis depend on the time-temperature-pressure history of the sample in a way which may never be completely understood. This has led to apparent controversy over the magnitudes of kinetic factors, energies and products when investigators compare results from different experiments. Nevertheless great progress has been made in the last decade in understanding the role of these variables in controlling the nature and quantity of the products.

The term "fast pyrolysis" has been used to describe a pyrolysis regime in which vapor production is maximized and the formation of char is minimized by rapid heating. It has been found in the last decade that it is possible to obtain high yields of pyrolysis oils or

gas using high heat flux (1-3). It has more recently been found that pyrolysis oil can be converted catalytically to high grade, high octane motor fuel. Thus there is a strong motivation to understand these relations.

While there is no hard boundary between "slow" and "fast" pyrolysis, it is necessary to understand the relation between the time and energy required for each and the different chemistry and the possible mechanisms available for supplying this heat. We hope this paper will help draw together the apparently disparate results using a time-temperature-pressure kinetic model and lead toward more effective methods of pyrolysis.

CELLULOSE AND BIOMASS PYROLYSIS KINETICS

Biomass is a composite plastic, consisting of cellulose, hemicellulose and lignin with cellulose constituting more than half the total and giving most of the mechanical strength. Cellulose has the best defined structure and thus has been studied more than lignin or hemicellulose. Furthermore it constitutes more than half the substance of most biomass and contributes most of the strength. Much of the following discussion applies primarily to cellulose, but qualitatively to all biomass.

The rates of pyrolysis reactions are usually represented in the form of a first order Arrhenius rate equation

$$dX/dt = -X A \exp(-E/RT) \quad 1)$$

where X represents the quantity of any reactant X at time t and temperature T. (A is the pre-exponential and E is the activation energy. R is the gas constant). If the biomass is heated at a constant rate of R °C/sec, simple substitution leads to

$$dX/dT = (-AX/R) \exp(-E/RT) \quad 2)$$

The values for A and E in Eqs. 1 and 2 are usually measured by thermogravimetric analysis (TGA) and describe the global pyrolysis (including all solid state reactions) in terms of a single A-E pair (2,3). While this oversimplification may be justified over a narrow temperature range for engineering purposes, the global approach ignores preliminary solid state reactions and thus is not able to predict the change of products with heating rate, the time required for pyrolysis or the temperature of pyrolysis.

Several reaction schemes for cellulose pyrolysis have been proposed involving competing parallel and consecutive reactions (2,3,5,6). Cellulose pyrolysis now appears to involve an initial drying step (not discussed here), followed by two parallel reactions which for instance differentiate between two subsequent paths as shown in Table 1. The first reaction involves cross linking (transglycolization) of the cellulose and leads to the formation of charcoal. The second reaction is a depolymerization leading to a low molecular weight liquid or solid depending on temperature and rate of formation. This was called the "active state" by Bradbury and Shafizadeh (4). These more volatile components may either immediately evaporate at low pressure or evaporate subsequently at higher pressures.

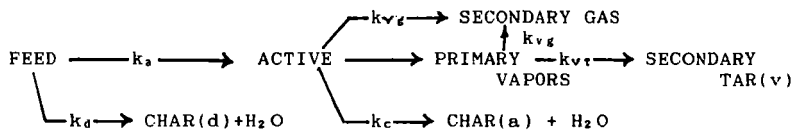
AN INTEGRATED MODEL OF CELLULOSE BIOMASS PYROLYSIS KINETICS

The justification for studying the various pyrolysis reactions is to predict the detailed course of pyrolysis under a wide variety of conditions. Diebold has recently collected previous work on various aspects of cellulose pyrolysis into a single integrated model of cellulose pyrolysis (5,6). The six reactions included are shown in Table 1. The temperature at which the reaction rate reaches 10⁻⁶/s and 1/s is listed for convenience in evaluating the relative strength of each reaction. Note that the reaction producing char reaches a rate of

10⁻⁶/s at 208 °C, while the depolymerization reaction does not reach 10⁻⁶/s until 225 °C. Thus slow pyrolysis favors charring. However the depolymerization reaction reaches a rate of 1/s at 379 °C, while the charring reaction does not reach a rate of 1/s until 703 °C. Thus rapid heating favors depolymerization and volatilization over charring.

The Diebold Kinetic Model (DKM) permits calculation of the relative amounts of the products of pyrolysis as a function of time-temperature history. The kinetic equation 1) using values in Table 1 are integrated using the Runge-Kutta technique on a microcomputer. A second-derivative test is used to determine the time increment. The model permits any type of heating history, but the results given here are those for a constant heating rate as given in Eq. 2).

Table 1 - Simplified Cellulose Pyrolysis Reaction Scheme



REACTION	k	A sec ⁻¹	E KJ	T(R=10 ⁻⁶) °C	T(R = 1) °C
Cellulose to char + H2O	k _d	6.69E+05	109	208	703
Cellulose to Active	k _a	2.80E+19	243	225	379
Active to Primary Vapor at 1 atm	k _v	6.79E+09	140	188	470
Active to primary vapor vacuum	k _{vv}	3.20E+14	198	231	440
Active to Char(b) + H2O	k _c	1.30E+10	153	224	518
Active to gas	k _{vg}	3.57E+11	204	335	651
Primary vapors to gas	k _{vg}	3.57E+11	204	335	651
Primary vapors to tars	k _{vt}	1.81E+03	61	70	700

Notes: Kinetic constants used in Diebold kinetic model. T(R = 10⁻⁶) is the temperature where the rate constant R = 10⁻⁶; T(R = 1) is the temperature at which R = 1.

While this model may not explain all aspects of cellulose pyrolysis, it goes a long way toward predicting the changes observed with time-temperature-pressure. Other values for kinetic factors and other pathways should be substituted as they become known. In particular, an improved model should include the effect of pressure explicitly in the vaporization rates given by k_v and k_{vv}. The nature and role of the "active" state needs to be better defined, since it plays a key role in this and other schemes. We will use this model here to predict heat flux requirements for slow and fast pyrolysis of cellulose.

DEPENDENCE OF TIME, TEMPERATURE AND PRODUCTS ON HEATING RATE

The dependence of the pyrolysis time, t_p and pyrolysis temperature, T_p on heating rate predicted by the DKM are shown in Table 2 and Fig. 1. The dependence of products on heating rate is shown in Fig. 2. (It is the nature of an exponential decay that it is never complete. We have therefore arbitrarily taken the time and temperature of pyrolysis as that time and temperature where the reaction is more than 99.9% complete.)

Table 2 - Cellulose Pyrolysis Time, Temperature and Products
 predicted by Kiebold Kinetic Model

PYROLYSIS CONDITIONS			PYROLYSIS PRODUCTS		
R Heat Rate R-°C/min	t _p Pyr Time sec	T _p Pyr Temp °C	Char- coal-%	Oil,Gas %	Water %
0.01	1650000	275	23.9	46.2	29.9
0.1	181200	302	12.4	73.2	14.9
1	19800	330	6.9	84.6	8.7
10	2142	357	4.2	90.3	5.4
100	234.6	391	2.6	94.3	3.1
1000	25.5	425	1.2	97.2	1.5
10000	2.778	463	0.005	98.7	0.007
100000	0.3042	507	0.003	99.4	0.003

Notes: Values calculated from Diebold model.

Here it is seen that pyrolysis temperatures vary between 280 and over 500°C as heating rates increase from 10⁻² to 10⁵ °/min. In slow "commercial" pyrolysis, char yields are still increasing with pyrolysis times of over a month, and pyrolysis is complete at temperatures below 300°C. These correspond to the conditions that have been used classically for the manufacture of charcoal (1). Most of the kinetic data of Table 1 were acquired in experiments using convenient "laboratory" heating rates of 1-100°C/min. The predicted char yields of 2.6-6.9% and temperatures of 330-390°C correspond to those observed experimentally in this range.

At even higher "heroic" heating rates, gas and oilyields are still increasing with rates of over 10⁴ °C/min where pyrolysis occurs at about 460°C. These conditions correspond to the experimental conditions of Diebold, Lede and Reed (7-9) produced by contact pyrolysis (see below). Thus it is clear that heating rate is a primary variable for controlling products in pyrolysis.

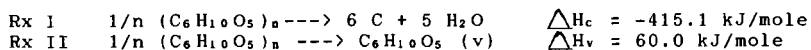
While the calculations in this paper are for cellulose, we believe the conclusions are qualitatively valid for all biomass.

HEAT OF PYROLYSIS AND HEAT FOR PYROLYSIS:

The energy required for pyrolysis, Δh_p , has long been a subject of interest to those involved in pyrolysis; yet no commonly accepted value is available to an engineer wishing to design a pyrolysis reactor, and even now it is not clear from the literature whether pyrolysis is endothermic or exothermic. It has been reported to vary from +370 J/g (endothermic) to -1700 J/g (exothermic)(5). One reason there is no commonly accepted value is that it is a difficult measurement to make under many of the conditions of pyrolysis (very slow or very rapid heating, large quantities of condensable vapors present, large temperature gradients in the sample). A more fundamental reason however is that the value depends on the particular form of biomass, the conditions of the experiment and the products formed, so that there is a unique value for each experiment. We will give here a method of calculating the heat of pyrolysis for known heating rates and products which, while approximate, underlines the factors that must be taken into account.

We define the "heat of pyrolysis" of biomass, Δh_p , as that heat required to effect the phase change from biomass to char-liquid-gas at

the temperature where pyrolysis occurs. (We define the "heat of pyrolysis as the heat required for the phase change plus the heat required to reach this temperature - see below.) A thermodynamic calculation of Δh_p can be made for cellulose based on the idealized reactions shown in Table 1. The idealized charring reaction for cellulose can be written as Rx I:



(Here we use the notation $1/n (\text{C}_6\text{H}_{10}\text{O}_5)_n$ for cellulose to emphasize its polymeric nature. The values above are calculated from the heats of combustion or formation of the products and reactants.) The second reaction represents the depolymerization of cellulose to levoglucosan, with simultaneous vaporization. (Levoglucosan is the principal decomposition product of cellulose.)

These two reactions can be combined in the appropriate ratio to give a value for the heat of pyrolysis depending on the relative amount of carbon formed, eg

$$\begin{array}{l} \Delta H_p = 59.96 - 475.1 F_c \text{ kJ/mole} \quad 3) \\ \text{or} \quad \Delta h_p = 370 - 6603 F_c \text{ J/g} \quad 4) \end{array}$$

where F_c is the weight fraction of carbon produced in the charring reaction. These values of the heat of pyrolysis should be considered as idealized because pyrolysis of cellulose gives charcoal (not exactly carbon) and other products beside levoglucosan. Nevertheless they illustrate the necessity for knowing the products in measuring the heat of pyrolysis.

Antal recently used a high pressure scanning calorimeter to measure the Δh_p of cellulose (2). He varied the amount of char formed by changing the pressure of the experiment. He found an approximately linear change in the Δh_p of cellulose from -170 kJ/g with a char production of 23% (typical of slow pyrolysis) to +270 kJ/g with a char production of 9% (typical of fast pyrolysis)(5).

These values can be used in a linear equation to predict the heat of pyrolysis on the basis of char content F_c , ie

$$\Delta h_p = 553 - 3142 F_c \text{ kJ/g} \quad 5)$$

where F_c is the fraction of charcoal produced. Note that the values for the coefficients resulting from the experimental values are similar in magnitude to those predicted from thermodynamic calculation in Reaction 4). The heats of pyrolysis calculated from the predicted char production and pyrolysis temperatures are listed in Table 3.

A quantity of more interest to the engineer is the heat for pyrolysis. We define the "heat for pyrolysis", h_p as the sensible heat required to raise a biomass particle to pyrolysis temperature, ($= c T_p$, where c is the heat capacity of the biomass) plus the heat required to pyrolyse it, Δh_p . (If the products of pyrolysis are then heated above this temperature, this heat must also be included.) Table 3 also shows values of h_p for pyrolysis of cellulose calculated from 2) and the heat capacity of cellulose, 1.31 J/g-°C (0.32 Btu/lb-F). Note that the variation of h_p with heating rate is small compared with the variation of Δh_p .

Table 3 - Heat of Pyrolysis and Heat For Pyrolysis of cellulose Calculated from char production

PYROLYSIS CONDITIONS Heat Rate R-°C/min	Pyr Temp °C	Char-coal-%	Δh_p J/g	h_p J/g
0.01	275	23.9	-198	162
0.1	302	12.4	163	559
1	330	6.9	336	769
10	357	4.2	421	889
100	391	2.6	471	984
1000	425	1.2	515	1072
10000	463	0.005	553	1159
100000	507	0.003	553	1217

Notes: Char yield calculated from Diebold Model. Δh_p calculated from $\Delta h_p = 553 - 3142F_c$; h_p calculated from $h_p = \Delta h_p = c(T_p - T_o)$ with $c = 1.3 \text{ J/g-}^\circ\text{C}$ for cellulose

HEAT FLUX REQUIRED FOR SLOW AND FAST PYROLYSIS
A. Small Particles & Slow Heating

The average heat flux required to pyrolyse a particle is given by

$$\dot{q} = \Delta h_p \rho V / t_p A \quad 6)$$

where \dot{q} is the rate of heat supply per unit area, ρ is the density, V is the volume and A is the heated surface area of the particle. If the particle is a cube, this simplifies to

$$\dot{q} = h_p \rho L / 6 t_p \quad 7)$$

where L is the length of the cube edge.

The data in Table 2 and 3 can be combined with this equation to predict the magnitude of heat flux required for slow and fast pyrolysis. Table 4 shows the heat flux required to pyrolyse a 1 cm cube of cellulose (or biomass). The values shown are calculated for heating the particle just to pyrolysis temperature. They assume that the particle is approximately isothermal and pyrolysis occurs everywhere at once.

The above calculation assumes that there is no resistance to heat transfer, and the particle will be essentially isothermal. However most forms of wood and biomass are relatively poor conductors of heat and at higher heating rates the results shown above will not be valid. The validity of these assumptions is tested by the Biot number, given by

$$N_b = \text{Heat flux to surface/Heat flux to interior} \\ N_b = H L / K \quad 8)$$

(where H is the heat transfer coefficient, characteristic of whatever method of heating is used; L is a characteristic length of the particle, typically the cube root of the volume; and K is the thermal conductivity.)

Unfortunately the heat transfer coefficient H is generally applied to convection or radiation heating with small temperature differences, where heat transfer is a strong function of ΔT . However for high temperature radiation and contact pyrolysis sources, the

change in ΔT is relatively small and the Biot number is approximated by

$$N_B = \frac{\dot{q}L}{K\Delta T} \quad 9)$$

The maximum heat transfer coefficients for the various heating mechanisms are also shown in Table 6.

Table 4 - Heat flux requirements and Biot number for heating of a 1 cm cube

PYROLYSIS CONDITIONS					
R	T _p	h _p		\dot{q}	N _B
Heat Rate	Pyr Temp			to 1 cm ³	Biot No.
R-°C/min	°C	J/g		W/cm ²	
0.01	275	162	:	8.20E-06	7.1E-06
0.1	302	559	:	2.57E-04	2.2E-04
1	330	769	:	3.23E-03	2.8E-03
10	357	889	:	0.035	0.030
100	391	984	:	0.35	0.304
1000	425	1072	:	3.50	3.0
10000	463	1159	:	34.78	30.2
100000	507	1217	:	333.41	289.9

Note: Heat flux calculated from $\dot{q} = h_p \rho L/6 t_p$
 Biot number calculated from $N_B = h_p \rho L^2/6 t_p K \Delta T$
 $K = 0.0023 \text{ J/s-cm-}^\circ\text{C}$

For Biot numbers less than 1, the particle will be nearly isothermal and will dry, then pyrolyse in sequence. For Biot numbers larger than 1, the resistance to heat transfer within the particle becomes large compared to that of the heat source and steep gradients exist in the particle. In this case the pyrolysis wave travels from the outside of the particle to the inside, producing simultaneous drying and pyrolysis.

The Biot number for a 1 cm cube is also shown in Table 4, calculated for the particle heating rates shown and assuming an average temperature difference of 500 K in. Here it can be seen that the assumption of an isothermal particle is valid for slow heating rates and small particles. However for a heating rate larger than 100 °C/min and a heating rate of 0.35 W/cm² there will be steep gradients in the particle, so that the heat flux will be altered and the drying and pyrolysis will occur simultaneously.

B. Large Particles & Rapid Heating

For high heat flux and larger particles, when the Biot number exceeds 1, it is necessary to calculate the non-steady state heat transfer for the particular particle geometry and surface temperature. While this can be quite complex for most cases, it is relatively simple for the one dimensional steady state case experiment described by Lede in contact pyrolysis (8). In this case a heated disk supplies sufficient heat to a beech dowel to pyrolyse and vaporize it at a rate V. The steady state temperature distribution in the rod is given by

$$T(x) = T_0 + (q/\rho cV)\exp(-Vx/\alpha) = (T_d - T_0)\exp(-Vx/\alpha) + T_0 \quad 10)$$

where T(x) is the temperature at a distance x from the heat source of strength q, T_p is the temperature at the pyrolysing interface and T₀ is the initial temperature of the rod. The density of the wood is ρ , c

is the heat capacity, α the thermal diffusivity and V the rate of pyrolysis. (Here we have taken the following values used by Lede for consistency; heat capacity, $c = 2.80 \text{ J/g-}^\circ\text{C}$; density = $\rho = 0.70 \text{ g/cm}^3$; thermal conductivity $\kappa = 0.0023 \text{ J/s-cm-}^\circ\text{C}$; thermal diffusivity = $\alpha = 0.0012 \text{ cm}^2/\text{s}$

Table 5 - Steady State Fusion-Pyrolysis of Birch Rod

HEAT FLUX	\dot{q}	10.00	100	1000	W/cm ²
Velocity (b)	V	0.01	0.11	1.14	cm/s
Penetration (c)	$X(1/e)$	0.10	0.01	0.001	cm
Heat stored	Q	89.76	8.98	0.90	J/cm ²
Induction Time (e)	t_i	9.0	0.09	0.0009	s

Notes and assumptions: (a) $T_p = 466 \text{ }^\circ\text{C}$, $T_o = 20 \text{ }^\circ\text{C}$

(b) The pyrolysis velocity, V was calculated from $V = q/(\rho c)(T_p - T_o)$

(c) The heat penetration $X(1/e)$ was taken to be the distance at which the temperature had fallen to $1/e$ of T_p , $VX/\alpha = 1$, $X = \alpha/V$.

(d) The heat stored in the rod, Q , was calculated as the integral of the sensible heat between $x=0$ and $x=\infty$, $= \alpha c \rho (T_p - T_o)/V$

(e) The induction time t_i is the time required to establish the steady state temperature gradient, $t_i = Q/\dot{q}$. This assumes the heat transfer intensity is constant before steady state is reached.

(f) Temperature Distribution $T = T_p \exp(-Vx/\alpha) + T_o$.

Note in Table 5 that the velocity and heat penetration increase linearly with heat flux. However, the induction time required to reach steady state varies inversely as the square of heat flux. At low flux, considerable char may build at the interface so that the steady state condition may never be reached.

HEAT TRANSFER MECHANISMS FOR FAST PYROLYSIS

The magnitudes of heating rates which can be obtained from various methods of heat transfer are shown in Table 6 (Reed, 1981 Cu Mtn.). Comparing the fluxes shown in Table 4 to the values in Table 5, it can be seen that the high heating rates required for fast pyrolysis of small particles can be achieved with convection, radiation or conduction.

Convection is the least satisfactory heat transfer mechanism for fast pyrolysis because the water and pyrolysis vapors produced during pyrolysis interfere with heat transfer. Also convection from gas sources with temperatures above $600 \text{ }^\circ\text{C}$ is unsuitable for oil production because they crack the pyrolysis oils which are only stable to about $600 \text{ }^\circ\text{C}$. Low temperature radiation sources (below $1000 \text{ }^\circ\text{C}$ are also unsatisfactory for fast pyrolysis of larger particles.

The production of pyrolysis oil is favored by radiation from a high temperature source or by "contact pyrolysis" (see below). In the case of radiation, the solid is heated rapidly, but the vapors are largely transparent and transient and so are not overheated (12). Unfortunately black body sources with temperatures above $2000 \text{ }^\circ\text{C}$ are expensive and difficult to use.

CONTACT PYROLYSIS

A new method of heat transfer, "contact pyrolysis", has been developed in the 1980's and appears to be especially suited for the production of pyrolysis oil vapor.

Table 6 - Heat Transfer Rates and Heat Transfer Coefficients from Various Devices

	Typical Temp diff ΔT K	Maximum Ht Transf \dot{q} W/cm ²	Maximum Ht tr coef H W/cm ² -K
CONVECTION			
Gas Free Convection	500	10	0.02
Gas forced convection	500	300	0.6
Air-Gas Flame	1500	200	0.13
Oxy-Acetylene flame	3000	3000	1.00
CONVECTION, ELECTRONIC			
Electric arc	10,000	20,000	2
RADIATION			
	Surface T °K		
Black Body	773	20	0.026
	1,273	150	0.12
	2,273	1,500	0.66
	5,273	44,000	8.3
Focused CO2 laser		100,000	NA
CONTACT PYROLYSIS	873	3,000	3.2

In 1980 Diebold showed that a moving hot wire would cut through a piece of wood at rates of several cm/sec with apparently no production of charcoal (7). Ledè et al have since shown that a wood dowel can be consumed at rates up to 3 cm/sec corresponding to heat transfer rates of 3000 J/cm² by pressing it against a heated disk (8). Furthermore the heat transfer rate is directly proportional to pressure, and a pressure of 30 atmospheres was used to attain the above heat transfer rate. The heat transfer is also proportional to the difference between the disk temperature and 466 °C. This was interpreted to show that the wood had a "fusion behavior" above 466°C (8,13). Reed has now developed a "heat flux concentrator" (see below) using a copper block to produce vapors for catalytic conversion to fuel (9).

Contact pyrolysis has several interesting and non-obvious features:

- o The thermal conductivity of metals is typically 3-4 orders of magnitude higher than that of hot gases or biomass, and so the heat transfer produced by direct contact is proportionally high.
- o The use of pressure at the heated interface retards the vaporization of the pyrolysis products so that they do not interfere with heat transfer, and instead the biomass pyrolyses to an oil or foam
- o When the resulting oil or foam is squeezed out of the interface region, it is immediately in a low pressure region and can vaporize very rapidly
- o The rubbing contact removes char or ash which would otherwise interfere with heat transfer

A HEAT FLUX CONCENTRATOR FOR CONTACT PYROLYSIS PRODUCTION OF PYROLYSIS OIL VAPOR

In order to produce vapors for catalytic conversion to hydrocarbon fuels, we have developed a "heat flux concentrator" shown

in Fig. 5 and 6. In operation, a wood dowel is rotated in a drill press and forced into a 1.2 cm diameter tapered hole in the heated copper block shown in Fig. 5. The rod is fed at a rate of 0.2 - 0.25 cm/sec. The vapors escape through 12 holes through the bottom of the block and are then captured in traps and in a gas burette. Alternatively, the vapors travel without cooling to a catalyst test furnace as shown in Fig. 6 where the products are captured (9).

The heat flux concentrator has been operated to produce pyrolysis vapor as an end product, or to test the operation of various catalysts. A preliminary mass balance on pyrolysis oil production is shown in Table 7 for pyrolysis runs. We observe that the walls of the pyrolyser and the exit holes become coated with a hard, shiny form of carbon like petroleum coke. We now believe that there is a high resistance to vaporization which causes plugging of the pyrolyser after the feeding of about 5 g. We are currently modifying the design to improve vaporization. A few catalyst runs have also been made and they will be described in more detail later.

=====

Table 7 - Preliminary Mass Balance on Contact Pyrolysis Experiments

Pyrolysis Run	T _p °C	Wood Consumed	g liq/ g wood	g gas/ g wood	g coke/ g wood	Mass out/ Mass in
5p	550	2.56	0.61	0.10	0.27	0.98
8p	600	5.59	0.57	0.10	0.33	1.00
9p	500	6.10	0.52	0.12	0.25	0.89
11p	700	4.21	0.57	0.13	0.14	0.85

=====

Acknowledgements

The authors would like to thank the Solar Energy Research Institute for support of this work under Contract HK-6-06059-1 and the Midwest Research Institute for thier support. The authors would especially like to thank their colleagues at SERI and elsewhere whose work has supplied the base on which this paper has been written.

REFERENCES

1. Stern, A. J. and Harris, E. E., "Chemical Processing of Wood", Chemical Publishing Co., New York, 1953
2. Antal, M. J., Jr., "Biomass Pyrolysis: A Review of the Literature, Part I-Carbohydrate Pyrolysis", in *Advances in Solar Energy*, ed K. W. Boer and J. A. Duffie, American Solar Energy Society, Boulder, CO, Vol 1, pp 61-112.
3. Antal, M. J., Jr., "Biomass Pyrolysis: A Review of the Literature, Part II-Lignocellulose Pyrolysis, in *Advances in Solar Energy*, ed K. W. Boer and J. A. Duffie, American Solar Energy and Plenum Press, New York, Vol 2, pp 175-255.
4. Bradbury, A. G., Sakai, Yoshio and Shafizadeh, F., "A Kinetic Model for Pyrolysis of Cellulose", *J. Appl. Polymer Science*, 23 3271 (1979)
5. Diebold, J. P., "The Cracking Kinetics of Depolymerized Biomass Vapors in a Continuous Tubular Reactor", Thesis T-3007, Colorado School of Mines, Golden, CO 1985.
6. Diebold, J. P., Scahill, "Ablative, Entrained Flow Fast Pyrolysis of Biomass", in *Proceedings of the 16th Biomass Thermochemical Contractors' Meeting*, Portland, OR May 8-9, 1984, PNL-SA-12403, 1984. See also, Diebold, J. P. "A unified Global Model for the Pyrolysis of Cellulose", (in preparation).
7. Diebold, J. P., "Ablative Pyrolysis of Macroparticles of Biomass," *Proceedings of the Specialists Workshop on the Fast Pyrolysis of Biomass*, Copper Mountain, CO., Oct. 12 1980, Solar Energy Research Institute, Golden, CO. 80401, SERI/CP-622-1096.
8. Lede, J., Panagopoulos, J., Li, H. Z. and Villiermaux, J., "Fast Pyrolysis of Wood: Direct Measurement and Study of Ablation Rate", *Fuel* 64, 1514 (1985)
9. Reed, T. B., Diebold, J. P., Chum, H. L., Evans, R. J. Milne, T. A. and Scahill, J. W., "Overview of Biomass Fast Pyrolysis and Catalytic Upgrading to Liquid Fuels," in *Proceedings of the American Solar Energy Society*, K. W. Boer, Ed., Boulder, CO June 11, 1986.
10. Roberts, A. F., "The Heat of Reaction During the Pyrolysis of Wood", *Combustion and Flame* 17, 79 (1971).
11. Reed, T. B., Diebold, J. P. and Desrosiers, R., "Perspectives in Heat Transfer for Pyrolysis", *Proceedings of the Specialists Workshop on the Fast Pyrolysis of Biomass*, Copper Mountain, CO., Oct. 12 1980, Solar Energy Research Institute, Golden, CO. 80401, SERI/CP-622-1096.
12. Chan, W. -C. R., Kelbon, M. and Krieger, B. B., "Product Formation in the Pyrolysis of Large Wood Particles", *Fundamentals of Thermochemical Biomass Conversion*, ed. R. P. Overend et al, Elsevier, New York, 1985.

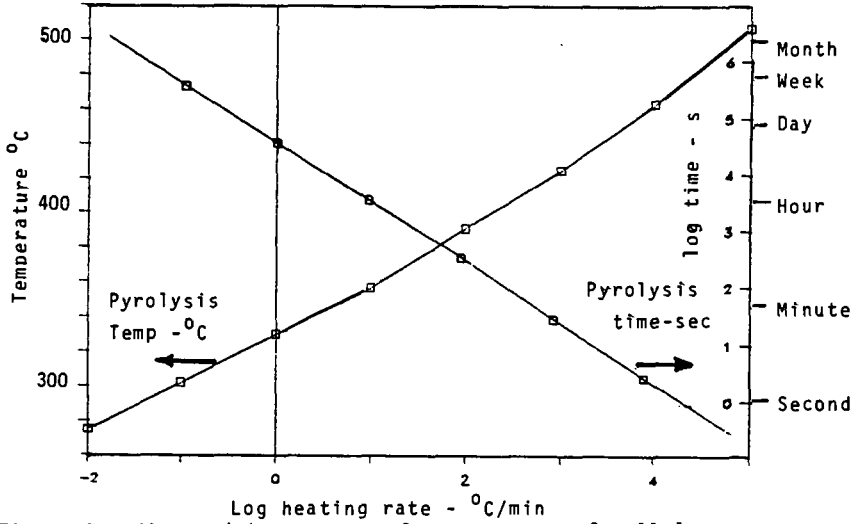


Figure 1 - Time and temperature for pyrolysis of cellulose as predicted by Diebold Kinetic Model

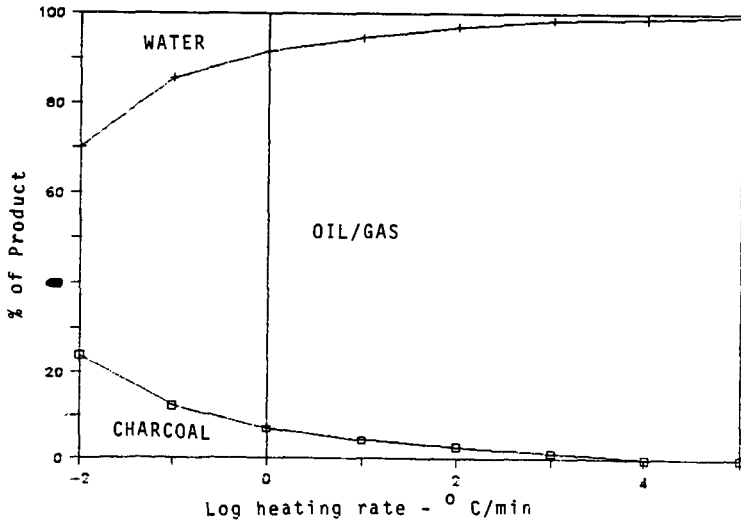


Figure 2 - Products of cellulose pyrolysis as predicted by Diebold Kinetic Model

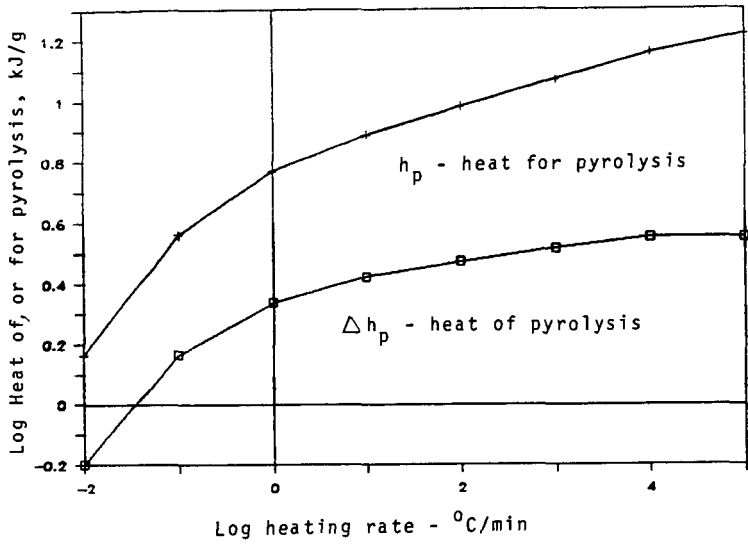


Figure 3 - Heat of pyrolysis and heat for pyrolysis as predicted from char yields and pyrolysis temperature

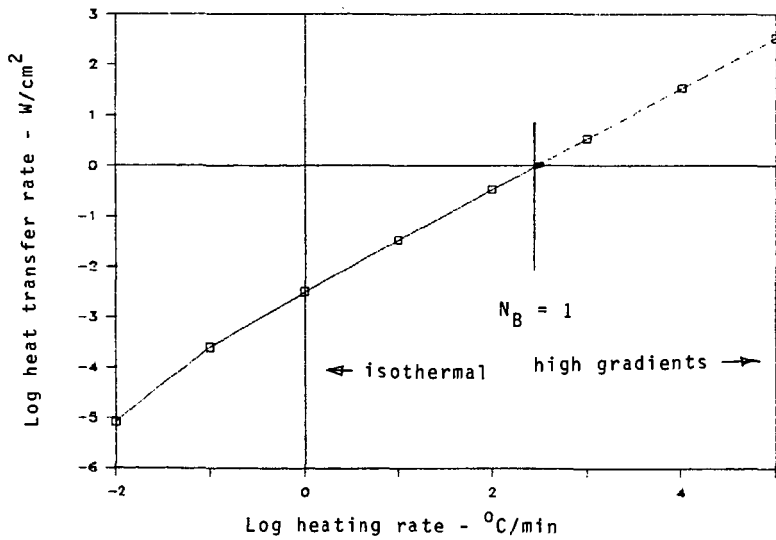


Figure 4 - Heat transfer rate required to support heating rate

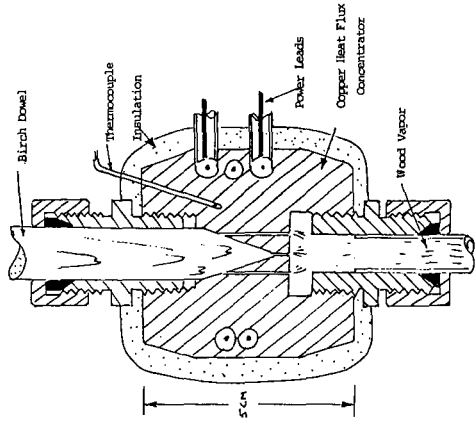


Figure 5 - Contact pyrolysis furnace for producing wood vapor.

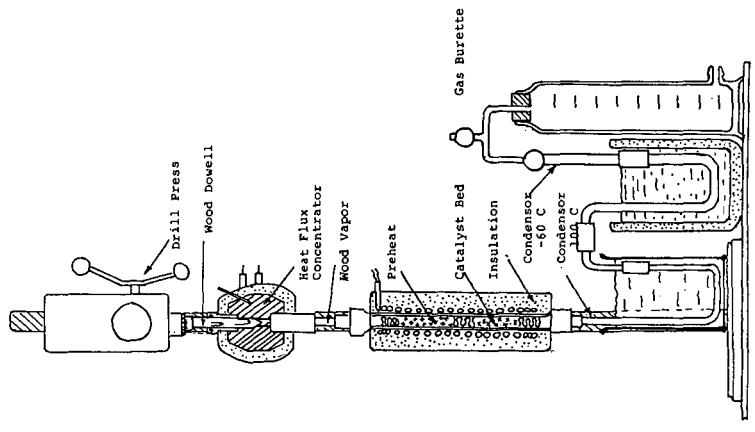


Figure 6 - Microanalytic test apparatus for catalyst testing

PRODUCTION AND CHARACTERIZATION OF PYROLYSIS
LIQUIDS FROM MUNICIPAL SOLID WASTE

James E. Helt and Ravindra K. Agrawal

Argonne National Laboratory
9700 S. Cass Ave.
Argonne, IL 60439

INTRODUCTION

Municipal solid waste (MSW) is a highly variable "raw material," by both season and location. However, it is generally accepted to have a composition within the ranges shown in Table 1 (1). Cellulosic materials, including paper, newsprint, packaging materials, wood wastes, and yard clippings, constitute over 50% of MSW.

A basic understanding of the pyrolytic reactions is important and relevant to both combustion and conversion of MSW. As MSW is heated the different components react differently at different temperatures. The volatile species can evaporate without major change, and the rest of the cellulosic components partially break down to volatile components leaving a carbonaceous char that contains the ash and noncombustibles. The volatile pyrolysis products consist of a gaseous fraction containing CO, CO₂, some hydrocarbons, and H₂, which are noncondensables. There is a condensable fraction containing H₂O, volatile hydrocarbons and low molecular weight degradation products such as aldehydes, acids, ketones, and alcohols. Finally, there is a tar fraction containing higher molecular weight sugar residues, furan derivatives, and phenolic compounds. The proportion and composition of these products are highly dependent on the cellulosic composition of the MSW, the pyrolysis temperature and the presence of inorganic compounds that could influence (catalyze) the pyrolysis reactions.

Pyrolysis of cellulose at temperatures below 300°C results mainly in char formation. Any lignin present in the MSW (Kraft paper, cardboard, and wood waste contain significant proportions) has a higher tendency for charring, whereas the cellulose and hemicelluloses readily decompose to volatile products at temperatures above 300°C. Most of the plastics present thermally degrade at a significantly higher temperature (400-450°C) (2).

BASIC MECHANISMS RESEARCH

The ANL/DOE program on pyrolysis of municipal solid waste (MSW) has two overall objectives: (1) to understand the basic thermokinetic mechanisms associated with the pyrolytic conversion of MSW and (2) to seek new processing schemes or methods of producing a liquid or gaseous fuel from MSW feedstock. To meet these objectives, we are performing laboratory experiments with the aim of determining the effects of different operating parameters on the pyrolysis-product compositions and deriving an analytical model of the pyrolytic process that describes the chemical kinetics.

This DOE-sponsored research has both ANL activities and subcontracted work. Argonne is performing closely controlled laboratory-scale parametric tests. The work is being performed on two experimental facilities: (1) a TGA to study the thermal degradation versus temperature, and (2) a bench-scale reactor to produce significant quantities of products to permit characterization. The goal is to determine how different operating parameters influence the product compositions.

Subcontracted activities are being performed at the Solar Energy Research Institute (SERI) and the Chemical Engineering Department at the University of Arizona. SERI has used their direct high-pressure molecular beam mass spectrometric sampling system to collect qualitative "fingerprints" and experimental data on the pyrolysis products generated from components of MSW and various refuse derived fuel (RDF) samples (3). They are also using the same experimental apparatus to distinguish between the primary and secondary reactions leading to the formation of the pyrolysis products (4). This data will be part of an overall data base to describe the influence of sample properties and reaction conditions on the solid phase and gas phase processes of low-temperature (<500°C) MSW pyrolysis to oils. Additionally, SERI has recently started a new task on the development of a rapid method of characterizing the liquid products from pyrolysis based on mass spectrometric data. This new task is composed of three parts: 1) compound class analysis by advanced pattern recognition techniques, 2) liquid product analysis via compound class analysis, and 3) correlation of chemical composition to fuel properties.

The University of Arizona has completed a small research effort on the fundamentals of direct liquefaction of MSW (5). They modified an existing autoclave and a real-time digital microprocessor control system so that it could be operated in a semi-continuous mode. Various components of MSW were studied in order to obtain meaningful data, not confused by the different thermokinetics of more than one distinct MSW component. Feedstocks included wood flour, cardboard, newsprint and rice (starch), as well as the important model compounds alpha cellulose and lignin. It was found that these MSW components could be converted to liquid oils and a high-heating value residual solid at temperatures of 325°C to 400°C and pressures of 1000 psi to 3000 psi.

A task which is related to the basic mechanisms work is also being performed by ANL (2). This task explores the possibility of using catalytic hydrotreating to upgrade the liquid products produced during conventional pyrolysis of MSW. The liquid products obtained from MSW pyrolysis processes are generally unsuitable for use as liquid fuels. Heating values are low and the liquids are very corrosive, viscous and unstable during storage. A major reason for these problems is the extremely high oxygen content of the pyrolysis products. The kinetics of catalytic reactions that remove oxygen-containing compounds from the pyrolysis liquids is being experimentally determined in a high-pressure, fixed-bed microreactor of the trickle-bed type. The reactions of interest involve the reduction of the oxygen-containing hydrocarbon with high pressure hydrogen using a solid catalyst. The catalysts which have been used are primarily commercially available hydrodesulfurization (HDS) catalysts containing molybdenum oxide with either cobalt or nickel oxide, supported on high surface area alumina matrix.

ANL BENCH-SCALE STUDIES

The emphasis of this paper will be on the bench-scale studies being performed at ANL and on the associated activities in characterizing the liquids produced in the pyrolysis reactions.

The reactor is a fixed bed contained inside a quartz tube (70-mm ID) and placed between two glass frits. The outside of the tube is enclosed in a furnace. The reactor tube can be purged from top to bottom with the desired gas(es). The reactor is operated in the nonisothermal mode with heatup rates as high as 30°C/min. Temperatures are recorded on a multipoint recorder to allow indication of existing temperatures and temperature gradients. There is a rotameter on the inlet gas line and a dry gas meter on the outlet. Cold traps are in the gas outlet downstream of the condenser unit. These traps are filled with ice or dry ice. Downstream of the traps, the gases that do not condense are collected in plastic sampling bags for analysis by gas chromatography (GC).

Experimental results on the thermal decomposition of typical MSW components (Whatman #1, newsprint, kraft paper, cardboard, aspen, and pine) over a temperature range of 275-475°C have been gathered. The details of these experimental runs may be found elsewhere (6). Also, information on the TGA runs used in support of this bench-scale work is available elsewhere (7,8).

CHARACTERIZATION OF LIQUIDS

Various liquid samples produced in the bench-scale apparatus have been analyzed with GC and GC/MS. The chromatograms were qualitatively compared to each other by both measurement of peak retention times and by observation of the patterns present. As a result, six different groups were identified:

- Group A - Most components elute early in the chromatogram as many sharp peaks within a small retention window.
- Group B - Bulk of components elute across a 6- to 20-min retention window and are a mix of both sharp and broad peaks.
- Group C - Many peaks are observed; the bulk of components elute across a 4- to 30-min retention window.
- Group D - Similar to C, but most components elute across a 4- to 20-min retention window.
- Group E - A few early peaks are observed, especially in the 5- to 7-min retention window.
- Group F - Similar to D, but many peaks are observed in the 9- to 11-min retention window.

The mass spectrum obtained from a typical tar sample is shown in Fig. 1. This tar sample was produced from a newsprint feedstock pyrolyzed in an inert atmosphere of helium. A computer search was performed using the 31,000 component NIH/EPA library in addition to a library of compounds from Battelle Pacific Northwest Laboratory (9). The results of the computer search and from interpretation of various standard spectra yielded tentative identification of numerous compounds. It is apparent that many compounds of homologous series are present. Recognition of just one of the compounds in a series leads to identification of all since they will most likely differ only by 14 amu (a CH₂ group) or by 31 amu (a CH₃O group). In some cases the same identification is made for more than one compound. Actually, different isomers of the compound are probably being found. The percent found was estimated by dividing the response of the most abundant ion for a compound by the total of the responses of the most abundant ions for all compounds.

In general, the classes of compounds included furfurals (9.4%), phenols (2.5%), methoxyphenols (16.9%), cyclic compounds such as methyl cyclopentanones (10.8%), methoxy benzenes (3.8%), and the substituted propane tentatively identified for the peak at scan number 1207 (36.8%). Although the compound eluting at scan 1207 is by far in the highest concentration, insufficient information is available from its spectrum to allow a reasonable identification. The base peak observed is 75amu, and a 115 amu ion is also present at 40% abundance.

With the computerized mass spectral matching capability, a substituted propane with a molecular weight of 192 g/mol (propane, 1,3-dimethoxy-2,2-bis(methoxymethyl)) was selected as the most probable compound. The sample was submitted for gas chromatograph/matrix isolation/Fourier transform infrared (GC/MI/FTIR) analysis to add to the information necessary for better identification.

A GC/MI/FTIR run provided useful information on the bulk of the material present in the sample at scan number 1207. Data from the GC/MI/FTIR analysis indicated that the computerized mass spectral identification of the component eluting at scan number 1207 is not far off. The compound does not contain phenyl groups, and computerized IR searches came up with compounds with an ethanol/ethane or propanol/propane backbone substituted with methoxy or ethoxy groups. In particular, three close matches are dimethyl acetaldehyde, $(\text{CH}_3\text{O})_2\text{-CH-CHO}$; 1-methoxy-2-propanol, $\text{CH}_3\text{O-CH}_2\text{-CH(OH)-CH}_3$; and 1,3-diethoxy-2-propanol, $\text{CH}_3\text{CH}_2\text{O-CH}_2\text{-CH(OH)-CH}_2\text{-OCH}_2\text{CH}_3$. The presence of methoxy or ethoxy groups is consistent with the tentative identification given for the compound.

Another compound present in a relatively large concentration but which cannot be identified is that eluting at scan number 1343. This compound has an apparent molecular weight of 110 amu, with ions at 71, 89, and 110 amu. It appears to be neither a methyl furfuryl, benzenediol, nor dimethyl cyclopentanone. The 71-amu ion probably results from a $\text{CH}_3\text{-CH}_2\text{-C=O}$ group, which can come from a tetrahydrofurfuryl structure or from a butyl ester. The compound's real molecular weight may be above 110 amu.

YIELDS AND ANALYTICAL RESULTS

With the Whatman No. 1 filter paper, the yields at 475°C of water vapor and gases were in the ranges 5-13 wt % and 26-34 wt %, respectively, of the original cellulose. The hydrogen balance suggests the higher water content (13%), whereas both the carbon and oxygen contents suggest a lower water yield (5 wt %).

Efforts have been made to analyze the gases collected in the sample bags. A Hewlett-Packard Gas Chromatograph is being used to identify major gas components. The preliminary GC analyses show that, for the Whatman No. 1 paper at 475°C, the gases produced are 56.6 vol% CO_2 and 43.4 vol% CO . No other gases were detected in significant quantities. The yield of CO_2 is, therefore, in the range of 18-23 wt % of the original cellulose and the yield of CO is 8-11 wt %. Roughly 25% of the energy in the feedstock is released in the gaseous products. These pyrolysis gases can be considered a low-Btu fuel.

The Whatman No. 1 paper (as received) contained 4.1 vol % moisture and 0.074 wt % ash. All results reported here are on a moisture-ash-free basis unless otherwise specified. Table 3 summarizes some analytical results of cellulose and condensed-phase cellulose pyrolysis products. A comparison of the results in Table 2 for cellulose and cellulose tars indicates that the elemental composition of these two materials is very similar. (The heating value of cellulose tars reported here may be low due to the loss of lower-molecular-weight products during the drying step.) Tars seem to have a slightly higher heating value than that of cellulose. These results strongly suggest that the nature of cellulose tars is similar to that of its parent cellulose.

As can be seen from Table 2, the cellulose chars are very different from the parent cellulose. When compared with the original cellulose, the cellulose chars have a carbon content that is roughly double, and H_2 and O_2 contents that are about one-half and one-third respectively. The richness in carbon content of the chars is indicated by their high heating value (7566 cal/g). Unfortunately, the low H_2 content of the chars make them an unlikely candidate for use as transportation fuels. Because of the high carbon content and low H_2 and O_2 content, the cellulosic chars are comparable to a low-volatile bituminous coal or a low-grade anthracite coal. However, since the chars contain no sulfur or nitrogen compounds that could form potential air pollutants upon combustion, they do have potential as a solid fuel. Tables 3 and 4 give the analytical results for newsprint and Kraft paper feedstock.

The atomic ratios (H/C and O/C) and the heating value of cellulosic chars indicate that they are very similar to coal. The H/C ratio of cellulose tars (1.73) is comparable to that of No. 2 fuel oil (1.84). Unfortunately, the high oxygen content indicated by the O/C ratio (0.91 compared to 0.01 for fuel oil) significantly reduces the heating value of the tars.

DISCUSSION

It should be noted that the tar analysis results of this study are very similar to those obtained from vacuum pyrolysis of small cellulose samples conducted by Agrawal et al (10). Also the tar yields are comparable to those obtained by Shafizadeh (11) using small samples of Whatman No. 1 paper under vacuum conditions. These findings support the assumption that negligible tar decomposition takes place in the reaction bed.

Efforts are also in progress to ascertain some of the possible heat and mass transfer limitations of the pyrolysis process. Fig. 2 depicts the residue and tar yields of 5-g and 15-g cellulose samples at a heating rate of 5°C/min. Increased sample weight shifts the weight-loss curve to a higher temperature by about 10°C. Fig. 2 also shows that increased sample weight decreases the tar yields. Efforts to explain this effect of sample weight on product yield are in progress.

Figures 3 and 4 summarize the data for the influence of heating rate on product yields from Whatman No. 1 paper. It is seen from Figs. 3 and 4 that increasing the heating rate or sample weight has a similar effect in shifting the weight-loss curve to a higher peak temperature. However, the shift in the weight-loss curve along the peak-temperature axis in the case of increased sample weight is due to mass transfer limitations, whereas, in the case of increased heating rate, this shift is due to combined effects of kinetics and heat transfer resulting in delayed decomposition. At a peak temperature of about 370°C, the product yields are essentially independent of the heating rates (Fig. 4).

The results in Table 6 illustrate the influence of sample weight and heating rate on product yields. The data show that increasing sample size reduces the tar yields and increases the char yields. The drastic decrease in tar yields is primarily due to increased vapor residence time in the reaction bed. If the vapor residence time is reduced in the reaction bed by using a fluidized bed or an entrained flow reactor, then secondary decomposition can be significantly reduced, and the effects of sample weight will not be as drastic. Thus, data collected in the loosely packed fixed-bed reactor of the present study may represent an extreme for an operating industrial reactor.

Increasing the heating rate appears to decrease the char yields but has little influence on tar yields. This implies that gas yields increase at the expense of char yields.

Table 7 summarizes elemental analyses of chars formed under various pyrolysis conditions. The elemental analyses of cellulosic chars suggest that the composition of chars is not strongly influenced by either the heating rate or sample weight.

Results to date strongly imply that, depending on the residence time, the tar yields for final pyrolysis temperatures above 300°C will be independent of heating rates. This observation is strengthened by the finding from TGA data analysis (7,8) that the apparent activation energy for cellulose decomposition is similar to that for tar formation.

Olefins and other hydrocarbon gases were not detected in the pyrolysis gases. This is not surprising since these fuels are not products of primary cellulose pyrolysis (12,13). The significant yields of olefins and hydrocarbon gases from flash pyrolysis studies are most likely a result of secondary tar decomposition. Cellulose tars start to decompose at about 550°C, and most of these studies were carried out over the temperature range of about 600-800°C. These observations suggest that results from flash pyrolysis studies are dominated by secondary tar decomposition reactions.

ACKNOWLEDGMENTS

This work was supported by the U. S. Department of Energy, Division of Biofuels and Municipal Waste Technology, under Contract W-31-109-Eng-38. The authors wish to acknowledge the support and guidance of J. Lazar, EMW Program Manager at ANL, and K. M. Myles, Section Head in the Chemical Technology Division at ANL.

REFERENCES

1. J. L. Kuester, Thermal Systems for Conversion of Municipal Solid Waste, Volume 5, Pyrolytic Conversion: A Technology Status Report, Argonne National Laboratory, ANL/CNSV-TM-120 (June 1983).
2. J. E. Helt et al., Pyrolysis of Municipal Solid Waste, Argonne National Laboratory, ANL/CNSV-45 (Dec. 1984).
3. R. J. Evans et al., Atlas of the Primary Pyrolysis Products of Municipal Solid Waste and Selected Constituents, Solar Energy Research Institute, SERI/SP-234-2597 (Oct. 1984).
4. R. J. Evans and T. A. Milne, Mechanisms of Pyrolysis of Municipal Solid Waste--Annual Report, Solar Energy Research Institute, SERI/PR-234-2852 (Nov. 1985).
5. D. H. White et al., Fundamentals of Direct Liquefaction of Municipal Solid Waste in a Semi-Continuous, Microprocessor-Controlled Autoclave, Argonne National Laboratory, ANL/CNSV-TM-180 (Sept. 1986).
6. J. E. Helt et al., Pyrolysis of Municipal Solid Waste: Annual Report July 1984-June 1985, Argonne National Laboratory, ANL/CNSV-54 (July 1986).
7. J. E. Helt and R. K. Agrawal, Pyrolysis of Municipal Solid Waste Components, AIChE Mtg., Chicago, IL (Nov. 1985).
8. R. K. Agrawal and J. E. Helt, Applications of Thermogravimetry in Energy from Solid Waste Research, 15th Annual North American Thermal Analysis Society Conference, Cincinnati, OH (Sept. 1986).

9. Personal communication Doug Elliot, Pacific Northwest Laboratory, Richland, WA.
10. R. K. Agrawal et al., J. Anal. Appl. Pyrol. 6, 325 (1984).
11. F. Shafizadeh et al., AIChE Symp. Ser. 75, 24 (1979).
12. M. J. Antal, Jr., Adv. Solar Ener. 2, 61 (1983).
13. F. Shafizadeh, J. Anal. Appl. Pyrol. 3, 283 (1982).

Table 1. Composition Ranges for Several MSW Samples^a

Component	Composition Range, wt %
Paper	30-50
Glass	8-10
Metals	7-10
Plastics	1-5
Rubber-Leather	1-3
Wood	1-4
Textiles	1-5
Food Wastes	10-20
Yard Wastes	5-20
Other	1-4

^aReference 1.

Table 2. Analytical Results of Feedstock, Tars, and Chars from Whatman No. 1 Paper (heating rate, 5°C/min; final temp., 475°C)

	Feedstock	Tar Product	Char Product
Heating Value, ^a cal/g	4170	4330	7566
Ash Content, wt %	0.074	-0.075	0.63
Moisture Content, wt %	4.1	--	--
Elemental Analysis, ^a wt %			
Carbon	44.7	42.3(43.6) ^b	81.0(27.3)
Hydrogen	5.9	6.1(47.5)	3.6(10.0)
Oxygen ^c	49.4	51.6(48.0)	15.4(4.7)
Yield, wt %	--	-46	-15

^aDry basis.

^bNumbers in parentheses give percent of original material (based on the reported yields).

^cDetermined by adding together the carbon and hydrogen contents and subtracting them from 100%.

Table 3. Analytical Results of Feedstock, Tars, and Chars from Newsprint (heating rate, 5°C/min; final temp., 475°C)

	Feedstock	Tar Product	Char Product
Heating Value, ^a cal/g	4722	5573	7866
Ash Content, wt %	.95	--	4.1
Moisture Content, wt %	8.3	--	--
Elemental Analysis, ^a wt %			
Carbon	48.0	47.5(45.5) ^b	78.0(24.4)
Hydrogen	5.4	5.6(47.7)	3.7(10.3)
Oxygen ^c	46.6	46.9(46.3)	18.3(5.9)
Yield, wt %	--	-46	-15

^aDry basis.

^bNumbers in parentheses give percent of original material (based on the reported yields).

^cDetermined by adding together the carbon and hydrogen contents and subtracting them from 100%.

Table 4. Analytical Results of Feedstock, Tars, and Chars from Kraft Paper (heating rate, 5°C/min; final temp., 475°C)

	Feedstock	Tar Product	Char Product
Heating Value, ^a cal/g	4445	5272	7333
Ash Content, wt %	1.3	--	4.3
Moisture Content, wt %	6.1	--	--
Elemental Analysis, ^a wt %			
Carbon	47.5	46.9(24.7) ^b	75.5(38.2)
Hydrogen	5.5	5.3(24.1)	3.9(17.0)
Oxygen ^c	47.0	47.8(25.4)	20.6(10.5)
Yield, wt %	--	-25	-24

^aDry basis.

^bNumbers in parentheses give percent of original material (based on the reported yields).

^cDetermined by adding together the carbon and hydrogen contents and subtracting them from 100%.

Table 5. Effect of Sample Weight and Heating Rate on Ultimate Product Yields from Whatman No. 1 Paper

Sample No.	Pyrolysis Sample Weight, g	Heating Rate, °C/min	Yields, %	
			Tar ^b	Char
FPLO8	5	5	46.14	14.55
FFL15	10	5	42.13	15.26
FFL13	15	5	38.54	15.66
FPMD3	5	20	47.18	12.65
FPMD5	5	30	47.76	11.93

^aProduct yields are given for a peak temperature of 475°C.

^bBased on weight percent Whatman No. 1 paper (dry basis).

Table 6. Effect of Sample Weight and Heating Rate on the Composition of Chars from Whatman No. 1 Paper

Sample No.	Pyrolysis Sample Weight, g	Heating Rate, °C/min	Ultimate Char Yield ^a at 475°C, wt %	Chars, wt %		
				C	H	O ^b
PFL08	5	5	14.55	81.80	3.75	13.45
PFL15	10	5	15.26	81.00	3.55	15.45
PFL13	15	5	15.66	81.90	3.45	14.65
PPH03	5	20	12.65	81.30	3.45	15.15
PPH05	5	30	11.93	80.30	3.55	16.15

^aYield from original Whatman No. 1 (dry basis).

^bDerived by adding together C and H contents and subtracting from 100%.

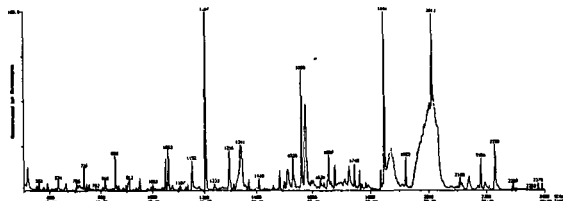


Fig. 1. Mass Spectrum Obtained from Sample 06298402

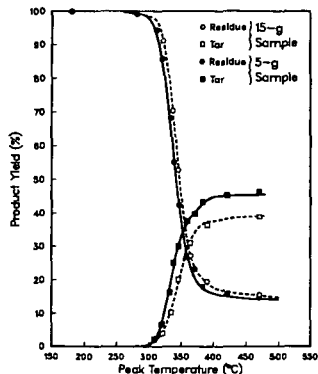


Fig. 2. Effect of Sample Weight on Product Yield for Whatman No. 1 Paper (heating rate, 5°C/min).

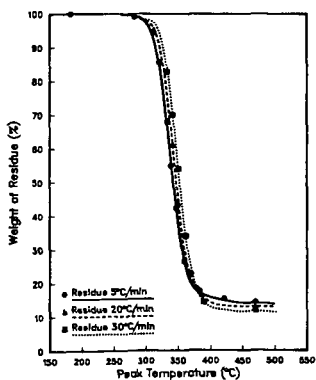


Fig. 3. Effect of Heating Rate on Weight Loss for Whatman No. 1 Paper

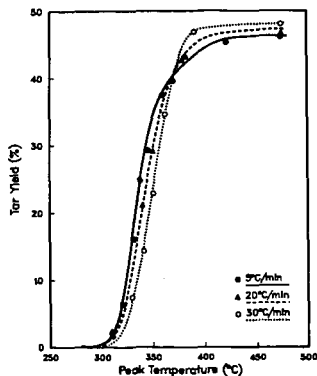


Fig. 4. Effect of Heating Rate on Tar Yields for Whatman No. 1 Paper

THE PRODUCTION AND EVALUATION OF OILS FROM THE STEAM PYROLYSIS OF POPLAR CHIPS

D.G.B. Boocock, A. Chowdhury, and S.G. Allen
Department of Chemical Engineering and Applied Chemistry, University of Toronto
200 College Street, Toronto, Ontario Canada M5S 1A4

and
R. Douglas Hayes
Energy, Mines and Resources, Ottawa, Canada

INTRODUCTION

In the early 1970's, as a response to the world oil crisis, two water-based technologies for the thermal liquefaction of woody biomass were studied extensively. The first of these, based on Bergstrom's earlier work (1), employed sodium carbonate as a soluble catalyst, and carbon monoxide as a reducing gas (2,3). The second technology, also based on earlier work, used nickel metal catalysts and hydrogen (4). In all cases the substrate was powdered wood slurried in water, and, in those studies using nickel metal as catalyst, it was not clear what role the catalyst played. In particular it was realised that the wood must yield gases or liquid before the catalyst could intervene. If liquids were formed, then the role of the catalyst/hydrogen system would be stabilisation, since under moderate heating rates, biomass alone in water does not yield significant quantities of oil. The stabilisation could also involve upgrading, if such things as oxygen content and viscosity were also decreased.

In subsequent experiments (5) we semi-continuously fed slurries of powdered wood along with nickel carbonate and hydrogen to a reactor. The feed, on entering the reactor, was heated sufficiently rapidly that the nickel carbonate decomposed to nickel oxide instead of reducing to nickel metal. In addition, when product was discharged from the reactor, both char and oil--the latter in 25 per cent yield--were present. We reasoned that the oil yield was initially higher, but that, because of the unavoidable, prolonged residence time up in the reactor, and the absence of the stabilising system (no nickel metal), some of the oil had charred.

As a test of this theory, powdered wood was heated rapidly, together with only water, in small reactors to 350°C, and then quenched (6). Oil yields (acetone-soluble) in up to 50 per cent by weight were obtained.

Until this time, all studies in both technologies had been confined to powdered wood or sawdust, the general opinion being that heat and mass transfer limitations in larger wood pieces would prevent liquefaction. However, we studied the liquefaction of single poplar chips (6.5 mm square cross section) in the same small reactors, and showed they were completely liquefied at 300°C and above (7). Steam entered the chips, swelling them and disrupting the matrix. The oil which was formed appeared to be stabilised by the presence of liquid water. The chemical conversions were obviously delayed relative to powdered wood, and some poplar clones yielded up to 6 per cent phenol from the chips, but not from the powdered form. Scanning electron microscopy showed liquefaction at the cellular level (8,9). On the surface the middle lamella merged with the cell walls and the matrix then flowed and engulfed the cells. Inside the chips, spherical structures appeared, particularly on the walls of vacuoles. These structures eventually filled irregular cavities which formed in the matrix. Gas or vapour bubbles could also be seen in the flowing matrix.

On the basis of these results it was decided that a laboratory unit should be constructed for the purpose of studying commercial-size (and larger) chips. The overall unit is shown schematically in Figure 1.

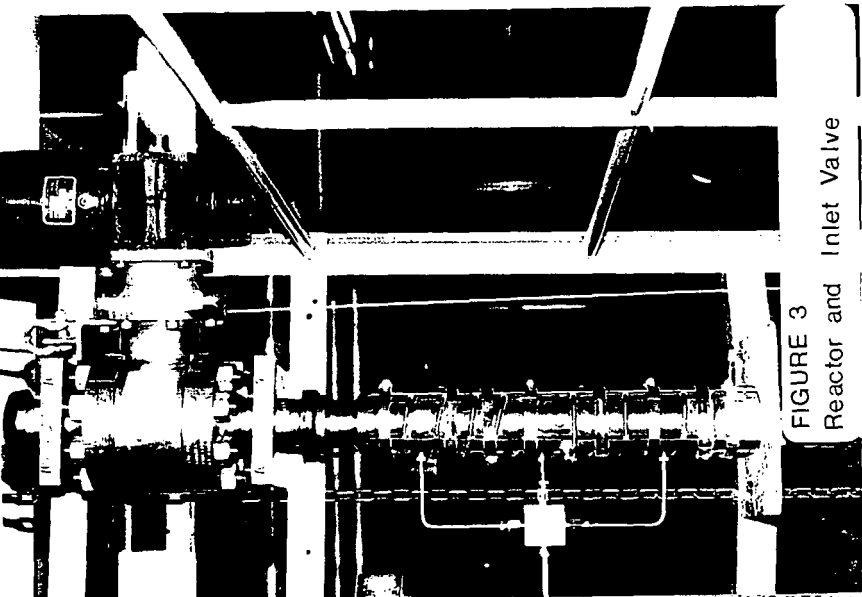


FIGURE 2
Reactor and Steam Vessel

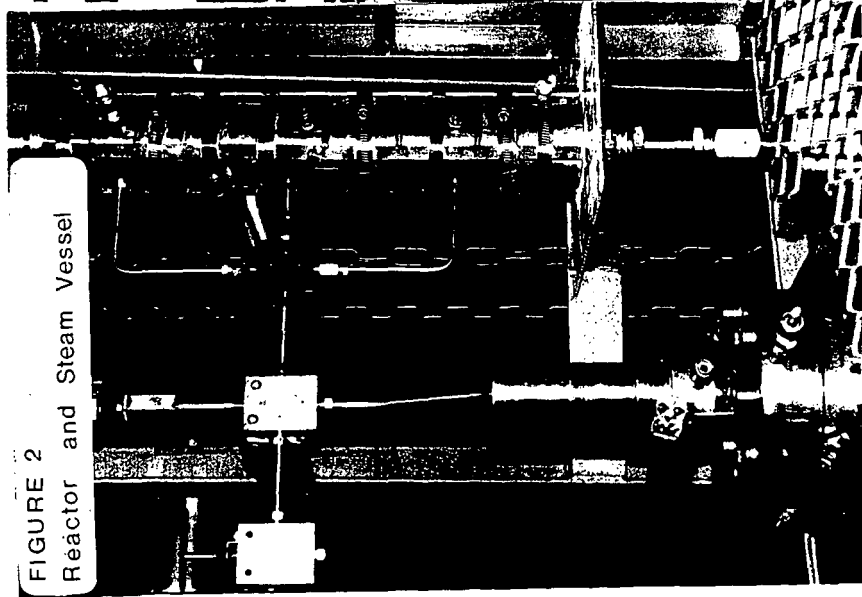


FIGURE 3
Reactor and Inlet Valve

FIGURE 1
CASCADE UNIT FOR
WOOD CHIPS LIQUEFACTION

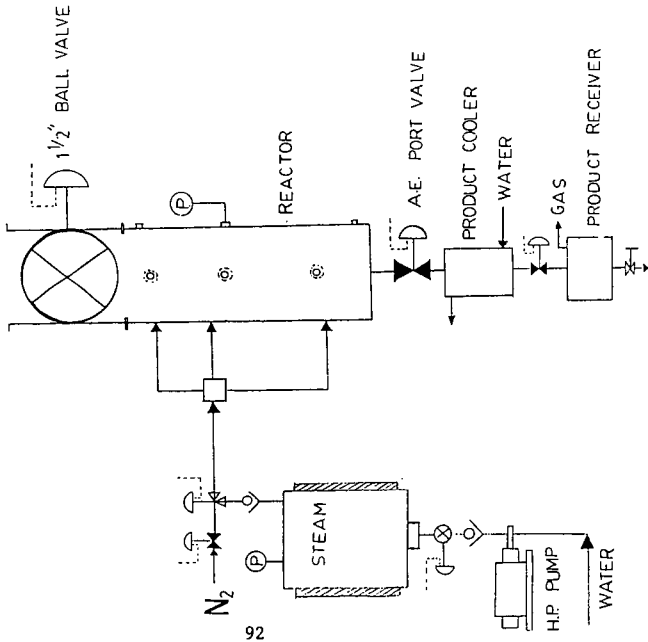
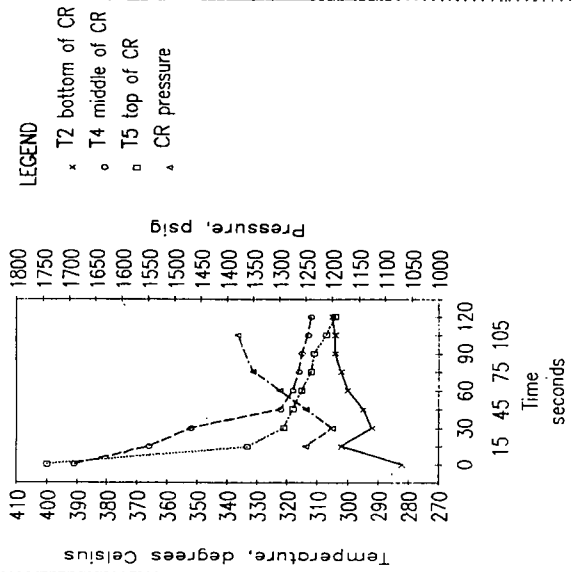


FIGURE 4
Temperature, Pressure Profiles

Steam for 7 Seconds
340 C, 2100 psig
1.0 L Water in SG



The Reactor

The reactor (Figures 2 and 3) was designed by THP Inc. according to ASME Code, Section VIII, Div. I., 1984 addenda. The rating was set at 24.1 MPa (3500 psi) at 350°C which allowed for 7.6 MPa (1100 psi) gas overpressure above the vapour pressure of water 16.5 MPa (2400 psi) at that temperature. A single ingot of TP 316 stainless steel was used for machining the reactor which has an internal diameter of 1.5 inches (3.8 cm) and an external diameter of 3.0 inches (7.6 cm). The length is 19 inches (48 cm) and the internal diameter is 600 mL which allows for a feed of 100 g of dry wood chips. At the top end an Oteco hub (Figure 2) is threaded and seal welded to the reactor body. A 1 inch Autoclave Engineering (AE) slim-line connector is threaded to the base of the reactor. A total of 9 holes are drilled in the reactor body to take 1/4 AE inch-slim connectors. The three on the left side of the reactor are for steam inlet lines. On the front face the top hole is for a rupture disc (20.67 MPa, 3000 psi). The middle hole is for a 1/8 inch thermocouple, and the bottom hole is for a vent line. On the right hand side, the upper and lower holes are for 1/8 inch thermocouples, and the middle hole is for a pressure gauge.

The reactor is clamped near its base by a split ring which is spot welded to a bracket bolted to the reactor frame. The split ring also supports a steel plate on which insulation, in the form of ceramic brick, (not shown in Figures) is stacked to the neck of the reactor. The brick is cut and fitted to the external contours of the reactor. A rectangular steel case is fitted outside the brick.

Heating is supplied to the reactor by two, 6 feet long (1.8 inch O.D.) heaters joined in parallel. These are coiled around the reactor as shown in Figures 2 and 3, and held close to the reactor by four longitudinal steel strips and eight circlips. The maximum power drawn by the heaters is 4 kw. The coils are operated through a temperature controller and with all the lagging in the place, the reactor can be brought to 365°C in 70 minutes.

Inlet Valve and Feed Basket

The inlet valve and its relationship to the reactor can be seen in Figure 3. The valve (Mogas Industries Inc.) is a 1.5 inch (3.8 cm) ball valve (ANSI 2500 series) rated at 24.8 MPa (3600 psi) at 370°C. It is joined to the reactor by a matching Oteco hub and supported on the frame by two brackets. The controller is air operated via solenoid valves. Failure of air pressure closes the valve. The valve is insulated by three layers of 1.5 inch thick glass wool, thus preventing excessive heat losses. The valve and controller together weigh 68 Kg and are attached to a pulley system to facilitate removal from the reactor when this is necessary.

The cylindrical feed basket is made of stainless steel mesh and is spot welded. The basket, besides facilitating feed addition, prevents contact of chips with the reactor walls and allows recovery of unconverted wood.

Outlet Valve

Another 1.5 inch ball valve was originally planned for the reactor outlet. However, because of initial cost considerations, this was replaced with a Crosby 0.5 inch ball valve (ANSI 1500) rated at 18.4 MPa (2665 psi) at 370°C. Special hubs were made by THP for connection to the reactor and the cooling lock. Considerable leaks were encountered with this system, probably because of misalignment of the hubs with the reactor body. Therefore, the system was replaced with a 0.5 inch AE seat and cone (port) valve rated 17000 psi at 350°C. The products thus had to negotiate two right angle turns before entering the product cooler. However, this was not considered a problem, because only water, oil and finely divided material would be exiting the reactor. The Crosby valve may be retested in the future after modification of the hubs.

Let-Down Lock and Collection Vessel

The cooling lock is a 20 inch long AE nipple, having an internal diameter of 0.688 inches (1.7 cm). The internal volume is 122 mL. An external copper jacket allows for use of a coolant, although at this time air cooling appears to be sufficient. Indeed excessive cooling is not desirable as the oil may not flow easily to the product collection vessel. At the time of writing, we are planning the installation of a larger lock (300 mL), since the total liquid discharge often exceeds the volume of the present lock.

The products discharge from the lock into a pyrex cylindrical vessel, approximately 5 inches in diameter and about 8 inches deep. Another smaller container such as a beaker can be placed inside the vessel if necessary. The collection vessel is sealed except for an outlet for the product gases which pass to a brine displacement vessel for volume measurement.

Steam Vessel and Injection

The top of the steam generator is visible at lower left in Figure 2. It is a 2 L AE autoclave equipped with a pressure gauge and thermocouple. The magndrive stirrer has been left in place but is not used. The steam transfer line can be seen passing upward from behind the magndrive to a two-way valve. When the steam line is closed, nitrogen flush gas can be passed from the transfer line on the left hand side to the reactor. Steam and nitrogen enter the reactor at three locations on the reactor as shown (Figure 2). If necessary, the hot generator can be charged with make up water using a Milton Royal high-pressure pump.

Control Panel and Safety Systems

The control panel is located in a room directly adjacent to that containing the unit. The panel contains main switches as well as switches to open and close the various valves. A digital readout and/or chart indicators allow the monitoring of thermocouple temperatures.

The major hazard of this type of equipment is the accidental release of steam to the atmosphere with subsequent injury to personnel. The equipment does contain an electrical override, in that the steam inlet valve can not be electrically operated, unless closure of the reactor inlet valve is initiated. However, this is not sufficient, since the reactor inlet valve takes 3-4 seconds to close, whereas the steam inlet valve opens in about 1 second. Thus if the switch for the steam inlet valve is moved to the open position immediately after the switch for the reactor inlet valve is moved to the closed position, then the contents of the steam vessel could discharge through the inlet valve. The system has, therefore, been provided with an extra safeguard in that the shaft of the inlet valve actuator now carries an extension arm. When the valve is fully closed, the extension arm activates a microswitch which only then allows the steam inlet valve to open. The equipment is also designed such that the main inlet valve cannot be opened if the steam valve is open. This is a purely electrical override but is sufficient, since the steam valve operates faster; i.e., it closed much faster than the reactor inlet valve can open. This, however, does not prevent the accidental discharge of the reactor contents to the atmosphere. To avoid this possibility, the reactor inlet valve has a keyed switch. The operator, after manually loading the wood, then inserts the key to close the reactor inlet valve. He then removes the key rendering the switch inoperable.

Polymethylmethacrylate sheet is installed around the equipment in locations where sudden steam leaks could otherwise injure the operators.

Operation of the Unit (Experimental)

Figure 4 shows typical temperature and pressure profiles (340°C steam injected

for 7 s). Before steam injection, the top and middle of the reactor had temperatures close to 400°C whereas the bottom of the reactor, where heat losses are greater, was at 300°C. After steam injection, the temperatures shown by the upper two thermocouples dropped over a period of about 2 minutes and came close to the temperature of the bottom thermocouple. Condensed steam was present in the base of the reactor, and the internal pressure of the reactor was controlled by the temperature of the surface of this water plus nitrogen and product gas overpressure. As might be expected, the pressure in the reactor is slightly higher than the equilibrium steam pressure corresponding to the temperature of the thermocouple at the base of the reactor (i.e., at the bottom of the water layer).

The following procedure is typical for a liquefaction experiment. The reactor was preheated and flushed with nitrogen with the inlet valve open. The stainless steel basket was loaded with wood chips (100 g, 8 per cent moisture) and then quickly lowered through the inlet valve. The nitrogen valve was closed, as was the inlet valve. Immediately the steam line was opened--usually for about 7 s. After 2 minutes, the products were discharged into the cooling lock, and after a further 30 s the valve to the collection vessel was opened. The gas separated and its volume was measured by displacement of water. Temperatures and pressures in the reactor and steam vessel were monitored throughout this procedure. The basket was retrieved through the inlet port after venting of the reactor.

The oil solidified and could be physically separated from the water by filtration (acetone free oil). The aqueous layer was centrifuged to yield a small insoluble fraction (aqueous-phase solids) most of which was acetone-soluble. An acetone flush of the reactor yielded further oil (acetone-wash oil). A small amount of acetone-insoluble material stuck to the walls of the basket (insolubles). The moisture content of the acetone-free oil was about 20%. However, heating the oil to 70°C for half an hour lowered the water content to less than 3%. This is a rather dramatic, and unexpected reduction in water content, but remelting the oil allows the separation and evaporation of water that was trapped when the oil originally solidified. This semi-dry oil softened around 50°C.

RESULTS AND DISCUSSION

The results from one typical run are discussed here. A steam temperature of 355°C was used, and the wood chips in this instance were soaked for 20 minutes with water for 20 minutes prior to addition. A further 51 g of water was added to the reactor in this way. The presoaking, which was intended to prevent charring, has no advantages and has now been discontinued.

A reasonable, overall mass balance was obtained, but this was not very meaningful, given the relatively large amounts of water involved in the reaction. Approximately 250 g of water were discharged in this run, and no particular effort was made at that time to limit the amount of condensate. A more important aspect is the carbon balance, and in this run slightly more carbon (45.6 g) was accounted for in the products than was in the feed (44.4 g). Figure 5 shows the distribution of carbon in the various product phases. The insoluble fraction is a composite of those acetone insolubles left on the basket and those in the oils. No aqueous phase acetone-insoluble solids were obtained with 355°C steam, and they only become significant when using steam below 340°C. The fraction of total carbon in the gas phase was close to 10 per cent. As in previous runs, about 90 per cent of this gas was carbon dioxide--the balance being mostly carbon monoxide. The total mass of gas was 18.6% of the wood mass. From our previous work on single chip (0.64 x 0.64 x 7.6 cm) liquefaction (7) this is approximately the percentage that would be produced at a water/wood ratio of 1.0 when the steam is generated internally. In that case, however, the oil chars due to the lack of water, so the mechanism for the increased gas production is probably different.

The elemental composition of the oil are also very similar to those obtained in

FIGURE 5
Wood Chips Liquefaction
 Carbon Distribution in Products

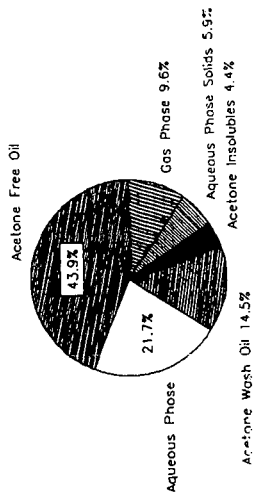
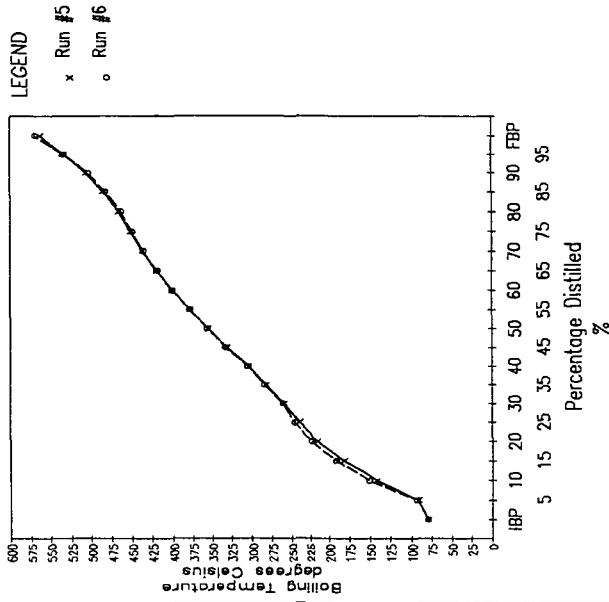


FIGURE 6
Boiling Point Distribution
 of Acetone Free Oils
 by ASTM Method D2887-73



Data provided by DC Research

the previous study, the carbon percentage being close to 70.0 and the hydrogen being around 6.5. The oxygen percentage (by difference) is thus in the low 20 per cent range. If complete oxygen removal was required by hydrotreating, then the viable oxygen limit in the substrate from an economic standpoint is about 20 per cent (11).

A distillation curve for the oils is shown in Figure 6. Approximately 60 per cent of the oil distills below 405°C, which is at the upper end of the range for heavy gas oil in petroleum distillation. Although the average molecular weight of the oil is not known at this time, it can be estimated from Goring's work (10) on the softening point of lignins that the value is less than 1000. The distillation results and the polar nature of the oil (which would increase boiling points relative to alkanes of similar molecular weight) support this estimation.

Continuing Work

Experiments are continuing to define the optimum temperatures and residence times for maximising oil yield and quality. In addition, the effect of water content and chip size are being investigated. Further results from these studies will be reported in the near future.

ACKNOWLEDGEMENTS

The construction and operation of the cascade autoclave system is contract supported by Energy, Mines and Resources, Canada, through the Bioenergy Development Program. We thank the Natural Sciences and Engineering Research Council of Canada for financial support to Stephen Allen through an Undergraduate Summer Research Award.

REFERENCES

1. H.O. Bergstrom and K.N. Cederquist, U.S. Patent 2177557, 1937.
2. H.R. Appell, Y.C. Fu, S. Friedman, P.M. Yavorsky and I. Wender, U.S. Bureau of Mines Technical Report of Investigation #7560 (1971).
3. H.R. Appell, Y.C. Fu, E.G. Illig, F.W. Steffgen and R.D. Miller, U.S. Bureau of Mines Report of Investigation, #8013 (1975).
4. D.G.B. Boocock, D. Mackay, M. McPherson, S.J. Nadeau and R. Thurier, Can.J.Chem.Eng., 47, 98 (1979).
5. D.G.B. Boocock, Final Report of Contract File #24SU.23216-3-6143 for Renewable Energy Division, Energy Mines and Resources, Canada, 1984.
6. D. Beckman and D.G.B. Boocock, Can.J.Chem.Eng., 61, 80 (1983).
7. D.G.B. Boocock and F. Porretta, J.Wood Chem. and Technol., 6, 127 (1986).
8. D.G.B. Boocock, F. Agblevor, A. Chowdhury, L. Kosiak, F. Porretta and E. Vasquez in Energy from Biomass and Wastes X, IGT Symposium, Washington D.C., April, 1986, in press.
9. D.G.B. Boocock and L. Kosiak unpublished results.
10. D.A.I. Goring, Pulp and Paper Canada, 64, T517 (1963).
11. M.J. Van der Burgt and H.P. Ruyter, Shell International Petroleum, Private Communication.

OIL PRODUCTION BY HIGH-PRESSURE THERMAL TREATMENT
OF BLACK LIQUORS: AQUEOUS-PHASE PRODUCTS

P. J. McKeough and A. Å. Johansson

Laboratory of Fuel Processing and Lubrication Technology
Technical Research Centre of Finland
02150 Espoo, Finland

ABSTRACT

Liquid-phase treatment of black liquors, from alkaline pulping, at 300 - 350 °C in a reducing atmosphere results in the formation of an oil-like product, which separates out from an aqueous phase containing the inorganic constituents. The process has several potential forms of application. This study was conducted in support of the development of one such application: a new recovery system for the kraft pulping process. Thermal treatment experiments were performed using different reactant gases. On the basis of analyses of the resultant gaseous and aqueous phases, the main reactions leading to aqueous-phase products were elucidated. This information was used to advantage in the compilation of a process scheme for the recovery of the cooking chemicals from the aqueous phase.

INTRODUCTION

A process producing liquid fuels from the organic matter of the black liquors from alkaline pulping is being developed at the Laboratory of Fuel Processing and Lubrication Technology, Technical Research Centre of Finland (VTT). The central operation in the process is the liquid-phase thermal treatment of black liquor at 300 - 350 °C under a reducing atmosphere (1). The treatment results in the formation of a hydrophobic oil which separates out from an aqueous phase containing the inorganic constituents (Figure 1).

The process can be applied in either of two basic ways:

- as a method to produce oil in conjunction with the kraft pulping process,
- as an entirely new system for recovering the cooking chemicals and energy from kraft spent liquors.

The first type of application exploits the favourable properties of black liquor as a feedstock for high-pressure conversion. In comparison to solid biomass, the advantages of black liquor as a feedstock include:

- no pretreatment required. Black liquor can be directly pumped into the reactor at dry solids concentrations as high as 60 %.
- black liquor contains alkaline compounds known to catalyze conversion reactions,
- cellulose, the most valuable component of wood, is not subjected to the conversion process.

In this type of application, the kraft cooking chemicals are recovered using the traditional method which is centred around the Tomlinson recovery boiler. Additional plant fuel (wood waste, peat, coal) is needed. Preliminary economic evaluations have indicated that this type of oil production process would be economic if oil prices were at their 1985 level.

In the second type of application, the Tomlinson recovery boiler is replaced by a safer and thermally more efficient recovery system, in which the oil produced by thermal treatment is used as plant fuel. This type of process is, in many respects, similar to the Hydrolysis Recovery Process developed by the St.

Regis Paper Company, USA (2), the essential difference being the use of a reducing atmosphere in the VTT process. The experiments described here-in were undertaken in support of the development of this second type of process.

The specific objectives of the present study were to elucidate the main reactions leading to aqueous-phase products, and, by applying this knowledge, to establish process schemes for the recovery of the cooking chemicals from the aqueous phase. Because the composition of the aqueous phase is dependent upon the composition of the reactant gas, several different gases were employed in these experiments.

It should be mentioned that research on conversion of black liquors is but a part of a wider biomass conversion program being undertaken at our laboratory. Other major parts to this program are:

- development of fixed-bed and fluid-bed gasification processes, including combined cycle power generation applications,
- supportive research for the first synthesis-gas plant using peat or wood as feedstock (the peat-ammonia plant of the Finnish company, Kemira),
- basic research on direct liquefaction processes for peat and wood (high-pressure liquefaction and flash pyrolysis),
- development of low-waste technologies.

EXPERIMENTAL

The kraft black liquor, employed in the experiments, originated from a laboratory cook of Scots pine (*Pinus sylvestris*). An analysis of the liquor is given in Table 1.

Table 1. Analysis of kraft black liquor¹.

	% of dry solids
Organic matter	78.9
Total Na	18.4
NaOH	3.0
Na ₂ S	5.5
Na ₂ SO ₄	0.04
Na ₂ CO ₃	1.1

¹ dry solids content of 30 %

A later batch of liquor, prepared in a similar way, was also analyzed for volatile acids (formic and acetic acids) and lactic acid, which are present as sodium salts in the liquor. On the basis of the analyses it can be concluded that the contents of these acids in the feed liquor used in the present experiments were approximately 6 % om, 4 % om, and 4 % om respectively, where % om denotes the percentage of black liquor organics.

The experiments were conducted in a 1-litre autoclave. In a typical experiment 500 ml of black liquor was placed in the autoclave and reactant gas was charged at sufficient pressure (5 - 9 MPa) to result in a total pressure of about 20 MPa at the reaction temperature. The autoclave was then heated at a rate of about 5 °C/min. A fixed time-at-temperature of 45 min was chosen for these experiments.

At the end of the reaction period, the autoclave was rapidly cooled, after which gases were released, measured, and analyzed. The organic phase and the aqueous

phase were separately recovered from the autoclave and weighed. The pH of the aqueous phase was measured. In many of the experiments the aqueous phase was also analyzed for formic, acetic, and lactic acids (present as sodium salts) and for CO₂ (chemically bound in sodium carbonate or bicarbonate). The former were analyzed by gas chromatography as their benzyl esters (3), the latter by measuring the amount of CO₂ liberated upon acidification with excess mineral acid.

The primary experiments were those employing either carbon monoxide or hydrogen as reducing gas. Two temperatures, 300 °C and 350 °C, were investigated. Experiments employing non-reducing carbon dioxide were also conducted in order to assess whether alkali neutralization by the reactant gas plays an important role in the thermal treatment process. One experiment was performed with a reactant gas of composition similar to that of a typical low-calorific fuel gas (producer gas) generated by gasification of biomass with air.

RESULTS AND DISCUSSION

The main experimental results are presented in Table 2.

Table 2. Results of autoclave experiments. Time-at-temperature: 45 min.

Experiment	1	2	3	4	5	6	7	8
Reactant gas	CO	CO	H ₂	H ₂	H ₂	CO ₂	CO ₂ /H ₂ ¹	Producer gas ²
Temperature, °C	300	350	300	350	350	350	345	350
Pressure, MPa	20	26	18	22	22	24	26	26
Yields, % of black liquor organics (% om)								
oil ³	24.9	26.9	0	23.2	22.6	0	22.1	20.2
bitumen ⁴	35.1	25.6	80.7	36.5	33.4	81.4	34.1	36.5
CO ₂ ⁵	30.1	32.1	0.4	2.4	2.4	0.6	5.2	3.9
H ₂	0.5	0.7	- 0.5	- 0.3	- 0.2	0	- 0.3	- 0.1
CO	- 31.8	- 28.6	0	0	0	0	0	- 3.8
CH _x -gases	0.4	0.6	0.1	0.7	0.8	0.7	1.0	0.7
H ₂ S	1.4	1.1	0.3	0.5	0.4	1.0	ND	0.4
CO ₂ /aqueous ⁶	2.0	19.0	10.0	ND	18.0	ND	19.0	ND
formic acid ⁷	35.7	10.6	6.2	ND	4.6	1.6	ND	ND
acetic acid ⁷	4.5	3.9	4.1	ND	3.8	3.9	ND	ND
lactic acid ⁷	1.3	0.3	1.5	ND	0.3	0	ND	ND
Aqueous-phase pH	8.5	8.5	10.2	9.5	9.4	8.9	8.4	9.1

¹ 60 % CO₂, 40 % H₂

² 14 % CO₂, 51 % N₂, 17 % H₂, 18 % CO

³ organic product as oil layer

⁴ heavier organic product

⁵ in gaseous phase

⁶ in aqueous phase as HCO₃⁻ or CO₃⁼

⁷ present as sodium salts

ND: not determined

Formation of oil phase

In this experimental program, complete separation of the organic product as a single oil layer was not achieved, even when reaction conditions were apparently similar to those successfully employed in other types of reactor in earlier development work (CO/300 °C) (1). In experiments in which an oil layer was

formed, part of the organic matter was also converted into a bitumen-like material. It was assumed that this separation of the organic product into two phases was dependent on certain physical parameters of the reaction system. This assumption has since been confirmed. In this study, concerned with reactions of aqueous-phase constituents, efforts were not expended in optimizing physical conditions for oil-layer formation. In Table 2, the yields of "oil" and "bitumen" are reported separately.

The oil yield data of Table 2 indicate that, at 300 °C, CO was effective in producing a distinctly oil-like product but H₂ was not. At 350 °C, H₂ was also an effective reactant gas, as were mixtures of CO and H₂ with other gases (for example, "producer gas"). CO₂, on the other hand, was not effective, confirming that the most important function of the reactant gas is to reduce organic matter in the liquor.

Interactions between gaseous and aqueous components

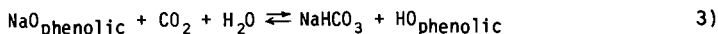
In all experiments the thermal treatment led to a decrease in the black liquor alkalinity, the final pHs being in the range 8 - 10 (Table 2). The chief neutralizing agents were the gases CO and CO₂. The decrease in alkalinity was least extensive in experiments employing hydrogen as reactant gas, but it was nonetheless quite significant, particularly at 350 °C (Expts. 4 and 5). In these cases, the neutralizing agent was CO₂, a product of the thermal decomposition of the organic matter (decarboxylation).

The electrolyte systems of kraft black liquor are well known (4). In principle this data can be applied to the product mixture of the thermal treatment process, allowing the following conclusions to be drawn:

1. In all cases, sulphur is present as HS⁻ in the aqueous phase, the final pHs (8 - 10) being lower than the pK_a for HS⁻ (~ 13.5) and higher than the pK_a for H₂S (~ 7). Very little H₂S should be formed.
2. HCO₃⁻ predominates over CO₃⁼², particularly at the lower end of the observed pH range. pK_a for HCO₃⁻ is ~ 10.
3. The phenolic hydroxyl groups of the lignin molecules are largely in an unionized condition, i.e. not bound to the sodium ion (pK_as: 9.5 - 11).
4. The carboxyl groups, which do not decompose during the thermal treatment, remain ionized (pK_as: 3 - 5). The three main fractions of the organic matter of the black liquor are lignin, aliphatic acids, and extractives. The aliphatic acid fraction contains the bulk of the carboxyl groups, but some are also encountered in the other fractions (5).

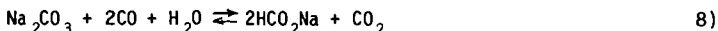
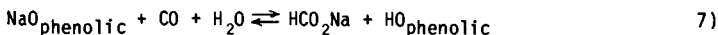
However, it should be noted that, because of mass transfer limitations, equilibrium between the gas and liquid phases is not necessarily established during all phases of the treatment process. For example, considerable amounts of H₂S were evolved during the treatment, the lower the pH the more H₂S (Table 2), indicating a higher pK_a value at the reaction temperature, and, after the rapid cool-down, lack of equilibrium between H₂S in the gas phase and H₂S in the aqueous phase.

When the neutralizing agent is CO₂, the main neutralization reactions can be written as follows:





When CO is the neutralizing agent, the equations become:



The results in Table 2 indicate that, at 350 °C, Reactions 1 to 4 occurred to a significant extent in all atmospheres. In the CO atmosphere, a significant amount of formate was also produced (Reactions 5 to 9). At 300 °C, the aqueous-phase composition in the CO experiment was considerably different from that in the H₂ experiment. In the CO atmosphere, a very large quantity of formate was formed. The increase compared to the CO/350 °C experiment was presumably due to a shift in the equilibria of Reactions 8 and 9. In the H₂ atmosphere at 300 °C, carbonate formation, although still significant, was less than at 350 °C (less decarboxylation of organic matter).

Stability of organic acid salts

A large fraction of the organic material of black liquor is comprised of aliphatic acids (5). In addition to the acids analyzed, there are significant quantities of less volatile aliphatic hydroxy acids. The acids, present as sodium salts in black liquor, are formed from wood polysaccharides during pulping. At the present time, the fate of the hydroxy acid components, other than lactic acid, during the thermal treatment process is not known with certainty. A recent study of cellulose conversion in alkaline solution suggests, however, that these components will not be converted into water-insoluble product, that is, oil, under these conditions (6). This is consistent with the energy yields of organic phase (oil and bitumen) observed in the present experiments. The yields are what one would expect if the organic phase were to originate almost entirely from the lignin fraction of black liquor. Forthcoming experiments will aim at confirming the origins of the oil product.

The present results (Table 2) indicate that sodium acetate was rather stable under the conditions of the thermal treatment, while sodium lactate decomposed to a large extent. Sodium formate decomposed in the CO₂ atmosphere, presumably due to a shift to the left of the equilibria of Reactions 8 and 9. In the H₂ atmosphere, formate was fairly stable. In this case, the decomposition of formate to carbonate was probably prevented by the following reaction (7):

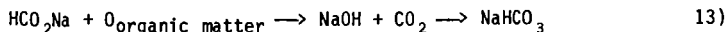


Consumption of reducing gas

From the point of view of oil formation, the most important reactions of CO or H₂ are the reduction reactions:



Sodium formate can also function as a reductant in a similar way (8):



However, the results of the $\text{H}_2/300^\circ\text{C}$ experiment suggest that the formate present in the black liquor feedstock (at 6 % om concentration) is not an effective reductant.

In addition to its being consumed as a reductant, CO is consumed in partial neutralization of black liquor alkalinity (Equations 5 to 9) and in production of H_2 by the water-gas-shift reaction:



From the data of Table 2, it has been possible to establish the consumption patterns of CO at 300°C and 350°C (Table 3).

Table 3. Consumption of CO.

		% of black liquor organics (% om)	
		CO/300 °C	CO/350 °C
I	Neutralization	18	3
II	Reduction	7	16
III	Shift	7	10
	Total	32	29

The total level of CO consumption, about 30 % om, is equivalent to a H_2 consumption of 2.1 % om, which is a much higher value than that observed in H_2 experiments: 0.3 - 0.5 % om (Table 2).

IMPLICATIONS FOR PROCESS DEVELOPMENT

The aqueous phase leaving the thermal treatment reactor contains the following compounds:

- NaHS ($\rightleftharpoons \text{Na}_2\text{S}$)
- NaHCO_3 ($\rightleftharpoons \text{Na}_2\text{CO}_3$)
- Sodium salts of aliphatic acids, with formate and acetate as two main components. The formate content is considerable when the reactant gas is CO.
- Other organic compounds in smaller amounts.

The organic acid salts and other organic compounds cannot be recycled, in their entirety, to the cooking stage. If not purged from the system, they will quickly build-up in concentration in the cooking liquor and retard the delignification reactions. Furthermore, particularly if the formate concentration is high, there may be insufficient sodium for binding to the hydroxide ion. In fact, various possibilities of converting sodium formate directly into sodium hydroxide were investigated in this study, but none of these proved to be technically feasible.

One example of a workable scheme for the recovery of chemicals is depicted in Figure 2. A part of the aqueous phase leaving the thermal treatment stage is recycled through a wet oxidation reactor where organic matter is oxidized to carbonate, CO_2 , and H_2O . The heat produced is employed in heating the feed

stream to the thermal treater. The rest of the aqueous phase is recausticized in the conventional way. In addition to the normal components of kraft green liquor, this liquor contains NaHCO_3 and some organic matter. The presence of organic matter should be an advantage because, according to the literature, a small but significant increase in pulp yield can be expected (2). The presence of NaHCO_3 will lead to a higher lime requirement in the recausticizing stage.

Wet oxidation is quite an economic process step in this scheme because the feed stream to it is already at the required temperature and pressure. Sulphide will be oxidized to sulphate, but it should be reduced again to sulphide in the subsequent heat treatment stage. This latter reaction will be investigated experimentally in the near future. For reasons of low gas consumption and low gas cost, producer gas is the reducing gas proposed for the scheme of Figure 2.

Preliminary economic evaluations of this scheme have indicated that it would be more economic than the conventional recovery process, particularly if a higher pulp yield were obtained. This process would also have a higher thermal efficiency than the conventional process.

CONCLUDING REMARKS

The black liquor treatment process being developed at VTT has several promising forms of application. The work described in this paper has furthered the development of one such application: a new recovery system for the kraft pulping process. Current research is being directed at gaining a better understanding of the oil-forming reactions occurring during thermal treatment.

ACKNOWLEDGEMENTS

This work was sponsored by the Energy Department of the Finnish Ministry of Trade and Industry. The authors particularly wish to acknowledge the contribution of Paula Ylinen, M. Sc., who undertook the study of the conversion of sodium formate into sodium hydroxide. Thanks are also due to the following staff members of the Laboratory of Fuel Processing and Lubrication Technology: Dr. Raimo Alén, Virve Tulenheimo, M.Sc., and Anja Oasmaa, M.Sc.

REFERENCES

1. Johansson, A. Biomass 4(1984)155-160.
2. Adams, W. S., & Maples, G. E. AIChE Symp. 76(1980)200, 114-119.
3. Alén, R., Jännäri, P., & Sjöström, E. Finn. Chem. Lett.(1985)190-192.
4. Rydholm, S. A. Pulping processes. New York 1965, John Wiley & Sons.
5. Sjöström, E. Appl. Polym. Symp. 37(1983)577-592.
6. Krochta, J. M., Hudson, J. S., & Drake, C. W. Biotech. & Bioeng. Symp. 14(1984)37-54.
7. Anon. Gmelins Handbuch der anorganischen Chemie. System-Nummer 21, Verlag Chemie, 1967.
8. Appell, H. R. et al. Conversion of cellulosic wastes to oil. U.S. Bureau of Mines, RI 8013, 1975.

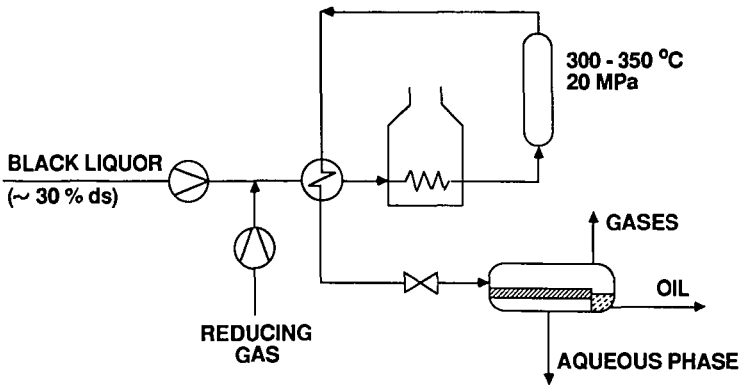


Figure 1. The thermal treatment process for black liquors.

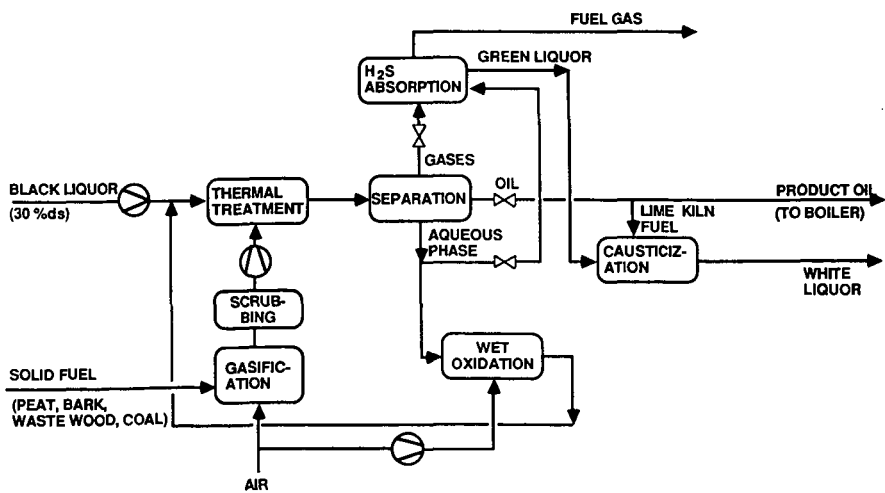


Figure 2. Preliminary scheme for a new kraft recovery process.

BIOMASS LIQUEFACTION UTILIZING EXTRUDER-FEEDER REACTOR SYSTEM

Don H. White, D. Wolf and Y. Zhao

Department of Chemical Engineering, University of Arizona, Tucson, Arizona 85721

ABSTRACT

Biomass including wood could provide liquid fuels on a regional basis if an economic liquefaction process can be developed. Through research sponsored by the U.S. Department of Energy (DOE), under its Thermochemical Conversion Program managed by Battelle PNL, the University of Arizona has developed a unique method of pumping concentrated, viscous biomass slurries, characteristic in biomass direct liquefaction systems. A modified single-screw extruder has now been shown to be capable of pumping solid slurries as high as 60 wt. % wood flour in wood oil derived vacuum bottoms. Preliminary experimental runs showed that a low-oxygen crude wood oil could be produced over a wide range of temperatures, pressures, with or without carbon monoxide and with or without a sodium carbonate catalyst.

INTRODUCTION

The modified extruder has now been shown to be capable of pumping slurries as high as 60 wt. % wood as compared to only 10-20 wt. % in conventional systems. The ability to handle such concentrated slurries which are in solid form at normal temperatures is expected to improve direct liquefaction wood oil quality and process economics. Various preliminary process design and economic studies indicated that the utilization of this newly-developed extruder-feeder in biomass direct liquefaction processes could lead to one or more of the process improvements listed below.

1. Elimination of recycle wood oil (or dramatically reducing it), which should result in less coke formation and better quality wood oil. In fact, even the reduced recycle will be wood oil vacuum bottoms, a heavy residue that might be decomposed further to a lighter oil.
2. Attainment of reactor temperature almost instantaneously, by the mode of adding heat (some by extruder-feeder preheater and remainder by superheater steam).
3. Attainment of near-plug flow in the reactor when using static mixers. This means that all biomass solids with nearly the same residence time in the reactor, have better control of conversion per pass and more uniform wood oil quality should be attained.

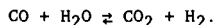
The extruder-feeder acts simultaneously as both a feed preheater and a pumping device into a 3,000 psi pressure reactor in the biomass liquefaction process. It could prove to be of importance in other processes where high concentration of solids in liquids are to be handled, like in the pulp and paper industry, hydrolysis of wood or other cellulose, other biomass liquefaction processes, coal liquefaction processes and some biomass gasification processes.

EARLY BUREAU OF MINES RESEARCH

In the early 1970's the Bureau of Mines showed that cellulosic materials, all other carbohydrates, wood wastes (largely cellulose and lignin), urban wastes (mostly cellulose plus other carbohydrates, proteins, fats, and small amounts of other organic materials), sewage sludge, agricultural wastes, and bovine manure can be converted to oil with carbon monoxide and water. Some plastics depolymerize and dissolve in the product oil; some remain as part of the unconverted residue (1,2).

Effect of Carbon Monoxide

Carbon monoxide and water react to form hydrogen and carbon dioxide in the following water-gas shift reaction:



Because some hydrogen adds to cellulose during its conversion to oil, it seemed at first reasonable to suppose that the hydrogen gas formed in the water-gas shift was responsible for converting cellulose. But when hydrogen was added to the reactor, it had little effect; an equivalent molar amount of carbon monoxide was much more effective. Early work showed that carbon monoxide consumption at lower temperatures (250°C) was low.

Effect of Water

The original experiments by the Bureau of Mines with carbon monoxide on low-rank coal (lignite) were successful without added water, because this coal has a large amount of moisture. However, addition of water was beneficial. It served as a vehicle (solvent) for the reaction. Cellulose forms water on being heated and the added water plus carbon monoxide improves the oil yield. However, added water also shifts the water-gas reaction in the direction of more carbon dioxide and hydrogen (more carbon monoxide is consumed); this side reaction may or may not be desirable.

The critical temperature of water is 375°C; above this temperature all the water is in the gaseous state. There were indications that the presence of liquid water is desirable. This may be accomplished by adding enough water so that some liquid is always present. The temperature must of course be below 375°C. If insufficient water is added, most of it will be in the gas phase, even below 375°C.

Nature of Conversion Reactions

The Bureau of Mines speculated on the possible chemical reactions in 1971 as follows:

"Cellulose, starch, and other carbohydrates can undergo a large number of reactions on treatment at elevated temperatures and pressures with carbon monoxide, water, and sodium carbonate or other alkaline salts. Since almost every carbon atom in a carbohydrate is bonded to an hydroxyl group (-OH), some dehydration will take place. Hydrolyses of the polysaccharides to glucose will also occur; glucose and the smaller units formed from it are soluble in water. Hydrolysis of the fats in the refuse to long-chain palmitic and stearic acids will also occur. Probably the most important overall reaction in converting cellulose to oil is the splitting out of oxygen to form molecules with high hydrogen-to-carbon ratios. Cellulose and other carbohydrates lose water and carbon dioxide just on being heated. Oxygen can also be lost by reaction with the added carbon monoxide to form carbon dioxide, by hydrogenation, by various disproportionation reactions, and by combinations of these reactions".

Later Bureau of Mines Research

Further research work in the early 1970's by the Bureau of Mines resulted in data on the reaction parameters (1). In general, the more readily hydrolyzable forms of cellulose, especially those containing pentosan units can be readily converted to a bituminous oil at temperatures as low as 250°C. Lignin and high-molecular-weight cellulose, containing crystalline cellulose, required higher reaction temperatures of about 350°C.

Wood is considerably more difficult to convert to oil than other biomass sources, but good oil yields were obtained by the Bureau of Mines in the presence of organic solvents as shown in Table 1 during wood liquefaction at 275°C. It was believed that some carbon monoxide was evolved during the decomposition of the wood and was apparently about equal to the amount of carbon monoxide consumed.

Table 1. - Effect of Water and Solvent on Wood Liquefaction

(50 g softwood sawdust, 1 hr at 275°C, 300 psig CO)

Cresol solvent, (g)	Water, ml	Catalyst		Pressure, psig	Conversion pct	Yield, pct	CO used g/100 g wood
		Type	Amount				
50	200	HCO ₂ Na	5	1,900	99.9	48	6
50	50	Na ₂ CO ₃	2	1,780	99.3	60	4
75	10	None	0	1,470	99.0	58	0
75	10	HCO ₂ H	1	1,500	99.3	58	0
75	10	HCO ₂ Na	1	1,560	99.8	60	0

The Bureau of Mines did considerable work at pressures below 2,000 psig and at 250°C. However, the products obtained at these mild conditions were pitches instead of oils. The lowest temperature at which a suitable oil could be produced was 300°C, at which temperature the combined water vapor and carbon monoxide pressure exceeded 2,000 psig.

The Bureau of Mines conducted some interesting experiments using formic acid or sodium formate in place of carbon monoxide. This lowered the operating pressure at 250°C to the range of 1,000 - 1,100 psig, and still gave good oil yields, as shown in Table 2 below. This technique would be less successful above 250°C because the formates decompose too rapidly.

Table 2. - Liquefaction of Wood in Absence of Carbon Monoxide

(50 g softwood sawdust 50 g Cresol solvent, 1 hr at 250°C)

Water, ml	Catalyst, g		Pressure, psig	Oil yield pct	Conversion pct
	Type HCO ₂ Na	Amount HCO ₂ H			
100	1	5	1,070	60	99.6
100	5	1	1,040	55	99.0
100	2.5	2.5	1,050	55	99.8
50	2.5	2.5	1,040	41	90

The unstabilized crude wood oil is very reactive to continued exposure to temperature. The Bureau of Mines studied the effect of recycling wood-derived oil. When using an initial carrier oil, such as mixed cresols, it was calculated that after 6 runs, using the product as recycle oil carrier, the original carrier oil would be reduced to about 9 percent. A series of runs at 250°C to 275°C showed that the product became too thick to use after only four cycles. A temperature of at least 300°C and pressures of 2,700-3,000 psig were needed to obtain a product with acceptable softening point.

OTHER RESEARCH ON BIOMASS LIQUEFACTION

There has been other research on biomass liquefaction by high-pressure, liquid-phase systems, but it appears to be fragmented and scattered. Remarkably, many of the concepts presented by the Bureau of Mines in the early 1970's appear to remain to some extent the "state-of-the-art" in biomass liquefaction, compared for example, with the extensive technology developed for coal liquefaction by Mobil, Exxon, Gulf and others, largely supported by the DOE and some by EPRI.

Battelle Pacific Northwest Laboratories

A fundamental study using pure cellulose (Solka-floc) was performed at Battelle, sponsored by the Division of Chemical Sciences, Processes and Techniques Branch, DOE (3). A series of 129 autoclave experiments analyzed by statistical methods indicated that carbon monoxide, while it promotes the attainment of high yields as claimed by the Bureau of Mines, is not necessary for the reaction to proceed. Analysis of the products by ¹³C-NMR, GC/MS, and gel permeation chromatography indicated that the non-volatile fraction of the oil consists of 44% aromatic carbon and 7% aromatic hydrogen, corresponding to a benzenoid polyaromatic with a substitution ratio of 5:1. However, the oxygen content of the non-volatile fraction and distillable oil is approximately the same. Since the oil contains a series of polyalkylated furans, this suggests that the char is a poly-furan rather than a conventional aphaltene derivative. Volatile products from the oil fraction consists of furans, cyclic ketones, linear and branched alkenes, and phenolics. The high proportion of phenolics relative to normal crude oil could explain the observed highly corrosive nature of the biomass-derived oils.

Albany Biomass Liquefaction Facility

The Albany facility operated on the basic PERC process, so designated because the original work was conducted at the Pittsburgh Energy Research Center. It was operated initially by the Bechtel Corporation, followed by the Rust Engineering Company (the latter for prime contractor, Wheelabrator Cleanfuel Corporation). The process involved reacting biomass in an oil slurry with carbon monoxide and hydrogen at temperatures up to about 380°C and pressures up to 4,000 psig.

The final Albany test run, Test Run No. 12, prior to shutdown and phaseout on June 30, 1981, produced over 11,000 pounds of wood oil is a sustained and controlled run. The oil had characteristics closely approximating the original design basis as shown below in Table 3.

Table 3 -- Summary of Properties of Albany Crude Wood Oil

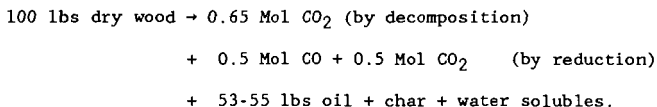
	<u>Design Basis</u>	<u>Run 12 Product</u>
Specific gravity	1.1	1.11
Viscosity	515 cp at 140°F	135 cp at 210°F
Heating value	13,390 Btu/lb (Calculated)	14,840 Btu/lb (measured)

Crude Wood Oil Analysis:

Carbon	72.62	78.9
Hydrogen	7.05	8.51
Nitrogen	0.13	0.5
Sulfur	0.14	0.08
Oxygen	20.05	12.3

Lawrence Berkeley Laboratory (LBL)

This laboratory provided technical assistance to the Biomass Facility at Albany, Oregon. For example, during the earlier period of Albany operations, it provided useful guidance from material balances on what chemical reactions might be occurring (5). It deduced that Douglas Fir wood converted to oil plus small amounts of water-soluble products and char at about 52-55 wt % efficiency. Based on an approximate stoichiometric analysis, the following changes occur.



Carbon monoxide used is about 200 SCF/100 lbs wood or 370 SCF 100 lbs product or 1300 SCF/bbl product. The yield of non-gaseous product can be less than 51% only if carbon monoxide is generated by decomposition of wood or by reaction of wood or its products with water. This appeared to be contrary to observations.

LBL researchers focused their attention on the prehydrolysis of wood to cut down swelling so that wood/water slurries containing up to 25 wt % wood could be pumped (6). This was done at 180°C, 45 min, with 500 ppm sulfuric acid. They used moist chips, water content of 75 wt.% and operated at about pH of 2 in a stirred autoclave. The wood chips disintegrated into fine particles and some courser but friable particles. When the resultant sludge passed through a disc refiner, a pumpable slurry was obtained.

LBL constructed a bench-scale liquefaction unit based upon the above water/oil/wood slurry concept. It was operated with limited success, but ran into plugging problems, possibly due to the small diameter of process tubing. Also, considerable wood oil product dissolved in the large water phase, and the economics of recycling this large water phase or treating it for disposal did not look attractive from the limited experimental data.

Crude Wood Oil Fuel-Burning Tests

Test runs were also made in the Albany facility to simulate the conditions proposed by LBL for its water/oil/wood slurry system, and in fact was the technique that produced the first significant quantities of wood oil. Combustion tests were conducted in a commercial boiler on oils produced by both LBL and PERC process modes at the Pittsburgh Energy Technology Center (PETC). Two barrels, approximately 100 gallons of wood oil from each process, were burned in a 20 Hp Johnson three-pass fire tube boiler designed to transfer 670,000 Btu per hour, with results as follows:

Table 4. Comparison of Heavy Liquid Fuels

	Test Run No. 8 PERC Distillate Oil	Test Run No. 7 LBL Crude Oil	Fuel Oil No. 2	Fuel Oil No. 6
Carbon %	84.5	78.1	87.3	87.0
Hydrogen %	9.5	7.7	12.5	11.0
Nitrogen %	0.2	0.1	--	0.3
Sulfur %	0.2	0.1	0.21	0.70
Ash %	0.2	0.2	--	0.10
Oxygen %	8.4	13.8	--	1.0
Heating value Btu/lb	19,840	17,360	18,610	14,940

Upgrading Crude Wood Oil by Hydrotreating

Currently, Battelle Pacific Northwest Laboratory has a major effort on the development of a hydrotreating process for wood oil product upgrading (7,8). Individual components from the product of direct liquefaction of biomass have been subjected to hydrogenation with a number of transition metal oxide catalysts. Sulfided cobalt-molybdenum has been found to be effective for the hydrodeoxygenation of phenolics. The product of choice from hydro-treating would be the aromatic product which maximizes oxygen removal and minimizes hydrogen consumption.

Other Interest in Biomass Liquefaction

This paper emphasized direct biomass liquefaction in the United States, but would be remiss if it did not point out the high interest in biomass liquefaction in other parts of the world, especially Canada and Europe. Low pressure pyrolysis is being investigated at the University of Sherbrooke, Canada (9). At the Royal Institute of Technology, Sweden, a research project in progress compares the dissolution of coal, peat and biomass in hydrogen donor solvent - tetralin at 350°C to 400°C, cold pressure of nitrogen 5.0 MPa and reaction time 15 to 120 minutes (10). At the University of Saskatchewan, Canada, the liquefaction of aspen poplar wood to produce a proto-oil was investigated (11). In the batch reactor studies, the water to wood ratio emerged as the most important parameter affecting yield and quality of oil. The Department of Scientific and Industrial Research, New Zealand, believes that biomass liquefaction has several inherent advantages over other processes for obtaining liquid fuels (12). The process is rapid and it does not require the production of reducing gases. This should allow smaller scale processing than other processes. Biomass is much less abrasive, and it is softer than coal.

CURRENT BIOMASS LIQUEFACTION RESEARCH AT ARIZONA

The advanced extruder-feeder biomass liquefaction reactor system was designed to experimentally convert wood flour to liquid wood oil fuels by direct liquefaction. The extruder-feeder system developed at the University of Arizona is incorporated into the system to develop 3,000 psig pressure at its discharge and preheat the slurry prior to entering the vertical reactor. As the wood flour slurry enters the reactor it is mixed with superheated steam and carbon monoxide. Gas dispersion as well as heat and mass transfer will be attempted by the use of static mixer elements inside the tubular reactor. The superheated steam is used to heat the wood flour slurry up to the reaction temperature of 350°C almost instantaneously, which is then maintained by the use of electrical band heaters surrounding the reactor. Steam and carbon monoxide also react via the water-gas shift reaction to provide hydrogen for the liquefaction. The liquefaction products are split into the vapor and liquid

fractions, condensed, cooled down and brought to atmospheric pressure by means of the let-down system. Computer control and real-time data acquisition have been implemented for the unit.

The University of Arizona in its limited experimental runs over the past year has consistently produced a low-oxygen crude wood oil, namely, in the 6-8 wt % oxygen range. A few samples of this oil are currently being evaluated for upgrading by hydrotreating by Battelle Pacific Northwest Laboratory (13). This may prove to be a good candidate of wood oil for upgrading to a petroleum-like transportation fuel.

Experimental data for some of the initial runs made at the University of Arizona over the period of August 29, 1985 through July 2, 1986 are shown in Tables 5, 6 and 7. These experimental runs were purposely planned to cover several extremes of operating conditions, namely, pressure, with and without reactant carbon monoxide, and with and without sodium carbonate catalyst. Experimental runs showing effects of residence time, temperature and various feedstock treatments have not yet been performed.

Table 5 -- Continuous Biomass Liquefaction Experimental Conditions

Run No.	Wood Four	Wood Oil Vacuum Bottoms	Feedstock H ₂ O, wt. %	Na ₂ CO ₃ Catalyst, pp hr.	Temp. °C	Press. psi	Feed Rate lb/hr	Residence Time Minutes
1	40	60	8	10	375	3,000	10	72
2	38	62	12.2	2	400	800	6	120
3	38	62	8.8	0	400	1,000	8	90
4	38	62	15	0	400	1,200	7	103
5	40	60	19.7	0	400	2,300	10	72
6	38	62	15	2	400	3,000	3	240
7	40	60	15	0	400	3,000	8	90

Table 6 -- Elemental Analysis of Crude Wood Oil Obtained by Liquefaction

Run No.	Crude Distillate, wt. %	Crude Distillate Analysis, wt. %			
		C	H	O	N
1	24.8	82.71	9.07	6.52	0.13
2	24.7	84.72	9.03	9.03	0.22
3	39.0	84.51	8.66	8.66	0.22
4	27.0	84.12	8.67	8.67	0.34
5	23.4	82.00	8.81	8.81	0.21
6	30.0	81.64	8.46	8.90	0.10
7	27.0	80.00	8.40	10.02	0.00

Table 7 -- Properties of Crude Wood Oil Obtained by Liquefaction

Run No.	Viscosity, C.S., 30°C	Heat of Combustion Btu/lb.	Water Content mg./mol	Aromacity (NMR)	
				Aromatic/Aliphatic, C	H
1	86	16,300	3.08	0.60	0.22
2	135	16,960	3.19	0.68	0.32
3	164	16,510	5.51	0.68	0.30
4	155	16,450	7.71	0.66	0.27
5	100	16,200	5.43	0.69	0.37
6	120	16,020	5.48	0.88	0.31
7	103	15,000	8.69	0.99	0.36

The crude distillate was obtained by vacuum distillation of the reactor effluent at 2-3 mm/Hg absolute pressure and temperatures starting at about 300°F and going up to 550°F. As can be seen it has a reasonably low viscosity at 30°C and a heat of combustion of about 16,000 BTU/lb. The aromatic content as determined by nuclear magnetic resonance is about 40 percent. Most important, the oxygen content has been reduced during liquefaction from about 42 wt.% in the white birch feedstock to about 6-7 wt.%, such that hydrotreating to a transportation fuel should be facilitated.

Even though the extruder-feeder has demonstrated the ability to feed 60 wt.% wood flour/sawdust feedstocks, these initial experimental runs were made with feedstocks ranging from 35 to 42 wt.% white birch wood flour. Thus, if one assumes the heavy vacuum bottoms are essentially inert as a carrier of the feedstock, then one would expect to generate 35 to 40 wt.% (less losses due to oxygen reduction) of crude wood oils in the once-through liquefaction system. Some results to date on the vacuum distillation of the reactor effluent, which contains the Albany vacuum bottoms carrier are as follows:

Table 8 -- Vacuum Distillation of Liquefaction Reactor Crude Product

Run No.	Run Date	Feedstock W.F., wt. %	Reactor Pressure psi	Percentage of Reactor Product Distilled, wt. %	Percentage of Reactor Product Condensed, wt. %
2	2/19/86	36	800	24.7	17.5
3	3/19/86	38	1,000	39.0	25.5
4	4/19/86	38	1,200	27.0	19.0
5	5/29/86	40	2,300	23.4	16.0
6	6/30/86	36	3,000	30.0	20.0
7	7/02/86	40	3,000	27.0	23.9
8	7/30/86	33	600	19.0	9.0
9	7/31/86	33	600	20.0	11.0

The liquefaction of wood to a crude wood oil having a much lower oxygen content and essentially little change in the hydrogen content means that for even a 100% of theoretical conversion to wood oil, there is a large loss of weight of product compared with the feedstock weight. Under certain liquefaction conditions, the elimination of oxygen from wood can occur by about 60 percent as water and 40 percent as carbon dioxide (14). Under other liquefaction conditions, the elimination of oxygen from wood is claimed to occur by about five percent water and 95 percent carbon dioxide (15). The off-gas of the above experimental runs were analyzed, but due to the water present from the steam injection, the ratio of water/carbon dioxide evolved from white birch wood has not yet been determined. Assuming a 50/50 ratio of

water/carbon dioxide evolving in these data, the theoretical loss of weight of wood going from 41.26 wt. % oxygen to 7.0 wt. % oxygen is 48 percent. Thus, 100 pounds of dry white birch biomass can theoretically produce about 52 pounds of crude wood oil, under the above assumption of liquefaction conditions. If one were to apply this theoretical yield to the amount of condensed distillate obtained as listed in Table 8, then yields greater than 100 percent theoretical are obtained. Even changing the assumption on the ratio of water/carbon dioxide rejection from the biomass over a range consistent with known H/C ratios of crude wood oils can only partially account for the high quantities of crude oil distillates obtained. One other conclusion that could be drawn (assuming the experimental data is reasonably correct) was that the Albany black vacuum bottoms are not inert at the liquefaction temperature of 375-400°C. Consequently, the thermal stability and possibility of obtaining distillable products from the Albany black vacuum bottoms were investigated.

The Albany black vacuum bottoms used at the University of Arizona came in drum lots from Albany, Oregon, where it was obtained by fractionating Douglas Fir wood oil in a fairly large vacuum fractionator. This material was used during the period August 29, 1986 through July 2, 1986 until essentially exhausted. A second lot of Albany vacuum bottoms, a brownish-black in color, was used in a "long run" of 52 hours duration conducted July 29-31, 1986. The elemental analysis of these two Albany vacuum bottoms and some related data are as follows:

Table 9 -- Elemental Analyses Related to Feedstocks and Carrier Oils

	Wt. % C	Wt. % H	Wt. % O	Wt. % N	Total CHON
Black Vacuum Bottoms	78.96	6.71	12.05	0.26	97.98
Brown Vacuum Bottoms	81.58	6.25	9.22	0.37	97.42
Distillate Black V.B.	85.21	7.60	5.32	0.23	98.36
White Birch Wood	46.98	5.61	41.26	0.04	93.89

First, to test the thermal stability of black vacuum bottoms, a series of three samples were heated in the absence of other reactants to 400°C for 2, 3 and 4 hours, respectively, in a pressure autoclave. The autoclave was cooled, all products except gases collected, and analyzed. Whereas the fresh Albany black vacuum bottoms were 99-100% soluble in THF, all three of the samples heated to 400°C for 2 to 4 hours showed that in all three cases 50 percent of the original samples were insoluble in THF, indicating a further cross-linking, polymerization, oxidation or carbonization of some type. Equally important, the other 50 wt. % of the original sample appeared to represent about 7 wt. % off-gas at 400°C and about 43 wt. % remaining as a "vacuum bottoms" containing some crude wood oil.

Secondly, when the fresh Albany black vacuum bottoms are further distilled at 2-3 mm/Hg absolute pressure, a total of 22.5 wt. % distilled as the temperature gradually was raised to 550°F, at which point no additional distillate was observable. A total of 16.3 wt. % of the original feed was condensed with 70°F cooling water with the balance being non-condensables at 70°F.

Yields of crude wood oil appear to be from 80 to 100 percent of the theoretical when all of the above data are used in the calculations. The weakest assumptions involve how much additional crude wood oil is derived from the Albany black vacuum bottoms carrier fluid. Another indication of the near-theoretical yield of crude wood oil is the low methane, ethane and hydrogen content of the off-gas, despite the liquefaction temperature being on the high side at 375-400°C.

CONCLUSIONS

A reasonably low-viscosity, low-oxygen crude wood oil can be obtained in the once-through, near-plug flow high-concentration solids vertical reactor system. Experimental conditions to date are on the high side of temperature and residence time, and on the low side with respect to pressure, quantity of steam, quantity of sodium carbonate catalyst, quantity of carbon monoxide reactant and quantity of superheated steam. The experimental unit exhibits good operability and has begun to provide good material balances, such that it appears that future runs can evaluate the many parameters affecting conversion, yield and quality of the crude wood oil.

REFERENCES

1. Appell, H.R. et al., "Converting Organic Wastes to Oil", BuMines RI 7560 (1971).
2. Appell, H.R. et al., "Conversion of Cellulosic Wastes to Oil", BuMines RI 8013 (1975).
3. Molton, P.M. et al., "Mechanism of Conversion of Cellulosic Wastes to Liquid Fuels in Alkaline Solution", Presented at Third Energy from Biomass and Waste Symposium, Sponsored by IGI, Held at Alexandria, Virginia (August 1978).
4. Berry, W.L. and P.L. Thigpen, "Operation of the Biomass Liquefaction Facility, Albany, Oregon", Presented at 13th Biomass Thermochemical Conversion Contractor's Meeting, Arlington, Virginia (October 1981).
5. Davis, H. et al., "Catalytic Biomass Liquefaction Quarterly Report" LBID-272, Lawrence Berkeley, Berkeley, California (April-June, 1980).
6. Ergun, S. et al., "Catalytic Biomass Liquefaction Quarterly Report", LBL-11019, Lawrence Berkeley Laboratory, Berkeley, California (February 19, 1980).
7. Elliott, D.C., "Bench Scale Research in Biomass Direct Liquefaction", Presented at the 14th Biomass Thermochemical Conversion Contractor's Meeting, Arlington, Virginia (June 1982).
8. Elliott, D.C., "Hydrotreating Biomass Crude Oils", Proceedings Annual Biomass Thermochemical Conversion Contractors Meeting, Minneapolis (October 1985).
9. Roy, C. C. et al., "The Pyrolysis under Vacuum of Populus Tremuloides and its Constituents", Presented at Fundamentals of Thermochemical Biomass Conversion: An International Conference, Estes Park, Colorado (October 1982).
10. Hornell, C. et al., "Dissolution of Peat and Wood in Tetralin compared with Coal", Presented at Fundamentals of Thermochemical Biomass Conversion: An International Conference, Estes Park, Colorado (October 1982).
11. Eager, R.G., et al., "Liquefaction of Aspen Poplar to Produce an Oil and Chemicals", Presented at Fundamentals of Thermochemical Biomass Conversion: An International Conference, Estes Park, Colorado (October 1982).
12. Miller, I.J., "Biomass Liquefaction as a Potential Process", Presented at Fundamentals of Thermochemical Biomass Conversion: An International conference, Estes Park, Colorado (October 1982).
13. White, D.H., Personal Communication with D.C. Elliott (August 1, 1986).
14. Espenscheid, W.F., "Liquefaction of Solid Carbonaceous Materials", U.S. Patent 4,052,292 (October 4, 1977).

15. Chen, N.Y. et al., "Liquefaction of Solid Carbonaceous Materials", U.S. Patent 4,247,384 (Issued January 27, 1981).

ACKNOWLEDGEMENT

This research was supported by Department of Energy Contracts DE-AC06-76RLO-1830 (Subcontract B-96249-A-Q from Battelle Pacific Northwest Laboratories) and DOE Contract EW-78-S-05-5679. Special thanks are given to M. Chehab, A. Homaidon, A. Lezzar, D. Joshi and B. Reyes, who performed much of the experimental work. We also appreciated the assistance of Professor N.R. Schott, while on Sabbatical at the University of Arizona. Many undergraduate students too numerous to list have also contributed to this research project and their help is greatly appreciated.

Characterization of Products Formed During
Coliquefaction of Lignin and Bituminous Coal at 400°C

by

Paul Altieri

and

Robert W. Coughlin

Department of Chemical Engineering
University of Connecticut
Storrs, Connecticut 06268

Abstract

The filterable solids from coliquefaction were about 30% benzene soluble compared to about 10% soluble when the same amounts of coal and lignin were reacted individually. In the case of coliquefaction, far more of the benzene-soluble material was also pentane-soluble oil. As a result of coreaction, significant amounts of nitrogen from the coal appeared in the liquid product in contrast to no observable nitrogen in the liquefaction product of coal alone under comparable conditions. Gaseous products were significant and contained CO₂ as a major component. More carbon-14 from the lignin got incorporated into the liquid product during coliquefaction of coal and lignin than in the case of liquefaction of lignin alone under comparable conditions.

Introduction

Recent reports (1, 8) have shown that liquefaction of bituminous coal can occur at temperatures as low as 300°C when the potentially abundant, renewable raw material, lignin, is present in the reaction mixture. Previous processes²⁻⁵ have generally required temperatures above about 400°C in order to rupture carbon-carbon bonds, a necessary step for depolymerization of coal. Lignin degrades thermally at temperatures as low as 300° with the production of substituted phenoxyl radicals. Heredy and Neuworth⁶ and Larsen et al⁷ reported that the presence of phenolic components in the reaction mixture aids the depolymerization of coal resulting in substantial coal liquefaction.

Thus it was hypothesized,⁽⁸⁾ that phenoxy radicals produced by lignin at temperatures ordinarily too low for depolymerization of coal abstract hydrogen from carbon-carbon bonds of coal molecules thereby making them more susceptible to thermal scission.

This paper reports the characterization of the liquid and solid products recovered after co-liquefying coal and lignin in the presence of the hydrogen donor solvent, tetralin. Products were investigated from three separate reactions:

1. Lignin and coal reacted together in tetralin
2. Lignin reacted in tetralin
3. Coal reacted in tetralin

Experimental

Materials And Reagents

Lignin

The lignin used was a "caustic" type obtained from autohydrolysis of aspen. It was purchased from Stake Technology LTD, Ontario, Canada. The lignin was dried in a vacuum oven at 85°C under low pressure (10 torr) for 24 hours and then stored in a dessicator for later use without any further purification.

Coal

Illinois No. 6 bituminous coal (particle size 74-105 micrometers) was obtained from the Pittsburgh Energy Technology Center. This coal has been found to have a 13.6% ash content which was accounted for when computing results on a moisture and ash free basis (maf basis). Crushed coal was sieved to the 74-105 micrometer particle size range, then dried and stored in the same manner as the lignin.

Reagents

All solvents were "Baker analyzed grade" from J. T. Baker Co. except guaiacol which was obtained from Pfaltz and Bauer Co. and tetralin which was obtained from Eastman Kodak Co. Hydrogen and nitrogen gases (98%) were supplied by AERO-All Gas Co.

High Pressure Liquefaction

Tetralin (200 ml), lignin (25 g), coal (25 g), and catalyst were mixed in an inner cylindrical vessel of sheet stainless steel. This was inserted in a one-liter 316 s.s. Magna-drive autoclave manufactured by Autoclave Engineers Inc. The bomb was sealed, pressure tested, flushed with hydrogen, and then pressurized with 1000 psig hydrogen. The system was then heated with agitation at 1500 rpm to 400°C for 1 hour. Approximately 45-60 minutes were required during which time the pressure rose from 1000 psi to 1900-2400 psi. After one hour at the desired reaction temperature, the system was cooled to around 40°C by flowing water through the internal coil for about two hours. Pressure in the cooled reaction vessel ranged

between 700-1000 psig. After venting gases the product material in the liner was removed and transferred to a tared container. Any liquid that remained in the bottom of the autoclave was removed with a pipette and added to the products together with liquid from rinsing the autoclave and liner with known amounts of fresh tetralin.

The product mixture consisting of both insoluble residue and liquid was weighed and then filtered through a tared glass fritted filter (ASTM 10-15). This insoluble, filtered residue was dried at 85°C under vacuum to constant weight.

Determination of Benzene and Pyridine-Soluble Fractions

The filtered residue material was extracted in a tared Soxhlet extraction thimble using benzene until the extract became clear (about 24-48 hours). The thimble was then dried at 85 C under vacuum to constant weight. The weight loss is reported as material which is benzene soluble.

The thimble containing the benzene-extracted solid residue was then extracted with 150 ml pyridine for 24-48 hours. Material soluble in pyridine was computed as weight loss.

Determination of Asphaltenes and Oil

The benzene extract was evaporated and the residue dried to constant weight, then redissolved in a minimum amount of fresh benzene with gentle warming. Then n-pentane (100 ml) was added to precipitate asphaltenes which were filtered and dried to constant weight. The filtrate remaining after asphaltene precipitation was evaporated to recover the "oil" (benzene and pentane soluble).

Carbon-14 Analysis

Various liquid product fractions were analyzed for carbon-14 by New England Nuclear Laboratories using a liquid scintillation spectrometer.

Analysis of Nitrogen Carbon and Hydrogen

Various liquid product fractions were analyzed for nitrogen, carbon and hydrogen content by the American Cyanamid Company. Oxygen content was obtained by difference. Two trials were performed for each sample.

GC/MS Characterization of Evolved Gases

Lignin (25 g), coal (25 g), and tetralin (300 ml) were reacted at 400 degrees centigrade for one hour at 2200 psi in a rocking autoclave (Parr #4021). The procedure was otherwise as discussed above.

After reaction the autoclave was cooled and then connected to the sampling valve of a Hewlet Packard #5985 GC/MS equipped with a stainless-steel column packed with Carbowax. The autoclave vessel was held at $\sim 200^{\circ}\text{C}$ while a small flow of gas was released and periodically sampled for GC/MS analysis. Temperature programming of the GC column from 20°C to 225°C over a time span of 60 minutes permitted adequate separation of components.

Results And Discussion

Table 1 summarizes mass balances for four experiments. The amount of gas formed was computed by difference.

Characterization of Solid Products of Reaction:

Figure 1 summarizes the work up and fractionation of the solid and liquid products of reaction. The individual fractions, P1 through P7 are further identified in Table 2.

Characterization of coal liquids as benzene-soluble and pentane-soluble goes back to Pelipetz et al (9) who viewed solubility in benzene as a measure of the extent to which coal has been hydrogenated; unreacted or partially reacted coal remains insoluble in benzene. Solubility in benzene and pentane is a measure of the "oil" produced. The portion that is soluble in benzene but insoluble in pentane (i.e. precipitated by pentane) is called asphaltenes. Asphaltenes are high-molecular weight intermediate products in coal liquefaction. The presence of asphaltenes in coal-derived liquids has been reported by both Pelipetz (9) and Weller (10). Stern (11) showed that both the quantity and the molecular weight of the asphaltenes present in the coal-derived liquid product affect its viscosity. These methods are also described by Mimal (12). As evident from Figure 1, we also employed pyridine solubility which was used by Whitehurst (13) to represent the extent to which coal is converted to liquid products (13).

The mass of solids filtered from the products of the reactions are plotted in Figure 2 (see Table 3 for experimental conditions). Figure 2 compares the solids from experiment 4-A (in which lignin and coal are co-liquefied) to the sum of the solids filtered in experiment 4-B (in which only lignin is used) plus experiment 4-C (in which only coal is used). The cross-hatched area of each bar graph represents benzene-soluble material (P4) which is greatly increased (by about a factor of four) when lignin is present in the reaction mixture.

Further characterization of the benzene-soluble solids (P4) is shown in Figure 3. Figure 3 shows that when lignin and coal are co-liquefied the production of asphaltenes

(benzene-soluble but pentane insoluble, (P5)) is increased more than the corresponding production of "oil" (soluble in benzene and pentane, (P6)).

The benzene-insoluble residue was partially soluble in pyridine in every case. Co-reacting lignin with the coal does not cause any substantial change in pyridine solubility of the benzene insoluble residue.

Three control experiments (5A, 5B and 5C) were conducted at room temperature but with all other aspects identical to experiments 4A, 4B and 4C. The results shown plotted in Figure 4 indicate essentially no liquefaction took place since the mass of filtered solid product was equal to the mass of coal and/or of lignin charged to the reactor. Benzene soluble solids are only about 2.5g in the case of the control experiments vs about three g for coal and lignin reacted separately at 400°C and about 11 g for the coreaction of coal and lignin at 400°C.

Characterization of Liquid Products:

Liquid products from reactions 4A and 4B were further characterized by analysis for carbon-14 and nitrogen. Because coal contains significant nitrogen but lignin contains very little, nitrogen analysis of liquid products indicates the relative contribution of coal. Because lignin contains significant carbon-14 but coal does not, the carbon-14 content of the liquid indicates the relative contribution of lignin. The half life of carbon-14 is 5730 years and coal was formed from biomass millions of years ago; therefore the carbon-14 remaining in coal is unmeasurable. Any detectable carbon-14 in the liquid must be contributed by the lignin which contains carbon-14 comparable in isotopic abundance to that in carbon dioxide in the atmosphere because the lignin was prepared from wood cut within recent years. Tetralin used as the solvent in the experiments contributed negligible carbon-14 because it was produced from petroleum formed millions of years ago.

Table 4 reports carbon-14 contents of the liquid products for the case when lignin and coal are present in the reaction mixture as well as when only lignin was present in the reaction mixture. The greater concentration of carbon-14 observed when lignin and coal are co-liquefied suggests ruptured coal molecules may incorporate lignin fragments. Coal may also catalyze the liquefaction of lignin or more lignin may get incorporated into the liquid because it reacts with coal fragments rather than self-polymerizing into a solid.

Table 5 shows the elemental analysis of the coal and Stake lignin used in the experiments. Table 6 shows that the liquid filtrate obtained from experiment 4-A when coal and lignin are coreacted contains 0.1% nitrogen compared to no detectable nitrogen in the liquid formed by reaction of coal alone.

The absence of nitrogen in liquid products from coal reacted alone at 400°C (experiment 4B) indicates that the nitrogen-containing portions of the coal molecules were not depolymerized. During co-reaction with lignin under the same conditions (experiment 4A), however, nitrogen does appear in the liquid products indicating more extensive depolymerization of coal molecules. The content of nitrogen (0.1%) indicates a rather uniform disintegration of the coal to form liquid because this value is close to what one would compute using the original nitrogen content of the coal and the apparent fraction of coal that was liquefied. Table 6 also shows the nitrogen content of three distilled fractions of the liquid obtained from experiment 4A. The lowest-boiling fraction is tetralin and contains no nitrogen. It appears the nitrogen is concentrated in the non-distillable residue as might be expected if the nitrogen occurs in the larger molecular fragments contributed by the coal.

Characterization of Gaseous Products

Mass balances (see Table 1) suggest the formation of significant amounts of gases during the reaction. An experiment was performed in which coal and lignin were reacted as in experiment 4-A and the reactor then cooled under pressure. Later, the reactor was heated to about 200°C and the product gas was sampled from the reactor at this temperature and analyzed by GC-MS. Table 7 shows the mass balance for this experiment and the components detected in the vented gas.

Based on the respective peak heights of the GC chromatogram, carbon dioxide was the most abundant gaseous product with water vapor being next. The gases estimated in Table 1 by difference from mass balances contain only a small contribution from water vapor, however, because liquid and solid products were collected and weighed after the reactor was opened at room temperature. The reactor was sampled for gas analysis by GCMS at 200°C, however, at which temperature the gas phase would contain considerably more water vapor than at room temperature.

Acknowledgement

The authors are grateful for support from the National Science Foundation under Grant No. CPE 8303505 and for nitrogen assays performed by the American Cyanamide Company.

References

1. Couglin, R. W., F. Davoudzadeh, *Nature*, 303, 5920, pg. 789-91, (1983)
2. Thorogood, R. M., C. L. Yeh and S. M. Morris, "Scaleup of the SRC-I Coal Liquefaction Process", paper presented at 3rd Annual Conference Coal Gasification and Liquefaction, University of Pittsburgh, August 3-5, 1976.
3. Schmid, B. K. and D. M. Jackson, "The SRC-II Process", paper presented at 3rd Annual Conference Coal Gasification and Liquefaction, University of Pittsburgh, August 3-5, 1976.
4. EDS Coal Liquefaction Process Development, U. S. DOE Report No. EE-2353-2, October 1977, Contract No. Ex-76-C-01-2353.
5. H-Coal Integrated Pilot Plant Phase I-Final Report, U. S. ERDA, No. HCP/T-1554/ (Vol. II) UC-90d, November 1977, Contract No. EX-76-C-01-1544.
6. Heredy, L. A. and M. B. Neuworth, *Fuel*, 41, 221 (1962).
7. Larsen, J. W., T. L. Sanis, B. R. Rodges, *Fuel*, 60, 335 (1981).
8. Coughlin, R. W., and F. Davoudzadeh, *Fuel*, Vol. 65, pg. 95-106 (1986).
9. Pelipetz, J., *Ind. Eng. Chem.* 40, 1259-64 (1948).
10. Weller, S. and J. Pelipetz, *Fuel* 29, 208-11 (1951).
11. Sternberg, W., *ACS Symposium Series*, Vol. 20, 111-122 (1975).
12. Mima, M. J., Analytical Methods for Coal Products, Vol 1, Ch. 19, (1979).
13. Whitehurst, D., Coal Liquefaction Fundamentals, ACS, Washington, D.C., (1980).

TABLE 1
Mass Balances For Liquefaction Experiments

Expt # (1)	Initial Mass Charged (g)			Total Mass Charged (g)	Liquid and Solid Pdts (g)	Gaseous(3) Pdts, % of Total
	Lignin	Coal	Solv.			
2-B(2)	25	25	223.0	277.0	241.6	12.8
4-A	25	25	190.8	240.8	215.3	10.6
4-B	25	0	190.8	215.8	186.2	13.7
4-C	0	25	191.0	216	203.0	6.0

- (1) Reactions run at 400°C for one hour in tetralin and 1000 psi hydrogen initial pressure.
 (2) Reaction run at 300°C for 3 hours in guaiacol.
 (3) Gaseous products are computed by difference.

TABLE 2
Definition of Quantities Used for
Characterization of Reaction Products

- P1 = Mass of Liquid Filtrate (g)
 P2 = Mass of Solid Filtered (g)
 P3 = Mass of Benzene-Insoluble Solids (g)
 P4 = Mass of Benzene-Soluble Solids (g)
 P5 = Mass of Benzene-Soluble Solids Precipitated by Pentane (g)
 P6 = Mass of Benzene-Soluble Solids that are Pentane Soluble (g)
 P7 = Mass of Benzene-Insoluble Solids that are Pyridine Soluble (g)

TABLE 3
Experimental Conditions

Expt #	Mass of Lignin (g)	Mass of Coal (g)	Volume of Tetralin (ml)	Reaction Temp. (C)	Reaction Time (hr)
4-A	25.0	25.0	200	400	1
4-B	25.0	-	200	400	1
4-C	-	25.0	200	400	1
5-A*	25.0	25.0	200	25	100
5-B*	25.0	-	200	25	100
5-C*	-	25.0	200	25	100

* - Control experiments

TABLE 4

Carbon 14 Analysis of Liquefaction Product

<u>Expt #</u>	<u>Reported Activity</u> <u>(1)</u>	<u>Experiment Description</u> <u>(2)</u>	<u>Lignin Molecules/ml</u>	<u>Carbon-14 Atoms/ml</u>
4-A	4.56*	Coal/lignin	4.58×10^{20}	1.98×10^{10}
4-B	3.30*	Lignin	3.82×10^{20}	1.65×10^{10}

- (1) Carbon-14 activity determined by liquid scintillation spectrometry, performed by New England Nuclear Company.
 (2) Reactions performed at 400 C for 1 hour with tetralin used as the solvent.

* Represents value obtained after background count of 2.5 dpm/ml has been subtracted.

TABLE 5

Elemental Analysis of Unreacted Lignin And Coal
(maf basis)

	<u>Stake Lignin</u>	<u>Illinois No. 6 Coal</u>
% C	60.58	82.20
% H	5.30	5.20
% O	34.11	6.81
% N	-	1.38
% S	-	4.15

TABLE 6

Results of Nitrogen Analysis of Liquid Filtrate Products⁽¹⁾

<u>Experiment</u>	<u>% Carbon</u>	<u>% Hydrogen</u>	<u>% Nitrogen</u>
4-A*	76.6	5.9	0.1
4-B**	76.3	6.1	-

Atmospheric Distillation of Liquid Product From Experiment 4A

<u>Fraction #</u>	<u>Boiling Range (°C)</u>	<u>Volume of Fraction (ml)</u>	<u>% Nitrogen</u>
1	188 - 190	130	-
2	192 - 195	5	.04
3	> 195	-	.34

* Coal and lignin co-liquefied at 400 C.

** Coal alone reacted at 400 C.

(1) Nitrogen analysis was performed by American Cyanamid Co.

TABLE 7

Characterization of Vented Gas for Experiment # 6-A

Expt# (1)	Initial Mass			Total Mass Charged (g)	Liquid and Solid Prod. (g)	Gaseous (2) Products,% of Total
	Lignin	Coal	Solv.			
6-A	24.8	25.0	220.8	270.6	244.0	9.98

- (1) Reaction run at 400C for 1 hour in tetralin and 1000 psi hydrogen initial pressure.
 (2) Gaseous products computed by difference.

Components detected in gas:

Major: CO₂, H₂O, CH₃OH

Minor: bicyclo(7,1,0)decane
 naphthalene
 1-nonyne
 tetralin
 methyl thiofurate

Figure Captions

- Flow diagram of treatment and characterization of solid and liquid products.
- Benzene solubility of solids filtered from products of experiments 4A, 4B and 4C. P3-benzene-insoluble portion. P4-benzene-soluble portion.
- Pentane solubility of benzene-soluble material extracted from solid products of reaction. P5-pentane-insoluble portion. P6-pentane-soluble portion.
- Benzene solubility of products from control experiments conducted at room temperature. Compare to Figure 2.

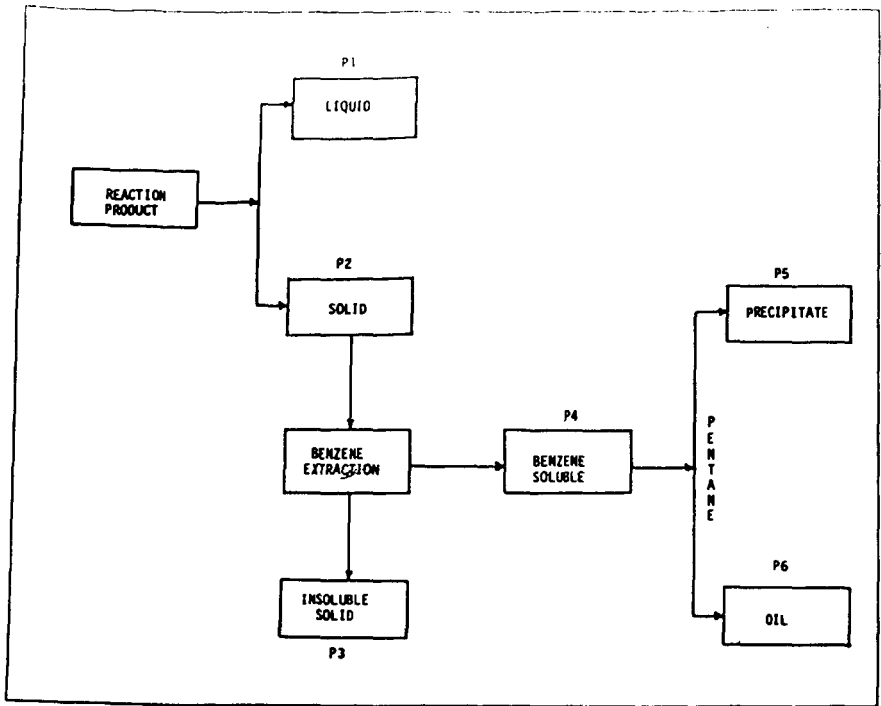


FIGURE 1

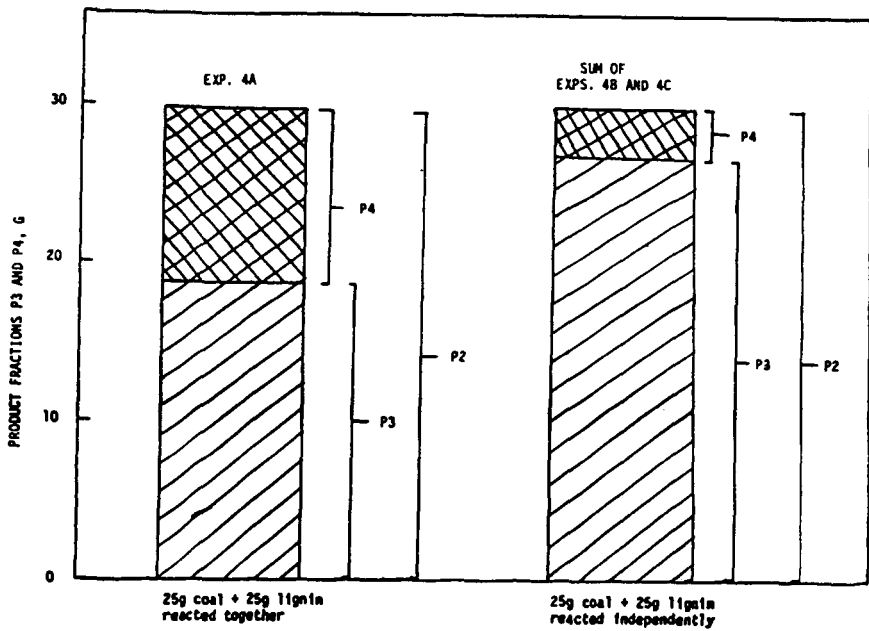


FIGURE 2

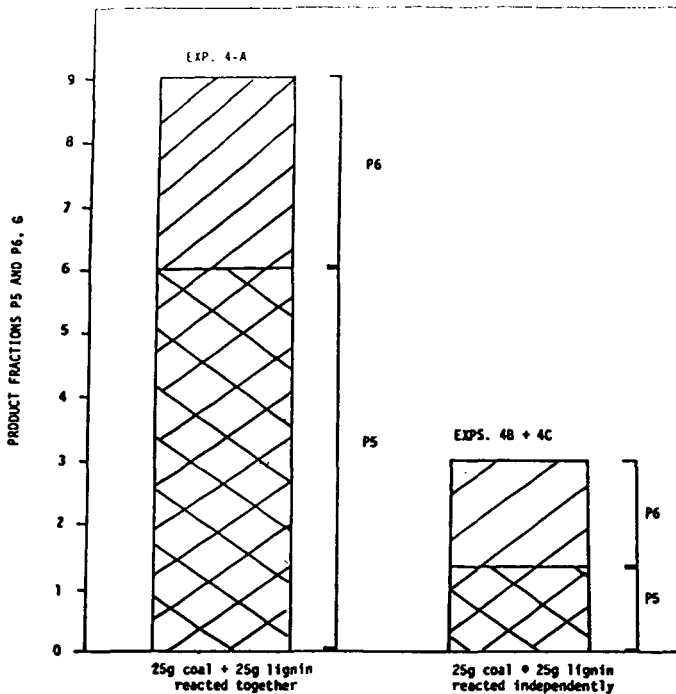


FIGURE 3

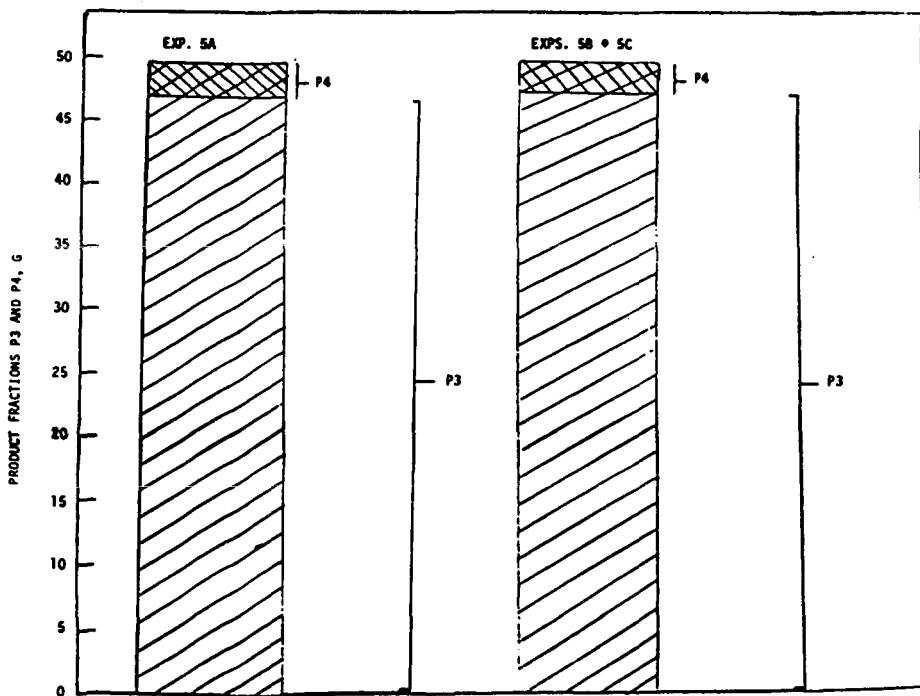


FIGURE 4

DEHYDRATION OF CARBOHYDRATES IN SUPERCRITICAL WATER

Ivan Simkovic, Tongchit Leesonboon,
William Mok, and Michael Jerry Antal, Jr.

Hawaii Natural Energy Institute and Department of Mechanical
Engineering, University of Hawaii, Honolulu, Hawaii 96822

INTRODUCTION

The State of Hawaii is a leading producer of sugarcane and pineapples. The phytomass waste that results from this production is mainly burned to generate electric power. To use lignocellulose materials more effectively some programs are under development. One of the most promising seems to be the conversion of phytomass under pressure and temperature higher or near the critical point of the solvent into chemicals. Near this point the chemical and physical properties of solvent are both liquid- and gas-like and the fluid could be very useful for production of chemicals with higher yields and selectivity obtained using more conventional conditions. The factors affecting supercritical (SC) processing are solvent, catalyst, parameters of the reactor and accesibility of substrate.

The dehydration of cellulose and chitin in supercritical acetone resulted in the formation of anhydrosugars with acceptable yields (1). We used water as a solvent because of its excellent characteristics as a solvent for carbohydrates, its ionic strength, and lower solubility of dehydration products. The reactions which we could suppose to take place under SC conditions in the presence or without inorganic acids or bases are mutarotation, epimerization, dehydration, degradation reaction to levulinic acid, saccharinic acids, as well as, aldol- and retro-aldol reaction. From all the products the most important seems to be 1,6-anhydro- -D-glucopyranose, 5-hydroxymethylfuraldehyde, 2-furaldehyde, and levulinic acid.

Most of the authors who studied production of chemicals from phytomass or its model compounds under SC conditions used batch or semi-continuous reactors (1-6). The negative effect of these reactors on reactions taking place are diminished heat transfer, lower reproducibility, and industrial applicability in comparison to flow reactors. In this paper we discuss the processing of D-glucose using the SC flow reactor under sub- and supercritical conditions.

EXPERIMENTAL

Prior to the initiation of flow, the system is brought up to pressure by an air compressor. Premixed reactant solutions were pumped into the reactor at a controlled flow rate by an HPLC pump. The solution flow through the reactor, pass a 10 port valve dual loop sampling system, and is collected in product accumulator. The flow of products into the accumulator displaces air through a back-pressure regulator which maintains the reactor system at the desired pressure.

The reactant flow is rapidly heated to reaction temperature by the entry heat guard, and maintained at isothermal conditions by a Trans-temp Infrared furnace and an exit heat guard. Samples captured in 5.4 ml sample loops are released into sealed, evacuated test tubes for quantitative analysis by GC, GC-MS, and HPLC instruments within the laboratory. The outer annulus of the reactor is a 4.572 mm ID Hastelloy C-276 tube, and the inner annulus is a 3.175 mm OD sintered alumina tube, giving the reactor an effective hydraulic diameter of 1.4 mm. The alumina tube accommodates a movable type K thermocouple along the reactor's axis, which provides for the measurement of axial temperature gradients along the reactor's functional length. Radial temperature gradients are measured as differences between the centerline temperatures and temperatures measured at 10 fixed positions along the outer wall of the reactor using type K thermocouples. The entire reactor and sampling system is housed in a protective enclosure which can be purged of air (oxygen) during studies involving flammable solvents (such as methanol).

The reactor apparatus can be characterized by the following representative nondimensional numbers: $Re = 420$, $Pr = 1.86$, $Sc = 0.86$, $Pe_h = 776$ (thermal diffusion), $Pe_m = 358$ (species diffusion), and $Da = 0.40$. We have determined from the temperature profile of the reactor during operation that radial temperature gradients within the annular flow reactor are negligible. A computer program, which accurately accounts for the effects of the various fluid (solvent, solvent and solute, air) compressibilities on flow measurements, calculates mass and elemental balances for each experiment.

RESULTS AND DISCUSSION

Results of experiments probing the dehydration chemistry of D-glucose in SC water ($P = 34.5$ MPa) are summarized in Table 1. We began the first experiment at 200°C . As can be seen under this condition no dehydration products were observed and only a small amount of D-glucose was epimerized to D-mannose. At 250°C we observed 5-hydroxymethylfuraldehyde as the only dehydration product. The presence of sulphuric acid or sodium hydroxide increased the conversion of substrate. The acid increased the yield of dehydration product and also 2-furaldehyde occurred as product of pentose dehydration. On the other hand, base decreased the yields of furan derivatives and produced lactic acid as a beta elimination, benzoic acid rearrangement, and retro-aldol reaction product. The decrease of flow rate and omission of catalysts increased the yield of 5-hydroxymethylfuraldehyde, as well as the conversion. A further increase of temperature to 275°C increased the conversion of substrate and yield of dehydration product. The presence of acid decreased yield of furan derivatives. In the presence of sodium hydroxide lactic acid was the predominant product. At 300°C and in absence of catalyst the yield of furan derivatives increased further. These results confirm that water is more selective for dehydration when used without catalyst in the SC flow reactor. In some experiments we were not able to identify some degradation products. This resulted in lower carbon balances than have been reported in our earlier work.

When the reaction was run under supercritical conditions (385°C, residence time of 24 seconds) the yield of furan derivatives decreased dramatically and products of retro-aldol reaction (acetol and formaldehyde) were observed. The levulinic acid was probably destroyed in this way. Under SC conditions gaseous products were also observed. Their presence indicate that decarbonylation, decarboxylation, and other fragmentation reactions were taking place. These were probably due to homolytic reaction processes.

CONCLUSIONS

The reactions of D-glucose at 34.5 MPa and temperature interval from 200 to 385°C in SC flow reactor are epimerization, dehydration, degradation to acids, and retro-aldolization. The experiments confirmed that water when used without catalyst is more selective for dehydration. Further research will follow to increase the yield of selected products.

REFERENCES

1. P. Koll and J. Metzger, *Angew. Chem.*, 1978, 17, 754-755.
2. P. Koll, B. Bronstrup, and J. Metzger, *Holzforschung*, 1979, 33, 112-116.
3. A. Calimli and A. Olcay, *Holzforschung*, 1978, 32, 7-10.
4. E. C. McDonald, J. Howard, and B. Bennet, *Fluid Phase Equilibria*, 1983, 10, 337-344.
5. R. Labrecque, S. Kallaguene, and J. L. Graudmalson, *Ind. Eng. Chem. Res. Dev.*, 1984, 23, 117-182.
6. M. T. Klein and P. S. Virk, *Ind. Chem. Fundam.*, 1983, 22, 35-46.

TABLE 1

Processing of D-Glucose in SC Flow Reactor at 34.5 MPa

PRODUCT	YIELD (%) ^a										
	52	24	11	3	20	8	1	1	1	1	--
$C_6H_{12}O_6$ ^b	--	--	4	2	2	1	1	--	--	--	--
$C_6H_{12}O_6$ ^c	--	23	27	25	5	31	18	5	21	3	
$C_6H_6O_3$ ^d	--	--	--	--	9	--	10	12	--	13	1
$C_5H_4O_2$ ^e	--	--	--	--	--	10	--	--	81	--	--
$C_3H_6O_3$ ^f	--	--	--	--	--	--	--	--	--	23	
$C_3H_6O_2$ ^g	--	--	--	--	--	7	--	--	--	10	
$C_2H_4O_2$ ^h	--	--	--	--	--	--	--	--	--	36	
CH_2O ⁱ	--	--	--	--	--	--	--	--	--	--	
CATALYST ^j	--	--	--	--	H ₂ SO ₄	NaOH	--	H ₂ SO ₄	NaOH	--	--
TEMPERATURE ^k	200	250	250	250	250	250	275	275	275	300	385
RESIDENCE TIME ^l	41	38	76	38	38	35	36	36	36	49	24
CONVERSION (%)	5	38	57	53	89	62	82	97	98	97	97 ^m

^a100 (moles of product/moles of reactant converted). ^bD-Mannose. ^cD-Fructose. ^d5-Hydroxymethylfurfuraldehyde. ^e2-Furaldehyde. ^fLactic acid. ^gAcetol. ^hGlycerinaldehyde. ⁱFormaldehyde. ^j5 mm of catalyst. ^kDegrees of Centigrade. ^lSeconds. ^mAlso gaseous products: Carbon monoxide (9.3 %), carbon dioxide (55.7 %), hydrogen (34.5 %), methane (0.2 %), ethylene (0.3 %), and ethane (0.1 %).

PYROLYSIS AND SOLVOLYSIS OF BIOMASS IN SUPERCRITICAL FLUID SOLVENTS

Susan H. Townsend and Michael T. Klein

University of Delaware
Department of Chemical Engineering
Newark, DE 19716

ABSTRACT

The reactions of diaryl ethers and alkanes were examined in water at varying densities. The ethers, namely benzyl phenyl ether (BPE), phenethyl phenyl ether (PPE) and dibenzyl ether (DBE) underwent parallel pyrolysis and hydrolysis. The former paths led to the usual products described in the literature, whereas the latter led to benzyl alcohol plus phenol, phenethyl alcohol plus phenol and two mols of benzyl alcohol for BPE, PPE and DBE, respectively. 1,2-Diphenylethane (DPE) and 1,3-diphenylpropane (DPP) fragmented according to the neat pyrolysis pathway only, even at the highest water density studied.

The solvolysis was evidently substitution at a saturated carbon atom to which was attached a heteroatom-containing leaving group. Kinetics analysis of the DBE experiments allowed decoupling of the pyrolysis and solvolysis rates, which further permitted correlation of the solvolysis rate constant with the solvent dielectric constant. Good correlation on this Kirkwood plot suggests the solvolysis proceeds through a transition state that is more polar than the reactants.

INTRODUCTION

The extreme pressure-volume-temperature behavior of fluids at or near their critical point has focussed considerable attention on the extraction of volatiles from, and synfuels-related processing of, high molecular weight, low-volatility materials including biomass [10]. More recently, it has been established that reaction in and with the solvent might assist [1, 7, 15]. However, information about the kinetics and mechanisms controlling these reactions is usually obscured during experiments with actual biomass by the complexity of the substrate and its structure. This motivates the use of model compounds whose structures and product spectra are well enough characterized to allow the deduction of reaction pathways, kinetics and mechanisms.

The present report is of a probe into the effect of supercritical water on the reaction paths of the

diaryl ethers BPE, PPE and DBE and the diaryl alkanes DPE and DPP. The thermal reactions of these compounds having been well studied previously, they afforded an excellent opportunity to explore the effect of supercritical water on their reactions.

EXPERIMENTAL

The model compounds were reacted neat and in water at conditions summarized in Table 1. The reduced density of water ($\rho_{r,w} = \rho/\rho_{c,w}$) ranged from 0.0 to 2.1. Except for PPE, the reactants, solvents, and GC standards were commercially available and used as received. PPE was synthesized according to the method of Mamedov and Khydyrov [8].

A typical experimental procedure was as follows: measured amounts of the reactant, solvent and the demonstrably inert [15] internal standard biphenyl were loaded into "tubing-bomb" reactors comprising one 1/4 in. stainless steel Swagelok port connector and two end caps. These constant volume batch reactors had a volume of 0.59 cm³. Sealed reactors were immersed into a fluidized sand bath and reached the desired reaction temperature, ± 2 °C, in about 2 minutes. After the desired time had passed, the reactions were quenched by immersion in a cold water bath.

Reaction products were collected as a single phase in acetone. Subsequent product identification was by GC-MS; and routine quantitation was by gas chromatography on an HP 5880 instrument equipped with a 50 M SE-54 or DB-5 fused silica capillary column and flame ionization detector. Response factors were estimated by analysis of standard mixtures.

RESULTS

Experimental results are presented in sections allotted to each model compound. Within each section, results are presented in terms of reaction products and kinetics, first for pyrolysis and then for reaction in water.

Benzyl Phenyl Ether. Neat pyrolysis of benzyl phenyl ether (BPE) at 332° C led to phenol and toluene as stable primary products, as indicated by their positive initial and zero final slopes in Figure 1, a plot of molar yield ($n_i/n_{1,0}$) vs. reaction time. Minor products included, in order of decreasing yield, o-hydroxydiphenylmethane (OHD), p-hydroxydiphenylmethane (PHD), diphenylmethane, benzaldehyde, benzene, 1,2-diphenylethane and t-stilbene. Linear regression showed the apparent first-order disappearance rate constant for BPE at 332° C to be $9.45 \times 10^{-4} \text{ s}^{-1}$.

BPE reaction in water, at 332° C and an overall water loading $\rho_{r,w} = 1.6$, was almost four times as fast as neat pyrolysis at the same reaction temperature. Figure 1 also illustrates the differences

between the product spectra for neat pyrolysis of BPE and its reaction in water at $\rho_{r,w}=1.6$. Benzyl alcohol, produced in only trace quantities during neat pyrolysis, was a major hydrolysis product. After reaching its maximum yield of 0.45 at 8 minutes, benzyl alcohol underwent secondary reaction to extinction by 45 minutes.

The ultimate yields of the stable products OHD and PHD were also dependent upon $\rho_{r,w}$. The maximum OHD yield of 0.098 observed during neat pyrolysis at 332° C was about one third of the value of 0.26 observed from reaction in water at $\rho_{r,w}=1.6$. Similarly the yield of PHD increased from a value of 0.05 after 45 minutes during neat pyrolysis to a value of 0.18, after only 30 minutes, during reaction of BPE in water.

The effect of $\rho_{r,w}$ on reaction of BPE in water is illustrated in Figure 2 as a plot of product selectivity ($s_i=y_i/x$) vs. $\rho_{r,w}$ for a constant reaction time of 5.6 minutes. BPE conversion (x) increased monotonically with reduced water density from a value of 0.85 at $\rho_{r,w}=0.0$ to essentially unity for $\rho_{r,w} \geq 1.5$. Selectivity to the pyrolysis product toluene decreased with increasing water density from 0.25 at $\rho_{r,w}=0.0$ to 0.05 at $\rho_{r,w}=2.1$. Selectivity to phenol, which resulted from both pyrolysis and solvolysis, increased from a low value of 0.58 at $\rho_{r,w}=0.0$ to 0.80 at $\rho_{r,w} \geq 1.1$. Selectivity to benzyl alcohol increased from 0.0 at $\rho_{r,w}=0.0$ to a maximum of about 0.50 at $\rho_{r,w}=1.2$, at which point secondary reactions of benzyl alcohol were significant by 5.6 minutes. Furthermore, but not illustrated in Figure 2, the selectivity to both OHD and PHD increased, as $\rho_{r,w}$ increased from 0.0 to 2.1, from lows of 0.08 and 0.03 to highs of 0.21 and 0.13 for OHD and PHD, respectively.

These results suggest that reaction of BPE in water is a combination of a thermal pathway leading to phenol and toluene and a hydrolysis pathway that yields phenol and benzyl alcohol. The thermal pathway is like that reported for BPE thermolysis by Brüker and Kölling [2], Schlosberg et al. [13], Sato and Yamakawa [11] and Kamiya et al. [5]. The hydrolysis reaction is the addition of one mol of water to one mol of BPE producing one mol each of phenol and benzyl alcohol. Selectivity to the hydrolysis pathway increased with increases in reduced water density.

Phenethyl Phenyl Ether. The major primary products from the neat pyrolysis of phenethyl phenyl ether (PPE) were phenol and styrene. Styrene underwent secondary decomposition to ethyl benzene, toluene, benzene and other minor products. PPE reaction in water also led to phenol and styrene, but in addition afforded phenethyl alcohol. Reactions in $H_2^{18}O$ showed incorporation of the label into the phenethyl alcohol.

The influence of $\rho_{r,w}$ on the selectivity to products at 413° C is summarized in Figure 3 as a plot of s_i vs. $\rho_{r,w}$ for a constant reaction time of 16 minutes. PPE conversion was about 0.40 at $\rho_{r,w}=0.0$ and leveled off at 0.25 for $\rho_{r,w}\geq 0.2$. Selectivity to styrene increased from 0.29 at $\rho_{r,w}=0.0$ to an average value of 0.52 for $\rho_{r,w}\geq 0.2$. Selectivity to phenol averaged at about 1.0. The selectivity to phenethyl alcohol increased from essentially zero at $\rho_{r,w}=0.0$ to 0.06 at $\rho_{r,w}=1.4$.

These results suggest that the overall reaction of PPE in water is by two paths, the first of which being pyrolysis to phenol and styrene and the second of which being hydrolysis to phenol and phenethyl alcohol. The neat pyrolysis pathway is identical to that observed by Klein and Virk [6]. The hydrolysis of PPE was equivalent to the addition of one mol of water to one mol of PPE to produce one mol each of phenol and phenethyl alcohol.

Dibenzyl Ether. Neat pyrolysis of dibenzyl ether (DBE) at 374° C led to toluene and benzaldehyde as major primary products. Its reaction in water at 374° C led to benzyl alcohol, toluene, benzaldehyde, and oligomers. DBE decomposition in water at $\rho_{r,w}=1.6$ was about 3.5 times as fast as neat pyrolysis; benzyl alcohol was the major and essentially the only primary product at this water density. The yield of benzyl alcohol reached a maximum and then decreased at longer times as it reacted to oligomers. The foregoing suggests that DBE reaction in water comprises two parallel pathways, with the first being identical to the neat pyrolysis reported by Schlosberg et al. [12] and also thermolyses in hydrogen donor noted by Brücker and Kölling [2], Cronauer et al. [3] and Simmons and Klein [14]. The second pathway is hydrolysis of one DBE mol to two benzyl alcohol mols.

1,2-Diphenylethane. Neat pyrolysis of 1,2-diphenylethane (DPE) at 500° C produced toluene as the major and primary product; t-stilbene, benzene, ethyl benzene, phenanthrene, and diphenylmethane were all minor primary products. Trace amounts of styrene and triphenylethylene were also present.

Reaction of DPE in water at 500° C and $\rho_{r,w}=1.4$ also led to toluene as the major primary product. Observed minor products were those formed during neat pyrolysis. Products' yields from neat pyrolysis and reaction in water were virtually identical. Thus, no additional pathways were identified for the reaction of DPE in water.

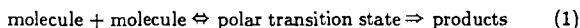
1,3-Diphenylpropane. Neat pyrolysis of 1,3-diphenylpropane (DPP) at 420° C led to toluene and styrene; styrene underwent secondary conversion to other products including ethyl benzene.

Minor products included 1,2-diphenylethane, benzene, and n-propyl benzene, all present in molar yields of less than 0.05. Reaction of DPP in water at 420° C and $\rho_{r,w}=1.6$ led to the same products in approximately the same molar yields as did pyrolysis. Thus pyrolysis was the lone operative pathway during reaction of DPP in water.

DISCUSSION

Reaction of the diaryl ethers BPE, PPE and DBE in water was via parallel pyrolysis and solvolysis pathways. The diaryl alkanes DPE and DPP, on the other hand, fragmented by only a neat pyrolysis pathway, even at the largest $\rho_{r,w}$ studied. Since all of the model compounds pyrolyse by a set of free-radical elementary steps, it is reasonable to suspect that solvolysis does not proceed through a transition state involving water and a thermally generated radical. In fact, the empirical observation that solvolysis occurred between water and an organic molecule with a saturated carbon to which was attached a heteroatom-containing leaving group suggests the chemistry may be like the classic liquid-phase nucleophilic substitution at saturated carbon. Solvolysis involving supercritical methanol and also a N-containing organic has been observed also [1]. Note that heterocyclics, devoid of saturated carbons, did not undergo solvolysis. Another mechanism must therefore govern the solvolysis reaction.

Thus the transition state is likely more polar than the reactants, which are neutral molecules. The class of reaction illustrated in Equation (1)



is amenable to division of the free energy of activation ΔG^\ddagger into an electrostatic and a non-electrostatic part, the former being influenced by the solvent dielectric constant as developed in the classic Kirkwood analysis. For the present reactions, where the activated complex is more polar than the reactants, the solvolysis rate constant should increase with increasing solvent dielectric constant [9] and afford a linear correlation of $\ln k_s$ with the function $(\epsilon-1/\epsilon)$.

The kinetics data for reaction of DBE in water at 374° C were reduced for pyrolysis and solvolysis rate constants for each $\rho_{r,w}$ studied. The solvolysis rate constant and Franck's [4] measurements of ϵ vs. ρ for water allowed construction of the Kirkwood plot of Figure 4. The linear relationship between $\ln k_s$ and $\rho_{r,w}$ supports the proposed polar transition state.

SUMMARY AND CONCLUSIONS

1. Reaction in water of the diaryl ethers was by parallel pyrolysis and solvolysis. The diaryl alkanes afforded only pyrolysis products, even at reduced water densities of greater than 1.4.
2. Whereas the pyrolysis occurred via a set of free-radical elementary steps, the solvolysis was likely via nucleophilic substitution that proceeded through a polar transition state.

REFERENCES

- [1] Abraham, Martin A.; Klein, Michael T.
I & E C Product Research and Development, **24**, 300-306, 1985.
- [2] Brücker, R.; Kölling, G.
Brenstaff-Chemie, **46**, 41, 1965.
- [3] Cronauer, D.C.; Jewell, D.M.; Shah, Y.T.; Modi, R.J.
Ind. Eng. Chem. Fundam., **18**, 153, 1979.
- [4] Franck, E. U.
"Organic Liquids: Structure, dynamics and chemical properties"
John Wiley & Sons, 1978.
- [5] Kamiya, Y.; Yao, T.; Oikawa, S.
A.C.S. Div. of Fuel Chem. Preprints, **24**, 116-124, 1979.
- [6] Klein, M.T.; Virk, P.S.
Ind. Eng. Chem. Fundam., **22**, 35-45, 1983.
- [7] Lawson, J.R.; Klein, M.T.
Ind. Eng. Chem. Fundam., **24**, 203-208, 1985.
- [8] Mamedov, S.; Khydyrov, D. N.
Zhurnal Obshchei Khimii, **32**, 1427-1432, 1962.
- [9] Moore, J.W.; Pearson, R.G.
"Kinetics and Mechanism, 3rd Edition"
John Wiley & Sons, New York, 1981.
- [10] Paulaitis, M.E.; Penninger, J.M.L.; Gray, Jr., R.D.; Davidson, P. (editors).
"Chemical Engineering at Supercritical Fluid Conditions"
Ann Arbor Science, Michigan, 1983.
- [11] Sato, Y.; Yamakawa, T.
Ind. Eng. Chem. Fund., **24**, 12-15, February, 1985.
- [12] Schlosberg, R.H.; Ashe, T.R.; Pancirov, R.J.; Donaldson, M.
Fuel, **60**, 155, 1981.

- [13] Schlosberg, R.H.; Davis, Jr., W.H.; Ashe, T.R.
Fuel, **60**, 201-204, 1981.
- [14] Simmons, M.B.; Klein, M.T.
Ind. Eng. Chem. Fund., **24**, 55-60, February, 1985.
- [15] Townsend, Susan H.; Klein, Michael T.
Fuel, **64**, 635-638, 1985.

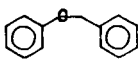
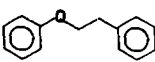
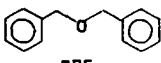
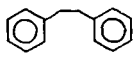
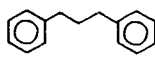
Reactant	T(°C)	$e_{r,w}$	t (min)
 BPE	332 377	0, 1.6 0.0-2.1	0-60 5.6
 PPE	413	0.0-1.4	16
 DBE	374	0.0-1.6	0-60
 DPE	500	0.0, 1.4	0-180
 DPP	420	0.0, 1.6	0-60

Table 1: Summary of Experimental Conditions

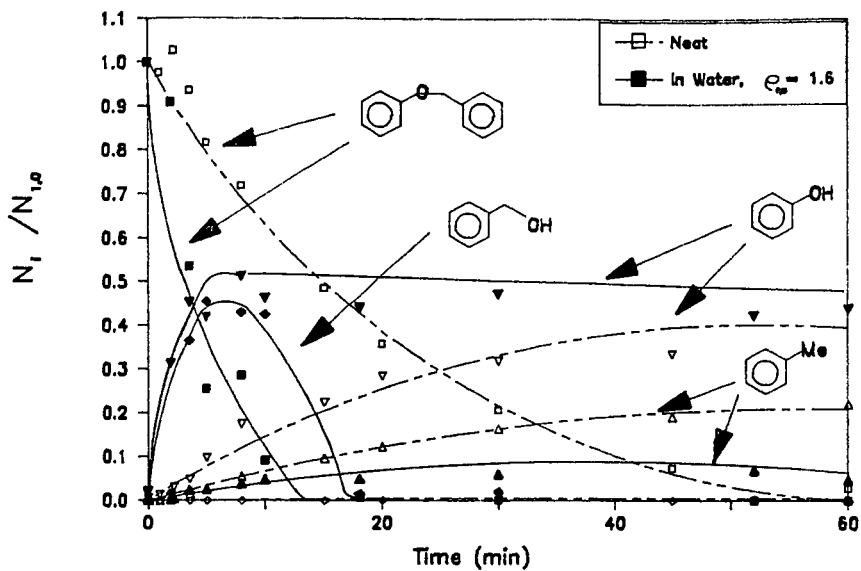


Figure 1: Reaction of Benzyl Phenyl Ether, Neat and in Water
 $T = 332^\circ \text{C}$

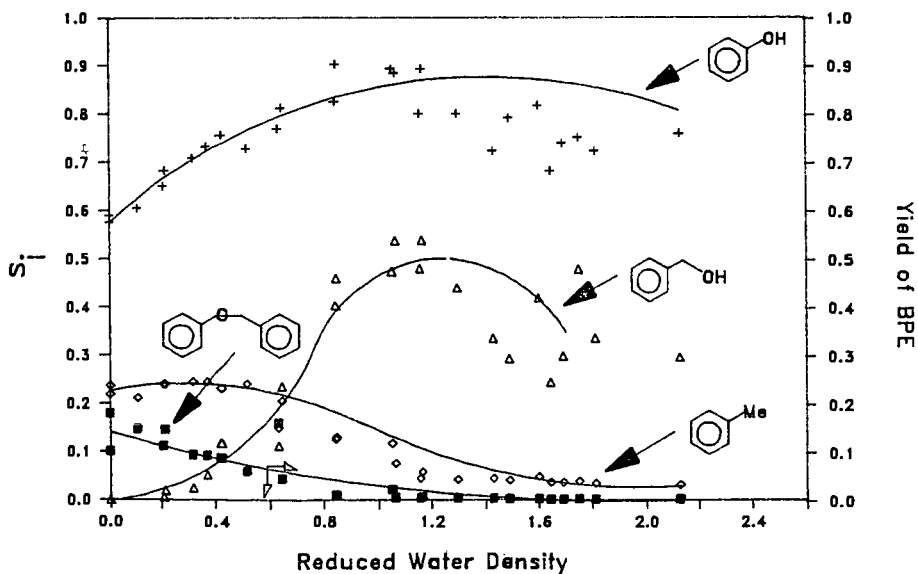


Figure 2: Reaction of Benzyl Phenyl Ether in Water
 $T = 377^\circ \text{C}$, $t = 5.6$ minutes

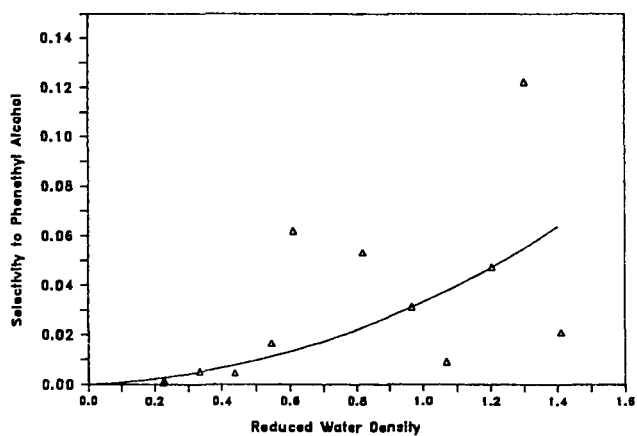
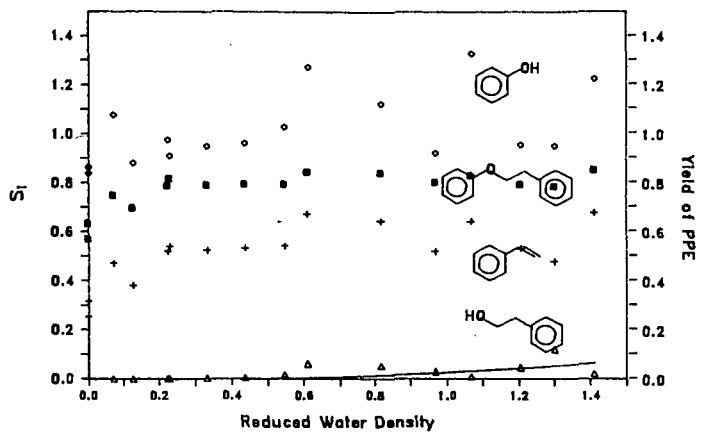


Figure 3: Reaction of Phenethyl Phenyl Ether in Water
 $T = 413^{\circ}\text{C}$, $t = 16$ minutes

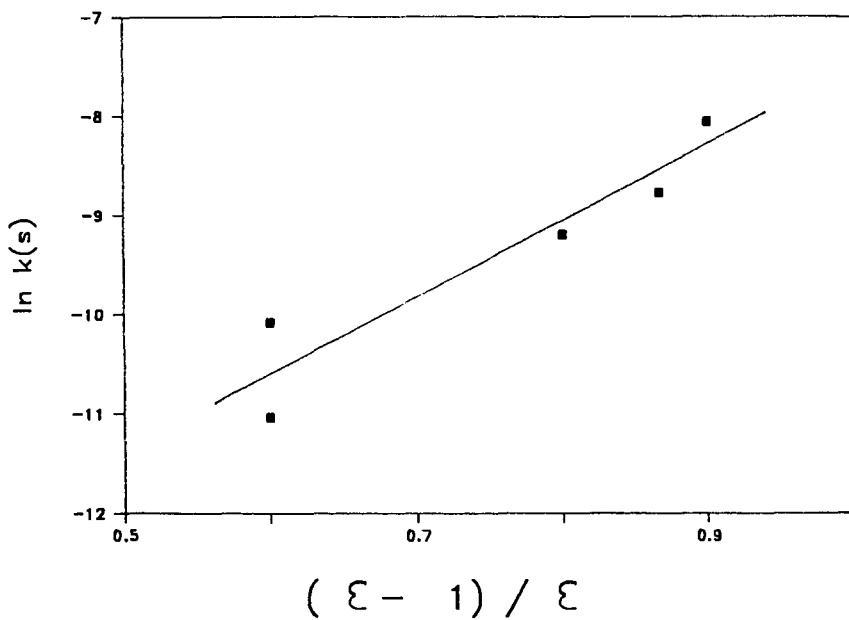


Figure 4: Variation of k_s with Solvent Dielectric Constant
Reaction of DBE in Water, $T = 374^\circ \text{C}$

Formation of Aromatic Compounds from Carbohydrates. X
Reaction of Xylose, Glucose, and Glucuronic Acid in Acidic Solution at 300°C

Olof Theander*

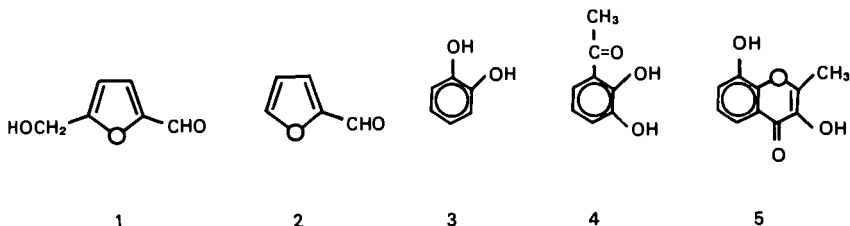
Department of Chemistry and Molecular Biology, Swedish University of
Agricultural Sciences, S-75007 Uppsala, Sweden

David A. Nelson* and Richard T. Hallen

Chemical Sciences Department, Pacific Northwest Laboratory, Richland, WA 99352
USA

INTRODUCTION

For several years our respective groups have investigated the formation of aromatic compounds from carbohydrates in aqueous solution at various pH-values under reflux or hydrothermolytic conditions. For instance, previous papers(1-6) in this series concerned the degradation of hexoses, pentoses, erythrose, dihydroxyacetone, and hexuronic acids to phenolic and enolic components. Of particular interest were the isolation and identification of catechols, an acetophenone, and chromones from pentoses and hexuronic acids at pH 4.5 (1,2). The formation of these compounds, as well as reductive acid(7), was found to be more pronounced than that of 2-furaldehyde(2) under acidic conditions. The aromatic precursors of 3 and 4 were also isolated from these reaction mixtures. This is in contrast to the high yields of 2 obtained from pentoses(8) and hexuronic acids(9) at very low pH. Similar products were obtained in lower yield from glucose and fructose under acidic conditions(10). However, the predominant product of these hexoses was 5-hydroxymethyl-2-furaldehyde (1) as would be expected from prior work(11). Surprisingly, similar products are noted at neutral and even alkaline pH with glucose and xylose(12). Previous hydrothermolytic studies of cellulose indicated that certain aromatic products could be obtained when the pH was maintained in the range of 4-11(13). This suggested that aldol condensation, a prime route for the production of aromatics from saccharides, could function under moderately acidic conditions.



The current research was initiated to study the competition between the formation of phenolic compounds (aldol involvement) and that of furans (dehydration and cyclization). Hydrothermolytic (liquefaction) conditions, 5-7.5 minutes at 300°C, were chosen to examine the effect on potential biomass

materials while exposed to mild acid. Xylose and glucuronic acids were previously found to provide higher yields of phenols than glucose. It is also of increasing interest for those involved with the hydrolysis of biomass, including steaming and autohydrolysis under slightly acidic conditions at 170-250°, to obtain substrates for various fermentation processes or as a pretreatment for other uses. It is very likely that the aromatic products, particularly those formed from pentosans and polyuronides, may have an inhibiting effect on fermentation processes. More information, therefore, is needed concerning the formation of aromatic components and their precursors from the high temperature, aqueous processing of biomass.

EXPERIMENTAL

A series of 3.0 mL capacity tubing autoclaves (316 stainless steel) were used. Each tube was 0.6 x 9 cm and sealed with Swagelok™ fittings. The tubes were charged with 0.27 g sodium glucuronate, 0.19 g D-xylose, or 0.22 g D-glucose, respectively. Buffered acid solutions (2.0 mL) were added to the tubes. For instance, sodium acetate-acetic acid buffer was used for the pH 3 to 4 reactions, while a potassium chloride-hydrochloric acid buffer was used for the pH 1.7-1.9 reactions. The void space of each tube was swept with nitrogen prior to insertion into a 300° sand bath. Interior tube temperature as reached 300° within 2.5 minutes, while quenching to below 100° required only 0.1 minute. The solutions after cooling, which in all nine experiments were dark brown, contained minimal or no precipitate. The tube contents were extracted with ethyl acetate, dried, and the solvent was removed. Gas chromatographic analyses were obtained with a Hewlett-Packard 5880A instrument using a DB capillary column.

RESULTS AND DISCUSSION

The yields of the solvent free extracts are presented in Table 1. Column A shows the standard wt.% yields. Column B was formulated to show a loss of

Table 1. Yields of Ethyl Acetate Extracts After Acidic Treatment of Glucose, Xylose, and Glucuronic Acid at 300°

	pH	Time (min.)	A*	B**
Glucose	1.7	5	37	52
Xylose	1.7	5	27	42
	3.6	5	40	62
	3.6	7.5	38	59
Glucuronic Acid	1.9	5	20	41
	3.0	5	22	45
	3.6	5	20	41
	3.6	7.5	31	63
	4.0	5	15	31

*A equals wt.% based on the amount of carbohydrate.

**B equals wt.% based on glucose or xylose minus 3 H₂O, and glucuronic acid minus 3H₂ and CO₂.

three moles of water for glucose and xylose and a loss of one mole of carbon dioxide for glucuronic acid. This represents the conversion of carbohydrates to furan or phenolic components. The standard yields (column A) give mixed results when pH is compared; i.e., xylose shows higher yields at higher pH, while glucuronic acid does not. This may reflect two different mechanisms, however. These solvent extracted yields are rather close to those obtained under basic conditions(13).

There was some change in pH after the acidic hydrothermolysis of glucose, xylose, and glucuronic acid. The aqueous phase of glucose and xylose increased from pH 1.7 to about 2.6 after 5 min at 300°. Those reactions of xylose buffered at pH 3.6 held that acidity level rather well. The pH of the glucuronic acid reactions tended to increase more than those of xylose regardless of buffer; i.e., pH 1.9 to 3.2, 3.0 to 3.4, 3.6 to 3.8, and 4.0 to 5.2. This probably could be partially attributed to the decarboxylation of the glucuronic acid.

Table 2 presents the quantitative results of those components volatile enough for gc analysis. At low pH the furan compounds predominate when both

Table 2. Major Identified Components of Glucose, Xylose, and Glucuronic Acid After Hydrothermolysis at 300° with Various Times and pH

Component	Glucose* pH 1.7 5 min	Xylose pH 1.7 5 min	Xylose pH 3.6 5 min	Xylose pH 3.6 7.5 min	Glucuronic Acid pH 1.9 5 min	Glucuronic Acid pH 3.0 5 min	Glucuronic Acid pH 3.8 5 min	Glucuronic Acid pH 3.8 7.5 min	Glucuronic Acid pH 4.0 5 min
1	19.9	—	—	—	—	—	—	—	—
2	8.4	46.5	6.9	2.9	2.7	0.7	—	—	—
3	—	—	3.5	6.5	3.8	4.2	16.7	4.0	8.5
4	—	—	—	—	0.5	0.5	4.1	0.9	0.6
5	—	0.4	6.3	8.5	2.3	3.3	—	0.7	—

* Values are reported as mole%; oil yields are reported in Table 1; those values not reported are <0.1%.

glucose and xylose are exposed to 300°. This is not unexpected since all pentoses form 2-furaldehyde(2) in high yield when exposed to aqueous acid solution(14). However, the presence of 2 in the glucose reaction mixture is of interest. The major product obtained from hexoses at elevated temperatures and aqueous acid is 5-hydroxymethyl-2-furaldehyde(1) with minor amounts of 2-(hydroxyacetyl)furan(15). The 2-furaldehyde has been detected after acidic

treatment of fructose(16), glucose(15,17), and is a major component after the thermolysis of cellulose in distilled water(13). One plausible explanation for the formation of 2 may involve loss of formaldehyde(18) from glucose with consequent pentose formation. It should be noted that the pyrolysis of 1 does produce a small amount of 2(19). However, the reaction conditions are sufficiently different to suggest a different mechanism for hydrothermolysis.

The xylose results are also notable with the increase of 3 and 5 at pH 3.6 and longer time. In contrast, 2 decreased with increased pH and time. During previous work(1) with xylose in refluxing acid at pH 4.5, 1,2-dihydroxybenzene (3) was not detected. However, 3 has been detected after xylose was exposed to refluxing caustic solution(12). The presence of 3 in basic solutions of xylose was attributed to retro-aldol and re-aldol reactions since both xylose and glucose yielded the same type of products. Unfortunately, this does not explain the presence of 3 in the acidic hydrothermolysis product, but it has been shown that the aldol reaction can occur at pH 4.0(13). Detection of 3,8-dihydroxy-2-methylchromone(5) has been noted previously in xylose solutions at pH 4.5(1,20). Since 5 is a ten-carbon product, it is presumed that at least two moles of xylose were necessary for its composition. Thus, the mole % values of 5 (Table 2) should be doubled to reflect this. Further support for this was recently demonstrated by E. Olsson, N. Olsson, and O. Theander in unpublished work during the preparation of 5 at pH 5 and 100% from 1-¹³C-pentose (prepared by a Kilij synthesis involving erythrose and K¹³CN). The major distribution of the ¹³C-label was at the 2-methyl and C-8a positions.

The results from glucuronic acid do not appear quite as informative as those from xylose. The 2-furaldehyde content decreased with increasing pH; none was observed beyond pH 3.0. Correspondingly, the amount of phenolic components (3 and 4) increased with pH, but reached a maximum at pH 3.6. The decrease of 3 and 4 after 7.5 min at pH 3.6 may be due to instability of those components toward the thermal conditions, however degradation of 3 at pH 4.5 was negligible at 100% (1). The results at pH 4.0 do suggest a contribution from the decreasing acidity. The decrease of 5 with increasing pH is also of interest since it had previously been isolated from glucuronic acid exposed to pH 4.5 and 100% (1,20). The Table 2 values obtained for 3, 4, and 5 from glucuronic acid may also represent only 50% of the mole percentage since each component may require more than one mole of glucuronic acid for its preparation.

Several unidentified components were also observed in the reaction mixtures of hydrothermolized glucuronic acid and xylose. Unfortunately, isolation attempts were not successful for these products. These components (m/e 164 and 162 from glucuronic acid and xylose, respectively) were found in moderate amounts.

It is evident from the results of this research that phenolic products, especially 3, may be obtained by the acidic hydrothermolysis of xylose and glucuronic acid containing materials. The phenolics and 2-furaldehyde could contribute toward the inhibition of fermentation organisms if acidic pretreatment procedures are not carefully controlled.

ACKNOWLEDGMENTS

This research was supported by the U.S. Department of Energy, Office of Basic Energy Sciences, under contract DE-AC06-76RLO 1830. O.T. thanks the Northwest College and University Association for Science (NORCUS) for the opportunity to conduct research at the Pacific Northwest Laboratory.

REFERENCES

1. T. Popoff and O. Theander, *Carbohydr. Res.*, 1972, 22, 135.
2. T. Popoff and O. Theander, *Acta Chem. Scand.*, 1976, B30, 705.
3. T. Popoff, O. Theander, and E. Westerlund, *Acta. Chem. Scand.*, 1978, B32,1.
4. K. Olsson, P.-A. Pernemalm, and O. Theander, *Acta. Chem. Scand.*, 1978, B32, 249.
5. O. Theander and E. Westerlund, *Acta. Chem. Scand.*, 1980, B34, 701.
6. R. Miller, K. Olsson, and P.-A. Pernemalm, *Acta. Chem. Scand.*, 1984, B38, 689.
7. M.S. Feather, *J. Org. Chem.*, 1969, 34, 1998.
8. C.D. Hurd and L.L. Isenhour, *J. Am. Chem. Soc.*, 1932, 54, 317.
9. E. Stutz and H. Deuel, *Helv. Chim. Acta*, 1956, 39, 2126.
10. T. Popoff and O. Theander, *Acta. Chem. Scand.*, 1976, B30, 397.
11. C.J. Moye and Z.S. Krzeminski, *Aust. J. Chem.*, 1963, 16, 258.
12. I. Forsskahl, T. Popoff, and O. Theander, *Carbohydr. Res.*, 1976, 48, 13.
13. D.A. Nelson, P.M. Molton, J.A. Russell, and R.T. Hallen, *I&EC Product Res. Develop.*, 1984, 23, 471.
14. R.W. Scott, W.E. Moore, M.J. Effland, and M.A. Millett, *Anal. Biochem.*, 1967, 21, 68.
15. R.E. Miller and S.M. Cantor, *J. Am. Chem. Soc.*, 1952, 74, 5236.
16. G. Bonn and O. Bobleter, *J. Radioanal. Chem. Chem.*, 1983, 79, 171.
17. P.C. Smith, H.E. Giethlein, and A.O. Converse, *Solar Energy*, 1982, 28, 41.
18. F.A.H. Rice and L. Fishbein, *J. Am. Chem. Soc.*, 1956, 78, 1005.
19. K. Kato, *Agr. Biol. Chem.*, 1967, 31, 657.
20. G. Lindgren and P.-A. Pernemalm, *J. Liq. Chrom.*, 1980, 3, 1737.

KINETICS OF ALKALINE THERMOCHEMICAL DEGRADATION OF POLYSACCHARIDES TO ORGANIC ACIDS

John M. Krochta, Joyce S. Hudson and Sandra J. Tillin

Western Regional Research Center
Agricultural Research Service
U. S. Department of Agriculture
Albany, CA 94710

INTRODUCTION

Very little research has been done to explore commercial application of the thermochemical degradation of polysaccharide materials to organic acids in alkaline solution. Much of the work on alkaline degradation of polysaccharides has been conducted at 100°C or lower to investigate mechanisms of degradation, reaction termination and the effects of molecular structure (1-4). However, little conversion of polysaccharides to acids occurs at these low temperatures. Most investigations at higher temperatures have involved study of the alkaline pulping process at approximately 170°C (5,6), where polysaccharide degradation is limited and not desired. Chesley et al. (7) proposed a commercial method for producing formic, acetic, glycolic and lactic acids from cellulosic materials. However, optimum process parameters were not clear, kinetic data was not obtained, additional acids were not identified, and most of the starting polysaccharide material was not accounted for. More recent work has provided additional information on the thermochemical degradation of cellulose to organic acids at reaction conditions of practical interest (8,9). However, no additional organic acids were identified, and the acid production data was difficult to interpret because of long heat-up times. No data has been reported for the important polysaccharide, starch, at reaction conditions of practical interest.

The object of this study was to obtain and compare kinetic data for the thermochemical degradation of starch and cellulose to organic acids in alkaline solution. Reaction conditions leading to substantial or complete degradation in short times were selected so that the results could have practical application to the production of organic acids. Data for the formation of seven identified acids were also collected to allow determination of reaction conditions leading to optimum yields. The reaction system used in a previous study (8) was modified to allow rapid attainment of reaction temperatures, thus making kinetic data more easily analyzed.

EXPERIMENTAL

Materials

Starch used in experiments was commercial, food-grade starch (CPC International Inc. Englewood Cliffs, NJ) having a moisture content of 13%. Cellulose was purchased commercially as a highly purified, finely powdered product (Cellulay-Cellulose, United States Biochemical Corp., Cleveland, OH) and had a moisture content of 6%.

Formic acid (88%) (Fisher Scientific Co., Fair Lawn, NJ), glacial acetic acid (J. T. Baker Chemical Co., Phillipsburg, NJ), glycolic acid, L(+)-lactic acid (grade L-1), DL- α -hydroxybutyric acid (sodium salt), α -hydroxyisobutyric acid and DL- α -hydroxyvaleric acid (sodium salt) (Sigma Chemical Co., St. Louis, MO) were used as standards in HPLC and GC analyses. Glutaric acid (Mallinckrodt, Inc., St. Louis, MO) was used as an internal standard in the GC analyses. Boron trifluoride (14% in propanol) (Eastman Kodak Co., Rochester, NY) was used as a derivatizing agent to produce propyl esters of the organic acids for GC analyses.

Reactions

All reactions were performed under nitrogen in a 1-L magnetically stirred autoclave equipped with a cooling coil (Model AFP 1005, Autoclave Engineers, Erie, PA). Each experiment was run by first adding 167g of aqueous solution containing 10g of NaOH to the autoclave and heating the sealed autoclave to the desired temperature plus 5-10°. A well-mixed slurry of 10g of starch or cellulose (moisture free) in 85g of water was then added to an adjacent Kuentzel vessel (Vessel KD-19.3-SS11, Autoclave Engineers, Erie PA) which had tubing with a ball valve leading from its bottom to the stirred autoclave. The tubing extended through the head of the stirred autoclave to below the surface of the alkaline solution. After addition of the starch or cellulose slurry, the Kuentzel vessel was quickly sealed and connected to a nitrogen cylinder. The Kuentzel vessel was pressured to 100 psi above the pressure in the stirred autoclave, and the starch or cellulose slurry was injected into the hot alkaline solution in the stirred autoclave by opening the ball valve. The resulting solution volume was 250ml and it contained 10g of starch or cellulose (0.25M based on glucose monomer) and 10g of NaOH (1.00N). This solution dropped below the target reaction temperature for a short time, but returned to the desired temperature in 1-3 min. The reaction was timed from the moment of injection.

Experiments were conducted at temperatures between 180 and 300°C, and the reactants were held at the selected temperature for varying times to determine the effect of reaction time. The temperature dropped quickly upon flow of water through the cooling coil and removal of the autoclave heater. The time required to cool the reactants to below 100°C was 5-15 min.

After cooling to room temperature, the autoclave was opened and the reaction products were suctioned out. In the case of cellulose, any unreacted material appeared as a solid residue in the reaction solution. Any residue was filtered from the reaction solution and then extracted with water. The filtrate was combined with extract, and an aliquot of the combined solution was titrated for total organic acids. The solid residue was dried at 40°C for 24 hr. in a forced-air oven and then at 98°C for 24 hr. in a vacuum oven. In the case of starch, any unreacted starch was soluble in the alkaline product solution. An aliquot of the solution was titrated for total acids. Unreacted

starch was precipitated quantitatively with acetone (10). A 5.0g aliquot of the product solution was neutralized with 2.0N HCl to pH 7 and 25ml of acetone was added. After sitting overnight, the starch precipitate was separated by centrifugation, washed with 20ml of a 1:3 acetone-water solution, separated again by centrifugation, and finally dried in the same manner as for cellulose solid residue.

High-Performance Liquid Chromatography

Filtered product solutions from reactions with starch and cellulose were analyzed using a Waters Associates high-performance liquid chromatograph model ALC 201 equipped with a refractive index detector model R-401 (Waters Associates, Milford, MA) to identify water-soluble products. This was accomplished by matching retention times of product compound peaks with retention times of standards. A 300 mm x 7.8 mm Aminex HPX-87H organic acid analysis column (Bio-Rad Laboratories, Richmond, CA) was used. Elution was carried out at 60°C using 0.002N H₂SO₄ at a flow rate of 0.5 ml/min. Data acquisition from the chromatographic system was by the Hewlett-Packard integrating recorder model 3388A (Hewlett Packard Co., Palo Alto, CA).

Gas Chromatography

To verify the compounds identified by HPLC, both standards and product solutions were converted to their propyl esters with BF₃-propanol according to the method of Salwin and Bond (11). Analysis of the esterified compounds was performed on a Hewlett Packard 5880A gas chromatograph equipped with a flame ionization detector and a bonded Superox FA (Alltech Assoc., Inc. Deerfield, IL) fused-silica capillary column (25m x 0.25mm I.D., 0.2 μm film thickness). The temperature program was 100°C to 240°C at 5°C/min and 10 min at 240°C. The injector temp was 225°C and the detector temp was 300°C. Carrier flow (He) was 1.0 ml/min. Injection volume was 1μl with a split ratio of 80:1.

RESULTS AND DISCUSSION

Degradation of Starch and Cellulose

An analysis of the data was performed to determine whether starch and cellulose degradation in alkaline solution could be described by second-order kinetics according to the equations:



$$\frac{dC_p}{dt} = -k_a C_p C_a \quad 2)$$

$$\ln \frac{C_a}{C_p} = \ln M + C_{p_0} (M-N) k_a t \quad 3)$$

$$M = C_{a_0} / C_{p_0} \quad 4)$$

$$N = (C_{a_0} - C_a) / (C_{p_0} - C_p) \quad 5)$$

where k_a is the reaction rate constant for starch or cellulose in alkaline solution, C_p is the concentration of starch or cellulose, C_{p0} is the concentration of starch or cellulose at $t=0$, C_a is the concentration of alkali, C_{a0} is the concentration of alkali at $t=0$, t is the reaction time, and N is the stoichiometric reactant ratio between hydroxide ion and polysaccharide.

The catalytic effect of the hydroxide ion would normally be represented as part of the reaction rate constant (k_a) for each temperature, because catalyst concentration normally remains constant. However, in the case of alkaline degradation of starch or cellulose, organic acids are produced which are converted to their salts by the alkali present, thus reducing the hydroxide ion concentration. Therefore, it seemed that this degradation reaction could be represented by second-order kinetics, with the hydroxide ion concentration determined by the stoichiometry of conversion of starch or cellulose to organic acids.

Figures 1 and 2 show experimental data plotted according to Equation 3 on semilogarithmic graphs to determine applicability of second-order kinetics. The linear plots indicate that the results conform to second-order kinetics quite well. Table I shows the reaction parameters determined for each temperature plotted in Figures 1 and 2.

Table I. Reaction Parameters for Alkaline Degradation

T °C	Starch		Cellulose	
	N	k_a liter/mole min.	N	k_a liter/mole min
180	1.44	0.0026	2.09	0.0034
200	1.17	0.0243	1.85	0.0194
220	1.16	0.1334	1.71	0.1189
240	1.16	0.3733	1.59	0.6000

Interestingly, although $M = C_{a0}/C_{p0} = 4.0$ for both starch and cellulose, extrapolating the data plotted in Figures 1 and 2 back to $t = 0$ gives $M = 5.0$ for starch and $M = 4.6$ for cellulose. Thus, M increased from 4.0 to 5.0 for starch and 4.6 for cellulose in very little or no time instead of the expected finite time. Considering that M eventually reaches infinity for the systems studied, this represents a small fraction of more easily degraded polysaccharide. The results of this paper apply to the more resistant fractions of starch and cellulose, which constitute the bulk of those polysaccharides.

Figure 3 shows the reaction rate constants determined from the slopes of the lines in Figures 1 and 2 plotted against the reciprocal of absolute temperature on a semilogarithmic graph. The slope of the line through the points allows determination of the reaction activation energy according to the Arrhenius equation: $k = k_0 e^{-E/RT}$. The value of E determined in this manner is 39,500 calories/mole, which appears to apply equally well to the degradation of starch or cellulose.

Production of Organic Acids

The values of N calculated for starch and cellulose shown in Table I reveal that as these polysaccharides were degraded by alkali, a smaller number of organic acid molecules were formed from each glucose monomer in starch compared to cellulose. This means that the organic acids produced initially from starch had a greater molecular weight than those produced from cellulose. This is illustrated clearly in Figure 4, which shows equivalents of organic acids produced from the degradation of starch or cellulose as a function of time. Although starch and cellulose degrade at the same rate, the rate of total organic acid formation was less for starch, and fewer equivalents of organic acids were produced in a given time from starch than from cellulose. The relative difference decreased as the temperature increased, and at higher temperatures the difference in total equivalents of organic acids produced disappeared at short times. A maximum concentration of approximately 0.45 equivalents/L of total organic acids was produced for both starch and cellulose for the reaction systems studied. Apparently, in starch degradation, the initially larger molecules of organic acids eventually break down into a larger number of smaller organic acids. Therefore, the total organic acid formation for starch ultimately equals that for cellulose. Since the starting concentration of starch and cellulose was 0.25 mol/L based on the glucose monomer, the average equivalent weight for the organic acids produced is $(0.25)(180)/(0.45) = 100\text{g/eq}$. This assumes that all the polysaccharide material degrades to acids.

The HPLC chromatograms of the alkaline degradation products of starch and cellulose were quite similar. Based on retention times of standards, formic, acetic, glycolic, lactic, 2-hydroxybutyric and 2-hydroxyvaleric acids were identified. The GC chromatograms of the propyl esters of the starch and cellulose chromatograms were also quite similar. Since GC gave much better separation of degradation products than HPLC, the GC chromatograms were used to calculate the yields of glycolic, lactic, 2-hydroxybutyric and 2-hydroxyvaleric acids. Formic and acetic were hidden under the GC solvent peak; thus, their yields were determined from the HPLC chromatograms. In addition, 2-hydroxyisobutyric, which was hidden under the HPLC lactic peak, was identified and quantified with GC. Tables II and III give the maximum yields of these acids at several temperatures. The corresponding times at temperatures to achieve maximums are included in the headings.

Table II. Maximum Organic Acid Yields from Degradation of Starch in Alkaline Solution

	Yields(1) %			
	240°C 30 min(2)	260°C 30 min	280°C 20 min	300°C 5 min
Formic	10.5	10.9	10.5	10.2
Acetic	1.6	1.9	2.3	2.1
Glycolic	3.4	4.5	5.3	5.6
Lactic	16.9	17.5	19.1	19.0
2-Hydroxybutyric	2.3	2.9	3.6	3.6
2-Hydroxyisobutyric	2.4	2.6	2.7	2.5
2-Hydroxyvaleric	1.1	1.4	1.6	1.3
Total	38.2	41.7	45.1	44.3

¹Based on starting dry weight of starch

²Maximum not yet attained

Table III. Maximum Organic Acid Yields from Degradation of Cellulose in Alkaline Solution

	Yields(1) %			
	240°C 32 min	260°C 18 min	280°C 6 min	300°C 3 min
Formic	10.8	10.9	10.7	10.2
Acetic	1.6	1.9	1.7	1.7
Glycolic	4.6	4.8	5.5	5.2
Lactic	19.8	19.9	20.4	18.5
2-Hydroxybutyric	3.4	3.3	3.5	3.4
2-Hydroxyisobutyric	2.1	2.1	2.1	1.9
2-Hydroxyvaleric	1.3	1.6	1.4	1.3
Total	43.6	44.5	45.3	42.2

¹Based on starting dry weight of cellulose

Consistent with the results for rates of total acids produced shown in Figure 4, it took a longer time to reach the maximum yields starting with starch compared to cellulose. The maximum yields of the identified product acids at each temperature were quite similar for starch and cellulose starting materials. The time required to reach the maximum yields decreased as temperature increased. The trade-off is the higher operating pressure at higher temperature. The total yields of the identified acids appear to reach an optimum at approximately 280°C for both starch and cellulose.

The similarity in maximum yields for the identified product acids from starch and cellulose suggests similar or identical reaction pathways. The slower rate for acid formation from starch could be explained by dissolved starch polymer or partially degraded starch polymer interfering with additional degradation of initial conversion products. The greater ease with which starch polymer dissolves in alkaline solution compared to cellulose is consistent with this possibility.

Although significant amounts of other organic acids are produced, lactic acid is the major product for the reaction conditions studied. As well as having numerous direct uses, lactic acid has the potential of being an important intermediate in the production of other valuable products (12, 13). Preliminary economic analysis indicates that production of lactic acid from alkaline degradation of cellulose has economic merit (9). It is also conceivable that all the hydroxy acids produced could be used together without separation to produce polyester materials.

CONCLUSIONS

Starch and cellulose can both be thermochemically degraded in alkaline solution to water soluble compounds of relatively low molecular weight. (A parallel study examines more completely the nature of these compounds (14).) Both starch and cellulose degradation processes can be described by second-order kinetics, with the hydroxide ion concentration determined by the stoichiometry of polysaccharide conversion to organic acids. The thermochemical degradation activation energy in alkaline solution for both starch and cellulose is 39,500 calories/mole.

The production of organic acids from starch proceeds more slowly than from cellulose. Ultimately, however, the yields of acids are quite similar from both. Formic, acetic, glycolic, lactic, 2-hydroxybutyric, 2-hydroxyisobutyric and 2-hydroxyvaleric acids are produced in significant amounts. The maximum yield of lactic acid is approximately 20%, and the maximum sum total yield of all identified acids is approximately 45% for the conditions investigated.

Increasing the yields of the desirable acids produced from the thermochemical, alkaline degradation of polysaccharides will require additional understanding of the reaction mechanisms and kinetics involved. Additional research should also proceed to determine the effect of other bases and supplementation of alkali catalysis by other catalytic materials.

REFERENCES

1. R. L. Whistler and J. N. BeMiller, *Adv. Carbohydr. Chem.*, **13**, 289 (1958).
2. J. N. BeMiller *in* *Starch: Chemistry and Technology*, Vol. 1, R. L. Whistler, E. F. Paschall, J. N. BeMiller and H. J. Roberts, Eds. Academic Press, New York 1965, Chap. XXI.
3. G. N. Richards *in* *Methods in Carbohydrate Chemistry*, Vol. III, R. L. Whistler, J. W. Green, J. N. BeMiller and M. L. Wolfrom, Eds. Academic Press, N.Y. 1963, Chap. 27.
4. P. M. Molton and T. F. Demmitt, *Plym. Plast. Technol. Eng.*, **11**(2), 127 (1978).
5. L. Lowendahl, G. Peterson and O. Samuelson, *Tappi*, **59**(9), 118 (1976).
6. E. Sjoström, *Tappi*, **60**(9), 151 (1977).
7. K. G. Chesley, C. W. Montgomery and L. T. Sandborn, "Production of Organic Acids and Salts Thereof from Cellulose Materials," U. S. Patent 2,750,414 (June 12, 1956); *Chem. Abstr.*, **50**, 14227 (1956).
8. J. M. Krochta, J. S. Hudson and C. W. Drake, *Biotechnology and Bioengineering Symp. No. 14*, Wiley, New York, 1984, p. 37.
9. B. R. Allen, W. J. Dawson and D. M. Jenkins, Report No. DOE/ID/12519-11, Battelle Columbus Laboratories, 505 King Ave, Columbus, Ohio 43201 (1985).
10. T. C. Taylor and G. M. Salzmann, *J. Am. Chem. Soc.*, **55**, 264 (1933).
11. H. Salwin and J. F. Bond, *J. Assoc. Off. Anal. Chem.*, **52**, 41 (1969).
12. E. S. Lipinsky, *Science*, **212**, 1465 (1981).
13. E. S. Lipinsky and R. G. Sinclair, Paper No. 34a, Am. Inst. Chem. Eng. 1985 Summer National Mtg, August 25-28, Seattle WA, The Engineering Societies Library, United Engineering Center, 345 East 47th St., New York, NY 10017.
14. J. M. Krochta, S. J. Tillin and J. S. Hudson, *J. Appl. Polym. Sci.*, in press.

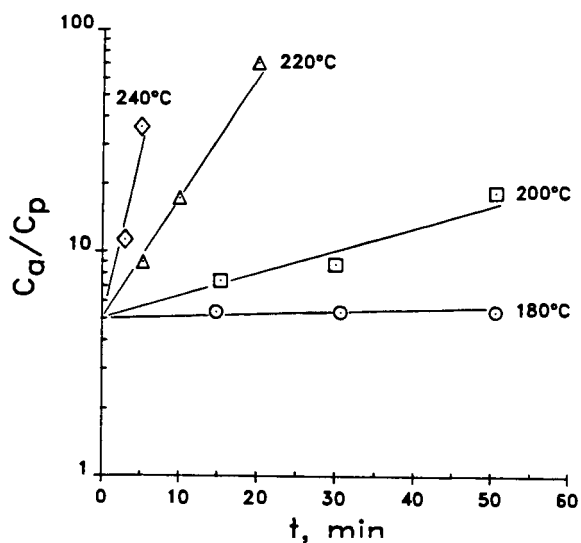


Figure 1. Effect of time on thermochemical degradation of starch in alkaline solution according to Eq. 3.

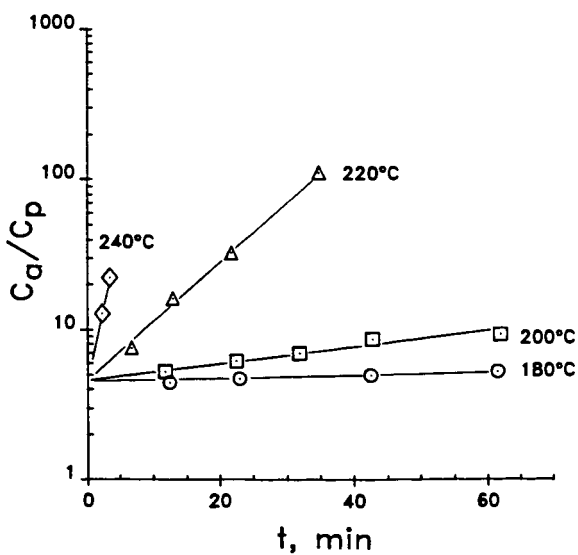


Figure 2. Effect of time on thermochemical degradation of cellulose in alkaline solution according to Eq. 3.

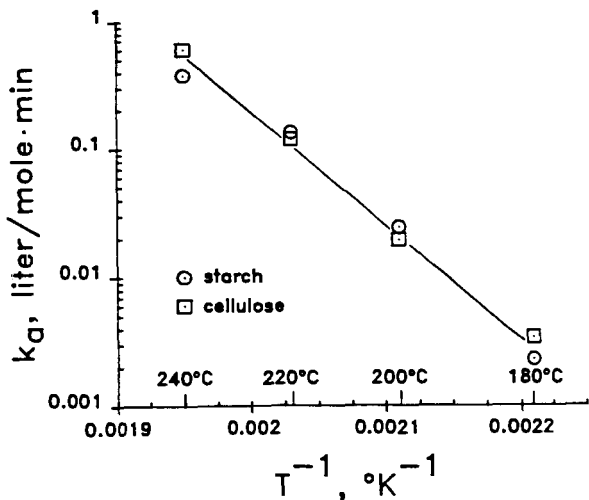


Figure 3. Relation of second-order reaction rate constants for starch and cellulose to temperature according to Arrhenius equation.

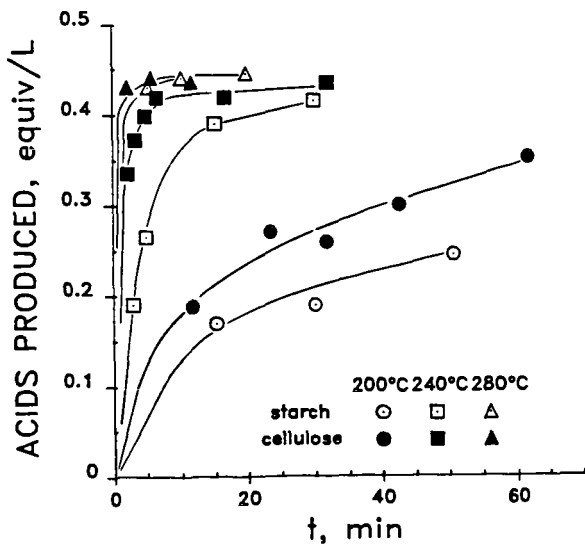


Figure 4. Effect of time on organic acid production from thermochemical degradation of starch and cellulose in alkaline solution.

ANALYSIS OF PARTIALLY CONVERTED LIGNOCELLULOSIC MATERIALS

J.L. Grandmison, A. Ahmed and S. Kaliaguine
Department of Chemical Engineering
Université Laval, Québec, CANADA, G1K 7P4

ABSTRACT

The systematic analysis of the solid residues of the supercritical methanol extraction of Populus tremuloides was performed for samples prepared at temperatures varying from 250 to 350°C and pressures from 3.4 to 17.2 MPa, using such analytical techniques as wet chemistry, chromatography, thermogravimetric analysis, diffuse reflectance FTIR spectroscopy and photoelectron spectroscopy. The results allow to monitor the continuous changes in chemical composition of the samples from partly extracted wood samples to highly recondensed polyaromatic structures.

INTRODUCTION

In the recent studies of thermal and thermochemical processes of wood liquefaction, considerable progress has been reported in the analysis of gaseous and liquid products⁽¹⁾. Some attention has been given to the composition of the solid products by wet chemistry analysis^(2,3).

For the last twenty years much work has been done in the study of the thermal stability of lignocellulosic materials by thermal analytical methods. Since these materials are complex mixtures of organic polymers, thermogravimetric (TG) analysis causes a variety of chemical and physical changes depending on the nature of the sample and its treatment prior to analysis. These problems have been reviewed recently⁽⁴⁾.

Lignocellulosic material can also be analyzed by IR spectrometry. This analytical method was used, for characterization of modified lignin and cellulose in various ways⁽⁵⁻¹³⁾. Quantification by infrared spectrometry, has been reported, for example in analysis of the three basic constituents in sweetgum and white oak chips pretreated at temperatures ranging from 140 to 280°C⁽⁵⁾ using the diffuse reflectance FTIR spectrometry (DRIFT). The technique is simple and applicable to powdered solids and dark samples⁽¹⁴⁾ and can be used for the characterization of the chemical bonds and their modifications by thermal processes.

In this paper we report our efforts to characterize the solid residues produced in a series of experiments for the semicontinuous extraction of Populus tremuloides in supercritical methanol⁽¹⁵⁾, at temperatures ranging from 250 to 350°C (Supercritical Extraction residues or SCE residues), by using wet chemistry and chromatographic⁽¹⁶⁾, thermogravimetric and spectral methods such as DRIFT⁽¹⁷⁾ and ESCA⁽¹⁸⁾.

EXPERIMENTAL PROCEDURE

The solid residues analyzed here were produced by supercritical extraction with methanol of Populus tremuloides in a tubular reactor⁽¹⁵⁾. The analytical procedures used for these residues were described previously as elemental analysis, Klason lignin test, thioglycolic acid lignin test, recondensed material and carbohydrates⁽¹⁶⁾, thermogravimetric (TG/DTG) and FTIR⁽¹⁷⁾ and ESCA⁽¹⁸⁾. Table 1 reports results obtained using these procedures as well as conditions of extraction for each SCE residues.

RESULTS AND DISCUSSION

Wet Chemistry and Chromatography

For the analysis of wood, the Klason lignin test, performed in concentrated sulfuric acid, is the accepted method for the determination of lignin content. We performed similar tests using also trifluoroacetic acid (TFA), the results of which are almost identical to those of the Klason tests. TFA has the advantage to allow further analysis of the saccharides in the acid soluble fraction as it can easily be evaporated from the solution.

The acid insoluble fraction, usually designated as "Klason lignin", is referred to in this work as Klason residue. Figure 1 shows that in the most severe extraction conditions the whole SCE residue is almost entirely constituted of Klason residue. The fact that this Klason residue cannot be considered as lignin has been established through elemental analysis and IR spectroscopy in KBr pellets⁽¹⁶⁾.

In order to determine if the solid residues still contain lignin the old method of forming a soluble lignin derivative with thioglycolic acid was used. This reagent reacts by displacement of α -hydroxyl and α -alkoxy groups in lignin and the derivative so produced can be solubilized by alkali and recovered. Results are reported in Table 1 and Figure 1 showing that thioglycolic acid lignin (TGAL) decreases from 15.6% in wood to 3.3-5.9% in the samples prepared at 350°C. It was shown by IR spectrometry that the TGAL keeps the characteristic features of lignin even for SCE temperatures of 350°C⁽¹⁶⁾.

This confirms our belief that the thioglycolic acid test is a suitable method for the determination of uncondensed lignin in SCE residues. In spite of the fact that 1) the Klason test induces some condensation reactions, 2) the thioglycolic acid test may only extract those lignin fragments containing benzyl alcohol groups or aryl ether groups⁽¹⁹⁾, we would like to suggest that 1) the thioglycolic acid lignin represents a good estimate of unconverted lignin, 2) the Klason residue represents the summation of unconverted lignin and of condensation products formed by pyrolysis reactions during the SCE process.

As a consequence we suggest that the difference between the Klason residue and the thioglycolic acid lignin is representative of recondensed material (RM) in SCE residues. The calculated values for recondensed material in these residues are reported in Table 1. Figure 2 gives the values for the percent recondensed material expressed on a dry wood basis.

Figure 3 shows the percentage of recondensed material, expressed on dry wood basis, plotted as a function of lignin conversion. This graph suggests different condensation reactions at 250°C and at 300-350°C. At 250°C in particular, the condensation seems to be a secondary reaction of lignin conversion. As also shown on the figure, for several experiments the percents of recondensed material are higher than the value which would be calculated assuming that all converted lignin is transformed to recondensed material (line A). It is believed that this indicates that the condensation reaction involves not only products of degradation of lignin but also some of carbohydrates.

The glucose and xylose contents were determined in the soluble TFA acid hydrolysis fraction by liquid chromatography using a cation exchange resin (Ca⁺⁺ form) column. The results are reported in Table 1. Most of the samples prepared at 300-350°C show only minor amounts of hydrolyzed material except for samples MP-16, MP-13 and MP-14 prepared at low pressure or low flow rate. The percents of glucose and xylose for these samples as well as those for the samples prepared at 250°C, expressed on dry wood basis, are plotted on Figure 4. The rather well defined curve indicates that cellulose and hemicellulose are simultaneously degraded at or below 250°C.

Thermogravimetric Analysis

Thermogravimetric analysis (TG and DTG) under nitrogen atmosphere was performed for aspen wood and the 16 partially converted wood residues. The TG and DTG curves are reproduced in Figure 5 for untreated wood and for 4 selected representative SCE residues.

The examination of TG and DTG curves, shows that:

- a) aspen wood loses weight starting near 230°C (pyrolysis of hemicellulose ⁽²¹⁾), and between 350 and 420°C with a maximum rate of weight loss at 385°C (cellulose and lignin pyrolysis ⁽²¹⁾); the weight lost at 700°C is 89.4%.
- b) the SCE residues can be classified according to their temperature of extraction.

For the residues of type I prepared at 250°C (like sample MP-6), the weight loss takes place between 350 and 420°C, with a maximum rate at 375-390°C. The weight lost at 700°C is between 82.5 and 94.6%.

For the type II residues produced at 300°C (like sample MP-12), a continuous weight loss is observed from 300 to 600-700°C, with a maximum rate at temperatures ranging from 380°C to 510°C. The total weight loss at 700°C is less important than for samples of the previous type, ranging from 27.2 to 57%.

For samples of type III prepared at 350°C (like samples MP-11 and MP-8), the weight loss is slower than for those of type II but happens roughly on the same temperature range (300 to 600-700°C) and with maximum rates occurring at higher temperatures, from 380 to 620°C. The weight loss at 700°C is significantly smaller ranging from 8.2 to 34.2%.

A closer analysis of these curves shows that there is a continuous change in the shape of the thermogram of the residues as the SCE pressure is increased for experiments at the same SCE temperature. As shown in Figure 6 the temperature T_{max} corresponding to a maximum on the DTG curve shows a continuous evolution with the parameters of extraction. Two maxima are observed at the lower SCE pressure of 3.4 MPa showing that when the extraction is performed less efficiently, some of the unconverted lignin and cellulose is still present at relatively high content in the residue prepared at 350°C.

The smooth evolution in the temperature of the high temperature DTG peak reflects a change in the nature of the volatile fraction of the recondensed material.

A very good correlation was found between weight lost between 200 and 420°C and the weight of trifluoroacetic acid soluble plus unconverted lignin previously determined by wet chemistry (correlation coefficient is 0.994 if one excepts sample MP-16). These data suggest that the material still not volatilized at 420°C would be identical with what we defined as the recondensed material. It was indeed verified that the correlation between recondensed material and weight % of the solid not volatilized at 420°C is also excellent (correlation coefficient 0.984 when point MP-16 is excepted). From thermogravimetric data the recondensed material in a given SCE residue can thus be further characterized by the weight fraction of RM volatilized between 420 and 700°C.

Diffuse Reflectance Infrared Spectrometry

DRIFT spectra were obtained for the 17 afore mentioned samples and the spectra of the five representative samples used to present the TG/DTG data, are reported in Figure 7.

The spectrum of aspen wood (Figure 7.A) shows the presence of the three fundamental wood constituents. The bands for cellulose are at 898 cm^{-1} β -anomer in pyranose ring ⁽²²⁾, at 1043-1171 cm^{-1} (C-O bonds in primary and secondary alcohols). The

band at 1745 cm^{-1} is due to uronic acid and acetyl groups in hemicellulose⁽²²⁾. The bands from 1246 to 1607 cm^{-1} , specially the one at 1505 - 1515 cm^{-1} , are typical for lignin⁽¹⁹⁾.

As shown by the other spectra in Figure 7, these bands are significantly modified by the SCE treatment.

Spectral region 2850-3050 cm^{-1} . A band at 3050 cm^{-1} (aromatic and/or alkene C-H stretching) becomes evident at 300°C (MP-12, Figure 7-C) and dominates this region at 350°C (MP-8, Figure 7-E). The band in the 2900 cm^{-1} region (aliphatic C-H stretching) which is broad in the initial wood sample, is progressively resolved in three separate bands (2850 , 2900 and 2950 cm^{-1}) as the SCE temperature is increased (MP-12, MP-11 and MP-8, Figures 7C, D and E). The overall pattern in Figure 7E corresponding to the most carbonized sample is similar to the ones reported for higher rank bituminous coal⁽²³⁾ and for vitrinite⁽²⁴⁾, with the 3050 cm^{-1} even more intense in our MP-8 sample. As it was shown earlier that this sample contains 89.2% of recondensed material it may be concluded that this material has a coal-like polyaromatic nature. This is supported by the changes in the next spectral region.

Spectral Region 800-950 cm^{-1} . The band at 898 cm^{-1} is discernible in wood and MP-6 (SCE temperature 250°C) but disappears from spectra of samples treated at higher temperatures where saccharides analysis has also shown the absence of cellulose. As carbonization proceeds, the out-of-plane bending of one isolated (868 - 874 cm^{-1}) and two adjacent (815 - 816 cm^{-1}) aromatic H increase.

The band at 950 cm^{-1} , which is visible in MP-8, is probably due to elimination reaction giving t-alkenes⁽¹⁹⁾.

Spectral Region 1440-1600 cm^{-1} . The characteristic aromatic ring vibration at 1505 - 1515 cm^{-1} , clearly visible in the spectrum of wood, is gradually hidden with an increase in the SCE temperature. This corresponds to the progressive decrease in lignin content of the residue. Inversely, two bands at 1443 - 1461 and 1600 cm^{-1} become very intense and dominate in the spectra of residues produced at 300 and 350°C (Figures 7-C, D and E). These changes parallel the modifications in the 2850 - 3050 cm^{-1} region. The band at 1443 - 1461 cm^{-1} can be attributed to methyl and methylene bonding and also to aromatic ring modes^(24,19). The band at 1600 cm^{-1} is also assigned to aromatic ring stretching. Its high intensity in spectra 7-C, D and E, could possibly be given the three following explanations⁽²⁴⁾:

1) aromatic ring stretching in combination with a chelated conjugated carbonyl structure, 2) aromatic ring stretching mode, with possible intensity enhancement due to phenolic groups, 3) aromatic ring stretching of aromatic entities linked by methylene and possibly ether linkages.

Spectral Regions 1035-1378 and 1700-1745 cm^{-1} . The bands from 1035 to 1171 cm^{-1} (primary and secondary alcohols), present in wood and samples obtained at 250°C , drop in the spectra of SCE residues produced at and above 300°C . The aromatic ethers bands (up to 1378 cm^{-1}) which include phenolic stretching near 1250 cm^{-1} , decrease also.

The hemicellulose band, at 1745 cm^{-1} , present on untreated wood almost disappears in residues prepared at 250°C . The unconjugated carbonyl and/or carboxyl and/or ester of conjugated acids at 1720 - 1735 cm^{-1} from original lignin is still visible at 250°C when hemicellulose is partly removed but at higher SCE temperatures it is hidden by the highly intense 1700 cm^{-1} band. This last band can be attributed to a conjugated carbonyl or carboxyl structure but it would be surprising that carboxyl could resist at severe SCE conditions. Further study is necessary for definite assignment of this band.

Quantification. Schultz et al⁽⁵⁾ reported recently correlations of FTIR absorbance ratios with such variables as the percents in glucose, xylose and Klason lignin for

wood chips pretreated by the RASH process at temperature ranging from 140 to 280°C. These correlations do not fit correctly our data so that we developed our own equations by non-linear least squares regression. For quantitative evaluation of absorbances, baseline was defined as shown on spectrum 7E.

These equations are as follows.

$$\% \text{ Klason Lignin} = 174.6 - \left(101 \times \frac{A_{2950}}{A_{1376}}\right) + \left(150.4 \times \frac{A_{2950}}{A_{1376}}\right) - \left(196.7 \times \frac{A_{1120}}{A_{1376}}\right) + \left(223.4 \times \frac{A_{1700}}{A_{1376}}\right) - \left(190.1 \times \frac{A_{1245}}{A_{1376}}\right) \quad (1)$$

$$\% \text{ Unconverted Lignin} = -17.13 + \left(17.53 \times \frac{A_{2900}}{A_{1429}}\right) + \left(70.77 \times \frac{A_{1605}}{A_{1429}}\right) - \left(90.18 \times \frac{A_{1090}}{A_{1429}}\right) + \left(122.2 \times \frac{A_{1043}}{A_{1429}}\right) + \left(46.72 \times \frac{A_{895}}{A_{1429}}\right) \quad (2)$$

$$\% \text{ Reccondensed mat.} = 242.2 + \left(263.8 \times \frac{A_{1330}}{A_{1090}}\right) - \left(240.7 \times \frac{A_{1245}}{A_{1090}}\right) - \left(873.4 \times \frac{A_{1043}}{A_{1090}}\right) - \left(327.6 \times \frac{A_{895}}{A_{1090}}\right) - \left(45.62 \times \frac{A_{866}}{A_{1090}}\right) \quad (3)$$

$$\% \text{ Glucose} = -33.07 + \left(74.06 \times \frac{A_{1506}}{A_{1461}}\right) - \left(46.28 \times \frac{A_{1376}}{A_{1461}}\right) - \left(84.12 \times \frac{A_{1330}}{A_{1461}}\right) + \left(74.39 \times \frac{A_{1245}}{A_{1461}}\right) + \left(65.39 \times \frac{A_{1130}}{A_{1461}}\right) \quad (4)$$

$$\% \text{ Xylose} = -51.54 - \left(17.74 \times \frac{A_{1700}}{A_{1429}}\right) + \left(38.53 \times \frac{A_{1600}}{A_{1429}}\right) + \left(18.17 \times \frac{A_{1245}}{A_{1429}}\right) - \left(13.44 \times \frac{A_{1171}}{A_{1429}}\right) + \left(40.60 \times \frac{A_{1130}}{A_{1429}}\right) \quad (5)$$

Calculated results for the 16 samples of SCE residues showed standard deviations from experimental values of 5.12, 1.28, 4.96, 3.62 and 1.62% and correlation coefficients of 0.99, 0.97, 0.99, 0.98 and 0.98 for equations (1) to (5) respectively.

ESCA

ESCA is a surface sensitive technique, based on the measurement of kinetic energies of photoelectrons ejected from a given atomic energy level under the action of a monoenergetic X-ray beam. It provides quantitative information on the elemental composition as well as on the chemical environment of each atom (bonding and oxidation state).

The kinetic energy of photoelectrons (E_k), as measured with respect to the vacuum level, is expressed as:

$$E_k = E_x - (E_B + \phi + E_c) \quad (6)$$

where E_x is the energy of the incident photon, E_B is the binding energy of the electron on its original level, ϕ is the work function of the spectrometer and E_c is the energy lost in counteracting the potential associated with the steady charging of the surface. ϕ and E_c are essentially corrections. ϕ is depending on the spectrometer and not liable to be modified between experiments. E_c is high on low conductivity samples and can be made lower by the use of a flood gun.

ESCA spectra corresponding to carbon 1s peaks of *Populus tremuloides*, 3 samples isolated at three different SCE temperatures and 2 reference compounds are illustrated in Figure 8. There is a general agreement in the literature on the assignment of components C_1 , C_2 and C_3 in wood derived materials: C_1 corresponds to carbon linked to H or C, C_2 has one link to oxygen, whereas C_3 has two. In the solid phase, C_1 is referenced at 285.0 eV and C_2 and C_3 are usually close to 287.0 and 289.5 eV (25).

In all SCE residues, a fourth C_{1s} component is found on the low binding energy side of the spectrum, shifted from the C_1 component by 1.4 ± 0.5 eV. This is thereafter

designated as the C_0 component. As the temperature of extraction is increased from 250 to 300°C, the C_0 component increases continuously whereas the general trend of C_1 , C_2 and C_3 components in a continuous decrease.

It is interesting to note that the uncorrected experimental C_{1s} binding energy for dibenz (a,h) anthracene is very close to the binding energy for this C_0 peak. As polyaromatic are electrical conductors, the charging is expected to be low and E_c close to 0. On this basis, C_0 component is assigned to carbon in polyaromatics. Usually, aromatic compounds show a shake up satellite located 5-7 eV above their C_{1s} peak (20). It can be seen however from Figure 8 that the intensity of this satellite in dibenz (a,h) anthracene is considerably lower than in o-biphenol. Thus the satellite from C_0 peak in SCE solid residues should only make a minor contribution to the overall C_{1s} band.

The ratio C_{RM}/C_{SR} (where C_{SR} is the carbon content of the whole solid residue as determined by elemental analysis, whereas C_{RM} is the calculated mass of carbon in the recondensed material contained in a given sample) was calculated for 5 samples (the elemental analysis for MP-13 was not available). Figure 9 shows not only that this ratio is correlated to the C_0 fraction of the C_{1s} peak, but that both values are almost equal for all samples.

Therefore it may be concluded that the ESCA technique provides a simple mean for the determination of the extent of recondensation reactions by a mere determination of the proportion of the C_0 component in the C_{1s} band of the solid residue.

LITERATURE CITED

- (1) Fifth Canadian Bioenergy R & D Seminar, Ed. Hasnain, S.; Elsevier, New-York, 1984.
- (2) McDonald, E.; Howard, J.; Fourth Bio-Energy R & D Seminar, Winnipeg, Canada, March 29-31, 1982.
- (3) Biermann, C.; Schultz, T.P.; McGinnis, G.D. J. Wood Chem. Technol. 1984, 4, 111-128.
- (4) Nguyen, T.; Zaverin, E.; Barrall II, E.M. J. Macromol. Sci.-Rev. Macromol. Chem a) 1985, C20, 1-65; b) 1985, C21, 1-60.
- (5) Schultz, T.P.; Templeton, M.C.; McGinnis, G.D. Anal. Chem. 1985, 57, 2867-2869.
- (6) Chua, M.G.S.; Wayman, M. Can. J. Chem. 1979, 57, 2603-2611.
- (7) Marchessault, R.H.; Coulombe, S.; Morikawa, H. Can. J. Chem. 1982, 60, 2372-2382.
- (8) Nassar, M.M.; Mackay, G.D.M. Wood and Fiber Sc. 1984, 16, 441-453.
- (9) Meier, D.; Larimer, D.R.; Faix, O. Fuel 1986, 65, 916-921.
- (10) Lephardt, J.O.; Fenner, R.A. Appl. Spectrosc. 1981, 35, 95-101.
- (11) Haw, J.F.; Schultz, T.P. Holzforshung 1985, 39, 289-296.
- (12) Dollimore, D.; Hoath, J.M. Thermochemica Acta 1981, 45, 103-113.
- (13) Shafizadeh, F.; Sekiguchi, Y. Carbon 1983, 21, 511-516.
- (14) Fuller, M.P.; Griffiths, P.R. Anal. Chem. 1978, 50, 1906-1910.

- (15) Poirier, M.; Ahmed, A.; Grandmaison, J.L.; Kaliaguine, S. I.&E.C. Prod. Res. Dev., submitted.
- (16) Ahmed, A.; Grandmaison, J.L.; Kaliaguine, S. J. Wood Chem. Technol. 1986, 6, 219-248.
- (17) Grandmaison, J.L.; Thibault, J.; Kaliaguine, S.; Chantal, P.D. Anal. Chem., submitted.
- (18) Ahmed, A.; Adnot, A.; Kaliaguine, S. J. Appl. Polym. Sci., accepted for publication.
- (19) Lignins. Occurrence. Formation. Structure and Reactions; Ed. Sarkanen, K.V.; Ludwig, C.H.; John Wiley and Sons; 1971.
- (20) Grandmaison, J.L.; Kaliaguine, S.; Ahmed, A. in Comptes Rendus de l'atelier de travail sur la liquéfaction de la biomasse, Sherbrooke, Canada, NRCC 23130, Sept. 29-30, 1983.
- (21) Shafizadeh, F. J. Anal. and Appl. Pyrolysis 1982, 3, 283-305.
- (22) Nakanishi, K.; Infrared Absorption Spectroscopy-Practical; Holden-Day, Inc.: San Francisco, 1962.
- (23) Gerson, D.J.; McClelland, J.F.; Veysey, S.; Markuszewski, R. Appl. Spectrosc. 1984, 38, 902-904.
- (24) Painter, P.C.; Snyder, R.W.; Starsinic, M.; Coleman, M.M.; Kvehn, D.W.; Davis A. Appl. Spectrosc. 1981, 35, 475-485.
- (25) Gelius, U.; Heden, P.F.; Hedman, J.; Lindberg, B.J.; Manne, R.; Nordberg, R.; Nordling, C.; Siegbahn, K. Physica Scripta, 1970, 2, 70.
- (26) Ohta, T.; Fujikawa, T.; Kuroda, H. Bull. Chem. Soc. Japan, 1975, 48, 2017.

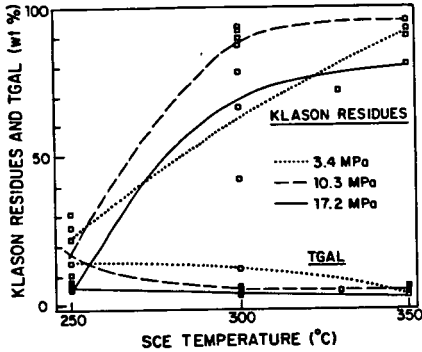


Figure 1. Klason residues and Thiolglycolic acid lignin in SCE solid residues.

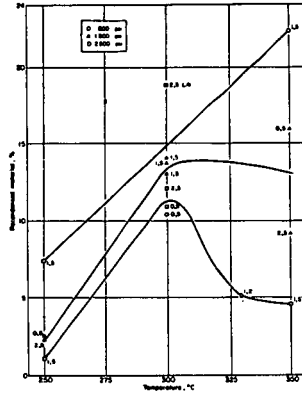


Figure 2. Effect of SCE conditions on recycled material (expressed on dry wood basis).

Sample	SCE Temperature °C	SCE Pressure MPa	SCE Flowrate l/h	Residue yield wt%	Klason residue wt%	TGAL residue wt%	Recond. material wt%	Klason material soluble wt%	Glw wt%	Xyl wt%	% C	% H	% O
Wood	-	-	-	100.0	17.6	15.6	-	78.5	47.6	27.2	46.1	6.50	47.4
MP-22	250	3.4	1.5	74.8	26.1	14.3	11.8	70.8	45.7	18.0	50.0	5.84	44.2
MP-6	250	10.3	0.5	55.4	30.5	22.2	8.3	64.1	38.1	12.8	53.5	5.29	41.2
MP-17	250	10.3	2.5	69.7	10.6	6.5	4.1	89.9	38.0	19.2	45.0	6.49	48.6
MP-15	250	17.2	1.5	68.4	7.6	5.4	2.0	90.6	26.9	12.3	44.1	6.97	48.9
MP-16	300	3.4	0.5	40.5	42.2	12.1	30.1	46.4	25.9	7.9	64.9	5.82	29.2
MP-20	300	3.4	2.5	31.0	78.1	12.3	65.8	-	0.0	0.0	75.9	5.12	19.0
MP-9	300	10.3	1.5	16.4	92.1	4.3	87.8	5.0	0.0	0.0	78.2	4.96	16.8
MP-12	300	10.3	1.5	15.9	92.5	3.8	88.7	1.6	0.6	0.0	88.4	4.62	15.0
MP-21	300	10.3	1.5	15.7	89.2	4.5	84.7	2.4	0.0	0.0	79.8	5.35	14.8
MP-13	300	17.2	0.5	18.4	65.8	6.8	59.8	27.2	10.3	3.3	64.8	5.47	29.7
MP-18	300	17.2	2.5	15.8	86.7	5.3	81.3	4.0	0.7	0.0	73.3	5.17	21.6
MP-27	330	17.2	1.2	8.4	71.4	4.8	66.7	19.8	7.1	0.0	74.1	6.08	19.8
MP-14	350	3.4	1.5	26.9	98.0	5.2	85.1	11.1	4.8	1.5	74.8	4.34	20.8
MP-11	350	10.3	0.5	18.2	92.3	3.8	88.5	8.8	0.8	0.0	83.5	4.89	11.6
MP-8	350	10.3	2.5	10.2	95.1	5.9	89.2	1.2	0.8	0.0	92.8	3.84	3.33
MP-24	350	17.2	1.5	6.1	80.3	3.3	77.0	3.1	0.8	0.0	76.3	5.90	18.8

Table I. SCE residues, extraction conditions and analyses

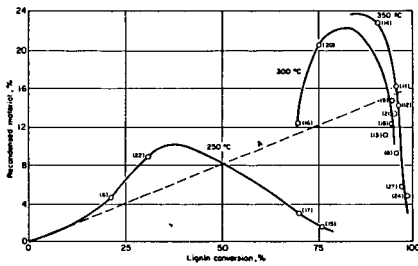


Figure 3. Recondensed material (expressed on dry wood basis) as a function of lignin conversion

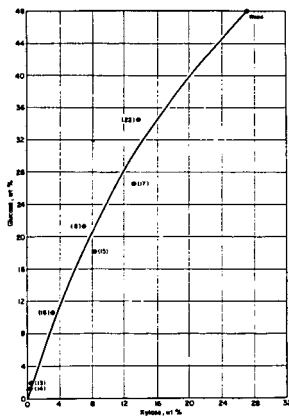


Figure 4. Residual hydrolyzed glucose as a function of residual hydrolyzed xylose (both expressed on dry wood basis).

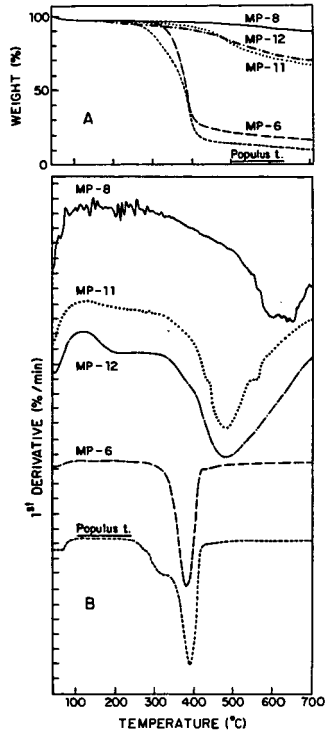


Figure 5. Thermogravimetric analysis of *Populus tremuloides* and of four SCE residues: TG (A) and DTG (B) in flowing nitrogen.

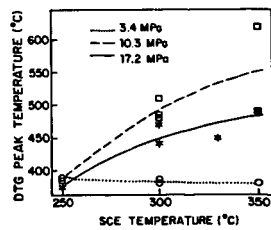


Figure 6. DTG peak temperature as a function of SCE temperature and pressure.

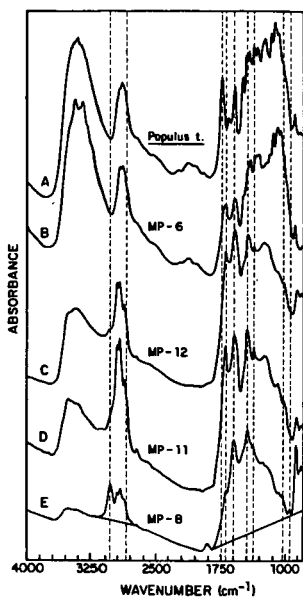


Figure 7. IRFT spectra of the same samples as in Figure 5.

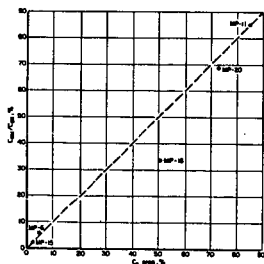


Figure 8. Relation between carbon in recomended material and polyaromatic carbon from ESCA C_a peaks

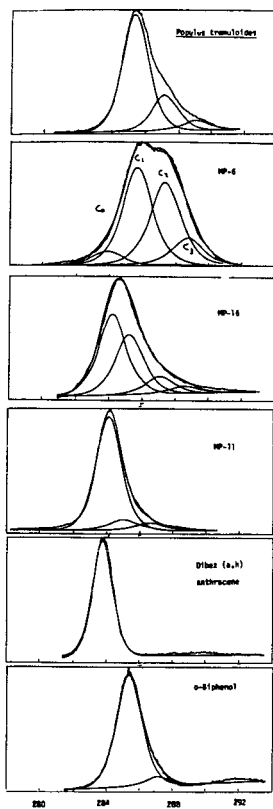


Figure 9. ESCA spectra (C_{1s} peaks) of *Populus tremuloides*, of 3 (three) SCE residues and of the standards compounds

**Some Aspects of Pyrolysis Oils Characterization
by High Performance Size Exclusion Chromatography (HPSEC)**

David K. Johnson and Helena Li Chum*,

Chemical Conversion Research Branch
Solar Energy Research Institute
1617 Cole Blvd., Golden, Colorado 80401

ABSTRACT

The utilization of biomass pyrolysis oils or isolated fractions of these feedstocks requires a fast overall characterization technique. Gas chromatographic techniques typically analyze only the volatile fraction (5%-50%) of underivatized oils. With proper choice of solvent and detector systems, the HPSEC on polystyrene-divinylbenzene copolymer gels of the whole oils can provide valuable information on the apparent molecular weight distributions and changes that occur upon aging or chemical fractionation. Several pyrolysis oils have been analyzed as well as fractions isolated by solvent elution chromatography. In order to understand better the observed low-molecular-weight region, a number of model substances of the main classes of compounds found in pyrolysis oils have been investigated. While hydrogen bonding between the phenolic groups and tetrahydrofuran occurs, solute-solute interactions can be kept very small by operating at very low concentrations of solute; solute-gel interactions do occur when polycyclic aromatic compounds predominate. HPSEC provides very good information on shelf life, reactivity of pyrolysis oils, and comparison of oils as a function of process conditions.

INTRODUCTION

Many biomass pyrolysis processes produce 55%-65% conversion of the dry biomass to a very inexpensive pyrolysis oil (1-3). Costs of the oils will range from \$0.02-\$0.08/lb of oil, depending on the biomass feedstock cost (\$10-\$40/dry ton biomass). Therefore, these inexpensive oils, rich in phenolic fractions, acids, and furan-derivatives can be feedstocks for further upgrading or could be used because of their reactivity, in applications such as thermosetting resins and other wood-bonding methods. One of the important considerations for this use or further processing is the stability of the oil. Fast techniques to determine such properties become necessary. We present a method of characterization of pyrolysis oils and chemically isolated fractions using high-performance size exclusion chromatography (4-5), a technique commonly employed in the determination of the molecular weight distribution of polymers. We discuss the potential of the method and its limitations. Classes of model compounds commonly found in these oils have been investigated in the low-molecular-weight range to shed light on interactions between solute and solvent, solute and gel material (polystyrene-divinylbenzene), and solute-solute which can be kept to a minimum by operating at very dilute conditions.

EXPERIMENTAL

High performance size exclusion chromatography was performed on Hewlett-Packard 1084 and 1090 liquid chromatographs using HP1040A diode array and HP-1037A refractive index detectors. Data were stored on a HP 85 microcomputer. The columns (300 x 7 mm) used in this study were purchased from Polymer Laboratories Inc. and were a PL 100 A (10 μ particles) and a PL 50 A (5 μ particles). The solvent employed was tetrahydrofuran (Burdick and Jackson, chromatographic grade) used as received.

Details on the preparation of pyrolysis oils at SERI in the entrained-flow, fast ablative pyrolysis reactor can be found in a report by Diebold and Scahill (2).

The lignin model compounds were prepared by J. A. Hyatt (6); all the other model compounds were purchased from the Aldrich Chemical Co.

RESULTS AND DISCUSSION

Comparison of Pyrolysis Oils Obtained from Various Sources. The HPSEC of four wood pyrolysis oils obtained from the entrained flow, fast ablative pyrolysis reactor at SERI are shown in Figure 1. The oils were obtained from two separate runs and collected from two different scrubbers. The apparent molecular weight distributions of the four oils are very similar, indicating little selectivity on the basis of molecular weight distribution. Figure 2, however, shows the HPSEC chromatograms of a number of other pyrolysis oils obtained under a variety of conditions from many different sources. Clearly, some of the oils contain components of high apparent molecular weight even to the extent that some are excluded from the pores of the column polymer, indicated by the peaks at about 4.5 minutes in the chromatograms. The oils also have varying amounts of more sharply resolved components at lower apparent molecular weight. Thus, HPSEC may be used to characterize pyrolysis oils obtained from different sources, and comparisons may be drawn regarding their relative apparent molecular weight distributions as long as the analyses were carried out under the same chromatographic conditions.

The wood oil obtained from the packed scrubber in Run 41 at SERI was also subjected to fractionation by sequential elution by solvents chromatography (SESC) according to the method of Davis et al. (7). The fractions obtained were also analyzed by HPSEC and the chromatograms are shown in Figure 3. The HPSEC shows a general trend to higher apparent molecular weight as the polarity of the eluting solvent was increased up to methanol. A number of the fractions appear to contain relatively large amounts of distinct components (the sharp peaks) of lower apparent molecular weight. The sixth fraction was produced by going back to a less polar solvent. A seventh fraction was produced using a more polar eluant of 10% acetic acid in methanol which could not be analyzed by HPSEC because it was insoluble in tetrahydrofuran. About three-quarters of the oil was found in Fractions 3, 4, and 5, the last being the major fraction. If the chromatograms in Figure 3 were combined taking into account the yields of the various fractions then, as expected, a close comparison could be made with the chromatogram in Figure 1 of the unfractionated oil.

Doubts have been expressed that these pyrolysis oils could have molecular weights as high as indicated by these chromatograms as they are obtained by condensation of the primary vapors from pyrolysis. Analysis by techniques requiring revaporization of the oils consistently does not detect high-molecular-weight components, possibly because they are difficult to vaporize and also because they may be thermally degraded to either higher or lower molecular weight components (8) or both. It has been suggested that the high apparent molecular weights observed by HPSEC are the result of solute-solute or solute-solvent associations producing high-molecular-weight complexes. To verify the results obtained by HPSEC, the three major fractions and the original unfractionated oil were subjected to proton NMR analysis. The spectra of Fraction 5 and the original oil contain broad peaks characteristic of irregular polymers such as lignin, while the spectrum of Fraction 3 contains sharp peaks indicative of a mixture of simpler, low-molecular-weight compounds; Fraction 4 is intermediate between 3 and 5. Thus, the HPSEC and proton NMR spectra appear to be in general agreement in that this pyrolysis oil

contains mixtures of possibly higher molecular weight polymeric components and simpler low-molecular-weight compounds.

Many of the chromatograms shown here are of samples whose history of handling and age are not known in detail. It has been suggested that because of the very reactive and acidic nature of these oils that the high molecular weights observed are produced as the oils get older and are exposed to ambient conditions. Consequently, a study has been started to examine the effects of aging and the conditions under which pyrolysis oils are stored. A pyrolysis oil was produced in the SERI entrained-flow, fast ablative pyrolysis reactor. In this reactor, the primary vapors are scrubbed out with water such that about 90% are dissolved out. One sample of this aqueous solution of pyrolysis oil was stored at 4°C and the other was analyzed by HPSEC. The sample to be analyzed was made up by dissolving a small amount of the aqueous solution in tetrahydrofuran. Storage was under ambient conditions. The THF solution was analyzed several times over the period of a week to look for changes in its HPSEC chromatogram as shown in Figure 4. At the end of this period, the sample kept at 4°C was also analyzed to determine the effect of aging on the oil. Actually, a physical change took place on the aqueous sample stored at 4°C in that a small amount of tar separated out on the bottom of the vial. Consequently, two samples were made up in THF from the cooled sample, one from the aqueous part and one from the tar. Figure 5 compares the HPSEC of the sample kept at ambient conditions to those of the cooled samples. The HPSEC of the tar sample shows it consists of relatively much larger amounts of material higher in apparent molecular weight. The aqueous fraction of the cooled sample appears very similar to the sample stored at 25°C, although the latter does appear to contain a slightly larger relative amount of apparently higher molecular weight material. The degree to which storage at lower temperature has prevented any increase in molecular weight of the pyrolysis oil with time is difficult to ascertain because of the fractionation of the refrigerated sample. The sample kept at ambient conditions did not have the opportunity to fractionate because of the solvent it was dissolved in.

The HPSEC of the unrefrigerated sample (Figure 4) did indicate that the pyrolysis oil "aged" over the period of a week with increasing amounts of apparently higher molecular weight components being produced with time. Most of the samples obtained from outside of SERI are much older than one week. Pyrolysis oils are generally very reactive so that unless they are effectively stabilized in some way, increasing molecular weight should be expected as they get older.

What are the Limitations of HPSEC as a Technique When Applied to Pyrolysis Oil Characterization. One of the major advantages of HPSEC as a technique is that with the proper choice of solvent to dissolve the sample, the whole of the sample may be analyzed under very mild conditions. Because HPSEC is an isocratic technique, differential refractometers may be used as detectors so that, again, all of the sample may be detected. This is not a great concern when applied to pyrolysis oils, as they tend to absorb quite strongly in the ultraviolet. With a modern UV-visible diode array detector, a number of wavelengths can be monitored to ensure all the components of the oil are monitored. However, the eluting solvent must be chosen such that all the sample is dissolved, and as pyrolysis oils are fairly polar and often contain water, the solvent will also need to be fairly polar. The combination of polar solutes and polar solvents means that solute-solvent interactions through hydrogen bonding must be a concern. Tetrahydrofuran, probably the most popular solvent for HPSEC, can form hydrogen bonds with certain species such as phenols producing a complex molecule exhibiting greater molecular size and lower retention volume than would be expected (9). When nonpolar solvents are used such as toluene or chloroform, the molecular size should be relatively unaffected, but oil solubility then becomes very limited. The use of solvents of greater solvating

power, such as dimethyl formamide, also generates problems (10) due to solute-solute association, interaction between polystyrene standards and the column gel and column gel-solvent interactions.

The other major limitation of HPSEC as a technique comes from the desire to correlate solute elution time with molecular weight. As stated in its name, this is a method of separation based on molecular size. HPSEC columns contain a polymer gel of polystyrene-divinylbenzene produced with a controlled pore size distribution. Solutes of different size are separated by the different degrees of their penetration into the pores of the gel. The parameter that can be obtained from HPSEC is effective molecular length; e.g., material excluded from a column containing gel with 100 Å pores should have an effective molecular length of 100 Å or greater. To correlate retention times to molecular weight, it is necessary to use calibration standards similar in structure to the solute whose molecular weight is being determined. The most common calibration materials used are polystyrenes of low polydispersity. Others used include straight chain alkanes, polyethylene glycols, and the related materials IGEALS™ that are 4-nonylphenyl terminated. If a column were calibrated with straight chain alkanes, it is unlikely to be much good for obtaining molecular weights of aromatic solutes, as a benzene ring is only about as long as propane, and anthracene is only about as long as hexane. When dealing with much larger molecules, it is difficult to estimate what their size might be in three dimensions in solution. Although pyrolysis oils have a high level of aromatic components, especially phenolics, they are a very complex mixture of components, and so it is unlikely that any one set of calibration standards would do a very good job. Despite these limitations, HPSEC can give an idea of the molecular weight distribution of an oil and certainly can be used in comparing oils. Establishing molecular weights for low-molecular-weight components is probably the most difficult task. Figures 6 and 7 compare the actual molecular weights of a variety of different types of compounds with their apparent molecular weights calculated from their retention times on 50 Å 5 μ HPSEC column calibrated with polystyrenes and IGEALS. If the calibration was good for all compounds, then they should all fall on the straight lines. The aromatic hydrocarbons follow the calibration, but the aromatic acids and naphthalenes deviate greatly and in opposite directions. The aromatic acids contain both carboxylic and phenolic groups and so probably have higher apparent molecular weights than their actual molecular weights because of hydrogen bonding with the solvent tetrahydrofuran. The naphthalenes have lower apparent molecular weights than actual not only because their condensed structure makes them relatively small for their molecular weight, but also because of interactions between these solutes and the column gel. Philip and Anthony (9) observed retention volumes that were longer than expected for anthracene, benzopyrene, and coronene, considering their molecular size. They attributed this behavior to interaction of these highly aromatic solutes with the phenyl groups of the polymer chains of the gels.

The phenols and lignin model compounds follow the calibration quite closely, tending to show slightly higher apparent molecular weights than they actually have, probably because of association with the solvent. This is encouraging for the HPSEC of pyrolysis oils as these types of compounds are more likely to be present. Heavily cracked oils, however, can be rich in polynuclear aromatics.

Solute-solute association has not been observed for any of these molecules or for others when using tetrahydrofuran as solvent. Retention time changes of less than 0.01 minutes were observed in changing sample concentrations in the mg/mL range (~4 mg/mL) to the ng/mL range (~3 μg/mL) when injecting 5 μl of these solutions. HPSEC of pyrolysis oil samples made up in this concentration range should also be free of

solute-solute association which would artificially increase the apparent molecular weight of the oils.

CONCLUSIONS

HPSEC has been shown to be a useful method of characterizing pyrolysis oils because it examines the whole of the oil. Using polystyrene-divinyl benzene polymer gel columns, tetrahydrofuran as solvent and polystyrenes and IGPALS as calibration standards a good indication of molecular weight distribution can be obtained for oils from a variety of sources. The high apparent molecular weights observed appear to be real, and some corroboration is seen in proton NMR spectra. Although some solute-solvent association can be expected, use of phenolic model compounds has shown that HPSEC can give a good indication of molecular weight. However, if the oils contained large amounts of either much more polar compounds or condensed aromatic compounds, then interpretation of HPSEC on the basis of molecular weight would be much more difficult. Pyrolysis oils are reactive materials and an awareness of the length of time and conditions under which they are kept must be maintained and is important for further processing.

ACKNOWLEDGEMENTS

This work was supported by the Office of Industrial Programs of the U.S. Department of Energy (FTP 587). Thanks are due to Mr. A. Schroeder, Program Manager, and to all producers of pyrolysis oils: J. Diebold, Tom Reed, J. Scahill, C. Roy, S. Kaliaguine, J. Howard, and to R. Evans and T. Milne for profitable discussions. Thanks also to J. A. Hyatt for supplying three of the lignin model compounds employed.

REFERENCES

- (1) Diebold, J. P., Editor, Proc. Specialists Workshop on Fast Pyrolysis of Biomass, Copper Mountain, October 1980, SERI/CP-622-1096, Golden, Colorado: Solar Energy Research Institute.
- (2) Diebold, J. P., and Scahill, J. W., "Entrained-Flow Fast Ablative Pyrolysis of Biomass," SERI/PR-234-2665, 1985, Golden, Colorado: Solar Energy Research Institute.
- (3) Overend, R. P., and Milne, T. A.; and Mudge, L. K., Editors, Fundamentals of Thermochemical Biomass Conversion, Elsevier: NY, 1985.
- (4) Provder, T., Editor, Size Exclusion Chromatography: Methodology and Characterization of Polymers and Related Materials, ACS Symposium Series, 245, Washington, D.C., ACS (1984).
- (5) Yau, W. W.; Kirland, J. J.; and Bly, D. D., Modern Size Exclusion Chromatography: Practice of Gel Permeation and Gel Filtration Chromatography Wiley: New York (1979).
- (6) Hyatt, J. A., Synthesis of Some Tetrameric Lignin Model Compounds Containing β -0-4 and 5,5'-Interunit Linkages, to appear in Holzforschung.
- (7) Davis, H. G.; Eames, M. A.; Figueroa, C.; Gansley, K. K.; Schaleger, L. L.; and Watt, D. W., 1985, "The Products of Direct Liquefaction of Biomass," Fundamentals of Thermochemical Biomass Conversion, edited by R. P. Coverend, T. A. Milne, and L. K. Mudge, London: Elsevier Applied Science Publishers, pp. 1027-1038.

(8) Evans, R. J., and Milne, T. A., Molecular Characterization of the Pyrolysis of Biomass. II. Applications, submitted to Energy and Fuels.

(9) Philip, C. V., and Anthony, R. G., "Analysis of Petroleum Crude and Distillates by Gel Permeation Chromatography," ACS Symposium Series 245 (17), 257-270 (1984).

(10) Chum, H. L.; Johnson, D. K.; Tucker, M.; Himmel, M., Performance Size Exclusion Chromatography using Styrene-Divinylbenzene Copolymer Gels, Holzforchung in press.

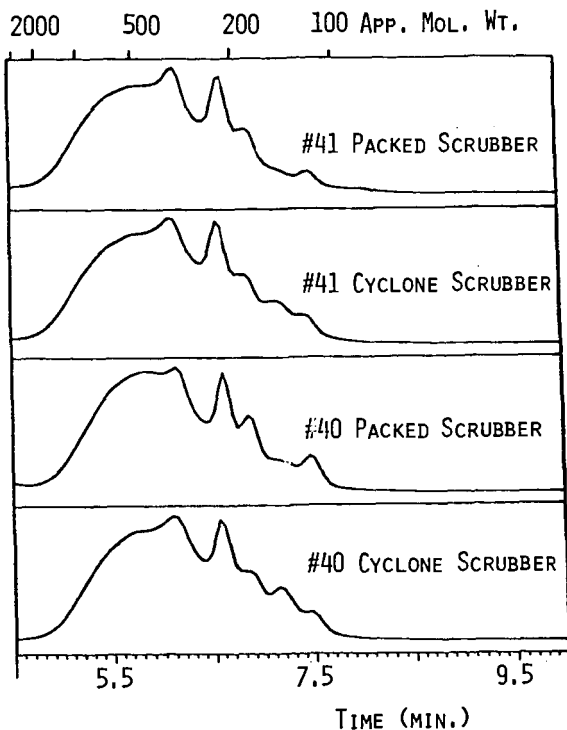


FIGURE 1. HPSEC OF WOOD PYROLYSIS OILS FROM THE SERI ENTRAINED-FLOW, FAST ABLATIVE PYROLYSIS REACTOR. ANALYSIS ON PL GEL 100Å, 10μ GPC COLUMN USING THF AT 1 mL MIN⁻¹ WITH DETECTION AT 330 NM (BANDWIDTH 140 NM).

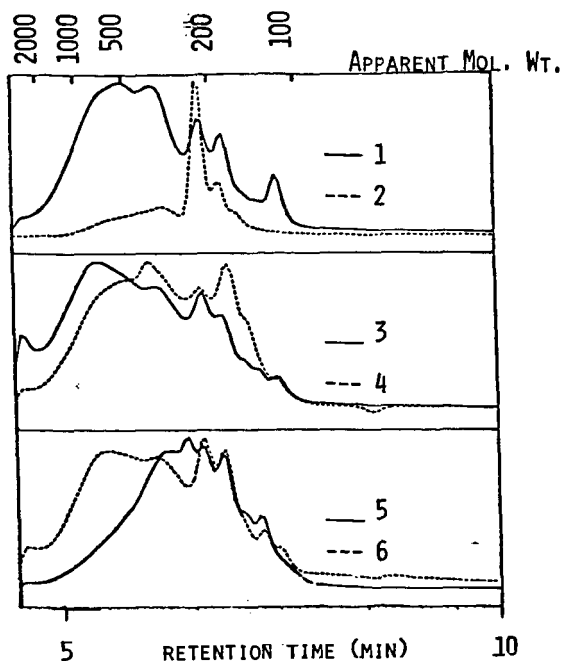


FIGURE 2. HPSEC OF WOOD PYROLYSIS OILS FROM A VARIETY OF SOURCES. ANALYSIS CONDITIONS AS PER FIGURE 1.

- 1 = OIL FROM D. S. SCOTT, U. OF WATERLOO, FLASH PYROLYSIS OF HYBRID POPLAR-ASPEN.
- 2 = OIL FROM C. ROY, U. DE SHERBROOKE, VACUUM PYROLYSIS OF AVICEL @ 306°C.
- 3 = OIL FROM C. ROY, U. DE SHERBROOKE, VACUUM PYROLYSIS OF ASPEN POPLAR @ 534°C, 2.2 MM OF HG.
- 4 = OIL FROM J. HOWARD, B. C. RESEARCH, SUPERCRITICAL ACETONE EXTRACTION OF ASPEN.
- 5 = OIL FROM S. KALIAQUINE, U. OF LAVAL, SUPERCRITICAL METHANOL EXTRACTION OF ASPEN @ 350°C, 1500 PSI.
- 6 = OIL FROM C. ROY, U. DE SHERBROOKE, VACUUM PYROLYSIS OF ASPEN @ 315°C, 0.7 MM OF HG.

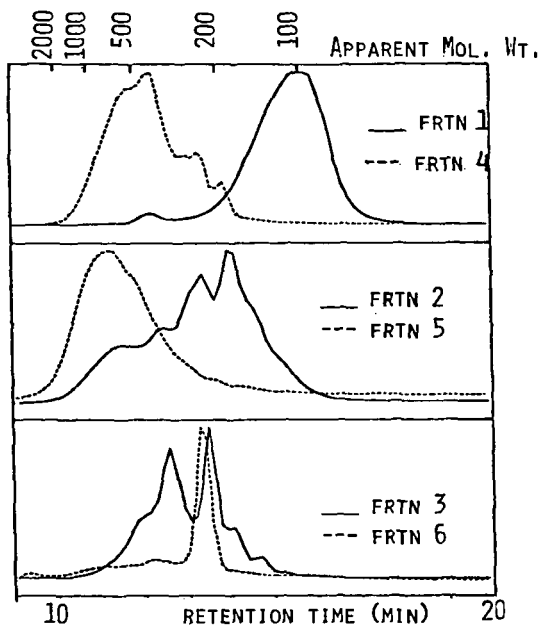


FIGURE 3. HPSEC OF SESC FRACTIONS FROM WOOD PYROLYSIS OIL RUN #41 PACKED SCRUBBER. ANALYSIS ON PL GEL 100 Å 10 μ GPC COLUMN USING THF AT 0.5 ML MIN⁻¹ WITH DETECTION AT 330 NM (BANDWIDTH 140 NM).

FRACTION 1 ELUTED WITH 15% TOLUENE IN HEXANE, YIELD 0.4%.

FRACTION 2 ELUTED WITH CHLOROFORM, YIELD 1.5%.

FRACTION 3 ELUTED WITH 7.5% ETHER IN CHLOROFORM, YIELD 15.6%.

FRACTION 4 ELUTED WITH 5% ETHANOL IN ETHER, YIELD 19.5%.

FRACTION 5 ELUTED WITH METHANOL, YIELD 38.1%.

FRACTION 6 ELUTED WITH 4% ETHANOL IN THF, YIELD 3.1%.

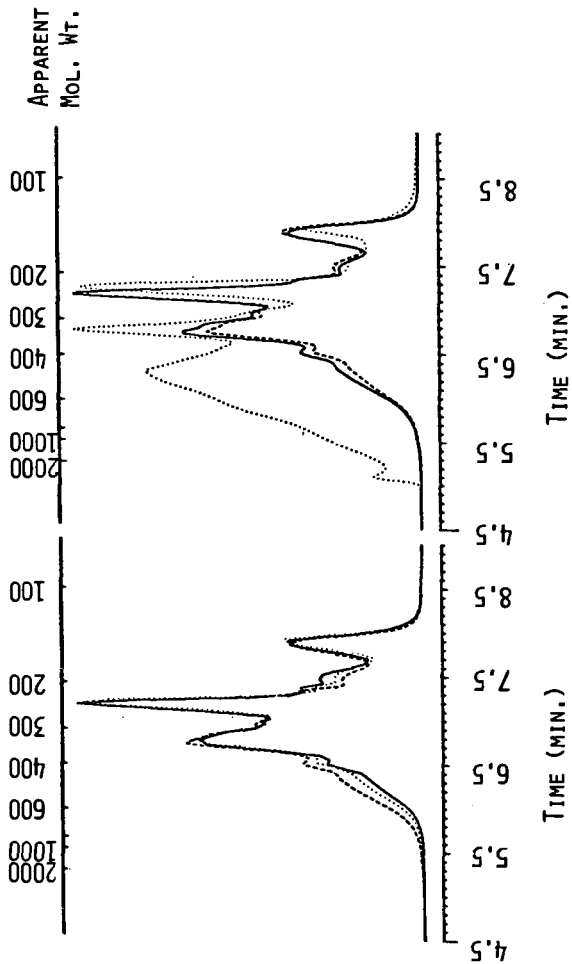


FIGURE 4. HPSEC OF PYROLYSIS OIL KEPT UNDER AMBIENT CONDITIONS AFTER 5 HRS (—), 3 DAYS (...), AND 7 DAYS (---). ANALYZED ON A PL GEL 50 Å, 5 μ GPC COLUMN USING THF AT 1 ML MIN⁻¹ WITH DETECTION AT 270 NM (BANDWIDTH 10 NM).

FIGURE 5. HPSEC OF PYROLYSIS OIL AFTER 7 DAYS KEPT UNDER AMBIENT CONDITIONS (—), TAR FRACTION OF REFRIGERATED SAMPLE (...) AND AQUEOUS FRACTION OF REFRIGERATED SAMPLE (---). ANALYSIS CONDITIONS AS PER FIGURE 4.

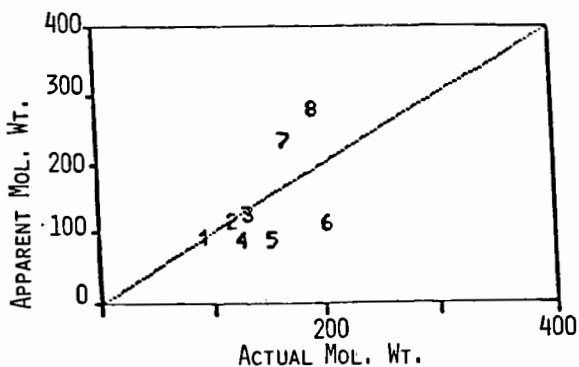


FIGURE 6. APPLICABILITY OF CALIBRATION FOR AROMATIC HYDROCARBONS, ACIDS, AND NAPHTHALENES. 1 = TOLUENE; 2 = PROPYL BENZENE; 3 = S-BUTYL BENZENE; 4 = NAPHTHALENE; 5 = 1,4-DIMETHYL NAPHTHALENE; 6 = 1-PHENYL NAPHTHALENE; 7 = VANILLIC ACID; 8 = 4-HYDROXY-3-METHOXY CINNAMIC ACID.

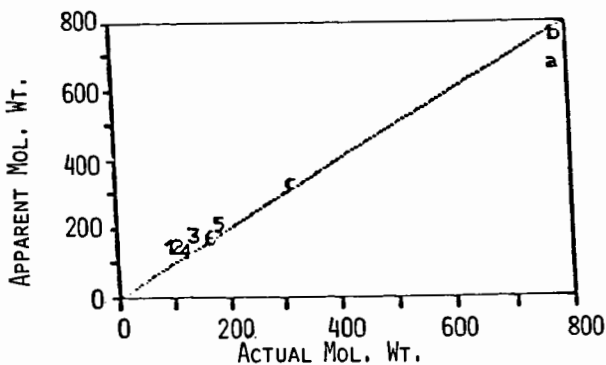


FIGURE 7. APPLICABILITY OF CALIBRATION FOR PHENOLS AND LIGNIN MODEL COMPOUNDS.

1 = PHENOL; 2 = P-CRESOL; 3 = 2-PROPYL PHENOL; 4 = GUAIACOL; 5 = SYRINGYL ALCOHOL; 6 = ACETOVANILLONE. LIGNIN MODELS: SEE

REF. 6 FOR DETAILED DESCRIPTION.

A = 5,5'-BIPHENYL TETRAMER HEXAOL, $C_{42}H_{54}O_{14}$

B = β -O-4 TETRAMER HEPTAOL, $C_{41}H_{52}O_{15}$

C = β -O-4 DIMER TRIOL, $C_{17}H_{20}O_6$.

CHROMATOGRAPHY OF NON-DERIVATIZED PYROLYSIS OILS AND UPGRADED PRODUCTS

E.J. Soltes and S-C.K. Lin
Dept. of Forest Science and TAES, Texas A&M University System
College Station, Texas 77843-2135

ABSTRACT

Over a period of several years [1], the Department of Forest Science at Texas A&M University has been conducting studies in the hydroprocessing (catalyzed high pressure hydrocracking plus hydrotreating or hydrodeoxygenation) of pyrolytic tars produced in biomass pyrolysis and gasification. Processing details are given elsewhere in this volume [2]. This paper discusses various chromatography techniques used to study composition of the volatile components of raw tars produced for these studies, the composition of products produced from these tars in the upgrading studies as well as a gel permeation / gas chromatography technique used to separate functionalities in raw and upgraded tars for kinetic studies of tar hydroprocessing. In all cases, no derivatization was required prior to chromatography.

METHODOLOGY

Capillary Gas Chromatography. We found suitable, for both the volatiles of tars and their upgraded products, the use of a 30-meter DB-5 bonded phase fused silica capillary column (J&W Scientific). The column was used in a Tracor 560 gas chromatograph (Tracor Inc., Austin TX) in the split injection mode (ca. 100:1). Temperature programming for the tars was held for 5 minutes at 30°C, then to 280°C at 3°C per minute. For the hydroprocessed tars, temperature was held at 30°C for five minutes, then programmed to 280°C at 4°C per minute. Signals were detected by a flame ionization detector and stored in raw form on diskettes for later reconstruction with the CAPS program of an IBM Instruments 9000 Computer.

Capillary GC-Mass Spec. The same columns were used in capillary GC-MS runs to determine composition of the separated components. Analysis was performed in subcontracts to Radian Corporation (Austin TX) using a Hewlett-Packard 5985A instrument. Conditions generally were on-column injection, hydrogen gas flow at 1 ml per minute, temperature programming was typically split 30°C to 100°C at 3°C per minute then to 280°C at 6°C per minute. Identification of peak contents was by comparison of spectra obtained with those reported in the literature, and the EPA/NIH Mass Spectral Data Base [4]. Computer-assisted component identification was not used.

Gel Permeation Chromatography. Although gas chromatography is suitable for the separation of volatile components, it cannot be used for the larger non-volatile molecules found in biomass tars. For these, gel permeation chromatography can be used. In earlier experimentation when evaluating various columns for this purpose, we determined that GPC columns can separate tar components not only by molecular size, but also somewhat surprisingly by functionality [2,5]. GPC separations were performed on a Model ALC/GPC 202 liquid chromatograph (Waters Associates) equipped with a refractometer (model R401). Four Styragel columns (30 cm x 7.8 mm i.d.) were used in series. THF, refluxed and distilled with sodium wire under a nitrogen atmosphere, was used to reduce tar viscosity, and tar/THF solutions (typically 25% tar in THF) were filtered through micropore filters (Millipore, 0.5 pore size) before injection. Maximum injection volume was 250 microliters.

Fractions separated were collected and subjected to GC analysis on the DB-5 column. Another 12-foot SP-2100 packed glass column (Supelco) was used to analyze the volatiles which were defined as the total amount of components detected by GC relative to a 1-decene internal standard.

More recent work shows satisfactory performance in the use of a single 5-micron PLgel column (60 cm x 7.7 mm I.D.; Polymer Laboratories) used with a Varian 5560 ternary liquid chromatograph equipped with ultraviolet (Varian UV-200) and refractive index

(Varian RI-3) detectors. Signals, as per the capillary gas chromatography, are stored in raw form on diskettes for later reconstruction with the CAPS2 program of an IBM Instruments 9000 Computer.

RESULTS AND DISCUSSION

GC of Raw Tars. Tars produced via the thermochemical conversion of biomass materials are very complex in chemical composition, with very few components in excess of 1% concentration [6]. Further, standard chemical separation techniques used to separate fractions of similar functionality are complicated by the wide range of molecular weights and difficult solubility of the various components. For example, one tar produced by the Tech-Air Corporation at their demonstration plant in Cordele, Georgia exhibited the gross composition shown in Table I [7]. Approximately 45% of the tar was water-soluble.

Despite the fact that the tars are produced by condensation of volatile matter, much of the tars appear to be of low volatility, typically 50 to 60%, when simple distillations are attempted. It appears that pot temperature above 200°C cause condensation reactions resulting in intractable pot solids.

Knowing that the volatiles content of raw pyrolytic oils is very low, and that higher temperatures such as might be experienced in the injection port of a gas chromatograph could cause condensation/ polymerization reactions, it was understandably with much hesitation that we initially attempted direct injection of tars into capillary columns for gas chromatography. After several hundred injections, we can now claim few problems in the use of capillary columns in split or splitless modes. Maintenance of column performance consists of occasional cleaning of the injection system, frequent baking of the column at 300°C to remove any volatile fragments resulting from thermal cracking of non-volatiles at oven temperature, and occasionally breaking off the first two or three cms of column containing the non-volatile matter. The bonded phase columns in particular appear to suffer little in performance with continued use.

Figures 1 and 2 show the gas chromatograms for the volatiles of Tech-Air pyrolysis oil and corn cob gasification tar, respectively. Note the similarity in chemical composition. Lignin appears to leave a strong signature in the volatile components, with the alkyl guaiacols predominating. Small concentrations of organic acids are found (see Table II), and these are responsible for the corrosivity of pyrolysis oils, as determined by corrosion tests using ASTM G31-72 [1,8]. Figure 3 gives the GC-MS chromatogram of the same oil and the same column as in Figure 1, except that on-column injection was used. Note that on-column injection results in less fractionation of the oil as seen in the higher concentrations of less volatile components.

GC of Hydroprocessed Tars. Tar, once hydroprocessed, is much easier to analyze for chemical composition than raw tar since it is nearly completely volatile, and thus easily subjected to gas chromatography and gas chromatography-mass spectrometry examination. Chromatograms of the hydroprocessed Tech-Air pine pyrolysis oil and the hydroprocessed corn cob gasification tar are shown in Figures 4 and 5 [9]. Alkyl cyclohexanes and their corresponding aromatic counterparts are predominant chemical species, derived from lignin phenolics (alkyl guaiacols) via hydrocracking and hydrotreating reactions. Some phenolics are still present due to incomplete hydrotreating. If desired, higher yields of phenolics are possible through less complete hydrogen consumption at milder reaction conditions. Alternately, the phenolics can be eliminated completely by saturation of chemical entities with hydrogen under more drastic conditions [10].

Some surprises in chemical composition of both the hydroprocessed pine waste tar and corn cob tars were contents of straight-chain hydrocarbons, similar and identical to the hydrocarbons found in conventional gasoline and diesel fuels. Straight-chain saturated hydrocarbons in the paraffinic series from C5 to C30 have been identified. The mechanisms by which these are produced are under investigation.

The two hydroprocessed tars examined were from different feed materials, and produced in two different processes in differing yields. Yet the volatiles chemical compositions of the tars, both before and after hydroprocessing are remarkably similar. This suggests that thermal conversion of biomass, followed by hydroprocessing of the tars

produced, might be a somewhat universal method for producing similar products from dissimilar biomass feedstocks.

GPC/GC of Raw and Hydroprocessed Tars. Figures 6 and 7 display gel permeation chromatograms for the Tech-Air pyrolysis oil and its hydroprocessed product. Fraction 1 at lower retention volumes is high molecular weight polymeric material; Fraction 2, larger molecules (size of C₁₄ to C₄₄ hydrocarbons); Fraction 3, phenolics; Fraction 4, aromatics; and Fraction 5, solvent used in hydroprocessing plus some smaller molecules. Note that this analysis results in separation of chemical functionality, and this fact was used in subsequent kinetic studies of the hydroprocessing reaction [2]. Figures 8 and 9 are gas chromatograms of the aromatic fraction 4 for the raw and hydroprocessed oil, respectively.

Other Chromatography. Other chromatography, especially that showing similarities in the compositions of oils and hydroprocessed oils from nine different biomass feedstocks will be discussed in the oral version of this communication.

ACKNOWLEDGMENTS

This research has been generously supported by the Texas Agricultural Experiment Station, the Center for Energy and Mineral Resources and the College of Agriculture, all parts of the Texas A&M University System, and by two USDA Special Research Grants (Agreements 59-2481-0-2-089-0 and 59-2481-1-2-123-0).

REFERENCES

- [1] E.J. Soltes and S-C.K. Lin, "Hydroprocessing of Biomass Tars for Liquid Engine Fuels", in: *Progress in Biomass Conversion*, Volume V, D.A. Tillman and E.C. Jahn, editors, pp.1-68, Academic Press, New York (1984).
- [2] E.J. Soltes, "Catalyst Specificities in High Pressure Hydroprocessing of Pyrolysis and Gasification Tars", Production, Analysis and Upgrading of Pyrolysis Oils from Biomass, American Chemical Society Meeting, April 5-10, Denver CO.
- [3] Y-H.E. Sheu, R.G. Anthony and E.J. Soltes, "Kinetic Studies of Upgrading Pyrolytic Oil by Hydrotreatment", *I&EC* (1985).
- [4] Heller, S.R. and G.W.A. Milne, *EPA/NIH Mass Spectral Data Base (Four volumes)*. NSRDS-NBS 63. U.S. Dept. of Commerce/National Bureau of Standards, Washington DC, 1978.
- [5] Y-H.E. Sheu, C.V. Philip, R.G. Anthony and E.J. Soltes, "Separation of Functionalities in Pyrolytic Tar by Gel Permeation Chromatography - Gas Chromatography", *J. Chromatog. Science* 22, 497-505 (1984).
- [6] E.J. Soltes and T.J. Elder, "Pyrolysis", in: *Organic Chemicals from Biomass*, I.S. Goldstein, editor, CRC Press, Boca Raton FL, 1981.
- [7] E.J. Soltes, "Biomass Degradation Tars as Sources of Chemicals and Fuel Hydrocarbons", in: *Wood and Agricultural Residues: Research on Use for Feed, Fuels and Chemicals*, E.J. Soltes, editor, Academic Press, New York NY (1983).
- [8] S-C.K. Lin, *Volatiles Constituents in a Wood Pyrolysis Oil*, M.S. Thesis, Forest Science, Texas A&M University, May 1978.
- [9] E.J. Soltes, "Hydrocarbons from Lignocellulosic Residues", *Appl. Polymer Symp.* 37, 775-86 (1983).
- [10] S-C.K. Lin, *Hydrocarbons via Catalytic Hydrogen Treatment of Pine Pyrolytic Oil*, Ph.D. Dissertation, Forest Science, Texas A&M University, May 1981.

TABLE I. GROSS FUNCTIONAL COMPOSITION OF TECH-AIR PINE PYROLYSIS OIL

	<i>Water Soluble %</i>	<i>Water Insoluble %</i>	<i>Total %</i>
Neutrals			
volatile	5.6	0.0	5.6
non-volatile	1.2	28.2	29.4
total	6.8	28.2	35.0
Phenols			
volatile	2.2	0.3	2.4
non-volatile	18.1	13.2	31.3
total	20.3	13.4	33.7
Acids			
volatile	5.2	0.0	5.2
Unextractables	13.1	2.0	15.1
Water	9.7	-	-
Losses	1.3	-	-
Total	56.4	43.6	100.0

TABLE II. RELATIVE ABUNDANCE AND PERCENTAGE COMPOSITION OF VOLATILE ACIDS IN PINE PYROLYSIS OIL

	<i>Formic Acid</i>	<i>Acetic Acid</i>	<i>Propionic Acid</i>	<i>Peak no.3</i>	<i>Butyric Acid</i>	<i>Peak no.5</i>	<i>Isovaleric Acid</i>
Relative Abundance	17.9	100.0	13.47	0.50	3.66	1.00	1.00
% Composition	0.32	1.70	0.24	0.01	0.06	0.02	0.02

Peaks no. 3 and 5 were not identified in gas chromatography, but exhibited acidic properties similar to the other components.

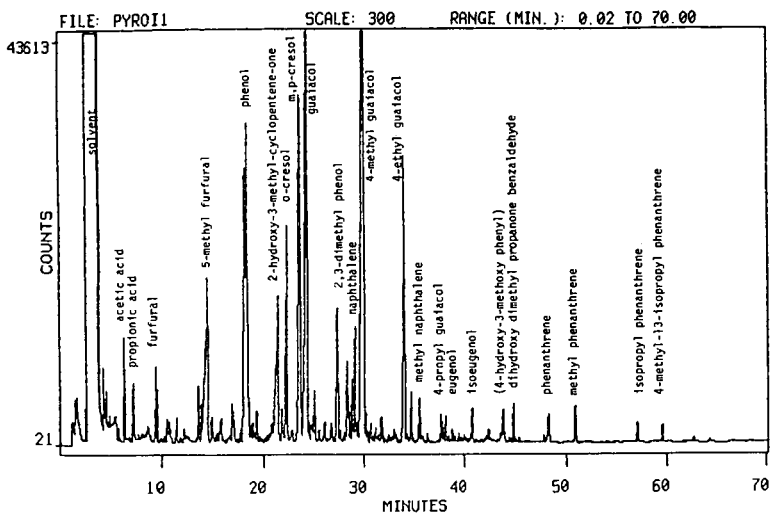


FIGURE 1. Volatiles of Tech-Air Pine Waste Pyrolysis Oil

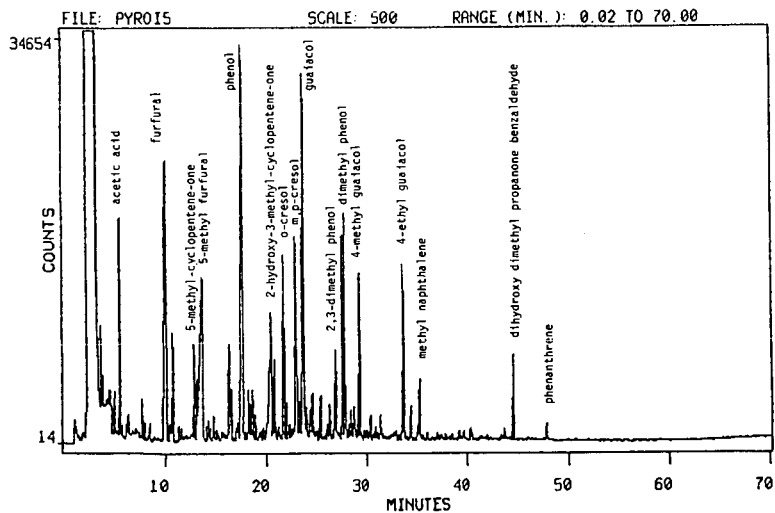


FIGURE 2. Volatiles of Corn Cob Gasification Tar

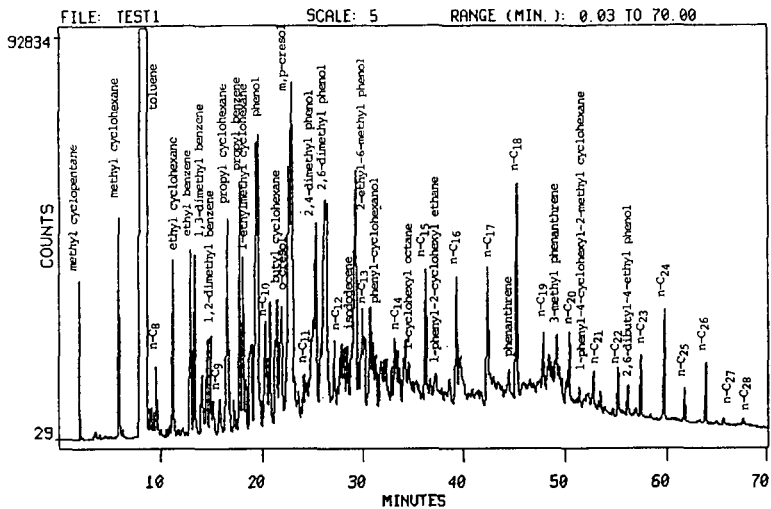


FIGURE 4. Volatiles of Hydroprocessed Tech-Air Pyrolysis Oil

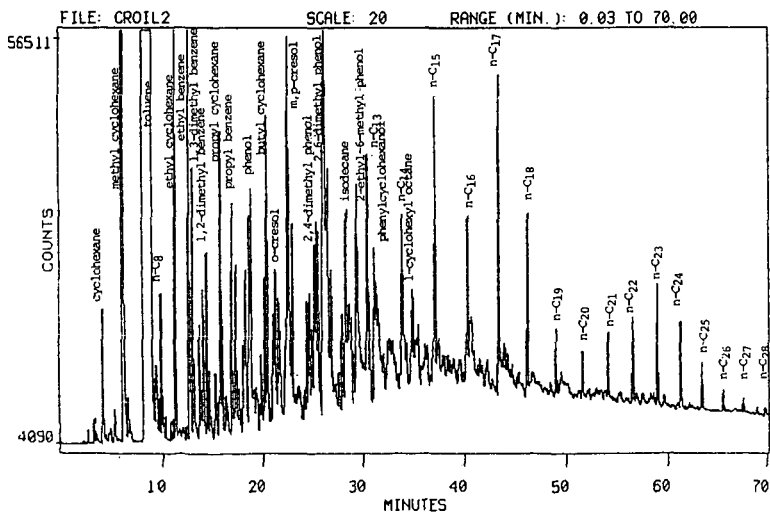


FIGURE 5. Volatiles of Hydroprocessed Corn Cob Gasification Tar

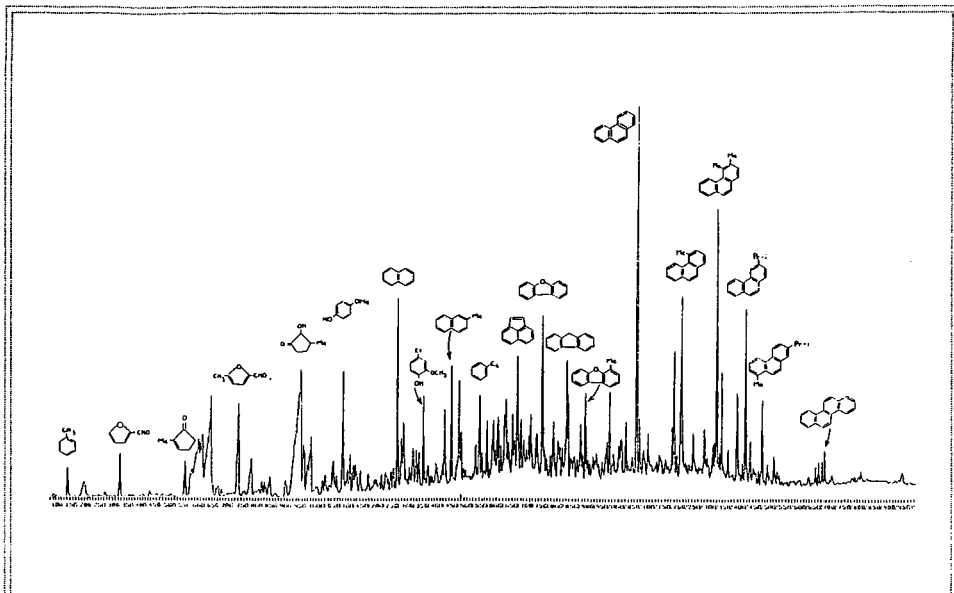


FIGURE 8. Aromatic Fraction (#4), Tech-Air Pyrolysis Oil

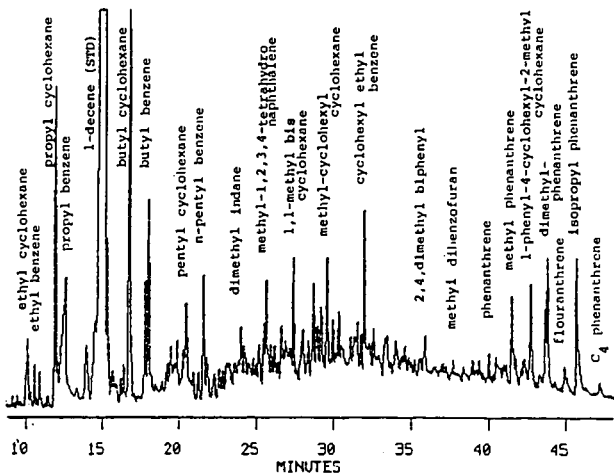


FIGURE 9. Aromatic Fraction (#4), Hydroprocessed Tech-Air Oil

PRODUCT ANALYSIS FROM DIRECT LIQUEFACTION OF SEVERAL HIGH-MOISTURE BIOMASS FEEDSTOCKS

Douglas C. Elliott, L. John Sealock, Jr. and R. Scott Butner

Pacific Northwest Laboratory*, P.O. Box 999, Richland, WA 99352

PROCESS RESEARCH IN DIRECT LIQUEFACTION OF BIOMASS

Significant progress has been made over the past fifteen years toward the development of processes for direct production of liquid fuels from biomass. Process research has generally progressed along two lines -- flash pyrolysis and high-pressure processing. Extensive analysis of the liquid products from these two types of processes has demonstrated the significant process-related differences in product composition. However, the effect of feedstock has received a lesser degree of attention.

Liquefaction Processes

Two generalized categories of direct liquefaction processes can be identified.(1) The first, flash pyrolysis, is characterized by a short residence time in the reactor (~1 second) at relatively high temperature (450-500°C) in order to obtain maximum yield of liquid product. The second, high-pressure processing, is usually performed at lower temperature (300-400°C) and longer residence time (0.2-1.0 hr). A typical operating pressure is 200 atm and often reducing gas and/or a catalyst is included in the process. The differences in processing conditions result in significant differences in product yield and product composition.

Product Analyses

Product analysis in support of the process development research in biomass direct liquefaction began at rudimentary level of determining solvent-soluble portions of the product. Analysis was soon extended to elemental analyses and proximate analyses, such as ash and moisture. Later, spectrometric analyses were performed followed by detailed chemical analyses used in conjunction with chromatographic separation techniques.

At all stages of development, the significant differences in composition between the products of flash pyrolysis and high-pressure processing have been evident. While polar solvents are most effective for both products, less polar solvents such as methylene chloride and even benzene and toluene have been used as extractants for high-pressure product oils. Comparative analysis has demonstrated the higher oxygen content and higher dissolved water content in the flash pyrolysis oils. Detailed analyses with spectrometric and chromatographic methods have added supporting evidence to these findings.

Variations in Product Due to Feedstock

While process-related differences in product composition have been evident, extensive study of the effect of feedstock on product composition has never been undertaken. Some limited comparative tests can be gleaned from the literature; however, most process research in direct liquefaction of biomass has been performed with woods of various species. Table 1 provides some of the results available in the literature for non-woody feedstocks. Significant differences in heteroatom content are evident, but only limited chemical analysis is available in most cases.

* Operated by Battelle Memorial Institute for the U.S. Department of Energy under contract DE-AC06-76RLO 1830

TABLE 1. Product Analyses from Liquefaction Tests with Various Biomasses

Feedstock	Temp. °C	Pressure psig	C	H	N	O	S	H/C
			percent					
<u>High-Pressure Processes</u>								
(2) newsprint	250	2,000	71.7	7.3	<0.3	~20.6	<0.1	1.21
(2) pine needles & twigs	250	2,000	72.2	8.7	1.05	18.0	0.10	1.43
(2) sewage sludge	250	2,000	77.0	10.7	2.80	8.8	0.64	1.65
(3) cellulose	250	2,000	72.4	7.0	.004	20.4	0.2	1.15
(3) sucrose	350	4,000	75.2	9.1	--	15.7	--	1.44
(4) municipal refuse	380	5,000	79.8	10.4	3.0	6.8	0.05	1.55
(4) manure	380	4,500 [∞]	80.4	9.4	3.0	6.9	0.26	1.39
(5) microalgae	400	4,000 [∞]	*81.2	8.6	5.4	3.5	--	1.26
<u>Flash Pyrolysis</u>								
(6) aspen	450	0	53.8	6.7	--	39.3	--	1.48
(7) sewage sludge	450	0	69.4	10.2	5.8	14.5	--	1.75
(8) poplar	500	0	49.8	7.3	0.0	42.8	0.0	1.74
(8) peat	520	0	67.1	9.0	3.4	20.3	0.1	1.59

[∞] estimate

* the microalgae analysis was calculated from the analysis of product fractions (oil and asphaltene) and the product distribution

The researchers at the Pittsburgh Energy Research Center (2,3,4) steadfastly maintained in their pioneering work that their oil products obtained from cellulosic wastes were paraffinic and cycloparaffinic in nature. They reported the presence of carbonyl and carboxyl functional groups but maintained that there was essentially no aromatic material produced except at higher temperature (then only in very small amounts). These conclusions were based on infrared and mass spectral analysis.(2) Later analysis of the sucrose-derived oil (3) included proton nuclear magnetic resonance spectral evaluation but resulted in the same conclusion. Most of the hydrogen was in methylene or methyl groups and about 4 percent was unsaturated but probably olefinic and not aromatic. Some ether linkages were also reported present in the sucrose-derived oil. Mass spectral analysis of the municipal refuse-derived oil (4) identified only two long chain fatty acids with certainty; however, not more than traces of aromatics were determined to be present. The manure-derived oil was found to be largely alicyclic hydrocarbon but contained heterocyclic nitrogen and alkyl phenolics.(4) These claims of the saturated hydrocarbon nature of the oil products are at odds with the reported elemental analyses (see Table 1). The low hydrogen to carbon ratios dictate that the oil products must contain a large fraction of aromatic or, at least, highly unsaturated compounds.

An algae-derived oil was reported to be principally n-paraffins and olefins with oxygen- and nitrogen-containing straight-chain hydrocarbons.(5) Polar compounds were reported to comprise 50-60 percent of the oil. Unfortunately, there is no indication of the type of analysis performed or detailed results of any kind; therefore, it is difficult to evaluate the veracity of these reported results.

The comparison of the peat and wood flash pyrolysis products is a good example of the effect of feedstock on product oil composition.(8) The poplar oil typically was composed of phenolic, ketone and furan compounds with a substantial fraction of low molecular weight organic acids. The main components of the peat oil were hydrocarbons, mostly straight chain olefins. Minor quantities of ketones were

noted but no acids, aldehydes or furans were identified by mass spectrometry. Phenols were also present in significant quantities.

A significant effort in comparing feedstock effects on product oil composition was reported by Russell et al.(9) Unfortunately, this effort did not include ultimate analysis of the oils for comparison. The report contains qualitative analysis by gas chromatography/mass spectrometry of five product oils derived from cellulose, hops field residue, softwood tree branches, peat, and sewage sludge. Phenols were a major component group for all feedstocks. Ketones and furans were also common. Hydrocarbons, aromatic and otherwise, were also identified primarily in the cellulose and softwood products. Nitrogen-containing products were absent from the cellulose and softwood products but could be found in the peat and sewage sludge-derived oils.

All of the above accounts can be contrasted with the large amount of analytical work on the chemical composition of wood-derived direct liquefaction products which has been reported over the past several years.(8,10-16) In all cases the majority of the product oils have been identified as phenolic with only minor amounts of pure hydrocarbon reported.

LIQUEFACTION EXPERIMENTS WITH MOIST BIOMASS

At Pacific Northwest Laboratory we have been testing the use of high-moisture biomass (marine and fresh-water biomass, post-harvest field residues and food processing wastes) in a thermochemical conversion system to produce useful fuels. Although the main focus of the work (17) has been gasification (catalytic production of methane) we have also performed a limited number of tests under high-pressure liquefaction conditions.

Feedstock Description

Five high-moisture biomass feedstocks were tested in these liquefaction experiments. They are characterized as follows:

Kelp - The sample used was a freshly harvested macrocystis kelp from Pacific Ocean seabeds off the southern California coast (El Capitan Beach, Santa Barbara Channel). It was packed in ice and flown to our laboratory where it was frozen in a polyethylene bag until used.

Water Hyacinth - Uprooted samples of hyacinths were recovered from the primary treatment lagoon at the Reedy Creek experimental sewage treatment facility near Orlando, Florida. The sample was packed in ice and flown to our laboratory where it was frozen in a polyethylene bag until used.

Spent Grain - The grain sample used was the residue following malting barley and water extraction of the sugars prior to fermentation. The sample was obtained from the Blitz-Weinhard Brewery in Portland, Oregon and was transported to our laboratory where it was frozen until used.

Napier Grass - Napier grass was collected after harvest by University of Florida researchers. The sample was bagged and shipped in a refrigerated container to our laboratory where it was stored in a freezer until used.

Sorghum - Grain sorghum was collected after the harvest of the grain by the University of Florida. The sample containing stems, stalks, and leaves was bagged and shipped in a refrigerated container to our laboratory where it was stored in a freezer until used.

Ultimate analysis, moisture contents and energy contents for the five feedstocks are provided in Table 2.

TABLE 2. Analysis of Moist-Biomass Feedstocks

	C	H	N	O	Ash	Moisture percent	HHV* BTU/lb
	percent, dried basis						
Kelp	26.9	4.0	1.2	30.2	38.4	88.9	7150
Water Hyacinth	43.0	5.8	5.6	29.5	15.3	94.9	7730
Spent Grain	48.6	6.8	3.4	35.3	3.4	80.5	9160
Napier Grass	44.5	5.9	<0.1	41.9	5.7	84.4	7870
Sorghum	44.7	5.8	0.2	37.5	7.9	77.0	8046

*HHV = higher heating value of dried biomass

Reactor Conditions

The experiments were performed batchwise in a one-liter, stirred autoclave. Approximately 300 g of moist-biomass was charged to the autoclave in a stainless steel liner. Sodium carbonate was added to the feedstock (approximately 0.1 g/g dry biomass) except in the case of kelp which already contains a high level of alkali as part of its chemical makeup.

The autoclave was then sealed, purged with nitrogen and then pressurized with carbon monoxide (approximately 50 atm). The reactor was heated to 350°C (approximately 30 minutes from 200° to 350°C) and held at that temperature for 30 minutes. The pressure within the autoclave at temperature typically increased from 270 atm to 340 atm over the period of the experiment. At the end of the allotted time cooling water was flushed through our internal cooling coil which brought the reactor temperature down to 200°C within 5 minutes.

Product Recovery and Analysis

After the autoclave had cooled completely, the gas product was vented. The typical gas composition included nearly equal parts of hydrogen and carbon dioxide with a 10-15 percent residual amount of carbon monoxide and minor amounts of hydrocarbons. [These results suggest a strong water-gas shift reaction as catalyzed by the sodium carbonate base.(18)] The autoclave was then opened and the two-phase liquid product was collected. The autoclave was rinsed with acetone and the resulting wash solution filtered. The liquid product was acidified to pH 2 with dilute HCl and then extracted with methylene chloride.

The soluble and insoluble products were analyzed for elemental content of carbon, hydrogen, nitrogen and oxygen with Perkin-Elmer 240 series instruments. The methylene chloride soluble oil product was also analyzed as a methylene chloride solution on a gas chromatograph equipped with a mass selective detector for qualitative analysis and a similar gas chromatograph equipped with a flame ionization detector for quantitative analysis. Identification of compounds was made by comparison of mass spectra with library listings of known compounds in conjunction with a comparison of chromatograph column residence time with similar known compounds. Quantitative analysis was based on a known amount of internal standard (trans-decahydronaphthalene) with detector response factors determined for various functional group types. Quantitation is estimated at within ± 20 percent. DB-5 capillary columns are used in both chromatographs.

LIQUEFACTION RESULTS AND PRODUCT DESCRIPTION

Liquefaction Experimental Results

Results from the liquefaction experiments with the five moist-biomass feedstocks are given in Table 3. The oil yield is based on the combined mass of acetone- and methylene-chloride soluble oils as a percent of the mass of dried feedstock calculated to an ash-free basis. The product oil elemental analysis is the calculated composite analysis for the combined acetone- and methylene chloride-soluble oils.

TABLE 3. Experimental Results for Liquefaction Experiments

	<u>Oil Yield</u> percent	<u>C</u>	<u>H</u>	<u>N</u>	<u>O</u>	<u>H/C</u>
		combined oil analyses				
Kelp	19.2	76.7	8.9	3.5	9.9	1.38
Water Hyacinth	26.0	76.3	9.9	3.3	10.5	1.54
Spent Grain	34.7	75.2	10.2	3.8	10.8	1.61
Napier Grass	34.4	74.5	8.5	0.4	16.7	1.36
Sorghum	26.6	75.9	8.7	1.7	13.7	1.36

The test results in Table 3 demonstrate oil product yields for liquefaction of the moist-biomass feedstocks at levels comparable to wood liquefaction. Reported yields for wood liquefaction in aqueous slurries, such as the LBL process, (19) have typically been in the 25 to 30 weight percent range. The quality of the moist-biomass liquefaction products fall in a general range which is also similar to reports for wood liquefaction products. However, certain examples of moist-biomass product oils appear to have elemental compositions suggesting higher quality products. Especially interesting are the high hydrogen to carbon ratios for the spent grain and water hyacinth products and the relatively low oxygen contents of the spent grain, water hyacinth and kelp products. A significant difference from wood-derived oils is the high nitrogen content in the oils from spent grain and aquatic biomasses.

Product Analysis Details

The detailed chemical analysis of the five moist-biomass derived oils by gas chromatography and mass spectrometry helps to better define the differences in oil composition. Over 190 different compounds and isomers were identified in the five oils. In order to better understand this large amount of information the components have been grouped by chemical functionality and these groups are listed in Table 4.

The compound groups consist of the following types of compounds:

esters/aldehydes/alcohols - four to six carbon oxygenates
cyclic ketones - five and six carbon rings, many unsaturated, most alkylated
furans - dihydrofuranones, hydroxymethyltetrahydrofuran
phenols - phenol and alkylated (up to five carbons) phenols
methoxyphenols - mono- and dimethoxyphenols and alkylated forms
benzenediols - dihydroxybenzenes and alkylated (up to five carbons) forms
naphthols - naphthols and methylated naphthols
aromatic oxygenates - bismethylguaiacol(?), phenylphenols, benzodioxin(?)
cyclic hydrocarbons-alkylcyclopentenes, alkylbenzenes(?), alkylindans, phenanthrene
long-chain hydrocarbons - C₁₄ to C₂₇ n-alkanes and olefins
fatty acids - C₁₂ to C₂₀ saturated and unsaturated acids
nitrogen cyclics-alkylpyrrolidinones, alkylaziridines(?), alkylpyrroles,
alkylindoles
amines/amides - C₈ to C₂₂ amines/amides(?)

TABLE 4. Chemical Functional Groups in Moist-Biomass Oil Products*

Compound Group	Kelp	Water Hyacinth	Spent Grain	Napier Grass	Sorghum
esters/aldehydes/alcohols	0 (1)	0 (0)	0 (1)	3 (4)	0 (0)
cyclic ketones	8 (13)	3 (9)	7 (10)	20 (25)	6 (12)
furans	0 (0)	1 (1)	4 (3)	2 (3)	2 (3)
phenols	11 (9)	22 (18)	26 (15)	35 (24)	21 (14)
methoxy phenols	3 (3)	3 (2)	3 (1)	5 (5)	10 (5)
benzenediols	11 (2)	6 (4)	0 (0)	6 (6)	25 (11)
naphthols	9 (5)	2 (3)	0 (0)	5 (9)	9 (6)
aromatic oxygenates	1 (2)	3 (3)	6 (2)	4 (5)	2 (2)
cyclic hydrocarbons	21 (15)	12 (18)	7 (9)	16 (24)	16 (19)
long-chain hydrocarbons	6 (3)	16 (15)	5 (4)	3 (9)	4 (4)
fatty acids	11 (3)	8 (7)	8 (4)	1 (2)	5 (4)
nitrogen cyclics	17 (11)	17 (11)	19 (7)	0 (0)	0 (0)
<u>amines/amides</u>	<u>3 (1)</u>	<u>6 (3)</u>	<u>15 (7)</u>	<u>0 (0)</u>	<u>0 (0)</u>
percent identified	10.3	17.8	14.2	20.4	17.8

* tabular listing is the mass percent of identified oil components in each compound group; the number in parentheses is the number of individual compounds and isomers in each compound group

Comparison to Earlier Results

These results verify that the carbohydrate structures found in biomass can be converted thermochemically to a mixture of primarily phenolic compounds. Hydrocarbons are not predominant yet they may survive the processing in a significant yield given an appropriate feedstock. Cyclic ketones are the other major component group which can be identified by GC/MS. Low molecular weight oxygenates and furans are minimized by the addition of base to the reaction medium as has been demonstrated by other researchers.(20)

The product compositions of the napier grass and sorghum-derived product oils shown many similarities to wood-derived oils. In comparing with high-pressure processed oil from Douglas fir the same groups of cyclic ketones, phenols, naphthols, and dihydroxybenzenes dominate. The traces of hydrocarbon in the sorghum and napier grass oils are significantly different from the Douglas fir and are apparently feedstock related. Nitrogen-containing compounds were not found in either the Douglas fir oils or the sorghum or napier grass oils reported here.

The large fraction of nitrogen-containing cyclic compounds is the distinguishing factor between the hyacinth, kelp and grain oils when compared to earlier wood oil analyses. Similar compounds were found earlier in peat and sewage sludge oils.(9) Our results now extend this trend to high protein feedstocks and green,

aquatic plants. It is obvious that a strong correlation exists between nitrogen content of the feedstock and the amount of nitrogen incorporated into the product oil. High-pressure liquefaction even with a reducing gas environment and alkaline catalysis cannot effect a preferential denitrogenation reaction. Substantial amounts of nitrogen are condensed into cyclic systems which remain in the oil product.

Utilization of Oil Products from Moist Biomass

The oil products from these high-moisture biomasses have properties similar to the more widely studied wood-derived oils. The numerous applications of wood-derived oil have been discussed by others (10a, 20). The moist-biomass oils should be amenable to the same types of applications. In addition, the nitrogen-containing compounds may be useful as chemical commodities. Indoles in particular may be recoverable for use as fragrances or flavors. The hydrocarbon component in the oils may facilitate the direct use of these oils as fuels.

The nitrogen-containing components in some of the moist-biomass oils is a source of concern when considering their use as fuels. Direct utilization of these oils would certainly lead to higher levels of emission of NO_x . The nitrogen-containing components have also been indicated as a source of fuel instability during storage and as cancer-causing agents in various chemical forms. Hydrotreating of these oil products to remove the nitrogen is a possible means of upgrading the products. However, hydrodenitrogenation of the heterocyclic compounds is a difficult and costly procedure compared to hydrodeoxygenation of the phenolics, which would also be accomplished in a hydrotreating type of oil upgrading.

Implications for Future Research

The high-moisture biomass feedstocks can be a source of useful liquid fuel products. The use of the high-moisture biomasses in high-pressure processing will allow their utilization in a thermochemical process without prior drying. Other research on the use of these feedstocks in high-pressure gasification has suggested the feasibility of feeding these materials as a slurry following maceration.(17) This same type of feeding should allow direct utilization of high-moisture biomass in high-pressure liquefaction processing. Experimental verification of this type of continuous processing needs to be undertaken.

The use of the nitrogen-containing feedstocks will lead to production of a nitrogen-containing oil product. Direct utilization of this oil product as a fuel will likely require development of appropriate emission control techniques in order to maintain air quality. Alternately, nitrogen-containing components can be removed from the oil product for use as specialty chemicals or by hydrotreating. Further development of hydrotreating technology specific to these oils may be necessary in order to process the heterocyclic nitrogen-containing compounds which require extensive processing in order to effect nitrogen removal.

ACKNOWLEDGMENTS

This research was performed as part of a project titled "Low-Temperature Thermochemical Conversion of High-Moisture Biomass Feedstocks" funded through the Biomass Thermochemical Conversion Program Office at Pacific Northwest Laboratory by the U.S. Department of Energy, Biofuels and Municipal Waste Technology Division, S. Friedrich, Program Manager. The authors also acknowledge the help of three coworkers at Pacific Northwest Laboratory, G. G. Neuenschwander, who operated the batch reactor, R. T. Hallen, who performed the chromatography and mass spectrometry, and W. F. Riemath, who performed the elemental analyses.

REFERENCES

1. D. Beckman and D. C. Elliott, "Comparisons of the Yields and Properties of the Oil Products from Direct Thermochemical Biomass Liquefaction Processes" Can. J. Chem. Eng. 63, 99-104, 1985.
2. H. R. Appell, I. Wender, and R. D. Miller, Conversion of Urban Refuse to Oil Bureau of Mines Solid Waste Program, Technical Progress Report-25, May 1970.
3. H. R. Appell, Y. C. Fu, S. Friedman, P. M. Yavorsky, and I. Wender, Converting Organic Wastes to Oil: A Replenishable Energy Source, Report of Investigations 7560, Pittsburgh Energy Research Center, 1971.
4. H. R. Appell, Y. C. Fu, E. G. Illig, F. W. Steffgen, and R. D. Miller, Conversion of Cellulosic Wastes to Oil, Report of Investigations 8013, Pittsburgh Energy Research Center, 1975.
5. L.-Y. Chin and A. J. Engel, "Hydrocarbon Feedstocks from Algae Hydrogenation," Biotech. & Bioeng. Symp. #11, 171-186, 1981.
6. D. S. Scott, J. Piskorz and D. Radlein, "Liquid Products from the Continuous Flash Pyrolysis of Biomass" Ind. & Eng. Chem., Proc. Des. & Dev. (24) 581-588, 1985.
7. J. Piskorz, D. S. Scott, and I. B. Westerberg. "Flash Pyrolysis of Sewage Sludge" Ind. & Eng. Chem., Proc. Des. & Dev. (25) 265270, 1986.
8. D. C. Elliott, "Analysis and Upgrading of Biomass Liquefaction Products," IEA Co-operative Project D1 Biomass Liquefaction Test Facility project Final Report, Volume 4, December 1983, PNL-5933, Volume 4, National Technical Information Service, Springfield, Virginia.
9. J. A. Russell, P. M. Molton and S. D. Landsman, "Chemical Comparisons of Liquid Fuel Produced by Thermochemical Liquefaction of Various Biomass Materials" presented at the 3rd Miami International Conference on Alternative Energy Sources, Miami, Florida, December 17, 1980, PNL-SA-8602, Pacific Northwest Laboratory, Richland, Washington.
10. a. D. C. Elliott, "Description and Utilization of product from Direct Liquefaction of Biomass" Biotech. & Bioeng., Symp #11, 187-198, 1981.
b. D. C. Elliott, "Analysis and Comparison of Products from Wood Liquefaction" Fundamentals of Thermochemical Biomass Conversion, Chapt. 55, 1003-1018, Elsevier Applied Science Publishers, London, 1985.
11. O. Karlsson and P. Björnbom, "Characterization of Peat and Biomass Liquids" Fundamentals of Thermochemical Biomass Conversion, Chapt. 56, pp. 1019-1026, Elsevier Applied Science Publishers, London, 1985.
12. H. G. Davis, M. A. Evans, C. Figueroa, R. R. Gansley, L. L. Schaleger and D. W. Watt, "The Products of Direct Liquefaction of Biomass" Fundamentals of Thermochemical Biomass Conversion, Chapt. 57, pp. 1027-1037, Elsevier Applied Science Publishers, London, 1985.
13. R. L. Eager, J. F. Mathews, J. M. Pepper and H. Zohdi, "Studies on the Products Resulting from the Conversion of Aspen Poplar to an Oil" Can. J. Chem. (59) 2191-2198, 1981; R. L. Eager, J. M. Pepper, J. C. Roy and J. F. Mathews, "Chemical Studies on Oils Derived from Aspen Poplar Wood, Cellulose and an Isolated Aspen Poplar Lignin" Can. J. Chem. (61) 2010-2014, 1983.

14. H. Menard, D. Bélanger, G. Chauvette, M. Grisé and A. Martel, "Liquid from Biomass by Pyrolysis: Analytical Aspects," Comptes Rendus De L'Atelier de Travail sur la Liquéfaction de la Biomasse, pp. 208-213, National Research Council of Canada, NRCC23120, 1983.
15. D. G. B. Boocock, R. K. M. R. Kallury and T. T. Tidwell, "Analysis of Oil Fractions Derived from Hydrogenation of Aspen Wood" Anal. Chem. (55) 1689-1694, 1983.
16. E. J. Soltes and T. J. Elder, "Pyrolysis" Organic Chemicals from Biomass, Chapt. 5, pp. 63-99, CRC Press Inc., Boca Raton, Florida, 1981.
17. R. S. Butner, D. C. Elliott and L. J. Sealock, Jr., "Low-Temperature Thermochemical Conversion of High-Moisture Biomass Feedstocks" Proceedings of the 1985 Biomass Thermochemical Conversion Contractors' Meeting, February 1986, pp. 193-209, PNL-SA-13571, Pacific Northwest Laboratory, Richland, Washington.
18. D. C. Elliott, R. T. Hallen and L. J. Sealock, Jr. "Aqueous Catalyst Systems for the Water-Gas Shift Reaction. 2. Mechanism of Basic Catalysis" Ind. & Eng. Chem., Prod. Res. & Dev. (22), 431-435, 1983.
19. C. Figueroa, L. L. Schaleger and H. G. Davis, "LBL Continuous Bench-Scale Liquefaction Unit, Operation and Results" Energy from Biomass & Wastes VI, pp. 1097-1112, Institute of Gas Technology, Chicago, Illinois, 1982.
20. D. A. Nelson, P. M. Molton, J. A. Russell and R. T. Hallen. "Application of Direct Thermal Liquefaction for the Conversion of Cellulosic Biomass" Ind. & Eng. Chem., Prod. Res. & Dev. (23) 471-475, 1984.

An Integrated Spectroscopic Approach to the Chemical
Characterization of Pyrolysis Oils

Barbara L. Hoesterey, Willem Windig, Henk L.C. Meuzelaar (Biomaterials Profiling Center); Edward M. Eyring, David M. Grant (Chemistry Department); and Ronald J. Pugmire (Fuels Engineering Department)

University of Utah
Salt Lake City, UT 84108

ABSTRACT

The hydrocarbon ("oil") fraction of a coal pyrolysis tar prepared by open column liquid chromatography (LC) was separated into 16 subfractions by a second LC run. The first 13 of these fractions were chosen for integrated spectroscopic analysis. Low voltage mass spectrometry (MS), infrared spectroscopy (IR), and proton (PMR) as well as carbon-13 nuclear magnetic resonance spectrometry (CMR) were performed on the 13 fractions. Computerized multivariate analysis procedures such as factor or discriminant analysis followed by canonical correlation techniques were used to extract the overlapping information from the analytical data. Subsequent evaluation of the integrated analytical data revealed chemical information which could not have been obtained readily from the individual spectroscopic techniques. The approach described is generally applicable to multisource analytical data on pyrolysis oils and other complex mixtures.

INTRODUCTION

Due to the extremely complex nature of pyrolysis tars obtained from recent or fossil biomass samples structural and compositional analysis of such tars poses a formidable challenge to analytical chemists. Even when armed with an arsenal of sophisticated analytical techniques a detailed qualitative analysis requires careful, laborious combination and integration of voluminous chromatographic and spectroscopic data. True quantitative analysis is generally not within reach of current analytical methodologies, especially if the tar contains nonvolatile and/or highly polar or reactive components. Although in recent years impressive advances have been made with the physical coupling of two or more chromatographic and/or spectroscopic techniques into so-called "hyphenated" methods, e.g., GC/MS, LC/MS, GC/FTIR, MS/MS, etc., true integration of the analytical data by means of multivariate analysis methods such as canonical correlation analysis is rarely ever attempted. Yet, intuitively the potential advantages and benefits of data integration methods are easily understood. With these considerations in mind the authors carried out the present feasibility study of a coal-derived pyrolytic tar using a combination of chromatographic (LC), spectroscopic (MS, IR, PMR, CMR) and chemometrics (factor, discriminant and canonical variate analysis) techniques. In order to reduce the complexity of the analytical problem to more manageable proportions, a completely distillable coal tar was selected. Moreover, polar and/or highly reactive components were removed by open column LC. Preliminary results of this integrated analytical approach will be presented here.

EXPERIMENTAL

A pyrolysis tar from a high volatile B bituminous Hiawatha seam coal (Wasatch Plateau field, Utah) was obtained from the fixed bed Wellman Galusha gasifier operated by Black, Sivalls and Bryson in Minneapolis. Open column liquid chromatography (LC) on silica gel using four solvents and solvent mixtures of increasing polarity; i.e. hexane; hexane/benzene 8/1; benzene/ether 4/1; and benzene/methanol 1/1, was used to separate the whole tar into broad compound classes as described by McClennen *et al.* (1). The hexane and hexane/benzene eluted fractions constituted

complex mixtures, principally composed of hydrocarbons. These fractions were combined and further separated by a second IC run. Fractions were eluted from the column with a nonlinear gradient beginning with 100% n-hexane and stabilizing at 10% benzene/90% hexane over a period of 30 min. Sixteen fractions were collected and weighed over a total of 40 minutes. Approximately 1 ml was taken from each sample for low voltage MS analysis. The remaining subfractions were then rotary evaporated and weights of residue were recorded. The calculated elution volumes are shown in Figure 1.

Low voltage mass spectra were run on an Extranuclear 5000-1 quadrupole mass spectrometer with Curie-point heating inlet. Low voltage mass spectra of subfractions 1-15 were obtained using 1/4 ul glass capillary probe tips as described by McClennen et al. [2]. Electron energy was set at 12 eV. Samples were scanned from m/z 20 to m/z 300. The inlet was heated to 200°C. Mass spectra were stored on an IBM 9000 computer and printed out in the form of bar plots. Examples of low voltage mass spectra are shown in Figure 2.

FTIR spectra were obtained using neat samples on NaCl (salt) disks. The instrument was a Nicolet 7000 series spectrometer, resolution 4 cm⁻¹, 200 scans, operated in the absorbance mode. Samples were scanned from 4000-600 cm⁻¹. Absorbance intensities were recorded for 20-30 peaks in each spectrum. In this way 33 wavenumber variables were obtained. Examples of FTIR spectra are shown in Figure 3.

Proton NMR spectra of the hydrocarbon subfractions dissolved in CD₂Cl₂ (with TMS) were taken using a Varian 300 superconducting instrument over the 1-10 ppm region. Integrated peak intensities for eight regions of the spectrum were tabulated for each subfraction, in addition to a table containing an overall view of the number of aliphatic, aromatic and olefinic protons present.

Carbon 13 NMR spectra of subfractions were also run in CD₂Cl₂ on the Varian SC 300 from 0-180 ppm. Peak intensities were measured using integration curves. Twenty three variables were chosen. Table 1 shows overall data from FMR and CMR.

Computerized multivariate analysis was carried out using the interactive SIGMA program package developed at the University of Utah Biomaterials Profiling Center which affords scaling, as well as factor, discriminant and canonical correlation analysis (3). Chemical components were numerically extracted using the Variance Diagram technique described by Windig et al. (4).

RESULTS AND DISCUSSION

The emphasis of this paper is on the general method of multisource data integration using Factor Analysis and Canonical Correlation Analysis. Figure 4 shows the variances calculated for the factors in each data set. For mass spectral and IR data, only eigenvalues greater than 1.0 are shown, whereas all factors were used for the FMR and CMR data. The dashed line shows eigenvalues <1.0, e.g. in the FMR, only Factor 1 had an eigenvalue > 1.0. Six factors from each data set were used for the canonical correlation analyses. Figure 3b shows the percent variance from the original factors that was represented in the subspace spanned by the canonical variate functions. Between 40% (MS) and 80% (FMR) of the original variance is represented by Canonical Variate functions 1 + 2.

Our discussion of the factor analyses presented in Figure 5 will first identify components characteristic of early eluting samples and then move on to later eluting samples. Investigation of the correlated mass peaks loading on factors 1 and 2 (Figure 5a) by means of the variance diagram method revealed 8 components. In Figure 5a component (a) (130°) represents the ion series C_nH_{2n-1}⁺, whereas component (b) (160°) shows C_nH_{2n}⁺ ions from monocyclics or alkenes. A large component (c) (190-240°) contains C_nH_{2n-1}⁺ ions (190°), C_nH_{2n-2}⁺ ion (220°) as well as fragment ions at m/z 149, 163, 177, and 191 characteristic of terpenoid resins or other C_nH_{2n-4}⁺ compounds (240°).

Aromatic compounds, such as short (C_n, n = 1, 2, 3) alkyl substituted benzenes occur at component (d) (280°), with longer chain (C_n, n = 5, 6, 7) benzenes + tetralins at 320°; component (e). Component (f) at 0° is thought to represent C_nH_{2n-10}⁺ series. Naphthalenes are found at component (g) (30°) and acenaphthene/biphenyl ions are present at component (h) (50°, Figure 5a). Note that

the scores in this factor space roughly describe a circle, with the exception of fraction 13, which is found near sample 10. Factor 3 (not shown) distinguishes sample 13 from the others with a component axis containing anthracene/phenanthrene moieties as well as an ion series at m/z 180, 194, 208.

Factor analysis was performed on the IR spectra of subfractions 1 to 13 using all 33 wavenumber variables. Figure 5b shows the factor score plot of the IR data on subfraction 1 to 13 in the F1 vs. F2 factor space. Samples 1-7 are very close together, implying that infrared spectroscopy does not detect much difference between these dominantly aliphatic mixtures. Analysis of the underlying correlation between variables by means of the variance diagram method showed component (a) 350° represents methyl and methylene absorptions such as 2870, 2850, 2920, 1460 and 720cm^{-1} . Component axes (b) 120° with peak 1516cm^{-1} and (c) 160° with 3050, 3015 and 1600 represented aromatic absorptions. A component axis (d) 240° , which points to subfractions 12 and 13, represents peaks 750, 2940, 1030 and 1180cm^{-1} .

Initially, we tentatively assigned 1030 and 1180cm^{-1} as C-O stretches, but further examination of infrared spectra of aromatic standards showed that these are probably CH in plane bends, e.g., 1030cm^{-1} (benzene). An interesting feature of the IR data is the peak at 2868cm^{-1} which correlates with the F1 aromatic axis, although it is believed to represent a combination of methyl and methylene stretches. Painter et al., (4) also found this behavior in IR spectra of coal macerals. The data strongly suggest a reinterpretation of this peak assignment.

Several peaks in the F1+ direction of Figure 5b can be assigned as olefin CH out-of-plane bends. These turned out to be important in the combined (canonical variate) space and will be discussed later.

The factor score plot F1 vs. F2 (91% variance) of the PMR data in Figure 5c shows a general distribution of samples forming a circle. The variance diagram of F1 vs. F2 from the proton NMR data shows that the positive F1 axis contains methyl and methylene groups attached to aliphatic (sp^3 hybridized) carbon groups, and olefinic protons. The F1 axis contains aromatic protons, split into two groups. The component axis at 200° represents methyl substituted benzenes ($\text{CH}_3 + 1$ ring aromatic), oriented toward fractions 9 and 10. The 170° rotation contains 2-ring and 3-ring aromatics and longer chain aromatic substituents (CH_2) oriented toward fractions 11-13.

Factor analysis of the CMR data gave 6 factors with eigenvalues >1.0 . The score plot of F1 vs. F2 (56% of the variance) (Figure 5d) shows that samples 1-7 appear to be similar in this dimension oriented along the negative side of F1. Components in this direction include aliphatic peaks such as at 23, 30, 32 and 38 ppm and (with weaker loadings), at 97 and 114 ppm, probably olefinic carbons. Fraction 8 is somewhat removed from fractions 1-7 but still on F1-, and therefore predominantly aliphatic in character. Fractions 9-13 are widely spread on factor F1+. A component axis at 350° represents peaks at 20, 122, 126, 131 and 135 ppm. Fractions 10 and 11 have an associated component which includes the peaks at 40 and 134 ppm. Fractions 12 and 13 have an associated component axis with the peaks at 127, 129, 132 and 142 ppm. All peaks on F1+ (except at 20 and 40 ppm) are likely aromatic carbons. The 20 and 40 ppm peaks are sp^3 hybridized carbon substituents on aromatic rings.

Canonical correlation of the factor analysis results from the MS, IR, PMR and CMR data using 6 factors from each data set gave four canonical variate functions with correlation coefficient greater than 0.90. The variance associated with the four CV functions is shown in Figure 4. Figure 6 is a score plot of CV1 vs. CV2 for the four data sets. The scores from each fraction analyzed by the four methods are connected by lines. A small polyhedron implies that the methods see the sample in a similar way. The later eluting samples (9-13) appear to group into clusters that are widely separated from one another (e.g., 9 and 10, 11 and 12, 13) whereas early eluting samples (1-7) are close together in this space. Figure 7 shows a consensus picture of the component directions from each method found in this CV space. Correlated variables consistent with an interpretation of aliphatic compounds are clustered around CV1-, near fractions 1-4. Fraction 7 appears also in this direction. A component axis of alkyl benzenes (m/z 92, 106...) from the MS data loads weakly in this CV space. From the original factor analyses it can be seen

that the mass spectral and PMR data clearly differentiated fraction 7 from the other fractions, but that other data sets grouped 7 with fractions 1-6. The PMR data showed no unique component associated with fraction 7. This says that the mass spectral picture of fraction 7 is in a sense unique, and does not appear in the CV space. A component axis corresponding to olefinic variables (IR, PMR, CMR) appears at 150°, in the direction of fractions 5 and 6. The mass spectral data shows ion series with 2 and 3 units of unsaturation, one or more of these apparently being a double bond. The positive half of CVI reveals three components, each one consistent with an assignment of aromaticity. The PMR and IR (CH in-plane bend modes) show increasing fused ring aromaticity in the ccw direction (300° to 50°). The mass spectral data identified the component at 300° with indane/tetralin, the 0° component as >C₃ alkyl substituted naphthalenes and the 50° component as acenaphthene/biphenyls. A component axis at 80° (mass spectral data only) showed peaks characteristic of alkyl anthracene/phenanthrenes. The CMR data has not been interpreted in as great a detail, but groups of aromatic peaks found in these three directions are not inconsistent with interpretations from the other data sets. A point of interest is provided by the two CMR aliphatic peaks, 20 and 40 ppm (0°), which correlate with aromatic carbons and are from alkyl substituents.

CONCLUSIONS

Valuable information was gained by correlating the four analytical techniques. For example, mass spectral peaks of samples containing 2 and 3 units of unsaturation, as determined by PMR, were shown to contain double bonds, whereas mass spectral peaks corresponding to molecules containing one unit of unsaturation were found to be cyclic. Since all the techniques showed the predominantly aromatic fractions to be very different from each other when moving to higher fused ring systems, a better understanding of spectral interpretation of aromatic hydrocarbons mixture data appears possible.

A major limitation of the present study is that only that portion of the analytical data common to all four analytical techniques was interpreted. Future studies will have to address the highly important portions of the analytical data unique for each analytical method in order to reap the full benefits of the integrated spectroscopic approach.

ACKNOWLEDGMENT

The expert assistance of Dr. Jim Liang, Mary West and Alireza Pezeshk in obtaining the analytical data, and of Dr. Liang and Dr. Charles Mayne in interpreting the results is gratefully acknowledged. Drs. George R. Hill and Larry L. Anderson are thanked for their stimulating support of this research. The work reported here is part of the research carried out at the University of Utah, under the auspices of the Consortium for Fossil Fuel Liquefaction Science funded under DOE contract RF-4-21033-86-24.

REFERENCES

1. McClellan, W.H.; Meuzelaar, H.L.C.; Metcalf, G.S. and Hill, G.S., Fuel, 62 (1983).
2. Meuzelaar, H.L.C.; Haverkamp, J.; Hileman, F.D., Tandem Mass Spectrometric Analysis (MS/MS) of Jet Fuels, Part I and II, Air Force Aero Propulsion Laboratory, Wright-Patterson Air Force Base, Ohio, AFWAL-TR-85-2047, Parts I and II, 1985.
3. Windig, W. and Meuzelaar, H.L.C., SIGMA, System for Interactive Graphics-oriented Multivariate Analysis, Proc. 34rd ASMS Conf. on Mass Spec. All. Topics, Cincinnati, 1986, pp. 64-65.
4. Windig, W. and Meuzelaar, H.L.C., Anal. Chem., 56, (1984) 2297-2303.
5. Kuehn, D.W.; Davis, A. and Painter, P.C., ACS Symp. Series, 252, Ch. 7, 100-119, 1984.

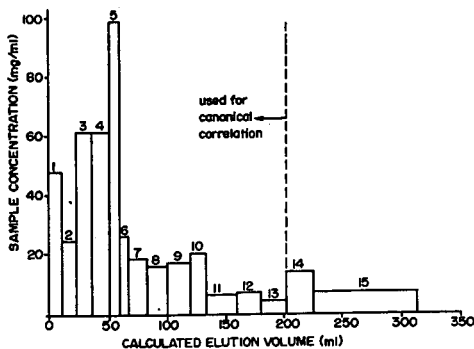


Figure 1. Reconstructed liquid "chromatogram".

TABLE I
INTEGRATED INTENSITIES OF ALIPHATIC OLEFINIC AND AROMATIC
REGIONS OF THE NMR SPECTRUM FOR SUBFRACTIONS OF THE
HYDROCARBON FRACTION OF BIAXINIA TAR

SUBFRACT.	(Proton NMR Data)				(Carbon 13 NMR Data)			
	ALIPHATIC (1-5 ppm)	OLEFINIC (4-6 ppm)	AROMATIC (6-9 ppm)	ALIPHATIC H- AROMATIC H	ALIPHATIC	OLEFINIC	AROMATIC	ALIPHATIC C- AROMATIC C
1	1.0				1	1.0		
2	1.0				2	1.0		
3	0.959	0.041			3	0.98	.02	
4	0.948	0.052			4	0.922	.078	
5	0.952	0.038			5	0.922	.078	
6	0.931	0.049			6	0.885	.063	
7	0.905	0.043	0.032	17.40	7	0.759	.121	.052
8	0.909	0.091	0.091	9.99	8	0.596		.404
9	0.827	0.173	0.173	4.78	9	0.513		.467
10	0.822	0.178	0.178	4.62	10	0.337		.643
11	0.789	0.211	0.211	3.74	11	0.333		.667
12	0.786	0.214	0.214	3.87	12	0.261		.739
13	0.849	0.151	0.151	5.62	13	0.211		.789

* integration from 50-150 ppm, olefinic and aromatic arbitrarily made equal.

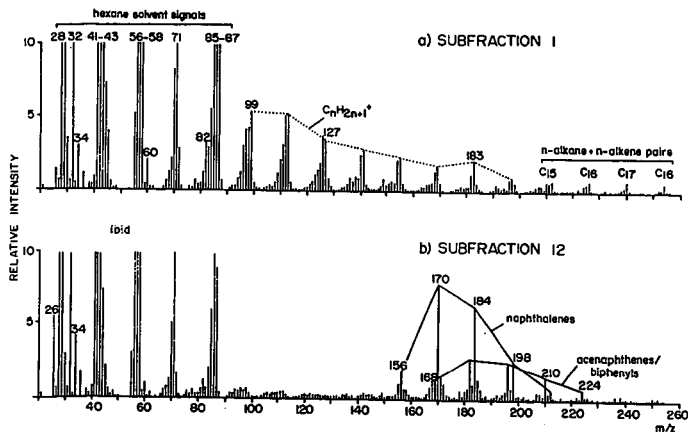


Figure 2. Low voltage mass spectra of (a) subfraction 1 and (b) subfraction 12.

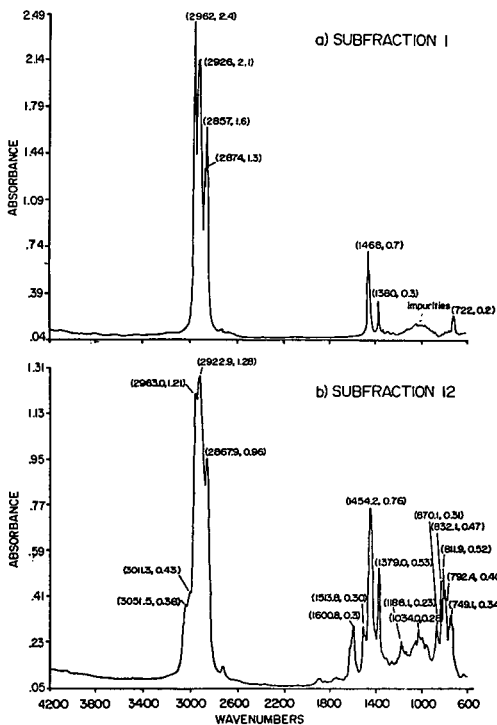


Figure 3. FTIR spectra of (a) subfraction 1 and (b) subfraction 12.

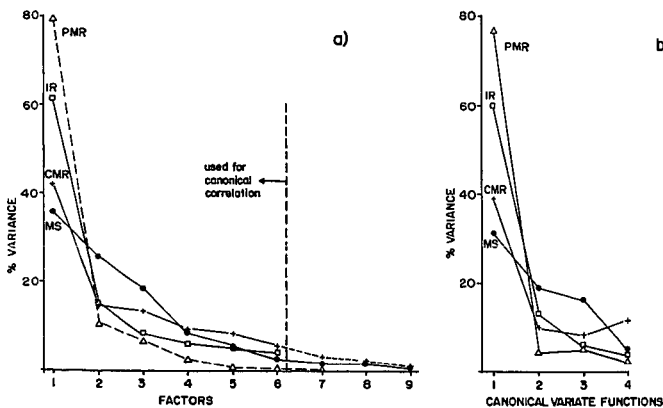


Figure 4. Percent total variance explained by (a) factors and (b) canonical variate functions.

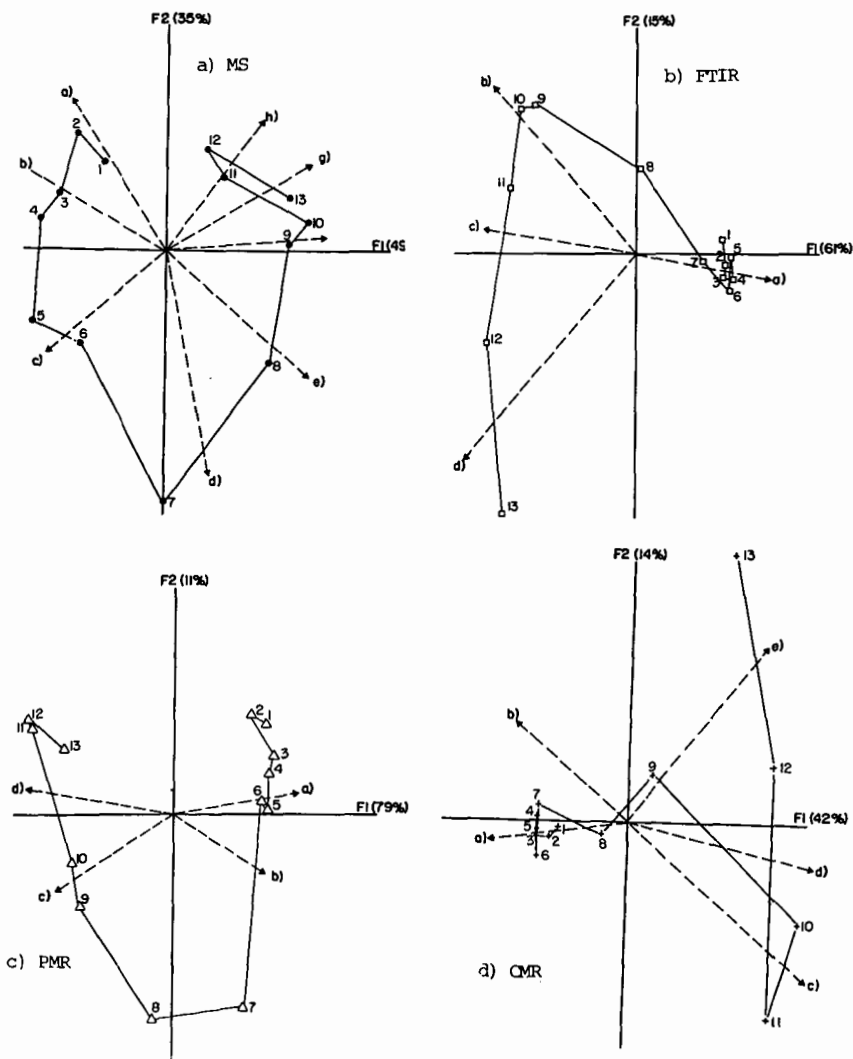


Figure 5. Factor score plots in FI/FII spaces of all four individual data sets.

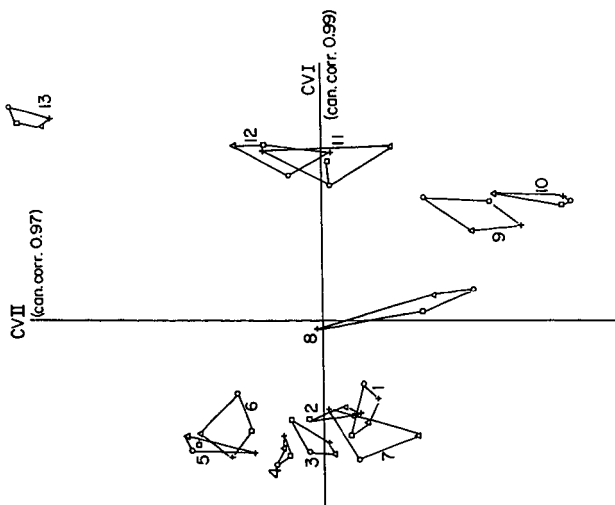


Figure 6. Combined score plots of integrated spectroscopic data in "common" CVI/CV2 space.

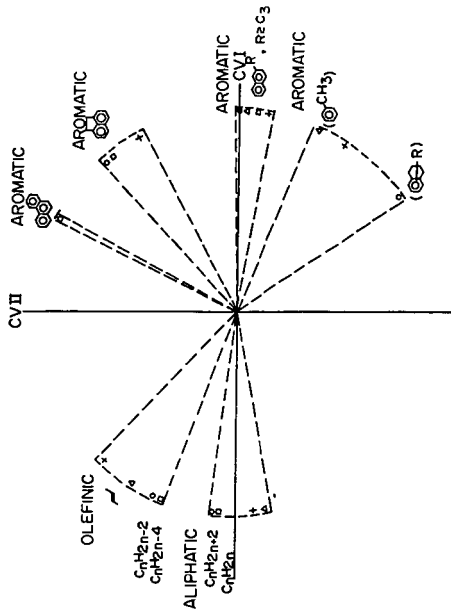


Figure 7. Combined loading plot of integrated spectroscopic data in CVI/CV2 space showing common chemical components.

CHEMICAL CHARACTERIZATION OF WOOD OILS OBTAINED IN A VACUUM PYROLYSIS PROCESS DEVELOPMENT UNIT. Hooshang Pakdel* and Christian Roy**,**

* Université Laval
Chemical Engineering Department
Pavillon Adrien-Pouliot
Sainte-Foy (Québec) G1K 7P4

** Assistant Professor at Université Laval and
Adjunct Professor at Université de Sherbrooke

INTRODUCTION

The identification and extraction of valuable chemicals from wood-derived oils is a very important goal for the biomass thermochemical conversion industry (1,2). Pyrolysis oils have been extensively studied and several pure compounds that are found in wood oils have already been separated (3,4). However to our knowledge there are only two general methods which have been reported for the fractionation of pyrolysis oils into chemical groups: the solvent extraction method (5) and the adsorption-chromatographic method (6). The former technique is rather tedious and quite often the phase separation is difficult due to the emulsion formation. The yield of extraction strongly depends on the solvent volume and extraction repetition number. The adsorption-chromatography method was used for this investigation with further modifications which will be discussed later.

Extensive work conducted by different authors utilizing GC and GC/MS sometimes leads to different results, which indicates the difficulties of carrying out accurate detailed analyses of the chemical constituents of pyrolysis oils. Examples of incomplete or even contradictory results can be found in the literature (3,7) and this paper for the analysis of vacuum pyrolysis oils. Other researchers have studied functional group distribution in pyrolysis oil (8). Although those techniques are long and tedious, they will lead to useful information about wood oil chemistry.

The majority of compounds found in pyrolysis oils are oxygenated with rather similar polarity. Therefore their gas chromatograms in general suffer from low resolution and consequently the quantitative analysis will be less accurate. Although this problem may be partially obviated by choosing narrow bore and long capillary columns, but they are very expensive and not very practical. Direct injection of a complex mixture into the gas chromatograph on the other hand, tend to deteriorate the column by building-up of non volatile matter in the column inlet, leading to gradual decomposition of the column stationary phase. Generally gas chromatography has a limited application and is not meant to be used for very complex and less volatile mixtures. GC/MS is a much more powerful analytical tool but would not be available in a great majority of cases. Besides it is quite costly and requires skilled operators for the interpretation of the results. Therefore development of new methods of separation and fractionation in particular are needed.

The primary objective of this work is to develop a separation and fractionation method for better and detailed analysis of pyrolysis oils. This will eventually enable us to make correlations between the oil properties and pyrolysis operation conditions. Full characterization of the oils will also shed some light upon the possible pyrolysis reaction mechanism and the upgrading of the oils. The secondary objective is to develop methods for extraction of valuable chemicals such as specialty and rare chemicals which are in increasing demand (9).

EXPERIMENTAL

The wood oil samples which have been characterized in this work have been obtained from pyrolysis of Populus deltoides (clone D-38) with no bark in a multiple-hearth vacuum pyrolysis reactor. The Process Development Unit (P.D.U.) has been described in detail by one of the co-authors in another paper (1).

The P.D.U. was tested for the production of high yields of oils from wood chips. One objective was to separate the bulk of the aqueous phase from the organic liquid phase by means of fractionation of the oil directly at the outlet of the reactor. This was achieved in the following way. The organic vapor product was removed from the reactor through six outlet manifolds which corresponded to the six heating plates of the reactor. The vapors were condensed in two condensing units named Primary and Secondary Condensing Units (P.C.U., S.C.U.). P.C.U. consisted of six heat exchangers in parallel and S.C.U. consisted of three traps placed in series. The pyrolysis oils which were obtained in both condensing units were subjected to sequential elution by solvent chromatography. The organic fractions were then analyzed as described below:

One gram of the oil sample was transferred into a glass column with 16 mm i.d. packed with 12.5 g of 60-200 mesh silica-gel in petroleum ether (30-60 °C b.p.). Fourteen fractions were collected, using different solvents as depicted in Table 1.

All the solvents were distilled before use and the silica-gel was washed with dichloromethane and dried in air. The other fractions were dried by rotary evaporator without heat. All the yields are shown in Table 1. FTNMR spectra of 5% solution in DMSO were recorded on XL 200 Varian instrument. Gas chromatographic analyses were performed on a 6000 Varian gas chromatograph with flame ionization detector and two injectors (on column and split). The capillary columns were J & W fused silica: DB5, 30 m X 0.25 mm i.d.; DB1, 30 m X 0.32 mm i.d. and DB1701, 30 m X 0.25 mm i.d. The results shown in this paper are on DB1 and DB5 columns. The carrier gas was He and N₂ as make up gas. The oven temperature was maintained at 50 °C for 2 min. then programmed to 150 °C and 290 °C at rates of 4 and 10 °C min⁻¹ respectively. Water's 840 data and chromatography control station with digital professional 350 computer and LA50 recorder were used as data processor.

Hydrolysis followed by sugar analysis was carried out according to the well know silylation technique. The procedure can be found elsewhere (10).

Gel permeation chromatographic (G.P.C.) analysis of the six oils from P.C.U. and one oil from S.C.U. (trap 1) were performed on ALC/GPC-201 Water's Associate liquid chromatograph equipped with a model R-401 refractometer. Four 30 cm X 7.8 mm i.d. columns packed with 100, 500, 10³ and 10⁴ μstyragel were used in series. The samples were prepared in THF (5%) and 15 μl were injected and eluted with THF. The following standards were used to calibrate the system: polystyrenes (M_w = 4000; 2000; 800 and 600), polyethylene glycol (M_w = 450, 300, 200), guaiacol, syringaldehyde and vanilline.

RESULTS AND DISCUSSIONS

The pyrolytic products can be divided into four parts as below:

- 1- Light organic chemicals such as phenols which can be analyzed by conventional analytical techniques, mainly liquid and gas chromatography and mass spectrometry.
- 2- High molecular weight, less volatile and presumably more polar com-

pounds resulting from incomplete thermal degradation of lignin, cellulose and hemicellulose which can not be easily characterized (8).

3- Char

4- Gases (e.g. CO and CO₂)

Part I will be discussed in this paper with appropriate references to Part 2 and 3.

The total oils from the six condensers (C₁ to C₆) and an oil sample from Trap 1 (S.C.U.) were analyzed by GPC for their molecular weight range distribution. The average molecular weights for the condensers 1 to 6 were: 342, 528, 572, 393, 233 and 123 respectively. The test for Trap 1 showed an average molecular weight of about 100. The molecular weight distribution of Trap 1 was as below:

MW<100 (40%); 100<MW<200 (46.5%); 200<MW<300 (10.5%) and 300<MW<500 (3%).

The pyrolytic oil in S.C.U. contains about 38.8% of the total oil which consisted of 17.9% water and 5.6% carboxylic acids (11). Due to its average low molecular weight however, it is expected that the majority of the S.C.U. oil can be analyzed if the interference due to the water can be eliminated.

G.P.C. analysis was carried out for a series of pyrolytic oils obtained in a batch reactor operated at various temperatures similar to P.D.U. hearth temperatures (12). The results showed a rather similar average molecular weight which indicates a fair selective separation of wood oil constituents at various temperatures in P.D.U.

The results of silica-gel column fractionation of the oils (C₁ to C₆) are shown in Table 1. The recoveries were approximately 4% higher probably due to the incomplete solvent removal. All fractions are designated as F1 to F14 in this part and all will be studied separately as shown in Table 1. F1 to F12 of all condensers were liquids with some differences in their colours and odors. The F13 and F14 were found to be very viscous and nearly solid. They became partially insoluble in water and methanol by redissolving them in water and methanol. F1 to F2 were not very soluble in methanol indicating their hydrocarbon nature. F4, 5, 6 showed some methanol insoluble matter which was identified as high molecular weight carboxylic acids in the range of C₁₈ to C₃₀ with a maximum at C₂₄ (11). These were separated and purified by crystallization in methanol. Although the high molecular weight carboxylic acids comprise very little percentage of the oil (~0.2%) but their finding is very interesting as only even carbon number acids up to C₂₄ have been already found in hardwood pyrolytic tar (13). The fractions 7 to 12 were slightly insoluble in dichloromethane and fully soluble in methanol. A preliminary composition analysis of each fraction was made and more work is in progress. The results are the followings:

Fraction 1:

This fraction mainly contains hydrocarbons with an odor typical of a fossil fuel mono-aromatic hydrocarbon. Proton nuclear magnetic resonance spectrum was recorded for a sample of C1-F1 (Condenser 1, Fraction 1) as an example and showed 4.5% aromatic, 2% olefinic, 18% methylenic hydrogens α to the rings and 19.5% β to the ring and 56% methylene and methyl hydrogens further away from the ring. This distribution indicates long alkyl and alkenyl side chains on benzene rings. A significant difference was observed in their gas chromatograms from C1 to C6. C1 to C5 showed some similarities in a few well resolved peaks eluting out of the gas chromatographic column at above

200 °C. Recently a series of short side chain alkyl and alkenyl benzenes (up to C₁₁ H₁₄ & C₁₁ H₁₆) were reported in wood pyrolysis oil (6). Condenser 6 on the other hand showed a broad range of hydrocarbons eluting above 100 °C. Materials eluting between 100 and 200 °C were rather less complex compared with the others eluting at above 200 °C. It is interesting to see in Table 1 that there is an increasing trend in quantity of the hydrocarbons up to the maximum in C₃ which falls down in C₅ and again reaches to the maximum at 18.5% in C₆. Whether further increase of the hearth temperature will increase and produce any more materials has not been tested but we have made an infrared spectroscopic study of the solid residue which were left behind accidentally in each hearth after the run (14). Their infrared spectra is shown in Fig. 1. Despite of the fact that a bulk of the pyrolytic oils were produced in condensers 1 and 2 but there are very small changes which can be observed in H-1 (Hearth 1) and H-2 (Hearth 2) (see Fig. 1). However significant differences were observed for H-3 to H-6. Spectrum H-6 which was operated at 448 °C shows only minor bands due to the remaining organic matter, mainly lignin or recondensed materials (15). These materials were measured to be approximately 20% of the total residue.

Fraction 2

This fraction was in low abundance in all the condensers and their quantities are significantly dependent on the hearth temperature. Similar to Fraction 1, Condenser 6 showed a maximum quantity of Fraction 2. With a slight tailing from the earlier or later fractions, but the overall separation of Fractions 2 was good. Qualitative analysis of Fractions 2 by GC showed significant differences for Condenser 6 in particular. This Fraction is similar to Fraction 1 and has aromatic nature but more polar than Fraction 1. Its gas chromatogram showed well resolved peaks but their identification has not been completed yet. Condenser 5 & 6 have completely different composition from the rest. Their GC peaks are moderately resolved. It was interesting to observe a complete change in the distribution of the compounds by 50 °C change in the bed heating temperature from hearths 4 to 5.

Fractions 3 - 11

These fractions have a particular value as their constituents are valuable and many of them can be characterized by gas-chromatography. F3-11 contributed between 23 - 36% of the condensers oil and 40.5% of the total P.C.U. oil. The total yield of these fractions therefore can be used as quality index to compare different oils. This paper contributes to a small part of these fractions and further work is in progress.

Table 2 lists some of the compounds which have been analyzed in these fractions which are mainly mono phenolic types and oxygenated heterocyclic compounds. All the chromatograms of F3 to 10 showed well resolved peaks but F11 suffered from peak broadening which is more likely due to the contamination from F12. Examples of a few chromatograms are presented in Fig. 2 and are compared with a chromatogram of the total oil from condenser 6 (Fig. 2a). From Fig. 2a, we could only identify a few compounds and the rest were coeluting and masked with the other non resolved and broad peaks. Consequently, any quantitative analysis of the total oil will be incomplete and less accurate. Although the total materials listed in Table 2, apart from water, contribute to only 23% of the total dry oil in P.C.U. but they show an interesting distribution of the compounds in the different condensers which can be correlated with their source materials.

Characterization of the low molecular weight carboxylic acids which we have developed in our laboratory (11) enables us to observe a close agreement between our results and the generally accepted source materials for two

formic acid and acetic acids, i.e. cellulose and hemicellulose (16). The former as a source for formic acid decomposes at higher temperature than the latter which is the source for acetic acid. This was observed in the P.D.U. by comparing the acid yields in the condensers. Carboxylic acid characterization was successfully achieved by analyzing the oils before any fractionation.

Finding of acetol in relatively high abundance in Condensers 5 & 6 may indicate a lignin type source or decomposition of recondensed materials in hearths 5 & 6. Since a large number of five carbon atom sugars, the source material for furan derivatives, are associated with hemicellulose especially in hardwood (3) therefore their finding in Condenser 2 with maximum abundance gives more support to the selectivity of the separation in the P.D.U. system. Finding of phenol with high proportion in Condensers 1 to 3 and some in Condenser 6 is also interesting and supports the suggestion that cellulose is also a source for phenol during wood pyrolysis (3). Since no any significant quantity of phenol was detected in Condenser 5 but some in Condenser 6, the decomposition of recondensed materials in the hearth 6 is more likely to be the source of phenol in Condenser 6. On the other hand *n*-propyl phenol has been found in a relatively high percentage in Condenser 6 which indicates a different source, i.e. lignin for the substituted phenols. Although guaiacol, catechol, eugenol and isoeugenol are spreaded in all condensers with an increasing trend toward Condenser 6 therefore it may be true that their production starts as soon as lignin starts to degrade, presumably at 250 °C or even below. Earlier these compounds have been found in the tarry residue from lignin pyrolysis (17). *p*-Cresol which we have identified in Condenser 6 has been recognized to be a degradation product of the lignin (18), more likely at high temperature around 440 °C. Finding of higher proportion of aromatic hydrocarbons in Condenser 6 also indicates that lignin is a possible source for hydrocarbons.

Fraction 12

Under the gas chromatographic conditions used, we were unable to observe any well resolved peaks. Typically the chromatogram showed lots of unresolved broad peaks indicating its higher polarity than the previous fractions. Its pH value was also significantly lower than the other fractions. The proton FTNMR spectrum was recorded for the Fraction 12 of Condenser 1 and showed hydrogen distribution of: aliphatic (4%), cyclic methylenes or methylenes α to the aromatic rings (20%), hydroxylic and methoxy groups (47%), olefinics and hydroxylics (17%), aromatics (8%), phenolics (3%) and aldehydics (1%). The total oil from Condenser 1 on the other hand showed: aliphatics (10%), cyclic methylenes or methylenes α to the aromatic rings (31%), hydroxylics and methoxys (30%) olefinics and hydroxylics (7%), aromatics (16%), phenolics (4%) and aldehydics (2%). Comparison of these two spectra shows that the F12 has higher hydroxyl group than the initial oil. More work is in progress for further fractionation of this fraction.

Fraction 13

This fraction contains the highest percentage of the high polar compounds, oligosaccharides in particular. Two techniques of ¹H-FTNMR spectroscopy and hydrolysis were applied to further study of these fractions which are briefly discussed in this paper as follows:

NMR spectra were recorded for the oils from the condensers and their F13's and comparisons were made. Fig. 3a and 3b represent the NMR spectra of Condenser 6 and its F13 as an example. Both spectra were recorded in DMSO. All the samples were freely soluble in DMSO. The peak assignments were made as: aliphatic hydrogens (12%), cyclic methylenes or methylenes to the aromatic rings (38.5%), methoxys and hydroxylic groups (29.5%), olefinics

and hydroxylics (4%), aromatics (12%), phenolics (3%), and aldehydics (1%), and F13, contained 2, 14, 60, 15, 5.5, 2.5 and 1% respectively.

The hydroxyl group assignments were also confirmed by addition of a few drops of deuterium oxide before recording the spectrum. Consequently we observed that approximately 50% of the resonance bands in the range of 3-4.2 ppm are due to the sugars hydroxyl groups. Similarly approximately 30% of the resonance bands in the range of 4.2 - 5.5 ppm are also due to the hydroxyl groups. Their spectra have some similarities with the typical sugars NMR spectra. From their NMR spectra we observed an increasing trend to the high hydroxyl content from Condenser 1, F13 to Condenser 6, F13.

The hydrolysis experiments were carried out to measure the oligosaccharide content of the oils. Primarily analysis was made for the total sugar content of the oils following silylation technique. We found only levoglucosan with 0.3, 0.4, 0.7, 1.7, 3.4, and 4.2% in Condensers 1 to 6 respectively. This finding was in close agreement with the previous data obtained on a series of the oils obtained in batch reactor operating at a similar range of temperatures as P.D.U. Hydrolysis of the total oils were carried out and their sugar content were measured. α and β Glucose and xylose were the most dominant sugars in hydrolysates. The total glucose content increased from Condenser 1 to 6 but xylose reached a maximum in Condenser 5 then decreased in Condenser 6. Their total sugar content were 3.14, 3.31, 6.85, 6.81, 14.23 and 14.05% for Condensers 1 to 6 respectively. Similar experiments were carried out on F13 for all Condensers. The results indicate that a complete recovery of levoglucosan was achieved in F13 but the hydrolysates showed approximately 30% loss. Further investigation is in progress to find the reason for this loss.

Fraction 14

This fraction comprised a small portion of the oils and a steady increase in their quantities was observed from Condenser 1 to 6. They may have presumably polymeric structure. Their infrared spectra showed a weak and broad hydroxyl stretching vibration band and very weak C=O and C-O absorption bands at 1700 and 1600 wavenumbers respectively. C-H stretching and vibration bands were also observed at very low intensities at 2920 and 1520 wavenumbers respectively.

CONCLUSION

The sequential elution chromatographic technique has been found particularly helpful in separating whole product oil produced by vacuum pyrolysis of wood into chemically distinguishable fractions. More than 30% of the P.C.U. oil that eluted first could be analyzed by GC and GC-MS with less unambiguity.

Now that sensitivity problems are being overcome, infrared spectroscopy and wet chemistry will be overtaken in some instances by high field $^1\text{H-NMR}$, a non destructive technique, and MS-MS spectroscopy and spectrometric techniques for characterization of the rest of the fractions namely F12, 13 and 14 in this investigation.

Fourier transform $^{13}\text{C-NMR}$ which has not been utilized in this investigation is likely to make a large contribution also in the near future to study these fractions.

Since variation in the distribution of the separated fractions and their composition in different condensers were in good agreement with their generally accepted source materials, the P.D.U. is considered to be capable of selective separation of oils.

Even though they are only present in relatively low concentration, the compounds such as methyl cyclopentene-ol-one, 3- hydroxy - 2- methyl - 4- pyrone, isoeugenol and acetaldehyde, for example, can serve to characterize various oils and monitor the pyrolysis liquefaction procedure. They can also be separated and extracted as fine chemicals.

ACKNOWLEDGMENTS

This study was supported by Energy, Mines and Resources Canada (Ottawa).

REFERENCES

- 1- Lemieux, R., C. Roy, B. de Caumia and D. Blanchette. Preliminary Engineering Data For Scale up of a Biomass Vacuum Pyrolysis Reactor. Production Analysis and Upgrading of Oils from Biomass, ACS Symposium, Denver, Col. April. 5 - 10, 1987.
- 2- Perdrioux, S. La Valorisation chimique du bois par carbonisation. Le Bois National - 2 juillet, 23-26 (1983).
- 3- Soltes Ed. J. and T. J. Elder. Organic Chemicals from Biomass. I.S. Goldstein, ed. CRC Press. 63-99 (1981).
- 4- Elliott, D.C. Analysis and Upgrading of Biomass Liquefaction Products. Final Report, Biomass Liquefaction. Tests Facility, IEA, Co-Operative Project D-1, Jan. 10 (1984).
- 5- Boocock, D. G. B. and Sherman K.M. Further Aspects of Powdered Poplar Wood Liquefaction by Aqueous Pyrolysis. The Canadian Journal of Chemical Engineering. 63: 627-633. (1985).
- 6- Hubert, G.D., M.A. Eames, C. Figueroa, R.R. Gansley, L.L. Schaleger and D.W. Watt. The Products of Direct Liquefaction of Biomass. Fundamentals of Thermochemical Biomass Conversion. R.P. Overend, T.A. Milne and L.K. Mudge eds. Elsevier Applied Science Publication, London, New York. 1027-1037. (1984).
- 7- Ménard, H., D. Belanger, G. Chauvette, A. Gaboury, J. Khorami, M. Grisé, A. Martel, E. Potvin, C. Roy and R. Langlois. Characterization of Pyrolytic Liquids from Different Wood Conversion Products. Fifth Canadian Bioenergy R & D Seminar. S. Hasnain, ed. Elsevier Applied Science Publisher. 418-425. (1984).
- 8- Nicolaides, G.M. The Chemical Characterization of Pyrolytic Oils. Master Thesis. University of Waterloo. (1984).
- 9- Singh B.B. Strategic Options for Commodity Chemical Producers in Transition to Specialty Market Sectors. World Congress III of Chemical Engineering. Tokyo - Japan. Vol I: 23-26 (1986).
- 10- Ménard, H., M. Grisé, A. Martel, C. Roy and D. Belanger. Saccharification of Biomass by Pyrolysis at Reduced Pressure Followed by Hydrolysis. Fifth Canadian Bioenergy R & D Seminar. S. Hasnain, ed., Elsevier Applied Sciences Publisher. 440-444 (1984).
- 11- Pakdel, H. and C. Roy. Production and Characterization of The Low-Molecular-Weight Carboxylic Acids from Wood in a Vacuum Pyrolysis Process Development Unit. In preparation.

- 12- Brouillard, D. Role of Wood Constituents on Pyrolysis Reactions. M.Sc.A. Thesis. Université de Sherbrooke, Québec (1986). (In French).
- 13- Goos, A.W. The Thermal Decomposition of Wood. Wood Chemistry. L.E. Wise and E.C. Jahn, eds. Reinhold New-York, chap. 20, 826-851 (1952).
- 14- Roy, C., R. Lemieux, H. Pakdel, B. de Caumia and D. Blanchette. Heat and Mass Balance Around a Multiple-Hearth Furnace for Vacuum Pyrolysis of Biomass. World Congress III of Chemical Engineering, Tokyo, Japan, Vol. 1: 621-624 (1986).
- 15- Ahmed, A., J.L. Grandmaison and S. Kaliaguine. Characterization of the Solid Residues of the Supercritical Extraction of Populus Tremuloides in Methanol. Journal of Wood Chemistry and Technology. 6 (2), 219-248 (1986).
- 16- Shafizadeh, F., R.H. Furneaux, T.G. Cochran, J.P. Scholl, Y. Sakai. Production of Levoglucosan and Glucose from Pyrolysis of Cellulosic Materials. Journal of Applied Polymer Science. 23: 3525-3539 (1979).
- 17- Allan, G. G. and I. Mattila. High Energy Degradation. Lignin - Their Occurrence, Formation, Structure and Reaction. K.V. Sarkanen, C.H. Ludwig, eds. Chap. 14 (1971).
- 18- Fletcher, T.L. and E.E. Harris. Products from the destructive Distillation of Douglas-Fir Lignin, Tappi, 35: 536 (1952).

TABLE 1 - PRIMARY CONDENSING UNIT PYROLYTIC OILS AND THE YIELD OF VARIOUS CLASSES OF COMPOUNDS OBTAINED BY SILICA-GEL COLUMN CHROMATOGRAPHIC ANALYSIS (a)

SAMPLE	FRACTION	FRACTION	FRACTION	FRACTION	FRACTION	FRACTION	FRACTION	TOTAL
025-PHE-450-RL	1	2	3-11	12	13	14		
Condenser 1	1.2 (0.12)	1.3 (0.13)	315.7 (31.57)	282.8 (28.28)	311.1 (31.11)	10.8 (1.08)	923.0 (92.3)	
Condenser 2	3.9 (0.39)	0.4 (0.04)	364.2 (36.38)	363.8 (29.96)	283.1 (28.28)	20.1 (2.01)	971.7 (94.10)	
Condenser 3	14.7 (1.46)	1.2 (0.12)	238.7 (23.70)	302.6 (30.04)	321.6 (31.93)	29.4 (2.92)	908.2 (90.2)	
Condenser 4	12.3 (1.22)	0.0 (0)	265.3 (26.37)	346.1 (34.40)	316.0 (31.40)	30.0 (2.98)	969.7 (96.4)	
Condenser 5	2.9 (0.29)	0.5 (0.05)	239.4 (23.87)	338.9 (33.79)	331.3 (33.03)	36.2 (3.61)	949.2 (94.6)	
Condenser 6	18.5 (1.84)	8.9 (0.89)	357.4 (35.61)	285.3 (28.43)	308.7 (30.76)	44.9 (4.47)	1023.6 (102.0)	

(a) See the text for description of the classes.

All figures in parentheses are expressed in weight percentage (as-received oil basis). Otherwise, numbers are mg.

Fraction 1: 128 ml with petroleum ether
 Fraction 2-11: 128 ml each with CH_2Cl_2 / Petroleum ether mixture, from 10 to 100% CH_2Cl_2 (10 % increments) for F2 to F11 respectively.
 Fraction 12: 128 ml with ether
 Fraction 13: 128 ml with water
 Fraction 14: 60 ml with 10% formic acid in methanol

TABLE 2- PRELIMINARY ANALYTICAL DATA OBTAINED FROM PRIMARY CONDENSING UNIT

CC #	COMPOUND	CONDENSER 1	CONDENSER 2	CONDENSER 3	CONDENSER 4	CONDENSER 5	CONDENSER 6
---	Water	46.54 (8.24)	50.58 (6.8)	59.45 (6.24)	83.63 (6.54)	85.03 (6.60)	28.52 (5.12)
---	Formic acid	13.89 (2.46)	27.37 (3.68)	38.77 (4.07)	59.33 (4.64)	72.02 (5.59)	11.36 (2.04)
---	Acetic acid	40.50 (7.17)	58.83 (7.91)	62.40 (6.55)	40.15 (3.14)	31.82 (2.47)	9.64 (1.73)
1	Acetol	---	---	---	0.89 (0.07)	0.52 (0.04)	7.24 (1.3)
2	Furfural	0.28 (0.05)	0.37 (0.38)	0.44 (0.05)	6.52 (0.51)*	4.64 (0.36)	0.50 (0.09)
3	Furfuryl alcohol	1.58 (0.28)	2.75 (0.37)	14.3 (1.5)	---	---	2.45 (0.44)
4	Angellactone	0.68 (0.12)	2.90 (0.39)	0.48 (0.05)	0.02 (0.002)	---	---
5	Cyclohexanol	---	---	---	---	---	---
6	-Butyrolactone	---	---	---	---	---	4.79 (0.86)
9	Me-Cyclopentan-1-one	---	---	0.51 (0.05)	---	---	---
10	5-Me-furfural	---	---	1.05 (0.11)	1.92 (0.15)	---	1.28 (0.23)
11	Phenol	5.2 (0.92)	5.50 (0.74)	9.53 (1.0)	1.41 (0.16)	1.54 (0.12)	2.73 (0.49)
12	Me-Cyclopentane-ol-one	0.14 (0.02)	0.82 (0.11)	1.81 (0.19)	4.35 (0.34)	---	---
13	m-Cresol	---	0.28 (0.35)	---	---	---	0.56 (0.1)
13a	p-Cresol	---	---	---	---	---	4.07 (0.73)
14	Guaiacol	0.02 (0.003)	1.12 (0.15)	0.95 (0.1)	1.79 (0.14)	0.52 (0.04)	0.45 (0.08)
16	5-Hydroxy-2-Me-4-pyrone	0.51 (0.09)	0.59 (0.08)	---	---	0.64 (0.05)	0.67 (0.12)
18	Dimethyl 2,3, phenol	---	---	---	---	---	8.74 (1.57)
19	Dimethyl 2,5, phenol	---	---	---	---	---	3.34 (0.6)
19a	Di-propyl phenol	---	---	---	---	---	---
20	Catrolone	1.13 (0.2)	2.01 (0.27)	2.48 (0.26)	4.6 (0.25)	7.73 (0.6)	0.52 (0.04)
22	Hydroquinone	---	---	---	---	---	5.02 (0.39)
23	Resorcinol	---	---	---	---	---	0.26 (0.02)
24	Syringol	1.81 (0.69)	2.37 (0.5)	10.86 (1.14)	10.23 (0.8)	5.02 (0.39)	8.35 (1.5)
25	Eugenol	3.11 (0.02)	0.45 (0.06)	0.28 (0.03)	0.26 (0.02)	0.26 (0.02)	0.45 (0.08)
27	Isoeugenol	3.22 (0.57)	3.05 (0.41)	6.29 (0.66)	5.37 (0.42)	6.57 (0.51)	12.48 (2.24)
28	Vanilline	---	---	---	---	0.13 (0.01)	---
---	Sugars**	17.73 (3.14)	24.25 (3.26)	64.88 (6.81)	87.08 (6.81)	183.33 (14.23)	57.20 (14.05)
---	Total	135.44 (23.98)	180.85(24.43)	273.48 (26.81)	306.76 (23.99)	431.97 (33.53)	173.56(31.16)
---	Total in P.C.U. = 1502.06 (27.89) %	---	---	---	---	---	---

* Could not be distinguished

** Total sugars after hydrolysis

All figures in parentheses are expressed in weight percentage (as-received oil basis). Otherwise, numbers are g.

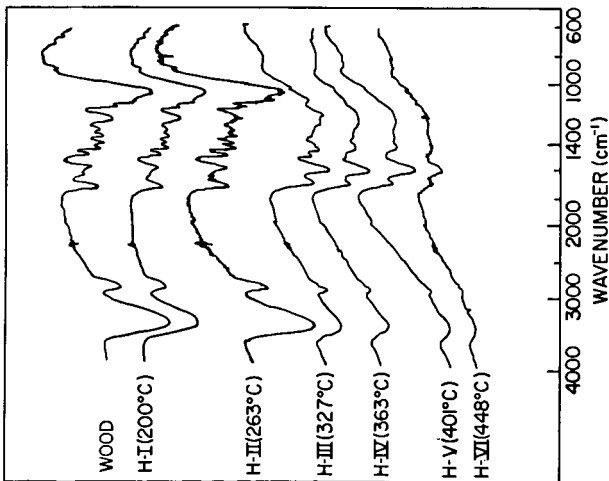


Fig. 1 - INFRARED SPECTRA OF WOOD AND SOLID RESIDUE. IN EACH RUNCH (INDICATED BY H.)

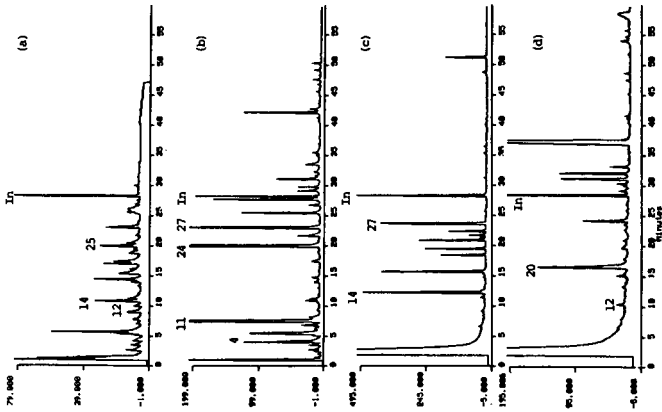


FIG. 2 - CAPILLARY GAS CHROMATOGRAMS OF: (a) total Condenser 6 oil; (b) Condenser 1 Fraction 1; (c) Condenser 2 Fraction 3 and (d) Condenser 3 Fraction 5. (See Table 2 for identification of peaks), In = Internal standard

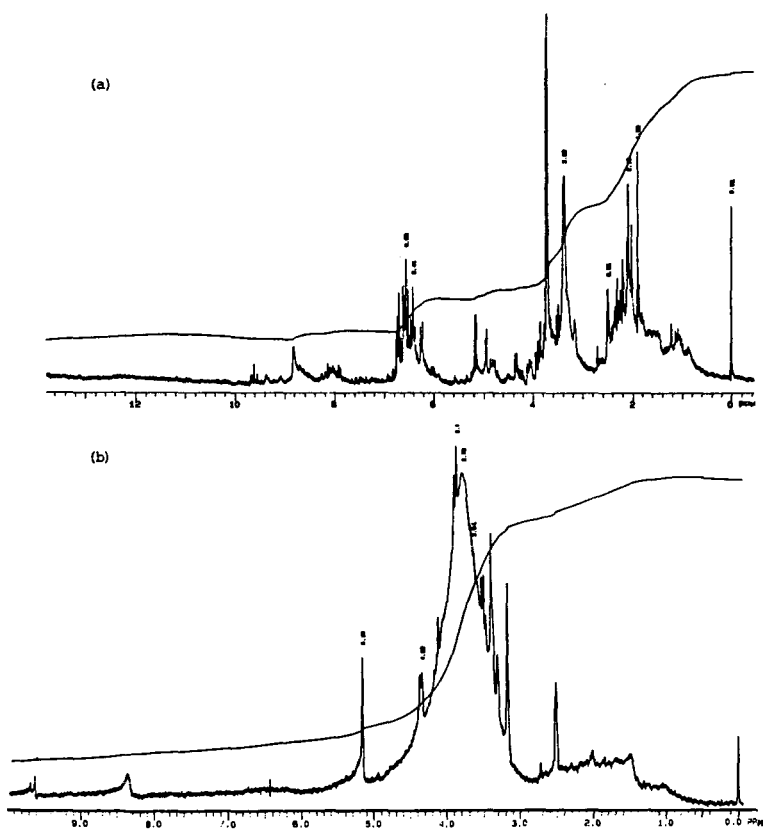


Fig. 3 - $^1\text{H-NMR}$ SPECTRA OF WOOD PYROLYTIC OILS
 (a) Condenser 6; (b) Fraction 13 Condenser 6

THE COMPOSITION OF OILS OBTAINED BY THE FAST PYROLYSIS OF DIFFERENT WOODS

J. Piskorz and D.S. Scott

Department of Chemical Engineering
University of Waterloo
Waterloo, Ontario, Canada N2L 3G1

Introduction

During the last six years a fluidized bed fast pyrolysis process for biomass has been developed at the University of Waterloo (The Waterloo Fast Pyrolysis Process). This process gives yields of up to 70% of organic liquids from hardwoods or softwoods, which are the highest yet reported for a non-catalytic pyrolytic conversion process. A fluidized sand bed is used as a reactor and optimum liquid yields are normally obtained in the range of 450°-550°C at about 0.5 seconds gas residence time with particles of about 1.5 mm diameter or smaller. Two units are in use, one with a throughput of 20-100 gms/hr, and another with a throughput of 1-4 kg/hr. Details of the process have been published by the authors in several publications [1], [2], [3].

Several studies have been published describing results from the flash pyrolysis of biomass. Most of these studies were carried out at higher temperatures and were intended to promote biomass gas production. However, the work of Roy and Chornet [4] reported high liquid yields from biomass pyrolysis under vacuum conditions. More recently, Roy et al. [5] have described a vacuum pyrolysis system for the production of liquids from biomass, based on a multiple hearth type of reactor. Knight et al. [6] have developed an upward flow entrained pyrolyzer for the production of liquids from the thermal pyrolysis of biomass.

However, few details of the chemical nature of the pyrolytic oils produced from wood or other biomass have been reported. Some recent studies of the composition of pyrolysis oils obtained from poplar wood were carried out by workers of the Pacific Northwest Laboratories of Battelle Institute [7] and the Universite de Sherbrooke [8]. Methods of quantitative determination of functional groups in the pyrolytic oils from wood were tested in our laboratory by Nicolaides [9]. However, more detailed characterisation exists in the literature for the products of the thermal degradation of cellulose [10,11,12,13,14]

Results

In previously reported tests (3), yields have been classified as gases, organic liquids, char and product water. Mass balances generally close to 95% or better. Elemental analyses were also reported for many runs, but identification of individual compounds was done only for non-condensable gases and for some volatile organics such as methanol, acetaldehyde, furan,

etc. However, more detailed analyses of liquid products have recently been carried out, and some of these preliminary results which are of particular significance are reported here.

All experimental results given were obtained at conditions of close to optimal feed rate, particle size and residence time for maximum liquid yield at the stated temperatures, as determined by over 200 bench scale runs and 90 pilot scale runs.

Table 1 shows the experimental yields of products from selected runs for four different woods whose properties are given in Table 2.

High organic liquid yields are characteristic of all four materials when undergoing fast pyrolysis in our process. The total liquid yield, including water of reaction, varies from 70% to 80% of the dry biomass fed, all of which can be directly used as a substitute fuel oil if desired. The liquids are single-phase, homogeneous fluids, which pour readily, and which contain from 15% to 25% water depending on the feed material and its moisture content.

These liquids are quite stable at room temperature. The water content, in a period of twelve months, was found to increase slightly presumably due to the slow processes of condensation-polymerization going on even at room temperature. At higher temperatures, 120°C and above, the oils become increasingly unstable and decompose with evolution of gas, and finally charification of a polymeric residue. All the pyrolysis vapors produce an oil mist following rapid quenching, but their polar character allows the easy utilisation of electrostatic precipitation in the recovery system of a pyrolysis process.

Preliminary small scale combustion tests carried out with the pyrolysis oil as produced (20% water content) showed that it burns readily in a furnace with a conventional pressure atomizing burner, providing the combustion box is preheated. If an air atomizing nozzle is used with a pilot flame, no pre-heating of the combustion chamber is necessary. Larger scale tests for extended periods have not yet been done, but preliminary work shows that the pyrolysis oil has potential as a substitute fuel oil.

Some properties of "wet" liquids as produced are given in Table 3. The elemental analyses of the pyrolytic liquids as given in Table 3 are very similar to those of the starting materials - wood. One could probably fairly accurately describe these liquids, therefore, by the term "liquid wood". Two major characteristics of these liquids are high oxygen content and high density (much higher than wood). Another specific property is a limited water solubility. In the case of pyrolytic sirups produced by the Waterloo process, water is dissolved in the organic phase. The addition of more water to the level of about 60% by weight causes a phase separation and this behaviour has been utilized in our work for analytical purposes, in that both

fractions were analyzed separately after dilution of the original oil product.

The details of the HPLC technique developed for analysis of the water soluble fraction are given below:

Column : Aminex[®] HPX-87H, high performance
cation exchange resin in hydrogen form
300 x 7.8 mm from Biorad

Eluant : H₃PO₄ 0.007 N

Flow Rate : 0.80 ml/min, isocratic

Temperature : 65°C

Detector : Waters R 401 Differential Refractometer

Internal Standard : n-propanol

The quantitative data obtained by the HPLC technique are presented in Table 4. A typical HPLC-chromatogram is shown in Figure 1.

To obtain relative response factors and retention times, the pure compounds were fed and then eluted, although some of them, such as cellobiosan and 1,6 anhydro- β -D-glucofuranose, had to be synthesized in-house [13]. Confirmation of compound identification was obtained by GC-MS [Hewlett-Packard 5970 Mass Selective Detector coupled to 5890A Gas Chromatograph]. For GC-MS analysis, sugars and anhydrosugars were first trimethylsilylated to the corresponding ethers. Small amounts of simple phenols and of furanoid compounds were also detected by GC-MS in the water soluble fraction. These components were not quantified by HPLC.

The yields of the water insoluble fraction are given also in Table 4. This fraction separated as a dark brown viscous liquid which solidified during drying into a hard, black, easily powdered material.

The carbon-13 NMR spectrum of this pyrolytic product is shown in Figure 2 together with similar spectra published by Marchessault et al. [15] for milled wood lignin (MW) and steam exploded lignin (EXW). The similarity of the spectra of the steam exploded lignin and our pyrolytic lignin is quite striking. It appears that the oils produced by the Waterloo Fast Pyrolysis process contain a significant fraction which is apparently derived from the natural wood lignin. This "pyrolytic lignin" represents nearly 80% of the original content of wood lignin. Evidence for this conclusion was first reported from the work of H. Menard [16] using thermogravimetric and infrared analysis.

The Waterloo NMR spectrum was recorded using a 9% solution in DMSO-d₆ at 62.9 MHz and 50°C with broad-band proton decoupling. Delay time between pulses was 10 seconds.

Conclusions

Four different woods under conditions of fast pyrolysis yielded very similar liquid products. Analyses show that this product is a complex mixture of chemicals.

The pyrolytic "wet" tar-sirup can be readily separated into two principal fractions by water extraction. The water-insoluble fraction is derived from lignin while the water-soluble fraction is carbohydrate in origin. Analytical results indicate large amounts of low molecular weight (<100) lactones and aldehydes, and a significant fraction of these are multifunctional in nature. Four major classes of chemicals can be differentiated,

1. sugars and anhydrosugars
2. carbonyl and hydroxycarbonyl compounds
3. acids - formic, acetic
4. "pyrolytic" lignin.

Results in Table 4 show that 81-92% of the content of the pyrolysis oils produced in this work from wood has been quantitatively identified.

Detailed analysis of pyrolytic oils is needed in order to allow possible mechanistic or kinetic models to be formulated which can explain the various observed aspects of fast biomass thermal degradation. A knowledge of chemical composition of these oils may also assist in the eventual future utilization, up-grading or separation of these compounds as higher value products.

Acknowledgement

The financial support for this work of the National Research Council of Canada and of the Natural Sciences and Engineering Research Council of Canada are gratefully acknowledged by the authors. The assistance of P. Majerski and A. Grinshpun with experimental measurements is also acknowledged with pleasure.

References

- 1 D.S. Scott and J. Piskorz, Can. J. Chem. Eng., 60 (1982) 666
- 2 D.S. Scott and J. Piskorz, Can. J. Chem. Eng., 62 (1984) 404
- 3 D.S. Scott, J. Piskorz and D. Radlein, Ind. Eng. Chem. Process Res. Devel., 24 (1985) 581

- 4 C. Roy and E. Chornet, Proc. 2nd World Congress Chem. Eng., Montreal, Vol. II, 315, (1981)
- 5 C. Roy, A. Lalancette, B. DeCaumia, D. Blanchette, B. Cote, M. Renaud and P. Rivard, Bio Energy 84, H. Egnéus and A. Ellegard (Eds.) Vol. III, 31, (1984), Elsevier App. Sc. Publ., London
- 6 J.A. Knight, C.W. Gorton and D.J. Stevens, Bio Energy 84, H. Egnéus and A. Ellegard (Eds.) Vol. III, 9, (1984), Elsevier App. Sc. Publ., London
- 7 D.C. Elliott, International Energy Agency Co-operative Project D-1, Biomass Liquefaction Test Facility, National Energy Administration, Stockholm, Vol. 4
- 8 H. Ménard, D. Belanger, G. Chauvette, J. Khorami, M. Grise, A. Martel, E. Potvin, C. Roy and R. Langlois, in S. Hasnain (Editor), Proc. 5th Bioenergy R & D Seminar, Elsevier, New York, (1984), p.418
- 9 G.M. Nicolaides, The Chemical Characterization of Pyrolysis Oils, MASC Thesis, Dept. of Chemical Engineering, University of Waterloo, Waterloo, Ontario, Canada, (1984)
- 10 F. Shafizadeh, J. Anal. Appl. Pyrol., 3 (1982), 283
- 11 T. Funazukuri, Ph.D. Thesis, Dept. of Chemical Engineering, University of Waterloo, Waterloo, Ontario, Canada, (1983)
- 12 J. Piskorz, D. Radlein, D.S. Scott, J. Anal. Appl. Pyr., 9 (1986) 121
- 13 D. Radlein, A. Grinshpun, J. Piskorz, D.S. Scott, J. Anal. Appl. Pyr., - accepted for publication (1986)
- 14 O.P. Golova, Russian Chemical Reviews, 44 (8), (1975)
- 15 R.H. Marchessault, S. Coulombe, H. Morikawa and D. Robert, Can. J. Chem., 60 (1982), 2372
- 16 H. Ménard, Université de Sherbrooke - private communication

Table 1
Pyrolysis Yields from Different Woods

	Brockville Poplar			White Spruce			Red Maple			IEA Poplar		
Kun #	51	58	50	42	43	45	14	63	81	27	59	A-2*
Temperature, °C	497	504	555	485	500	520	532	508	515	500	504	497
Moisture content, wt%	-	5.2	+	-	7.0	+	3.8	5.9	9.5	6.2	4.6	3.3
Particle Top Size, µm	-	1000	+	-	1000	+	590	590	1000	590	1000	590
Apparent Residence Time, sec	0.64	0.47	0.57	0.70	0.65	0.62	0.69	0.47	0.44	0.55	0.48	0.46
Feed Rate, kg/hr	2.24	2.10	4.12	2.07	1.91	1.58	2.16	1.98	1.32	2.24	1.85	0.05
Yields, wt% of m.f. wood												
Organic liquid	62.9	62.9	59.0	63.1	66.5	66.1	67.3	67.9	65.0	65.8	66.2	65.7
Water	10.3	9.7	10.2	10.7	11.6	11.1	7.4	9.8	10.0	9.3	10.7	12.2
Char	14.4	16.5	10.6	16.3	12.2	12.3	9.0	13.7	12.1	12.1	11.8	7.7
Gas:												
H ₂	0.02	0.02	0.07	0.04	0.02	0.01	0.04	0.01	0.02	0.02	0.01	--
CO	4.95	4.71	8.40	4.16	3.82	4.01	6.96	4.12	4.83	5.32	4.44	5.34
CO ₂	6.14	5.89	7.06	3.38	3.37	2.69	4.02	4.89	5.36	6.30	5.75	4.78
CH ₄	0.45	0.44	0.97	0.34	0.38	0.43	0.75	0.36	0.57	0.48	0.37	0.41
C ₂ H ₆	0.22	0.19	0.40	0.16	0.17	0.16	0.24	0.16	0.21	0.20	0.13	0.19
C ₂ H ₄	0.06	0.05	0.11	0.02	0.03	0.05		0.04	0.07	0.04	0.05	--
C ₁	0.06	0.07	0.10					0.07	0.10		0.08	0.09
C _n	0.13	0.16	0.28	0.03	0.04	0.06	0.04	0.14	0.41	0.09	0.19	3.10
Total Gas	12.0	11.5	17.4	8.1	7.8	7.4	12.1	9.8	11.6	12.4	11.0	10.8
Overall recovery wt%, m.f.	99.7	100.5	97.2	97.8	97.7	96.7	95.7	101.2	98.7	99.7	99.8	96.4

* Bench Scale Unit

Table 2
Properties of Feed Materials

Source	Whole Tree Poplar	White Spruce	Red Maple	IEA Poplar Wood
	Brockville Plantation, Whole Tree Except Leaves and Roots Ontario MNR Clone C-147	Eastern Canada Clean Wood Sawmill Sawdust and Mill Scrap		Clean Wood only Ontario MNR Clone D-38
Moisture, wt%	5.2	7.0	3.8 - 25.2	4.6
Ash, % of	1.19	0.50	0.40	0.46
Elemental Analysis, %				
C	49.06	49.63	48.5	49.45
H	6.23	6.36	6.1	6.05
O	43.6	43.1	--	44.4
N	1.08	0.2	--	0.07

Table 3
Properties of Pyrolytic Liquids

Run #	Brockville Poplar			White Spruce			Red Maple	IEA Poplar
	51	58	50	42	43	45	63	59
Yields, wt% of wood as fed	74.1	73.3	70.5	75.2	79.2	78.5	77.9	77.6
Water content, wt%	19.8	18.7	21.7	21.9	22.4	21.8	18.0	18.6
pH	2.6	2.4	2.8	2.1	2.1	2.3	2.4	2.4
Density, g/cc	1.19	1.20	1.18	1.22	1.22	1.22	1.19	1.23
Elemental analysis, wt%, m.f.								
Carbon	54.1	54.7	55.6	53.5	54.0	56.6	54.7	53.6
Hydrogen	7.1	6.9	6.9	6.6	6.8	6.9	6.4	7.0

Table 4
Analysis of Liquid Products

Run #	Brockville Poplar	White Spruce	Red Maple	IEA Poplar
Temperature	504	500	508	A-2 504
Yields, wt% of feed, m.f.				
organic liquid	62.9	61.5	67.9	69.8
1. oligosaccharides				0.70
2. cellobiosan	1.11	2.49	1.62	1.30
3. glucose	0.55	0.99	0.64	0.41
4. fructose	1.34	2.27	1.51	1.32
5. glyoxal	1.42	2.47	1.75	2.18
6. methylglyoxal				0.65
7. levoglucosan	2.52	3.96	2.84	3.04
8. 1,6 anhydroglucofuranose	--	--	--	2.43
9. hydroxyacetaldehyde	6.47	7.67	7.55	10.03
10. formic acid	5.40	7.15	6.35	3.09
11. formaldehyde	--	--	--	1.16
12. acetic acid	6.30	3.86	5.81	5.43
13. ethylene glycol	0.87	0.89	0.63	1.05
14. acetol	1.70	1.24	1.15	1.40
15. acetaldehyde	--	--	--	0.02
16. methanol				
Water-solubles-total above	27.7	33.0	29.9	34.2
Pyrolytic lignin	24.8	20.6	20.9	16.2
Amount not accounted for (losses, water soluble phenols, furans etc.)	10.5	7.9	17.1	18.3

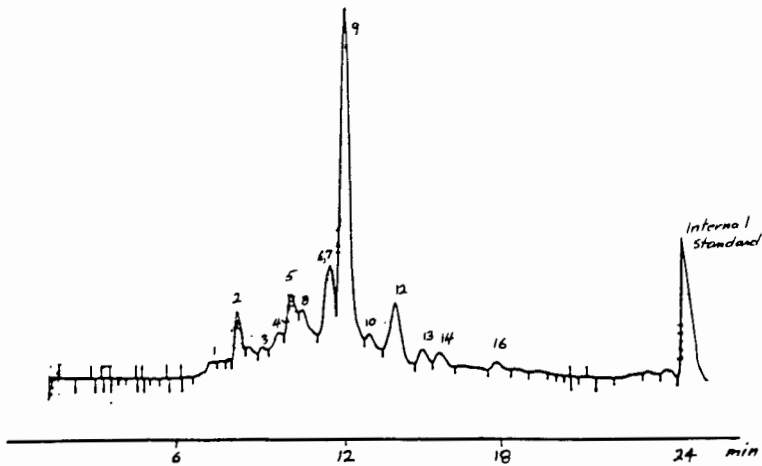


Figure 1 Chromatogram of Wood tar from run # A-2

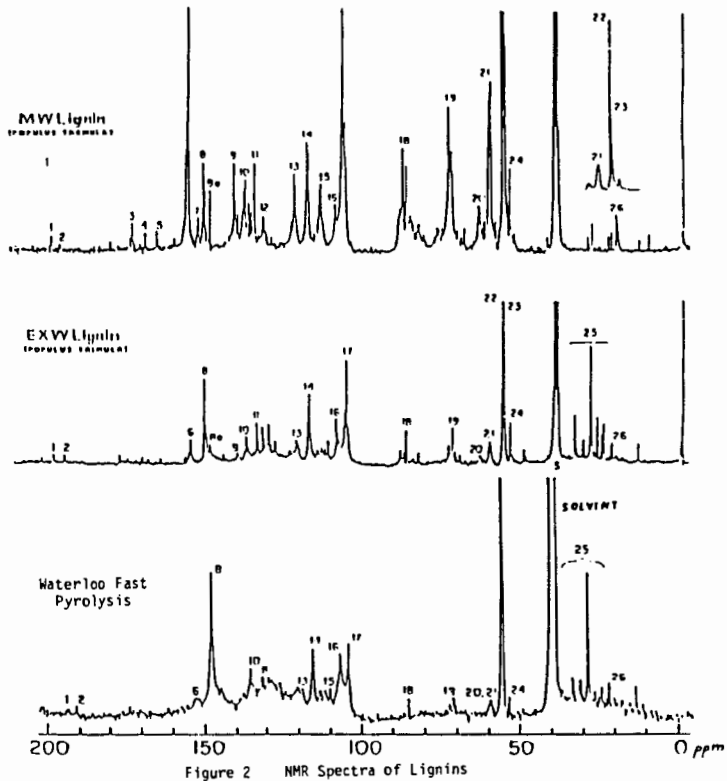


Figure 2 NMR Spectra of Lignins

AN OVERVIEW OF BIOMASS THERMOCHEMICAL LIQUEFACTION RESEARCH SPONSORED BY
THE U.S. DEPARTMENT OF ENERGY

Don J. Stevens

Pacific Northwest Laboratory*

P. O. Box 999
Richland, Washington 99352

BACKGROUND

Biomass represents an important energy resource in the United States both at present and as a potential energy contributor for the future. In 1981, for example, it is estimated¹ that biomass contributed about 3.5% of the nations' energy supply, approximately equivalent with nuclear energy which contributed 3.8% in that year. With proper resource management and the development of efficient conversion processes, the Office of Technology Assessment has estimated² the potential contribution of biomass to the United States energy supply could range as high as 17 quadrillion Btu per year--almost 20% of current United States energy consumption. Similarly, the Energy Research Advisory Board (ERAB) has estimated³ that biomass could potentially supply the nation with about 10 quadrillion Btu by the year 2000.

A wide variety of biomass resources such as wood and forest product residues, grasses, agricultural crops and their residues, and animal wastes can be used as energy feedstocks. As an abundant, renewable, domestic energy resource, biomass can help the United States reduce its dependence on imported oil and natural gas. Liquid fuels derived from biomass are expected to contribute significantly to the energy potential from this resource.

Liquid fuels from biomass offer several advantages over the biomass resource itself. Perhaps most important, liquid fuels have a higher energy density. The energy content of wood, for instance, is about 8500 Btu/lb, roughly half that of liquid hydrocarbon fuels. The effective bulk energy density of biomass solids on a volumetric basis is even lower if the void space between the solids is considered. A cubic foot of dry wood chips for instance, has an energy content of about 90,000 Btu. This is less than one-tenth the energy density of gasoline which contains about 928,000 Btu/ft³. The higher energy density of liquid fuels from biomass allows the products to be transported more economically and to be more easily stored. Liquid fuels also match existing end-use patterns, particularly in the transportation sector. Biomass is the only renewable energy technology capable of addressing this need for transportation fuels.⁴

Thermochemical conversion processes offer promising methods for converting biomass to gasoline-compatible liquid fuels. Thermochemical conversion processes employ elevated temperatures to convert the biomass feedstock. Thermal conversion processes are well suited to conversion of wood and crop residues which account for about 96% of the biomass resources in the United States.² These processes can convert 85 to 95% of the organic material in such feedstocks with little sensitivity to variations in the feed material.

Biomass direct liquefaction processes are those which produce liquids as primary initial products, usually at moderate temperatures (250 to 600°C). Pyrolytic and catalytic liquefaction processes which produce biocrude oils are examples. The biocrude oils would be suitable for some uses as produced or for upgrading into gasoline-compatible fuels. As will be described in greater detail later, the biocrude oils are quite different chemically than petroleum crude oils, and different refining and upgrading procedures are necessary. Indirect liquefaction processes,

*Operated for the U.S. Department of Energy by Battelle
Memorial Institute under Contract DE-AC06-76RLO 1830

by comparison, first convert the biomass to simple gaseous components including H₂ and CO and then synthesize these into liquid products. Methanol production is an example. Mechanical extraction of natural products from various biomass species followed by limited thermal or physical treatment can also supply liquid fuels. Various seed oils, for instance, have been used as extenders for diesel fuels.

In this paper we present an overview of biomass direct liquefaction research being sponsored by the U.S. Department of Energy's Biomass Thermochemical Conversion Program. Pacific Northwest Laboratory provides field management for this program as shown in Figure 1.

BIOMASS DIRECT LIQUEFACTION RESEARCH

Liquid fuels research sponsored by the Thermochemical Conversion Program focuses on biomass direct liquefaction processes capable of producing true hydrocarbon fuels. This is achieved by first converting the biomass feedstock to a biocrude product using various liquefaction processes. The crude oils produced in these processes are subsequently upgraded into true hydrocarbon products. The ability to generate true hydrocarbon fuels is very important to ensure compatibility with existing gasoline based fuels and fuel distribution systems. Thermochemical conversion processes are necessary for producing true hydrocarbons from biomass.

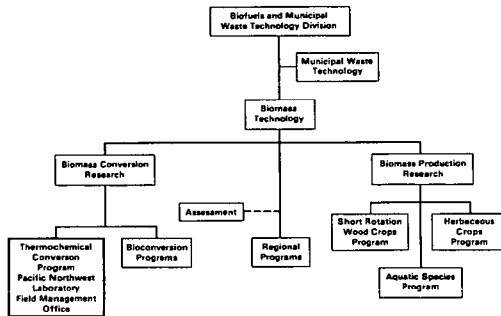


Fig. 1 - Organization of the Biomass Thermochemical Conversion Program

Projects being funded by the Biomass Thermochemical Conversion Program are shown in Figure 3. The research is directed at exploring of methods for generating biocrude liquids and at upgrading them into high value hydrocarbon fuels.

PRODUCTION OF BIOCRUDE LIQUIDS

The initial step in the conversion of biomass to hydrocarbon fuels is the production of an intermediate biocrude liquid. This step can be accomplished using several different approaches. These are discussed below.

PYROLYTIC LIQUEFACTION - Pyrolysis refers to the heating of biomass in the absence of air. Traditionally, pyrolysis has been used to produce charcoal. Conventional pyrolysis typically produces about one-third each gases, pyrolysis oils, and char. The process is inefficient because large quantities of low-value liquids and gases are formed in addition to desired solid products. Batchwise, often primitive, conversion units have also added to the inefficiency of conventional pyrolysis processes.

In recent years, the concept of rapid pyrolysis has emerged as a promising alternative for producing liquid fuels. By carefully controlling both the heating rate and the temperature, the yields of liquid biocrude products can be increased to over 65% by weight on a moisture, ash-free basis.⁵ Under some conditions, up to about 20% high value olefinic products can be produced.⁶

Georgia Tech Research Corporation, Atlanta, Georgia, is conducting research on rapid pyrolysis of biomass with the goal of producing low cost liquid products. The research makes use of an entrained flow pyrolyzer where biomass is converted primarily to liquid products under conditions of moderate heating rates and temperatures. The system, as shown schematically in Figure 3, consists of an entrained, upflow reactor and an oil recovery system that allows partial on-stream fractionation of the product. Georgia Tech Research Corporation has established the interdependence of the reaction temperature and residence time on pyrolysis oil yield. Testing over temperatures from 400 to 550°C gave mass yields of moisture-free oil ranging from 31 to 53%. Additional testing should complete parameter optimization studies.

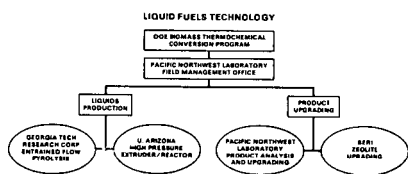


Fig. 2 - Liquid Fuels Projects Sponsored by the Thermochemical Conversion Program

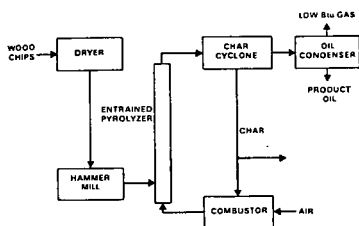


Fig. 3 - Schematic Diagram of Entrained-Flow Pyrolysis Reactor at Georgia Tech Research Corporation

CATALYTIC LIQUEFACTION - Catalytic direct liquefaction research, at this time, is based on a concept first proposed by the Pittsburgh Energy Research Center. In this concept, biomass is mixed with recycled wood oil and sodium carbonate catalyst along with a H_2/CO reducing gas. The mixture is injected into a high-pressure vessel (3000 psi) and heated to about 350°C. The product stream is cooled and flashed into a pressure let-down vessel. The oil phase product is withdrawn and part of it is recycled for use as slurry medium.

In 1980 and 1981, this process and an aqueous slurry version, proposed by Lawrence Berkeley Laboratory, were tested in a DOE research facility located at Albany, Oregon. This research showed the technical feasibility of producing biomass derived liquids by both the oil slurry and aqueous slurry process variations. In one test run during 1981, over 11,000 lbs of direct liquefaction oils were produced during operation in the oil slurry mode. The tests, however, also showed the need to reduce the large oil recycle requirement in order to improve process economics. The Thermochemical Conversion Program is attempting to improve the competitiveness of direct liquefaction through the use of increased feedstock slurry concentrations.

The University of Arizona, Tucson, Arizona, is conducting research on an advanced concept for direct liquefaction that would use very concentrated biomass slurries. The goal of this work has been to use a polymer extruder as a slurry feeding/pumping device. The modified extruder/feeder system is capable of handling slurries as concentrated as 60% wood solids in biomass oil. Conventional systems, by comparison, typically cannot handle slurries containing over about 20% wood. The University of Arizona had designed and constructed an integrated extruder/static mixer liquefaction system as shown in Figure 4. The static mixer is expected to allow adequate mixing and agitation of the viscous slurries.

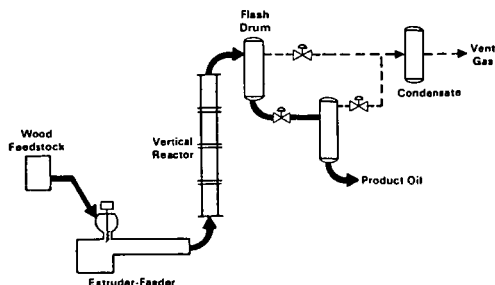


Fig. 4 - Schematic Diagram of Catalytic Liquefaction Unit at the University of Arizona

The University of Arizona has completed construction of the research unit and has begun experimental operation. Results to date show that the unit can be operated consistently and reliably over a variety of experimental conditions. The biocrude product produced is low in oxygen content and has a high heating value. Properties of the oil are summarized in Table 1.

Table 1 - Properties of Crude Oil from the Wood Produced by the University of Arizona (Dry Basis)

Elemental Analysis:

C	83.4%
H	7.9%
O	8.5%
Heating Value (HHV)	16,000 Btu/lb

During 1987, the University of Arizona will operate the experimental unit to determine the effect of lowering or eliminating both the carbonate catalyst and the reducing gas. Preliminary results show that the reactor can operate when those two additives are eliminated, but the effect on product quality has not yet been determined.

PRODUCT CHARACTERIZATION AND UPGRADING

In addition to research on liquefaction concepts, the Thermochemical Conversion Program is also sponsoring research on the characterization of the biocrude products and their subsequent upgrading into gasoline compatible hydrocarbon fuels. This research is described below.

Pacific Northwest Laboratory, Richland, Washington, is conducting research on the characterization and upgrading of both pyrolytic and catalytic liquefaction oils. Characterization studies indicate that there are significant differences between the pyrolytic and the catalytic liquefaction oils. As shown in Table 2, pyrolysis oils contain more oxygen and are less viscous than the catalytic liquefaction products. The catalytic liquefaction products contain large quantities of phenolic compounds while the pyrolysis oils have large concentrations of organic acids. These differences directly impact the methods for upgrading these products.

Table 2 - Biomass Liquefaction Products Comparative Analytical Data

<u>Elemental Analysis (MAF)</u>	<u>Catalytic Liquefaction Oil (PERC-Albany TR12)</u>	<u>Pyrolysis Oil (Georgia Tech #11)</u>
Carbon	81.0%	59.2%
Hydrogen	10.2%	7.0%
Oxygen	8.8%	33.8%
Nitrogen	0.1%	0.1%
Sulfur	1.5%	1.4%
<u>Moisture and Heating Value</u>		
% H ₂ O	7.3	19.7
raw ² HHV	14,200 Btu/lb	7,950 Btu/lb
MAF HHV	15,300 Btu/lb	9,800 Btu/lb
<u>Other Properties</u>		
viscosity cps @ 40°C	400,000	62
density g/ml @ 23°C	1.14	1.24
pourpoint	27°C	-15°C

Research at PNL has concentrated on upgrading the biocrude liquids to gasoline-like motor fuels. This research uses nickel/molybdenum and cobalt/molybdenum catalysts in a continuously fed, bench-scale reactor to hydrotreat the liquefaction crude oils. Initial research has focused on the catalytic liquefaction oils due to their lower initial oxygen content and higher stability. Hydrotreating under conditions of 350 to 400°C at pressures of 2000 psi selectively eliminates oxygen and yields primarily hydrocarbon materials. Comparisons of key constituents and of relative properties of the crude and upgraded products are shown in Tables 3 and 4. Research indicates that the octane number for the hydrocarbon product is about the same as straight run gasoline from petroleum sources.

Table 3 - Comparison of Typical Constituents of Biomass Catalytic Liquefaction Biocrude Oil and Hydrotreated Product (Albany TR-7 Oil)

<u>Biomass Crude Product</u>	<u>Refined Biomass Oil</u>
Cyclic Keytones	Cyclohexane
Unsaturated Cyclic Keytones	Alkyl-Cyclohexanes (to C-10)
Alkyl-Phenols	Benzene
Methoxy-Phenols	Toluene
Di-Phenols	Xylene
Napthols	Other Alkyl-Benzenes

Table 4 - Comparison of Properties of Biocrude Oils and Hydrotreated Product (Albany TR-7 Oil)

	<u>Biocrude Oil</u>	<u>Refined Biomass Oil</u>
Hydrogen to Carbon Ratio	1.21	1.61
Oxygen Content (% MAF Basis)	11	0.3
Density (g/cm ³)	1.19	0.83
Viscosity (cPs @35°C)	100,000	1.1
Heating Value (HHV, MAF Basis)	15,800	18,900

Pacific Northwest Laboratory also initiated research on the upgrading of the pyrolytic liquefaction oils. The pyrolytic oils are expected to be less expensive to produce but more difficult to upgrade due to their higher oxygen content and lower stability. The lower stability of the oil results in extensive char formation and reactor plugging when the pyrolysis oils are hydrotreated under conditions similar to the catalytic liquefaction products. Preliminary research has indicated that a two-step process may be feasible for upgrading the pyrolysis oils. The initial step would use a mild treatment with a nickel catalyst at relatively low temperature (260 to 280°C) followed by a second hydrotreating step similar to that use with the catalytic liquefaction products. Additional research on this concept will be conducted in FY86.

Solar Energy Research Institute (SERI), Golden, Colorado, is also conducting research on the upgrading of biomass pyrolytic liquefaction oils. The concept being explored uses zeolite catalysts to convert the pyrolysis oils to hydrocarbon fuels. The pyrolysis oil vapors would be reacted on the catalyst directly downstream from the pyrolysis reactor, eliminating the need for intermediate condensation of the pyrolytic products. The zeolite catalysts could also eliminate the need for hydrogen in the upgrading process. The zeolite catalysts are known to produce gasoline-like hydrocarbons from a variety of oxygenated feedstocks such as methanol.

Preliminary studies at SERI using mass spectroscopic techniques showed that zeolite catalysts are reactive with respect to the biomass tars and will produce hydrocarbon products. During 1986, SERI completed modification of their ablative pyrolysis reactor to include a slipstream reactor so the pyrolytic vapors could be directly upgraded. Using a zeolite catalyst donated by Mobil Corporation, SERI has now shown that the catalyst can effectively deoxygenate biomass vapors to produce hydrocarbons. In 1987, research is continuing to determine catalyst lifetimes, the extend of carbon deposition, and related factors in order to optimize reaction conditions.

ADDITIONAL INFORMATION

Detailed descriptions of all the research and development projects funded by the Biomass Thermochemical Conversion Program are given in the Proceedings of the 1985 Biomass Thermochemical Conversion Contractors' Meeting, October 1985. This document, PNL-SA-13571/CONF-8510167, is available from the National Technical Information Service, United States Department of Commerce, 5285 Port Royal Road, Springfield, Virginia 22161.

REFERENCES

1. J. Haggin and J. H. Krieger, "Chem. and Eng. News." March 14, 1984.
2. Office of Technology Assessment, "Energy from Biological Processes." Washington, D.C., U.S. Government Printing Office, 1980.
3. "Solar Energy Research and Development: Federal and Private Sector Roles." Draft Report to the Solar R&D Panel of the Energy Research Advisory Board, September 2, 1982.
4. P. Collins, "Energy From Biomass: Building on a Generic Technology Base." ANL/CNSV-TM-157, November 27, 1984.
5. "Comptes Rendus De L'Atelier de Travail sur la Liquefaction de la Biomasse." Sherbrooke, Quebec, Canada, September 29-30 1983.
6. M. Steinberg, P. T. Fallon, and M. S. Sundaram, "Flash Pyrolysis of Biomass with Reactive and Non-Reactive Gases." Portland, Oregon, Battelle, Pacific Northwest Laboratory, May 8-9, 1984.

CATALYST SPECIFICITIES IN HIGH PRESSURE HYDROPROCESSING
OF PYROLYSIS AND GASIFICATION TARS

E.J. Soltes, S-C.K. Lin
Dept. of Forest Science and TAES, Texas A&M University System
College Station, Texas 77843-2135

and

Y-H.E. Sheu
Texaco Chemical Company, Austin Laboratories
Austin, Texas 78761

ABSTRACT

Over a period of several years [1], the Department of Forest Science at Texas A&M University has been conducting studies in the hydroprocessing (catalytic high pressure hydrotreating or hydrodeoxygenation accompanied by hydrocracking) of pyrolytic tars produced in biomass pyrolysis and gasification. Upgrading through hydroprocessing results in good yields of volatile hydrocarbon and phenolic products. This paper compares the performance of twenty different catalysts selected for hydroprocessing of a pine pyrolysis oil, describes the use of noble metal catalysts with tars produced from nine different biomass feedstocks (oil from pine pyrolysis and the tars from pine wood chip, pine plywood trim, pecan shell, peanut shell, sugarcane bagasse, corncob, rice hull, and cottonseed hull gasification), and compares the use of several catalysts in a trickle bed reactor for kinetic studies of the hydroprocessing reaction.

METHODOLOGY

Feedstock and Materials. Pine pyrolytic oil produced by Tech-Air Corporation from sawdust and bark in the Cordele GA demonstration plant was used as the base oil in this study. A barrel of this oil was generously provided by American Can Company. Other tars from agricultural residues were produced in a modified gasification-pyrolysis reactor (100 kg capacity updraft gasifier run under conditions to promote tar production).

Catalysts used for the batch reactor studies were used in the form purchased from Strem, Harshaw, or donated by UOP (Table 1). For the trickle bed reactor studies, the 5% Pt/Al₂O₃ powder catalyst was mixed with Ludox AS-40 binder in proportions that the final catalysts contained 30% SiO₂. A paste was made when the binder was added, and this paste was taken up into a syringe with a 1/16 inch plunger. The catalysts was extruded, dried and calcined in air at 756°K (483°C) for four hours. In order to obtain an active catalyst, the Pt/Al₂O₃ pellet was reduced *in situ* prior to the experiments. The reduction was done by passing H₂ through the catalytic bed at 673°K, 8270kPa at a flow rate of 200 cm³/min (21.1°C, 1 atm) for one hour.

For Harshaw's catalysts, the sulfided form was used. Presulfiding of the catalysts was done *in situ* prior to the experiments. A mixture of 90% H₂ and 10% H₂S by volume was passed through the catalyst bed at a flow rate of 40 cm³/min (measured at 21.2°C, 1 atm) at 673°K and atmospheric pressure until the outlet gas showed no further sign of H₂S consumption.

Decahydronaphthalene (decalin) purchased in purified grade from Fisher Scientific and methyl cyclohexane produced by hydrogenation of toluene were used as hydrogen-donor solvents in the hydroprocessing reactions.

Batch Reactor Studies. Some twenty catalysts (Table I) were used in preliminary screening studies [2,3]. A number of experiments were conducted using the various catalysts at differing reaction conditions in attempts towards optimization for each catalyst, but the results obtained could not be tabulated to effect some ranking order. Standard conditions chosen were those found to be effective for the 5% Pd and 5% Pt catalysts in the preliminary study - 60g stripped pine pyrolytic tar (water removed through azeotropic distillation with toluene), 100g solvent (decalin or methyl cyclohexane), 20g catalyst, 1000 psi (@ ambient temp.) hydrogen feed and 400°C for 60

minutes in a rocking reactor (Aminco 4 3/8 inch o.d. series, 1500 ml capacity, rated at 5500 psi). After the reactions, the following were calculated (Tables II and III): *hydrocarbon conversion %* (total liquid product corrected for solvent and water concentrations), *water yield %* (water produced as % of pyrolytic tar feed - a measure of hydrotreating or hydrodeoxygenation activity), *gases and losses %* (balance of products by difference as % of pyrolytic tar feed - a measure of excess hydrocracking activity in the production of gaseous hydrocarbons). For a few catalysts with limited catalytic activity, a fourth component of the reaction product was calculated: *tar residue %*. Tar residue is the heavy tar deposited on catalysts and insoluble in the reaction solvent selected (determined by weighing dirtied catalyst after reaction, subtracting weight of catalyst used, and expressing as % of pyrolytic tar feed).

Trickle-bed Reactor Studies. A schematic for the trickle-bed reactor system is shown in Figure 1 [4,5]. The reactor proper consists of a 32-inch long 316 SS tube, 3/4 inch O.D., 0.065 inch thick. The bottom 12 inches contained an inert support, Pyrox 3 mm dia. glass beads, with the top 20 inches packed with catalyst. The reaction temperature was non-isothermal, viz. 22 inches of the reactor was immersed in a salt bath (Hotec heat transfer salt, a mixture of 53% potassium nitrate, 40% sodium nitrite, 7% sodium nitrate; air bubbled through bath to ensure uniform temperature profile), so that the salt around the bottom half of the catalyst bed (10 in) was at temperature, while the temperature of non-immersed top half decreased linearly from near reaction temperature at the top of the salt bath to 190°C at the top of the reactor. By using non-isothermal conditions, the temperature inside the reactor increased gradually along the reactor length, preventing the volatiles in the pine pyrolysis oil from flashing into the gas phase suddenly. With the catalyst packed at the top of the reactor, the pyrolysis oil was hydrotreated before the oxygen-containing compounds could polymerize at high temperature. The NiW catalyst is a strong cracking catalyst and was thus not effective in hydrotreating: oxygen-containing components in the oil polymerized in the reactor.

Under typical operating conditions, H₂ feed was 100 cc/min (at 60°C, 1 atm) per gram of pine pyrolysis oil input; liquid feed was used at a ratio of 2 grams decalin per gram of pine pyrolysis oil; weight hourly space velocity (g oil input per hr / g catalyst in the reactor) was 0.5 to 3.0 hr⁻¹; salt bath temperature was 673 to 673°K; H₂ pressure was 5272 to 10443 kPa (750 to 1500 psig); and, catalyst bed was 60 g. for each load. After the reaction, the catalyst was regenerated by burning in air to remove coke deposited on the catalyst during the reaction, then reactivated for the next run.

Sample and Product Chemical Analyses. Analytical techniques used to determine the chemical composition of raw oils and hydroprocessed products are given elsewhere in this volume [6].

RESULTS AND DISCUSSION

Batch Reactor Studies. Results for the 20 catalysts using the batch rocking reactor using decalin as hydrogen-donor solvent are given in Table II; those for the methyl cyclohexane solvent system in Table III. The 5% noble metal catalysts in both solvent systems generally gave superior results in hydrocarbon conversion and water yield. Note that hydrocarbon conversion efficiencies may appear low because these are expressed on a mass and not energy basis. With 27% oxygen content in the raw pyrolytic tar feed, maximum hydrocarbon conversion is 73% plus hydrogen uptake; maximum water yield is 30% (27 X 18/16). These data will be discussed in the oral presentation.

Trickle-bed Reactor Studies - Oxygen Removal. The effect of reaction temperature, pressure and space velocity on oxygen removal (hydrotreating, hydrodeoxygenation) are shown in Figures 2 through 4. The points in the figures are the experimental data and the solid lines were evaluated by using an oxygen removal model. A clear trend is observed for the effect of reaction temperature and pressure, while changes in space velocities did not affect oxygen removal. The Pt/Al₂O₃ catalyst exhibits the best activity for oxygen removal for pine pyrolysis oil among the four catalysts tested. The NiW catalyst was not effective in oxygen removal, and was dropped from further consideration.

Trickle-bed Reactor Studies - Kinetic Modeling. The proposed kinetic model for hydroprocessing pyrolysis oil consists of the kinetic scheme as shown in Figure 5. Terms used in this and subsequent figures are defined as follows (see other paper in this volume [6] for examples of the GPC chromatograms):

<i>heavy nonvolatiles</i>	- nonvolatiles in GPC fractions 1 and 2.
<i>light nonvolatiles</i>	- nonvolatiles in GPC fractions 3 and 4
<i>phenols</i>	- volatiles in GPC fraction 3 detectable by GC
<i>aromatics</i>	- volatiles in GPC fractions 4 and 5, excluding solvents
<i>alkanes</i>	- volatiles in GPC fraction 2
<i>coke + H₂O + outlet gases</i>	- 1 minus liquid yield
<i>liquid yield</i>	- $\frac{(\text{wt. of fractions by GPC}) - (\text{solvents in hydroprocessed oil})}{\text{pine pyrolysis oil input}}$

An elaboration of the kinetic model is outside the scope of this preprint. The outcome, expressed as experimental and predicted values of the lumped species in the kinetic model at various reaction conditions (temperature, pressure and space velocity effects) is presented in Figures 6 through 14.

Effect of Reaction Temperature (Figures 6 to 8). Temperatures selected for study were 623, 648 and 673°K. All reactions were run at 8720 kPa and WHSV 2 hr⁻¹.

Effect of Reaction Pressure (Figures 9 to 11). The effect of reaction pressure was evaluated at 5272, 6996, 8720 and 10443 kPa at 673°K and WHSV 2 hr⁻¹.

Effect of Space Velocity (Figures 12 to 14). WHSV was evaluated at 0.5, 1.0, 2.0 and 3.0 hr⁻¹. Pressure used was 8721 kPa; temperature, 673°K.

Results are essentially self-evident in these figures, but will be discussed in detail in the oral version and final manuscript of this communication.

ACKNOWLEDGMENTS

This research has been generously supported by the Texas Agricultural Experiment Station, the Center for Energy and Mineral Resources and the College of Agriculture, all parts of the Texas A&M University System, and by two USDA Special Research Grants (Agreements 59-2481-0-2-089-0 and 59-2481-1-2-123-0).

REFERENCES

- [1] E.J. Soltes and S-C.K. Lin, "Hydroprocessing of Biomass Tars for Liquid Engine Fuels", in: *Progress in Biomass Conversion*, Volume V, D.A. Tillman and E.C. Jahn, editors, pp.1-68, Academic Press, New York (1984).
- [2] E.J. Soltes, "Diesel Fuels from Pine Pyrolytic Oils". Final Report, USDA Energy Grants FY1980 No. 59-2481-0-2-089-0 (1982).
- [3] S-C.K. Lin, *Hydrocarbons via Catalytic Hydrogen Treatment of Pine Pyrolytic Oil*, Ph.D. Dissertation, Forest Science, Texas A&M University, May 1981.
- [4] Y-H.E. Sheu, R.G. Anthony and E.J. Soltes, "Kinetic Studies of Upgrading Pyrolytic Oil by Hydrotreatment", I&EC (1986).
- [5] Y-H.E. Sheu, *Kinetic Studies of Upgrading Pine Pyrolytic Oil by Hydrotreatment*, Ph.D. Dissertation, Chemical Engineering, Texas A&M University, May 1985.
- [6] E.J. Soltes and S-C.K. Lin, "Chromatography of Non-Derivatized Pyrolysis Oils and Upgraded Products", THIS volume.

TABLE I.

CATALYSTS SCREENED FOR HYDROTREATING AND HYDROCRACKING OF BIOMASS THERMOCHEMICAL TARS

5% Pd/alumina	2% Pt/alumina	0.5% Pd/alumina
5% Pd/carbon	5% Pt/alumina	0.5% Pt/alumina
5% Re/alumina	5% Pt/carbon	0.5% Re/alumina
5% Rh/alumina	Harshaw CoMo-0603	silicated gamma alumina
5% Ru/alumina	Harshaw HT-400	NiO-WO ₃ / silica alumina
Raney Ni	Harshaw Ni-4301	UOP Lomax
NiCO ₃	ZrO ₂ on alumina	UOP Unibon

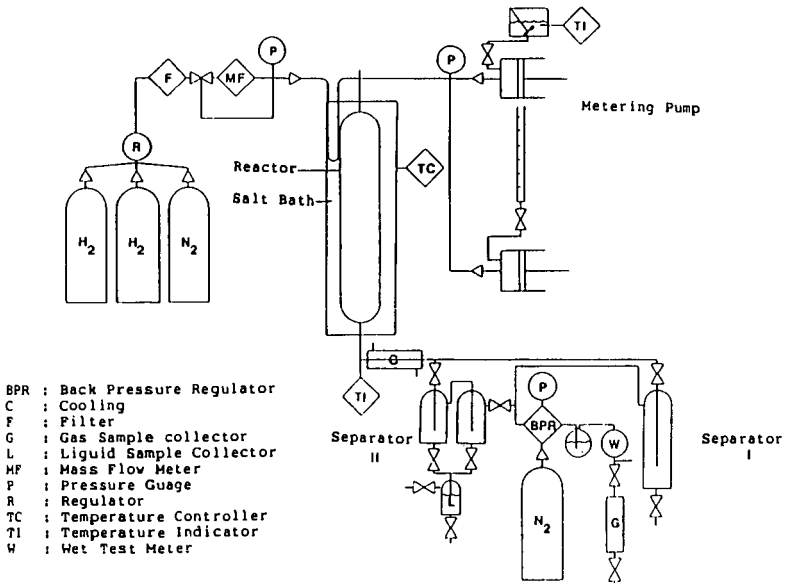


Figure 1. Schematic process of trickle-bed reactor system

TABLE II. HYDROPROCESSING OF TECH-AIR PINE PYROLYSIS OIL IN DECALIN SOLVENT¹

Catalyst Type	Hydrocarbon Conversion ² %	Water Yield ² %	Tar Residue ² %	Gases & Losses ² %
5% Pd/alumina	55.7	25.3	-	19.0
5% Pd/carbon	35.7	21.7	-	42.5
5% Pt/alumina	44.5	24.5	-	31.0
5% Pt/carbon	33.1	17.7	-	49.2
5% Rh/alumina	39.3	15.8	-	44.8
5% Ru/alumina	25.8	20.0	-	54.2
5% Re/alumina	44.3	18.2	-	37.5
UOP Lomax	43.5	8.3	-	48.2
UOP Unibon	33.3	6.6	-	60.1
Raney Ni	40.1	19.6	-	40.3
2% Pt/alumina	51.4	5.0	-	43.6
0.5% Pd/alumina	18.4	9.8	-	71.2
0.5% Pt/alumina	25.7	10.8	-	63.5
0.5% Re/alumina ³	-	10.1	75.4	-
Ni-4301	11.9	8.3	40.3	39.5
CoMo-0603	4.2	6.0	41.2	48.6
HT-400	3.4	7.5	57.9	31.2
ZrO ₂	25.1	7.4	35.9	31.6
silica alumina	3.3	13.2	69.9	13.6
silicated gamma alumina	11.4	6.7	45.3	36.6

¹ conditions as described in text

² defined in text

³ hydrocarbon conversion very small; gases and losses % could not be calculated

TABLE III. HYDROPROCESSING OF TECH-AIR PINE PYROLYSIS OIL IN METHYL CYCLOHEXANE SOLVENT¹

Catalyst Type	Hydrocarbon Conversion ² %	Water Yield ² %	Tar Residue ² %	Gases & Losses ² %
5% Pd/alumina	54.5	8.9	-	36.6
5% Pd/carbon	37.4	8.2	-	54.5
5% Pt/alumina	44.2	5.0	-	50.8
5% Pt/carbon	19.1	6.7	-	76.5
5% Rh/alumina	38.9	16.6	-	44.5
5% Ru/alumina	24.9	12.4	-	62.8
5% Re/alumina	37.1	20.0	-	42.8
UOP Lomax	38.0	5.0	-	57.0
UOP Unibon	35.6	7.5	-	56.9
Raney Ni	40.1	19.1	-	40.1
2% Pt/alumina	21.3	2.4	-	76.3
0.5% Pd/alumina	53.9	8.9	-	37.2
0.5% Pt/alumina	46.5	10.1	-	43.3
0.5% Re/alumina ³	-	5.0	69.3	-
Ni-4301 ³	-	10.0	50.2	-
CoMo-0603 ³	-	4.8	46.6	-
HT-400 ³	-	8.3	60.6	-
ZrO ₂ ³	-	5.0	63.4	-
silica alumina ³	-	12.4	74.0	-
silicated gamma alumina ³	-	1.7	61.7	-

¹ conditions as described in text

² defined in text

³ hydrocarbon conversion very small; gases and losses % could not be calculated

TABLE IV. PROPERTIES OF RAW AND HYDROPROCESSED¹ BIOMASS PYROLYTIC TARS

	RAW TARS								
	Tech-Air	Wood Chips	Pecan Shell	Sugarcane Bagasse	Peanut Shell	Corncob	Rice Hull	Cotton Hull	Plywood Trim
Elem. Anal. ²									
C, wt %	65.79	54.34	68.37	55.94	60.89	58.34	64.62	67.91	74.08
H, wt %	27.08	36.31	25.90	36.90	28.27	34.30	25.26	23.47	13.10
O, wt %	—	36.18	20.32	36.33	38.67	34.30	23.02	23.02	16.33
N, wt %	—	0.14	0.61	0.31	3.03	1.04	3.44	1.80	0.33
Heat Content	23.18	24.32	23.93	22.39	27.65	24.88	24.26	23.86	24.61
MJ/kg									
Spec. Gravity ²	1.14	1.22	1.11	1.15	1.10	1.26	—	—	1.10
Ash Content ²	1.03	0.22	0.20	0.57	0.77	1.32	0.68	3.16	0.12
%									
Water Content	10.0	6.4	13.0	19.6	15.0	3.1	5.0	5.0	10.6
%									
HYDROPROCESSED ¹ TARS									
	Tech-Air	Wood Chips	Pecan Shell	Sugarcane Bagasse	Peanut Shell	Corncob	Rice Hull	Cotton Hull	Plywood Trim
Elem. Anal. ²									
C, wt %	83.20	79.48	81.58	78.62	78.50	83.40	81.78	82.05	81.14
H, wt %	12.70	9.79	10.96	9.26	9.85	9.22	10.53	10.80	9.51
O, wt %	4.10	10.57	6.41	11.25	10.24	5.49	5.53	5.53	8.45
N, wt %	—	0.26	1.06	0.75	1.41	1.89	2.16	1.38	0.90
Heat Content ²	40.26	38.19	40.24	38.15	38.33	39.32	37.37	41.02	38.91
MJ/kg									
Spec. Gravity ²	0.87	0.90	0.90	0.94	0.95	0.88	0.93	0.90	0.89
Conversion ³									
wt %	71.7	58.1	67.3	57.4	74.7	58.8	63.4	64.7	59.2
energy %	111.9	83.5	98.4	78.4	87.7	90.1	92.7	105.7	83.7

¹ conditions used: 15g 5% Pd/alumina catalyst, 100g decalin, 400 C, 60 minutes, 6900 kPa Hz

² not corrected for moisture

³ conversion, wt %, is (wt % of product minus wt of solvent) over tar dry weight times 100.

conversion, energy %, is wt % times heat content of product over heat content of raw tar.

TABLE V. SPECIFICATIONS FOR THE CATALYSTS USED IN THE TRICKLE BED REACTOR STUDY¹

Catalyst Type	Pt/Al ₂ O ₃	CoMo	NiMo	NiW
Manufacturer	Strem 78-166	Harshaw HT-400	Harshaw HT-500	Harshaw Ni-4301
Size	powder	1/16" E. ²	1/16" E. ²	1/16" E. ²
Composition	5% Pt	3% CoO, 15% MoO ₃	3.5% NiO, 15.5% MoO ₃	6% Ni, 19% W ³
Surface Area, m ² /g	100 ³	200	200	230
Pore Volume, cc/g	0.52 ³	0.45	0.46	0.37
Pore Size, dia, Å	100	94	88	104

¹ conditions as described in text

² E. = extrudate

³ for the pellet catalyst

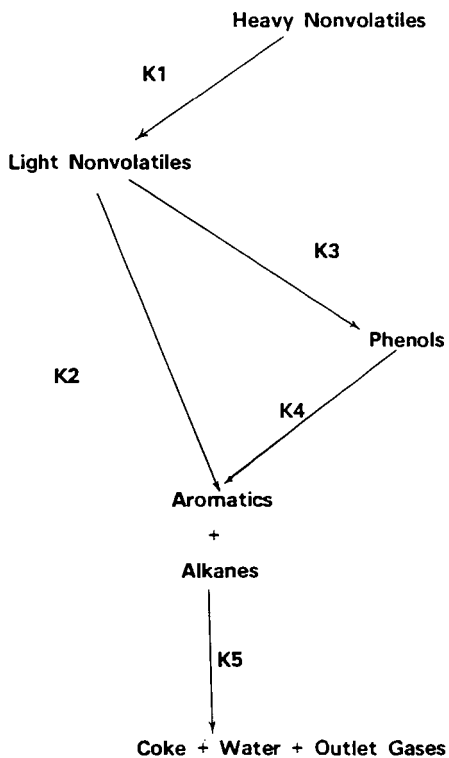


FIGURE 5.
Lumped Kinetic Scheme

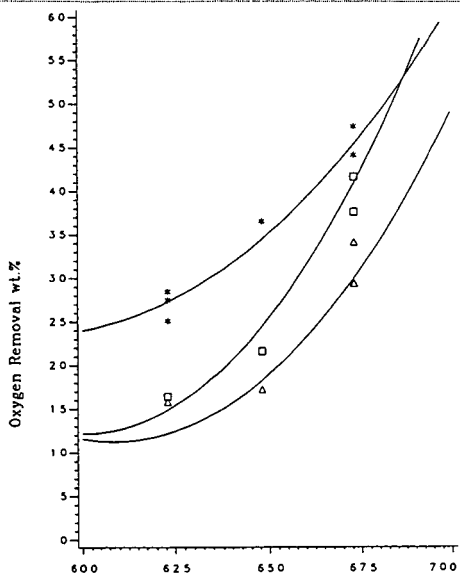


FIGURE 2 - Reaction Temperature, K

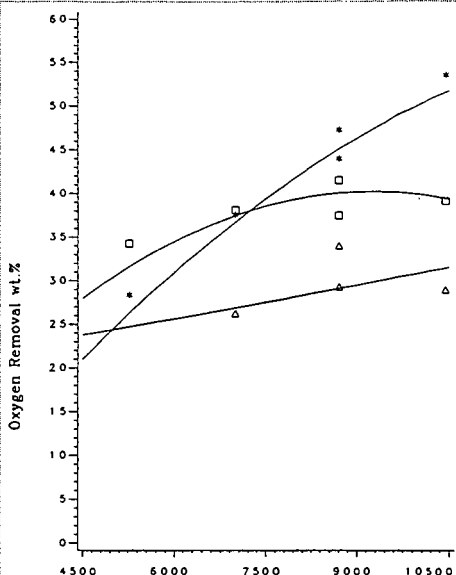


FIGURE 3 - Reaction Pressure, kPa

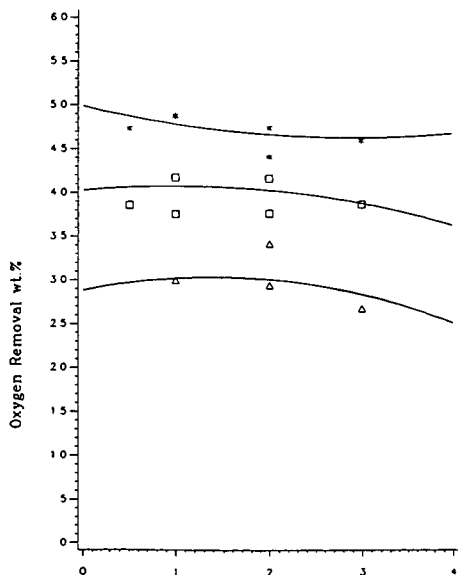


FIGURE 4 - Space Velocity, hr⁻¹

Effects of Reaction Temperature, Reaction Pressure and Space Velocity on Oxygen Removal - Trickle-Bed Reactor Study

- * Pt catalyst
- CoMo
- △ NiMo
- Model Predictions

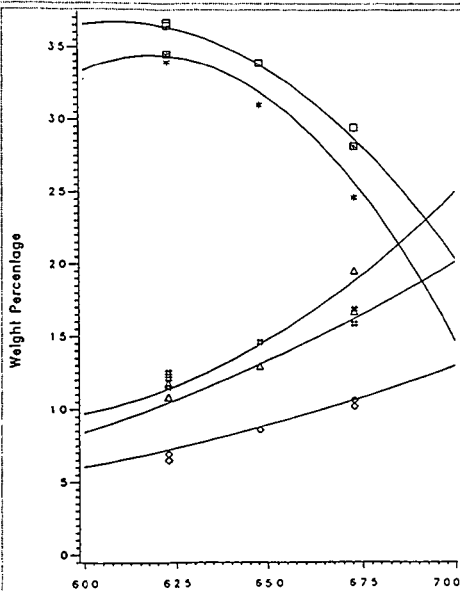


FIGURE 6 - Pt/Al₂O₃ Catalyst

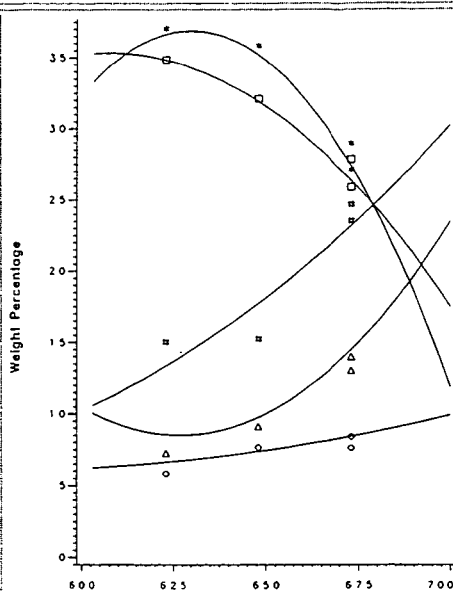


FIGURE 7 - CoMo Catalyst

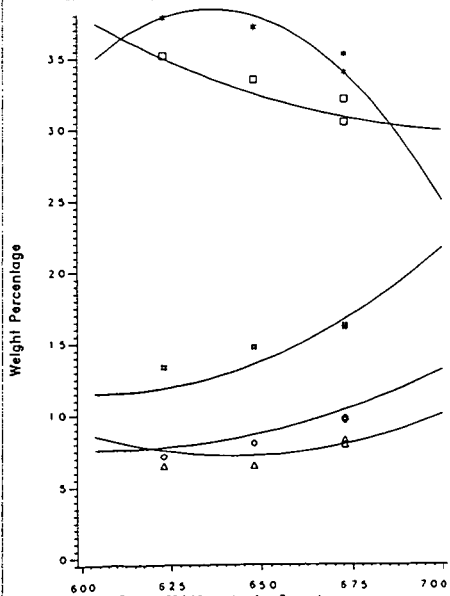


FIGURE 8 - NiMo Catalyst

Effects of Reaction Temperature, K_1 on Hydroprocessing - 8720 kPa, WHSV 2 hr⁻¹ Trickle-Bed Reactor Study

- * Heavy Nonvolatiles
- Light Nonvolatiles
- Phenols
- △ Aromatics + Alkanes
- Coke + Water + Outlet Gases
- Model Predictions

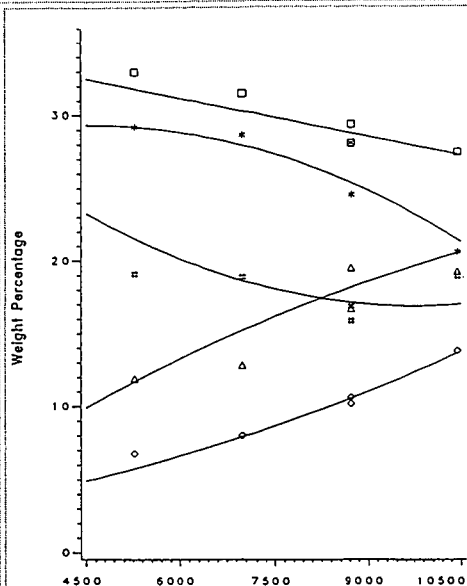


FIGURE 9 - Pt/Al₂O₃ Catalyst

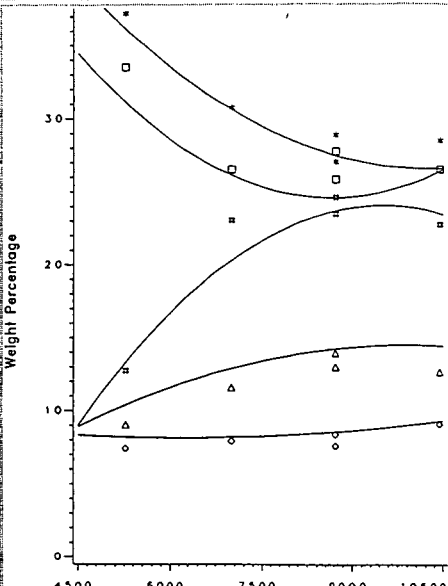


FIGURE 10 - CoMo Catalyst

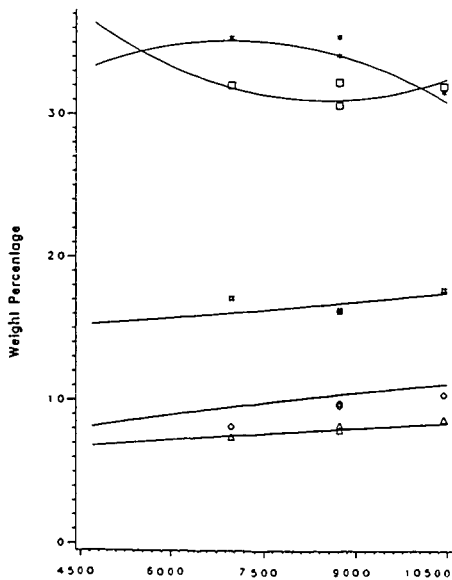


FIGURE 11 - NiMo Catalyst

Effects of Reaction Pressure, kPa, on Hydroprocessing - 673 K, WHSV 2 hr⁻¹ Trickle-Bed Reactor Study

- Heavy Nonvolatiles
- ◻ Light Nonvolatiles
- ◊ Phenols
- △ Aromatics + Alkanes
- Coke + Water + Outlet Gases
- Model Predictions

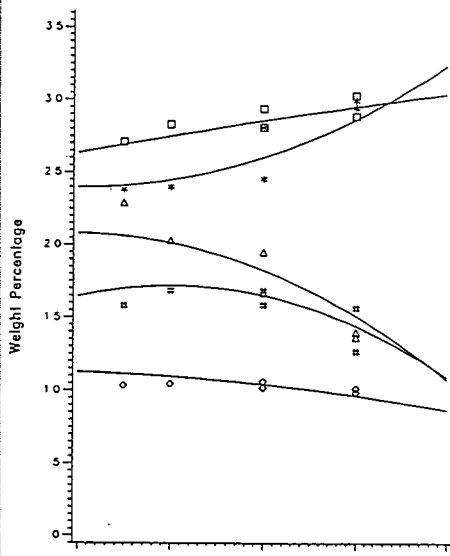


FIGURE 12 - Pt/Al₂O₃ Catalyst

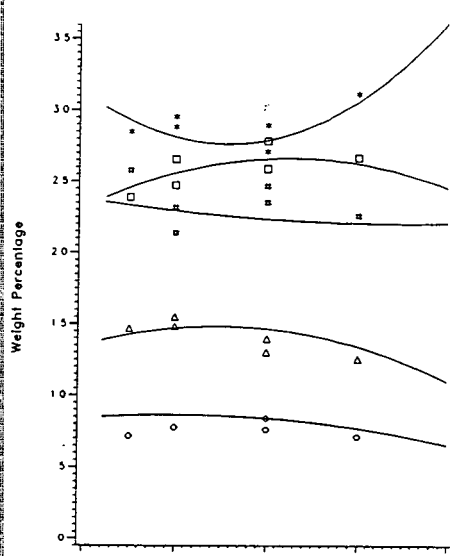


FIGURE 13 - CoMo Catalyst

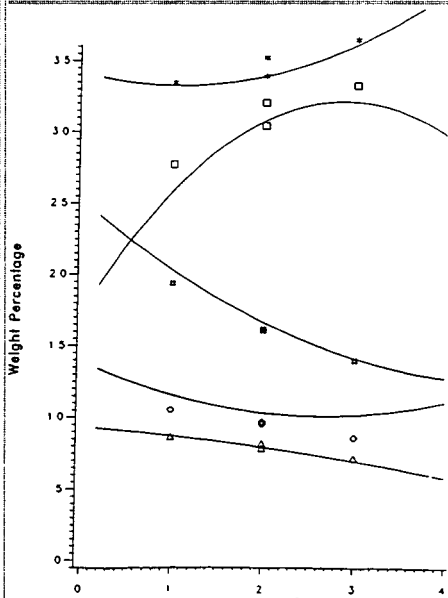


FIGURE 14 - NiMo Catalyst

Effects of Space Velocity,
hr⁻¹, on Hydroprocessing -
8720 kPa, 673 K
Trickle-Bed Reactor Study

- Heavy Nonvolatiles
- Light Nonvolatiles
- Phenals
- △ Aromatics + Alkanes
- Cake + Water + Outlet Gases
- Model Predictions

CHEMICAL AND STOCHASTIC MODELING OF LIGNIN HYDRODEOXYGENATION

Peter M. Train and Michael T. Klein

Center for Catalytic Science and Technology
and
Department of Chemical Engineering
University of Delaware
Newark, DE 19716

Abstract

An *a priori* Monte Carlo simulation of the product spectrum resulting from the thermal and catalytic depolymerization of lignin has been developed. The simulation combines model compound reaction pathways and kinetics, deactivation parameters, and stochastic models of polymer diffusion into a Markov-chain based simulation of the reaction of lignin polymers. Predicted product class ratios of single-ring phenolics were in reasonable agreement with experimental data pertaining to lignin liquefaction, especially as regards neat pyrolysis. The advantage of catalytic liquefaction was suggested by the increase in single-ring product yields, especially those of phenols and hydrocarbons, relative to pyrolysis.

Introduction

The intensity of research in the U. S. and abroad into the liquefaction of coal has largely been directed toward reduction of the demands on petroleum feedstocks. Both traditional fossil fuel feedstocks and alternative feeds are rich in sulfur and nitrogen, and removal of these heteroatoms has therefore been studied in detail. Oxygen removal is less well studied although large quantities of oxygen are found in biomass and coals. Herein we focus attention on the former feed.

Wood comprises cellulose, hemicellulose and lignin portions, with proportions of the latter typically one-third by weight. The potential for upgrading lignin to useful chemicals or fuel additives has been demonstrated [5]. Moreover, the structural elements of lignin are well enough understood to make it an attractive substrate for study. The study of lignin thus provides an opportunity for generalization about the reactions of lignites and low-rank coals that share similar structural features.

Lignin pyrolysis is to rather low yields of useful single-ring phenolics (10-15%), and as many as 33 different phenolics form, each in low yield, rather than any one in a usefully high yield [1,3,7,8,9,10]. Much of the original lignin weight is lost to a high molecular weight char, suggested by model compound experiments to form via a polymerization of ortho oxygen-containing guaiacyl moieties characteristic of lignin [11]. Petrocelli [16] has suggested that the catalytic hydrodeoxygenation (HDO) of lignin should reduce char formation by removing some of the guaiacyl oxygen as water and thus circumventing the polymerization to char; the single-ring phenolic fraction is also substantially simplified as a result.

This motivated the development of a model compound based and thus predictive computer simulation of lignin liquefaction. This would allow scrutiny of the feasibility of various lignin upgrading schemes by testing various processing strategies in a quantitative link of the competing factors of reaction, diffusion, catalyst deactivation, substituent effects and multiple bond identities.

A stochastic model of depolymerization has several advantages over deterministic models. First, substrate heterogeneities, including substituent effects, multiple linkage types, and an unusual molecular weight distribution are easily addressed in a stochastic model. Second, a Monte Carlo model can account for the molecular weight of each reactive moiety separately, which facilitates proper modeling of the diffusion and reaction in a porous catalyst. Thus, the classic approximation of equal reactivity need not be invoked. Finally, the processes involved in chemical kinetics may well be stochastic, so it seems reasonable to model them as such.

Background and Model Development

Stochastic Kinetics

The stochastic approach to chemical kinetics is well known [14] and has been applied by McDermott [13] and Squire [19] to model the decomposition of a simplified lignin polymer and coal, respectively. In one approach, the stochastic simulation of the polymer decomposition begins by dividing the total reaction time into small time steps of equal duration, after the passage of which the reactions of the polymer bonds are tested by comparing a characteristic reaction probability to a random number. Reaction occurs when this transition probability is greater than the drawn random number. In this manner, each bond along the polymer chain is tested for reaction, and the procedure is repeated through time in increments of Δt until the desired final time is reached. This process is equivalent to mapping out a first-order Markov chain through time, as illustrated in Figure 1, where the new physical state of the system depends solely on the previous state of the polymer. The Monte Carlo simulation is the average result of a large number of Markov chains.

The transition probability for the first-order reaction of A to B follows the Poisson distribution and has the general form shown in Equation 1:

$$P_{AB} = 1 - e^{-k_{AB}\Delta t} \quad (1)$$

Thus both the size of the time step and the overall rate constant dictate the likelihood of reaction. For the present model of the catalytic liquefaction of lignin, the appropriate k_{AB} for a given moiety included factors for diffusion limitations and catalyst age. Thus, the transition probability for each reactive moiety in lignin had a catalytic and thermal component, as in Equation 2:

$$P = 1 - e^{-(\eta\Phi w_c k_c + k_t)\Delta t} \quad (2)$$

where η = catalytic effectiveness factor; Φ = catalyst activity; k_c = intrinsic catalytic reaction rate constant, $1/\text{g}_c\text{-s}$; w_c = catalyst bed loading, g_c/l ; Δt = reaction time step, s; k_t = intrinsic thermal reaction rate constant, s^{-1} .

Lignin Structure

The lignin reactant was assembled randomly. This was accomplished by transferring the detailed information contained in chemical models for lignin structure [4,18] into probabilities of substituent and bond types present on each position of an average aromatic ring as illustrated in Figure 2. Four ring positions were required to define a lignin ring, and two of these identified as P1 and P2 contained primarily oxygen-bearing substituents and linkages, whereas the other two identified as H1 and H2 contained hydrocarbon substituents. Coupling this substituent distribution information with the details of the initial distribution of lignin molecular weights allowed random generation of linear lignin polymers of appropriate lengths.

In practice, a drawn random number was placed onto the integral probability distribution of substituent and linkage types at each of the four ring positions. This assembly determined each substituent and linkage type along a lignin polymer chain whose length was determined by placing a drawn random number on the integral molecular weight probability distribution. Repetition according to the Monte Carlo technique allowed generation of an appropriate starting lignin.

Lignin Reactions

The reaction pathways and intrinsic kinetics parameters were deduced from related model compound experiments reported elsewhere [6,8,11,12,13,15,16,20]. The operative reaction pathways and kinetics parameters elucidated are summarized in Table 1.

Catalyst Deactivation

Model compound reactions in a flow microreactor allowed observation of the decay of catalyst activity with time on stream. This is illustrated in Figure 3 for the reaction of 2-hydroxydiphenylmethane at 2250 psig H_2 , 250°C and $WHSV=0.49 \text{ hr}^{-1}$ [20]. Best fit models relating the observed activity losses to the quantity of oxygen-containing species lost (C_c) to char were of the form

$$\Phi = e^{-\alpha C_c} \quad (3)$$

and

$$\Phi = \frac{1}{1 + \alpha C_c} \quad (4)$$

and associated deactivation parameters (α) are listed in Table 1.

Catalyst Effectiveness

The parallel events of diffusion and reaction of lignin oligomers in catalyst pores were modeled in terms of a catalyst effectiveness factor, which was a function of oligomer molecular weight and degree of polymerization (DP) as follows:

$$\eta = \frac{1}{\phi} \frac{3\phi \coth 3\phi - 1}{3\phi} \quad (5)$$

$$\phi = f(k_c, DP) \quad (6)$$

For relatively short lignin polymers ($DP < 200$), Rouse's model for coiling polymers in dilute solutions [17] dictated that the Thiele modulus ϕ be proportional to the square-root of DP. The diffusion of longer polymer chains ($DP > 200$) was modeled using de Gennes reptation theory, in which diffusion is inversely proportional to the square of molecular weight [2]. Under these conditions, and the Thiele modulus was proportional to DP.

Integration

Equations 3, 4 and 5 and the intrinsic model compound kinetics of Table 1 were integrated into a stochastic model of lignin depolymerization in terms of the transition probabilities of Equation 2. The resulting simulation was capable of predicting the product spectrum resulting from the thermal or catalytic depolymerization of kraft and milled-wood lignin.

Results and Discussion

Simulations of kraft lignin pyrolysis and catalytic liquefaction were at 380 and 400°C. The predicted product yields from catalytic liquefaction of kraft lignin at 380°C, 2250 psig and 2.47 g_{lignin}/g_c in a batch reactor (case 1) illustrated in Figure 4 increase with time to 0.23 and 0.17 for single-ring products and char, respectively after 30 min.

Figure 4 also illustrates the effects of catalyst deactivation and internal transport. Simulations run in which both were either included or neglected provided limiting cases. Intrinsic kinetics resulted in the highest yields of single-ring products and the lowest yield of char, whereas allowing for catalyst deactivation and diffusional limitations resulted in the lowest single-ring product yield and highest char yield.

The effects of polymer diffusion and catalyst deactivation were also considered separately. The remaining curves of Figure 4 illustrate. The diffusional limitation was largest initially, where polymer molecular weight was high, as both single-ring products and char evolved at lower rates initially than in the limiting case of no internal transport limitations. Moreover, inspection of the yields of these products after 30 min shows that transport had little effect on the ultimate evolution of single-ring products and char. Finally, the remaining curve in Figure 4 illustrates that the effect of catalyst deactivation was largest at longer reaction times, and lower ultimate yields of single-ring products were accompanied by greater quantities of char.

The more rapid catalytic liquefaction relative to thermal depolymerization is illustrated in Figure 5 as a plot of the number molecular weight distribution parametric in reaction time. For catalytic depolymerization, a 15% yield of single-ring products was realized after only 10 min at which time the thermal yield of single-ring products was only 4%.

The temporal variation of monomer and char yield for pyrolysis and catalysis are illustrated in Figure 6 along with a measure of the selectivity to char over single-ring products. The yields of single-ring products were greatly increased upon reaction over a catalyst compared to thermal treatment alone, and char formation was decreased by roughly half. This agrees with the experimental findings of Petrocelli [16] and Train [20] that single-ring product yields were roughly doubled compared with pyrolysis. Moreover, the selectivity to char decreased rapidly to roughly 0.5 with catalytic treatment compared with the steady increase predicted with pyrolysis.

The identities of the major products in the single-ring product fraction are shown in Figure 7 as a plot of product yield versus reaction time. Whereas products containing two oxygen substituents (guaiacols and catechols) accounted for nearly half of the monomeric products evolved from pyrolysis, yields of these products were only 5% of the single-ring products formed by catalytic liquefaction. As a result, yields of both phenols and hydrocarbons increased substantially with catalytic treatment.

Finally, the simulation predictions are compared with experimental kraft lignin pyrolysis [8,9] and catalytic liquefaction [20] results in terms of the products of the monomer fraction in Figure 8. The agreement between simulated and experimental kraft lignin pyrolysis at 400°C is quite favorable. The agreement between simulated and experimental catalytic liquefaction at 380°C is still qualitatively good but quantitatively poorer.

Conclusions

The Monte Carlo simulation is a convenient and flexible tool for predicting the depolymerization of macromolecular substrates. Not only intrinsic kinetics but also catalyst deactivation and diffusional limitations can be addressed. The simulation predictions herein were in good qualitative agreement with experimental results, and agreement between predicted and experimental proportions of hydrocarbons, phenols, guaiacols and catechols in the monomer fraction was excellent. The practical significance is the prediction that removal of at least one of the oxygen-containing substituents from phenolic rings by catalytic HDO should reduce char formation and simplify the resulting phenolic product spectrum.

References

- [1] Chan, R. W.-C.; Krieger, B. B. *Journal of Applied Polymer Science* 26, 1981.
- [2] de Gennes, P. G. *Journal of Chemical Physics* 55(2), 1971.
- [3] Domburg, G. E.; Sergeeva, V. N.; Kalninh, A. I. *Thermal Analysis - Proceedings Third ICTA, Davos* 3, 1971.
- [4] Freudenberg, K.; Neish, A. C. Springer-Verlag, New York, 1968.
- [5] Goheen, D. W. *Adv. Chem. Ser.* 59, 1966.
- [6] Hurff S. J.; Klein, M. T. *Ind. Eng. Chem. Fundamentals* 22, 1983.
- [7] Iatridis, B.; Gavalas, G. R. *Ind. Eng. Chem. Prod. Res. Dev.* 18(2), 1979.
- [8] Jegers, H. E. Master's thesis, University of Delaware, 1982.
- [9] Jegers, H. E.; Klein, M. T. *Ind. Eng. Chem. Process Des. Dev.* 24, 1985.
- [10] Kirshbaum, I. Z.; Domburg, G. E.; Sergeeva, V. N. *Khim. Drev.* (4), 1976.
- [11] Klein, M. T. PhD thesis, Massachusetts Institute of Technology, 1981.
- [12] Klein, M. T.; Virk, P. S. *Ind. Eng. Chem. Fundamentals* 22, 1983.
- [13] McDermott, J. B. PhD thesis, University of Delaware, 1986.
- [14] McQuarrie, D. A. Methuen & Co. LTD, London, 1967.
- [15] Petrocelli, F. P.; Klein, M. T. *Macromolecules* 17, 1984.
- [16] Petrocelli, F. P. PhD thesis, University of Delaware, 1985.
- [17] Rouse, P. E. *Journal of Chemical Physics* 21(7), 1953.
- [18] Sarkanen, K. V.; Ludwig, C. H. (editors). Wiley, New York, 1971.
- [19] Squire, K. R.; Solomon, P. R.; Di Taranto, M. B.; Carangelo, R. M. *ACS Division of Fuel Chemistry Preprints* 30(1), 1985.
- [20] Train, P. M. PhD thesis, University of Delaware, 1986.

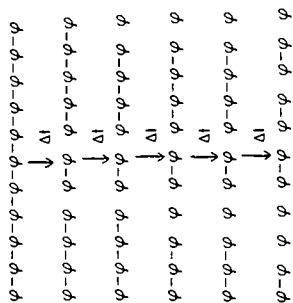


Figure 1: Random reaction trajectory of a polymer chain.

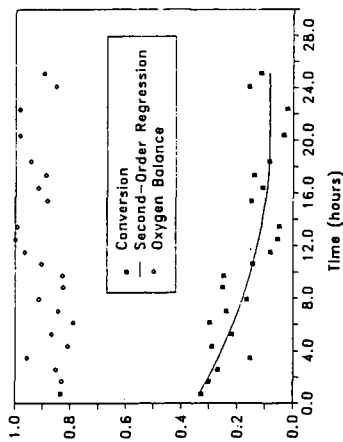


Figure 3: Catalyst deactivation in the reaction of 2-hydroxyphenylmethane over Co-AlO_x at 250°C, 2200 pmg, WHSV=0.49 hr⁻¹

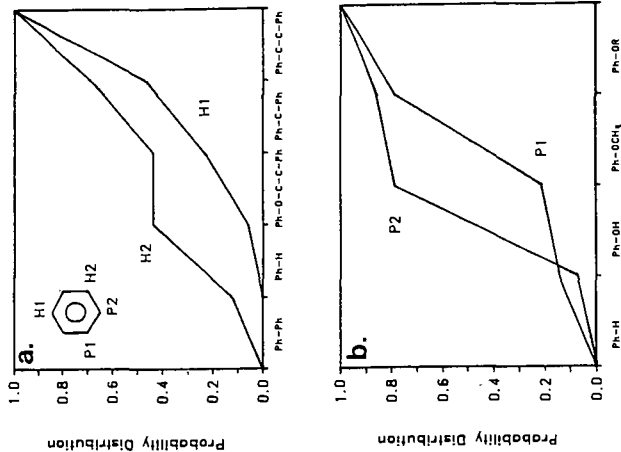


Figure 2: Cumulative probability distributions function for substitutions on aromatic ring positions (a) H1, H2 and (b) P1, P2.

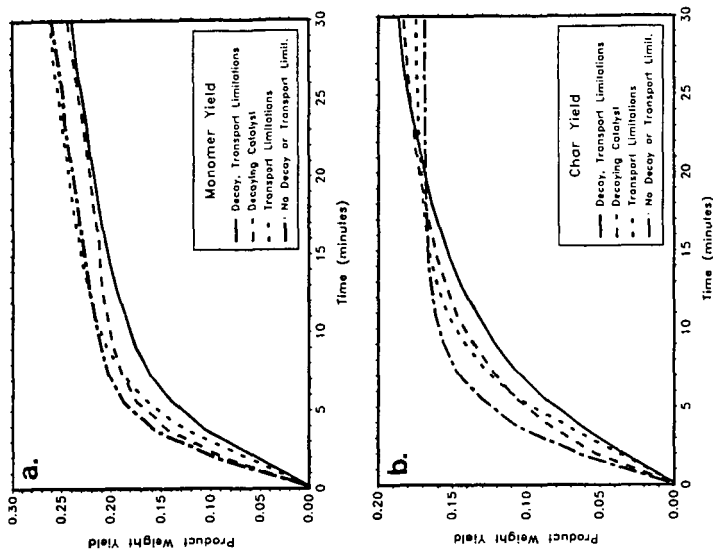


Figure 4: Effects of catalyst deactivation and transport limitations on lignin depolymerization (case 1). (a) monomer yield (b) char yield.

Reaction	Primary Products	$\log_{10} k^A$ (sec/mol)	Thermal St. Source	$\log_{10} k^A$ (sec/mol)	Catalytic Parameters (1/gc-h)	Source
Veratrols	Guaiacol	11.4	48	4.8	21.7	[28]
	Phenol	10.6	47.4	4.8	21.7	[28]
Guaiacol	Catechol	12.8	48.3	5.2	22.1	[16]
	Char	11.8	45.2	11.8	19.8	[16]
	Phenol	11.8	45.2	11.8	19.8	[16]
Catechol	Char	4.9	25.2	5.5	28.3	[16]
	Phenol	4.9	25.2	5.5	28.3	[16]
Anisols	Phenol	9.1	42.2	9.9	29.7	[16]
	Benzenes	17.2	68.7	9.9	29.7	[16]
Phenol	Benzenes	-1.9	6.7	-1.9	6.7	[16]
Diphenylmethane	Toluenes/Benzenes	12.7	68.6	2.9	21.6	[28]
OHO	Phenols/Toluenes	9.6	43.4	9.2	36.1	[16]
	o-Cresols/Benzenes	9.6	43.4	7.8	35.2	[16]
Diphenylmethane	2-Toluenes	18.2	45.3			[16]
	Ethylbenzenes/Benzenes	8.6	44.3			[16]
2-Phenylphenol	Phenols/Benzenes	x	x	-2	8.2	[16]
	2-Phenol	x	x			
PPE	o,o'-Biphenol	11.1	65.9			[12]
	Phenols/Ethylbenzenes	5	26.8			[12]
GCE	Guaiacols/AV	14.6	72.1			[11]
	Phenols/Benzenes	14.6	72.1	8.7	35.4	[16]
4-Phenylphenol	2-Phenol	8.7	32.2	8.7	32.2	[28]
	Phenols/Benzenes	8.7	32.2	8.7	32.2	[28]

OHO = 2-hydroxyphenylmethane
 PPE = 2,2-bis(4-phenylphenoxy)propane
 GCE = Guaiacol/ethylene glycol
 AV = Acrylonitrile
 AV = Acrylonitrile

Deactivation Parameters [28]	Free of Activity Function
Single-ring Phenolics	Equation 4
Cerane Linkages	Equation 3
Ether Linkages	Equation 3

Table 1: Summary of model compound kinetics and reaction pathways.

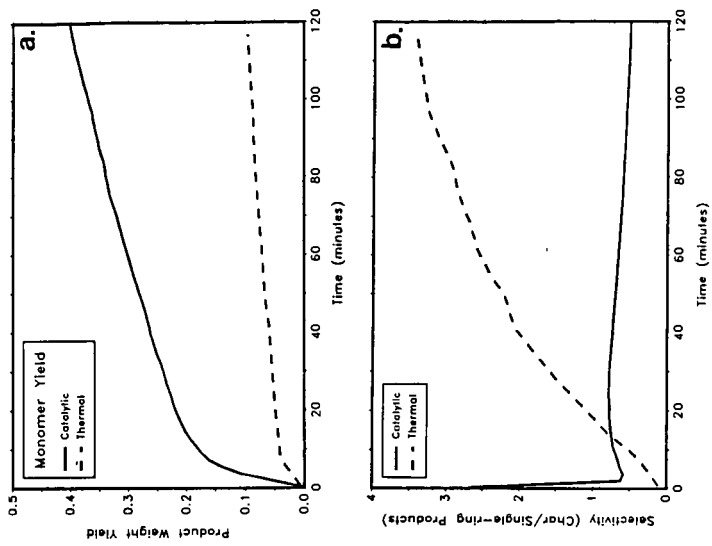


Figure 6: Comparison of thermal and catalytic liquefaction strategies. (a) monomer yield (b) selectivity (char/monomer)

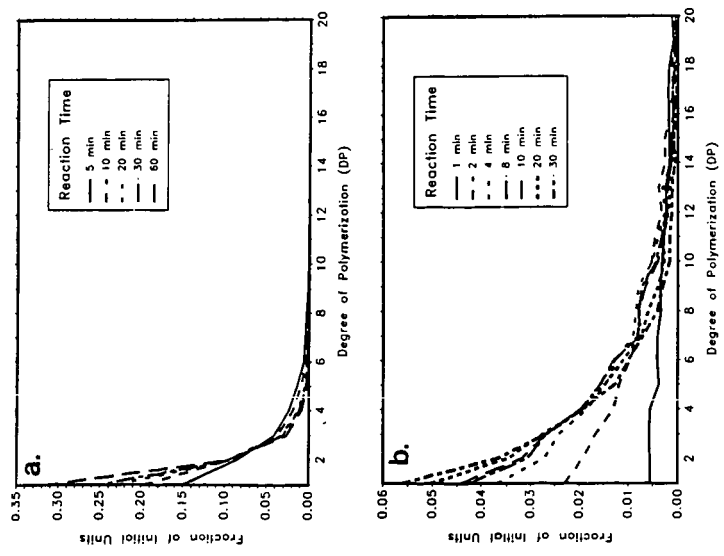


Figure 6: Temporal variation of the molecular weight distribution of a reacting lignin polymer. (a) catalytic (b) thermal

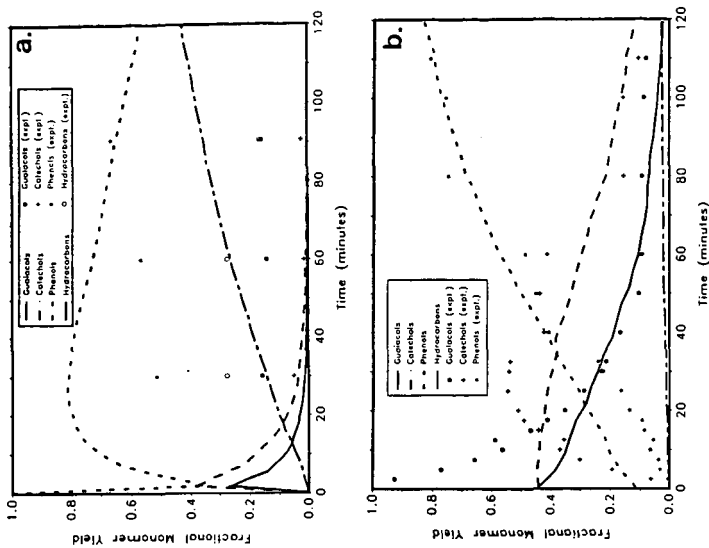


Figure 8: Comparison between simulation and experimental results. (a) catalytic (b) thermal

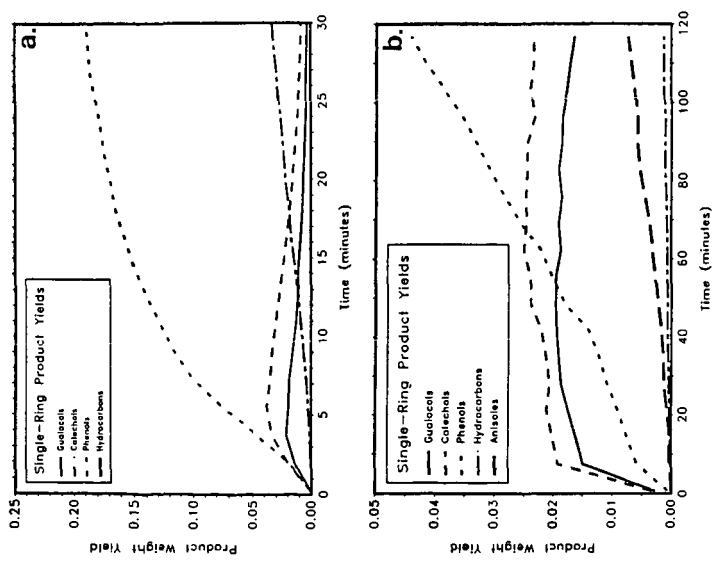


Figure 7: Comparison of single-ring product classes produced by thermal and catalytic liquefaction strategies. (a) thermal (b) thermal

Catalytic Hydrodeoxygenation and Dealkylation of a Lignin Model Compound

Matthew Ratcliff, Fannie Posey, and Helena Li Chum*,

Chemical Conversion Research Branch
Solar Energy Research Institute
1617 Cole Blvd., Golden, Colorado 80401

ABSTRACT

A comparison is presented of the hydrotreatment of 4-propylguaiacol (4PG) exploring two catalysts: MoS₂ on γ -alumina and the dual functionality MoS₂/NiS on phosphated γ -alumina at 250°-450°C and 500 psig of hydrogen. The catalyst with acidic support was found to promote substantial dealkylation of 4PG into a number of alkylated phenols such as methyl- (predominantly meta- and para-), ethyl-, and methylpropylphenols. The main reaction product on the less acidic catalyst was 4-propylphenol. At 350°C, mild deoxygenation to phenols can be maximized, whereas higher temperatures favor the formation of hydrocarbons, aromatic and saturated. Higher space velocities also favor mild deoxygenation to phenols. These studies are relevant to the conversion of lignins into phenolic compounds. Transformation of phenols into methyl aryl ethers produces a suitable gasoline octane enhancer and extender.

INTRODUCTION

In the production of liquid fuels from lignocellulosic materials, the carbohydrate components can be converted into ethanol fuels in fermentation processes. However, the lignin fraction, composed of phenylpropane units, is not amenable to such a conversion, but can be transformed into phenolic compounds and hydrocarbons. The phenolic fraction, when converted into methyl aryl ethers, can be blended with gasoline, together with the hydrocarbon (primarily the aromatics) fraction. Singerman (1) demonstrated that methyl aryl ethers produced from coal liquids are fully compatible with gasoline to replace or supplement the aromatic components (e.g., benzene, toluene, xylenes). The most desirable phenols for conversion into methyl aryl ethers are phenol, cresols, and xylenols because the resultant ethers have high octane numbers and their boiling points fall within the range of gasoline. We are investigating the conversion of lignins into phenols and hydrocarbons (2) by mild hydrodeoxygenation (HDO) routes.

The approach taken is based on coal and petroleum hydrotreating processes as well as early work in the field of hydrodeoxygenation (HDO) of lignins (refs. 3-7), that has recently been reviewed (8). MoS₂ on γ -alumina catalyst was considered the best for the hydrocracking stage of the Hydrocarbon Research Institute's Lignol Process (9), in which hydrotreating was followed by thermal dealkylation for the production of phenol and benzene. An optimal catalyst for the conversion of lignins into phenols would possess the following characteristics: high conversion at modest temperatures to minimize char formation from lignin, high selectivity to phenols to prevent higher hydrogen consumption that accompanies hydrocarbon formation, dealkylation capability for side chain removal or rearrangement, tolerance to water formation, durability, and reasonable cost.

In order to select the best catalysts, well-defined lignin model compounds (e.g., 4-propylguaiacol, or 2-methoxy,4-propylphenol) containing representative functionalities have been employed. The aim is two-fold: mild deoxygenation into 4-propylphenol and partial dealkylation into methyl-, and ethyl-phenols. A commercial

catalyst and a custom-synthesized heterogeneous catalyst (10) have been screened for their HDO and dealkylation activities. The results reported here are preliminary but illustrate the utility of bi-functional HDO catalysts in lignin-model compound hydrodeoxygenation.

EXPERIMENTAL

Equipment. A trickle-bed reactor was constructed from 1/2-in. OD 316 stainless steel (SS) tubing with a 0.035-in. wall thickness and Swagelok tube fittings. The catalyst bed was supported by a 90 micron SS frit which in turn was supported by a 1/16-in. K type thermocouple. The thermocouple entered the reactor from the bottom through a Tee fitting (see Fig. 1). The reactor was suspended vertically in a Lindberg oven (Model 55035). The outlet lines were heat taped and nominally maintained at 160°C between the reactor and the high-pressure condenser. The condenser was constructed from a Whitey 150 mL SS sample cylinder to which copper tubing was silver soldered. During operation, the condenser was maintained at -5°C. The pressure letdown valve was a Whitey SS-22RS-4. A second condenser made from a 3-oz Fisher-Porter bottle was installed downstream of the letdown valve and was immersed in a Dewar filled with isopropanol/dry ice. The rest of the gas handling train consisted of a gas sampling port, Matheson rotameters for flow measurement, and a heavy walled flask containing saturated KOH for scrubbing H₂S before venting to the exhaust system. The parallel gas train which splits at the three-way ball valve, upstream of the letdown valve, allowed continuous operation during liquid sampling from the condenser (Fig. 1). The feed mixture was injected into the reactor by a calibrated Isco model LC-5000 high-pressure syringe pump. Hydrogen was supplied from a high-pressure cylinder with a regulator.

The trickle-bed reactor currently in use has been modified to improve mass balance and ensured adequate catalyst particle wetting and minimized liquid channeling. Thicker wall tubing has been employed in the reactor, and VCR glands were welded to both ends, adapted to a pipe threaded Conax fitting at the top and a 1/2 in. to 1/4 in. Swagelok reducer at the bottom. Directly below the reactor is a high-pressure condenser constructed from a Whitey SS sample cylinder of 150 mL volume. During operation the condenser is maintained at -5°C.

Materials. The catalysts used include MoO₃/γ-Al₂O₃ supplied by Strem Chemicals (#42-1500). The MoO₃ content was 10%-12%, and the surface area was 64 m²/g in the form of 3/16 in. x 1/8 in. pellets. The pellets were ground with a mortar and pestle and sieved to 20-14 mesh before loading into the reactor. NiO/MoO₃ on phosphoric acid co-precipitated γ-alumina was supplied by M. Maholland and S. Cowley at the Colorado School of Mines. Their detailed preparation and properties are described elsewhere (10). The Ni and Mo contents of the catalyst were 3% and 11.7%, respectively. The P:Al atomic ratio was 0.5, surface area was 8.2 m²/g, and the average pore diameter was 210 Å. The catalysts were presulfided in-situ by injecting a solution of 5 vol % methyldisulfide in hexane in the presence of hydrogen at 100 psig. The liquid and gas flow rates were calibrated to maintain approximately 10 vol % H₂S in hydrogen. The presulfiding was performed at 200°C for two hours then 400°C for an additional two hours.

Research grade hydrogen (99.999%) was used as supplied. 4PG was used without further purification as supplied by Frinton Laboratories (#1035). The feed mixture was 75 vol % 4PG in research grade hexanes with 0.25 vol % methyldisulfide (Aldrich #15,031-2) to maintain catalyst sulfidation. Burdick and Jackson UV-grade acetonitrile was used as supplied to dilute the liquid samples prior to analysis.

Analysis. The liquid samples (generally 0.75-1 g) were diluted to 100 mL in acetonitrile.

Water Determination:

The diluted samples were mixed 1:1 with an internal standard solution of absolute methanol in acetonitrile. The separation and quantitation of water was performed on a Varian 3700 gas chromatograph equipped with an autosampler, integrator, and a glass column 6 ft x 0.2 mm ID packed with Porapak QS. The carrier gas was high-purity helium.

Hydrocarbons and Phenolics Determination:

The individual reaction products were identified on a Hewlett Packard Model 5985 GC/MS. Each identification was checked by search and comparison with computer library spectra and by comparison with mass spectra generated from known standards for most of the compounds. The components were also identified by their retention times and were quantified on the Varian 3700 using a Supelco SPB5 wide bore capillary column, 30 m x 0.75 mm ID, 1- μ film. The column temperature was programmed starting at 40°C, held for two minutes then increased at a rate of 3 degrees/minute to 280°C. The injector and flame ionization detector temperatures were 220°C and 280°C, respectively. Helium carrier gas was used at 12 mL/min.

Gas Analysis:

Gas samples were analyzed on a Carle Model 111H gas chromatograph equipped with two thermal conductivity detectors, one for H₂ and the other for light hydrocarbons. After sample injection, hydrogen was separated by a Pd diffusion tube at 600°C and then a 5 ft x 1/8 in. Porapak Q (80/100) column using N₂ as the carrier gas. The remaining gases were separated on a series of three columns: (1) 6 ft x 1/8 in. Molecular Sieves, (2) 2.5 ft x 1/8 in. Squalane, and (3) 12 ft x 1/8 in. n-octane Poracil C using He as the carrier gas. The columns were accessed sequentially by automatic valves which are controlled by a Hewlett Packard 3388A integrator.

Operating Procedure. The reactor was operated in the integral mode for catalyst screening. The reactor was loaded with 1-1.5 g of catalyst which was presulfided as described above. A typical experiment was performed as follows. The chilled water circulator, oven, and heating tape were switched on and set to the desired temperatures. The hydrogen pressure regulator was used to pressurize the system to 500 psig. The syringe pump was loaded with the feed mixture and calibrated to the desired flow rate. Once all the temperatures had stabilized, the syringe pump was switched to inject the feed into the reactor and the hydrogen flow rate adjusted with the letdown valve to give the desired rate of 900 mL H₂/mL 4PG (equivalent to a typical petroleum hydrotreating rate of 5000 SCF/bbl). The system was allowed to equilibrate for one hour before sampling began. Liquid samples were obtained by switching to the parallel gas train, thereby isolating the condenser which was then depressurized. Samples were removed with a syringe through a septum at the bottom of the condenser. One gas sample was obtained toward the end of each run by switching to the parallel gas train, attaching an evacuated SS sample cylinder to the sampling port, and opening the letdown valve slightly to fill the cylinder.

Results and Discussion

4-Propylguaiaicol has been hydrotreated under a variety of conditions using MoS₂/ γ -Al₂O₃ and NiS-MoS₂/P: γ -Al₂O₃ catalysts in the temperature range of 250-450°C, at two molar hourly space velocities (MHSV 0.007 and 0.017 moles 4PG/g cat.*h which correspond to WHSV = 1.17 and 2.82 g 4PG/g cat.*h, respectively). Based on early

experiments to determine the effect of hydrogen pressure on the reaction, we found that decreasing the pressure from 1000 psig to 500 psig increased the selectivity of propylphenol formation 89% with no significant effect on the overall conversion using the MoS₂ catalyst. Therefore, all experiments reported here were performed at 500 psig.

The major phenolic product from the MoS₂/γ-Al₂O₃ catalyst was 4-propylphenol having a maximum selectivity of 47% at 350°C and MHSV = 0.007 (see Table 1). At higher temperatures, hydrocarbon products such as propylbenzene, methylpropylbenzenes and propylcyclohexane are predominant. No reaction conditions studied so far with this catalyst have given significant yields of dealkylated products. This result is not surprising given that γ-Al₂O₃ is not a very acidic support.

Table 1. Selectivities of Major Products on MoS₂/γ-Al₂O₃

Temp. (°C)	Conversion (%)	Propylphenols (%)	Propylbenzenes (%)	Propylcyclohexane (%)
250	38	7.3	2.9	0
300	36	35.7	8.7	0
350	82	48.5	8.5	1.3
400	95	11.1	14.6	4.0
450	99	5.9	25.5	5.5

All reactions run at 500 psig, MHSV = 0.007 moles 4PG/g cat.*h. Conversion = (moles 4PG_{in} - moles 4PG_{out})/moles 4PG_{in} * 100. Selectivity = moles product/moles 4PG converted * 100.

The product slate obtained from 4PG on the NiS-MoS₂/P:γ-Al₂O₃ catalyst is notably different from that of the MoS₂/γ-Al₂O₃ catalyst. 4-Propylphenol remained the major product up to 350°C; however, significant dealkylation to phenol, cresols, and ethylphenols occurred (see Table 2). Figures 2 and 3 compare the selectivities of dealkylated phenolics from the two catalysts used. The more acidic catalyst support gave higher yields of dealkylated phenols at 300°C than the neutral support did at 450°C (6% vs. 3.5%, compare experiments 11 and 16 in Figures 3 and 2, respectively). This selectivity toward dealkylated phenols increased by a factor of 5 at 350°C (compare experiments 15 and 16). Interestingly, GC/MS data suggests that the major cresols formed are meta- and para-cresol having a selectivity as high as 15.5% at T = 400°-450°C and MHSV = 0.017 moles 4PG/g cat.*h. Again, at higher temperatures the yields of phenols decrease at the expense of hydrocarbon production. This product shift can be offset by increasing the space velocity as demonstrated in Figure 4. At 450°C and MHSV = 0.017, the selectivity to phenols is about 4 times the selectivity at MHSV = 0.007 (compare experiments 19 and 20 in Figure 4).

The gas analyses from the NiS/MoS₂ on phosphated γ-alumina catalyzed reactions support the evidence from the liquid analyses that the more acidic catalyst increases side chain cracking. At 400°C only 0.2 mole % of propane was detected in the gas from the Mo/γ-Al₂O₃ catalyst, whereas using the more acidic catalyst support, 0.5 mole % of propane was formed plus from 0.1 to 0.5 mole % propene depending on the reaction temperature and space velocity. Water formation increased with increasing reaction temperature and followed the decrease in phenols selectivity above 350°C because of hydrocarbon formation.

Table 2. Selectivities of Major Products on NiS-MoS₂/P:γ-Al₂O₃

Temp. (°C)	Conversion (%)	Propylphenols (%)	Ethylphenols (%)	Cresols (%)	Phenol (%)
300	53	32.2	1.8	4.0	0
350	63	48.1	9.8	16.2	4.4
400	96	4.4	5.6	13.3	7.0
450	100	0.7	1.7	4.4	4.4

All reactions run at 500 psig, MHSV = 0.007-moles 4PG/g cat.*h. Conversion and selectivity as defined in Table 1.

The results reported here, while preliminary, demonstrate the direction of our research efforts to test systematically, well characterized catalysts and develop, with researchers at the Colorado School of Mines, bi-functional catalysts for lignin hydrotreating. The data show that increasing the acidity of the catalyst support significantly increases the selectivity to dealkylated products. Additional catalysts with controlled acidity are under investigation to confirm the product trends described above. Complementing the model compound study, lignin investigations using a 300 mL stirred Autoclave Engineers high-pressure reaction vessel, operated in the semicontinuous mode are underway (11).

ACKNOWLEDGEMENTS - This work is supported by the Biofuels and Municipal Waste Technology Division of the U.S. Department of Energy under the Biochemical Conversion/Alcohol Fuels program (FTP 616). The authors acknowledge profitable discussions with Professor S. Cowley and Mr. M. Maholland, as well as the preparation and characterization of the dual functionality catalyst employed in this work.

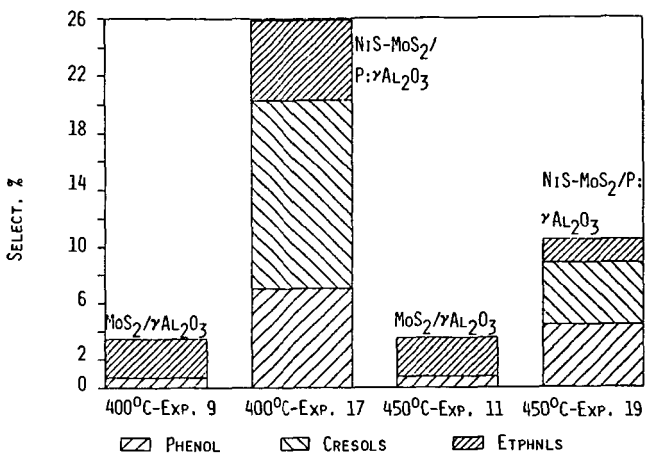


FIGURE 3. COMPARISON OF DEALKYLATED PHENOLS FROM 4-PROPYLGUIAIACOL HYDRO-TREATED ON $\text{MoS}_2/\gamma\text{Al}_2\text{O}_3$ AND $\text{NiS-MoS}_2/\text{PHOSPHATED-}\gamma\text{Al}_2\text{O}_3$, $\text{MHSV} = 0.007$ MOLES $4\text{PG}/\text{G CAT.}\cdot\text{H}$.

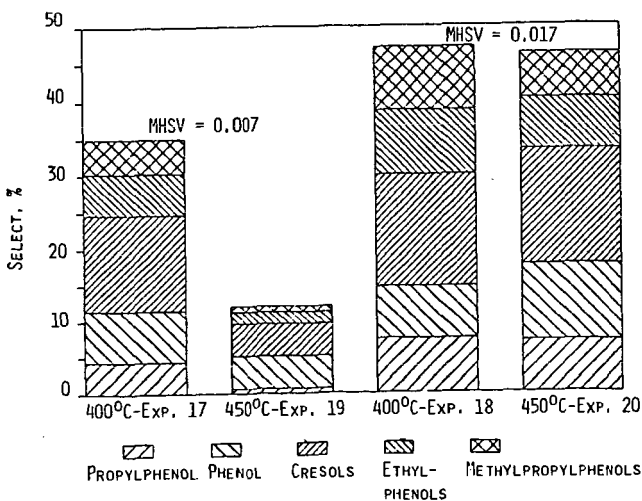


FIGURE 4. EFFECT OF SPACE VELOCITY AND TEMPERATURE ON THE SELECTIVITY OF PHENOLS FROM 4-PROPYLGUIAIACOL HYDROTREATED ON $\text{NiS-MoS}_2/\text{PHOSPHATED-}\gamma\text{Al}_2\text{O}_3$, $\text{MHSV} = \text{MOLES } 4\text{PG}/\text{G CAT.}\cdot\text{H}$.

CATALYTIC HYDROTREATING OF BIOMASS-DERIVED OILS

Eddie G. Baker and Douglas C. Elliott

Pacific Northwest Laboratory^(a)
Richland, WA 99352

INTRODUCTION

Pacific Northwest Laboratory (PNL) is investigating the catalytic upgrading of biomass-derived oils to liquid hydrocarbon fuels. Tests have been conducted in a 1-liter, continuous feed, fixed-bed catalytic reactor at 250-450°C and 2,000 psig. This is envisioned as the second stage in a two-stage process to produce hydrocarbon fuels from biomass. Given that biomass can be converted to a liquid product, widely reported as phenolic (1-4), then oxygen removal and molecular weight reduction are necessary to produce usable hydrocarbon fuels. Upgrading biomass derived oils differs from processing petroleum fractions or coal liquids because of the importance of deoxygenation. This topic has received only limited attention in the literature (5-9).

HYDROTREATING BIOMASS-DERIVED OILS

Two types of biomass-derived oils have been studied at PNL. The first type of oil is produced by high pressure liquefaction at relatively long residence times. Oils identified as TR7 and TR12 in Table 1 were produced by this type of process at the Albany, Oregon Biomass Liquefaction Experimental Facility. These highly viscous oils consist primarily of substituted phenols and naphthols. The other type of oil is produced by low pressure flash pyrolysis at somewhat higher temperature and very short residence times. These oils are highly oxygenated and contain a large fraction of dissolved water. Because of the soluble water these have a much lower viscosity. The flash pyrolysis oil produced at Georgia Tech is typical of this type of oil. The fourth oil shown in Table 1 was made at PNL by pretreating the Georgia Tech pyrolysis oil to produce an oil more similar to the high pressure oils. Details of the pretreating step are given by Elliott and Baker (10).

Figure 1 shows some model reactions that are typical of what is required to produce liquid hydrocarbon fuels from biomass-derived oils. The three compounds, 2-methyl-2-cyclopentene-one, 4-methyl guaiacol, and naphthol are typical components of biomass-derived oils. The single ring compounds are upgraded primarily by deoxygenation. Hydrogenation of the aromatic structure is not desirable if high octane gasoline is the intended product, but it may be necessary as part of the pathway to cracking multiple ring compounds. Previous studies showed CoMo, NiMo and in particular sulfided CoMo to be the most effective catalysts for this combination of reactions (6). The heavy fraction of biomass-derived oils is not as well characterized and the reaction mechanism for upgrading is unknown. Use of an acidic support (such as a zeolite) compared to alumina may be beneficial for upgrading the high molecular weight fraction.

(a) Operated for the U.S. Department of Energy by Battelle Memorial Institute under Contract DE-AC06-76RL0 1830.

TABLE 1. Feedstock Oils for Hydrotreating Tests

	TR7		TR12		Georgia Tech Pyrolysis Oil		Treated Georgia Tech Pyrolysis Oil	
	As Fed	Dry	As Fed	Dry	As Fed	Dry	As Fed	Dry
Elemental Analysis, wt %								
Carbon	74.8	77.5	72.6	76.5	39.5	55.8	61.6	71.6
Hydrogen	8.0	7.9	8.0	7.8	7.5	6.1	7.6	7.1
Oxygen	16.6	14.1	16.3	12.5	52.6	37.9	30.8	21.1
Nitrogen	< 0.1	< 0.1	< 0.1	< 0.1	< 0.1	< 0.1	< 0.1	< 0.1
Ash	0.5	0.5	3.0	3.0	0.2	0.3	0.0	0.0
Moisture	3.5	0.0	5.1	0.0	29.0	0.0	14.1	0.0
Density, g/ml @ 55°C	1.10	--	1.09	--	1.23	--	1.14 ^(a)	
Viscosity, cps, @ 60°C	3,000	--	17,000	--	10 ^(c)	--	14,200	
Carbon Residue, wt% ^(b)	13.5	13.9	26.9	28.3	--	27-31 ^(c)	--	

a) at 20°C

b) TGA simulated Conradson carbon, see reference 12

c) Viscosity and carbon residue were measured for other similar pyrolysis oils

EXPERIMENTAL

The reactor system used for this study is a nominal 1-liter, continuous feed, fixed-bed reactor operated in an upflow mode. It has been described in detail previously (10,11). Operation in the downflow mode (trickle-bed) plugged the outlet line of the reactor with coke-like material and tests in this mode were discontinued. The oil feedstock, preheated to 40-80°C, is pumped by a high-pressure metering pump. Hydrogen from a high-pressure cylinder is metered through a high-pressure rotameter into the oil feed line prior to entering the reactor vessel. The reactor is 7.5 cm I.D. by 25 cm and holds approximately 900 ml of catalyst.

A two phase flow pattern exists in the reactor. Gas and volatile products move through the reactor quite rapidly. Unconverted, non-volatile material does not leave the reactor until it reaches the top of the liquid level and overflows into the product line. Pressure in the system is maintained by a Grove back-pressure regulator. Liquid product is recovered in a condenser/separator and the offgas is metered and analyzed before it is vented.

Catalysts used in the most recent hydrotreating tests are shown in Table 2. The Harshaw catalysts are conventional extruded CoMo and NiMo hydrotreating catalysts. The Haldor Topsoe catalysts are a composite system using low activity rings in the bottom of the bed to prevent plugging from carbon and metals, and high activity extrudates in the top of the bed. The last two catalysts are specialty catalysts incorporating a zeolite in the base to provide more acidity and promote cracking reactions.

TABLE 2. Catalysts Used for Hydrotreating Tests

Supplier Catalyst ID	Harshaw		Haldor Topsoe ^(b)			PNL/ Union Carbide	Amoco
	HT-400	HT-500	TK-710	TK-750	TK-770	CoMo/Y	NiMo/Y
Active metals, wt%	3% CoO 15% MoO ₃	3.5% NiO 15.5% MoO ₃	2% CoO 6% MoO ₃	2.3% CoO 10% MoO ₃	3.4% CoO 14% MoO ₃	3.5% CoO 13.9% MoO ₃	3.5% NiO 18% MoO ₃ 2.5% P ₂ O ₅
Support	Al ₂ O ₃	Al ₂ O ₃	Al ₂ O ₃	Al ₂ O ₃	Al ₂ O ₃	Y-zeolite/ Al ₂ O ₃	Y-zeolite/ Al ₂ O ₃
Form ^(a)	1/8-in E	1/8-in E	3/16-in R	3/16-in R	1/16-in E	1/16-in E	1/16-in E

a) E - Extrudate, R- Rings, size given is O.D.

b) All three catalysts used in a layered bed

RESULTS AND DISCUSSION

The following discussion deals primarily with recent tests with TR12 oil and CoMo catalysts. Results of previous tests with other oils and catalysts will be summarized as they relate to the most recent efforts.

Tests with Cobalt-Moly Catalysts

Most of the test work has been done with the TR12 and TR7 oils and various sulfided CoMo catalysts. Table 3 shows results obtained with the TR12 oil and the Haldor Topsoe composite catalyst system at about 400°C, 2,000 psig and three different space velocities. Typically, the liquid product yield from the TR12 oil is about 0.9 l/l of oil fed. At the low space velocity (0.11) the oil is 96% deoxygenated and is about one-third high quality aromatic gasoline (C₅ - 225°C). At even lower space velocities (~0.05) a liquid product containing about 60% gasoline and almost no oxygen can be produced. At higher space velocities (up to 0.44) deoxygenation is still good, nearly

TABLE 3. Results of Hydrotreating TR12 Oil with Haldor Topsoe Composite Catalyst

Run No.	HT-34	HT-34	HT-34
Temperature, °C	397	395	403
Pressure, psig	2,020	2,015	2,030
Space Velocity, LHSV, hr ⁻¹	.11	.30	.44
Hydrogen Consumption, l/l oil fed	548	296	212
Product Yield, l/l oil fed	.92	.88	.94
Deoxygenation, wt%	96	87	79
Product Inspections			
Oxygen, wt%	0.8	2.5	3.8
H/C ratio, mole/mole	1.5	1.3	1.3
Density, kg/l	0.91	1.0	1.03
Yield C ₅ - 225°C, LV%	37	24	11

80%, but hydrogen consumption decreases 50% or more resulting in a lower H/C ratio, higher density, and lower gasoline yield. The theoretical hydrogen requirement to deoxygenate TR12 is about 200 l/l of oil. This indicates that at the low space velocity 350 l H₂/l oil is being used for hydrogenation, hydrocracking and other reactions. At the highest space velocity only about 50 l H₂/l oil is being used by these other reactions.

Table 4 shows results from hydrotreating TR7 with Harshaw CoMo/Al₂O₃ catalyst. Tests with the Harshaw catalyst and TR12 oil were similar to those with the Haldor Topsoe composite catalyst indicating the differences between Tables 3 and 4 are due primarily to the oil. At similar processing conditions, the products from TR7 are higher quality than those obtained from TR12. Analysis of TR7 and TR12 oils indicates TR7 is primarily single ring phenolics which when deoxygenated become gasoline boiling range aromatics. The TR12 oil is primarily double ring phenolics which require additional cracking and hydrogenation to produce light distillates.

When the Georgia Tech pyrolysis oil was hydrotreated with a sulfided CoMo catalyst at conditions similar to those used with TR7 and TR12 the runs had to be terminated due to severe coking in the bed. The temperature had to be reduced to 250^o-270^oC to prevent coking. The properties of the oil produced at these low temperatures are shown in Table 1 under the heading of treated Georgia Tech pyrolysis oil. This oil was further hydrotreated at 350^oC and 2,000 psig with a sulfided CoMo catalyst and the results were similar to those obtained with TR7 and TR12. This is the basis for a proposed two stage upgrading process for biomass pyrolysis oils (10).

Results to date indicate 400^oC is about the optimum temperature for hydrotreating biomass-derived oils. At 350^oC a much poorer quality oil is produced. At 450^oC the product quality improves somewhat compared to 400^oC but the yield is reduced due to increased gas production.

TABLE 4. Results of Hydrotreating TR7 Oil with Harshaw CoMo/Al₂O₃*

Run. No.	HT-15	HT-14	HT-14
Temperature, °C	398	394	389
Pressure, psig	2,003	2,021	2,026
Space Velocity, LHSV, hr ⁻¹	0.10	0.30	0.55
Hydrogen Consumption, l/l oil fed	616	435	202
Product Yield, l/l oil fed	0.99	1.0	0.88
Deoxygenation, wt%	~100	94	88
Product Inspections			
Oxygen	0.0	1.1	2.6
H/C ratio, mole/mole	1.65	1.41	1.32
Density, kg/l	0.84	0.91	0.96
Yield C ₅ -225 ^o C, LV%	>87	60	28

* adapted from reference 11

Other Catalysts

In early tests with the TR7 oil where gasoline boiling range material was the primary product, the CoMo catalysts were preferred over NiMo because they retained the aromatic character and antiknock properties of the product. The NiMo catalysts were more active for hydrogenation and produced primarily saturated cyclic compounds (naphthenics) with a lower octane rating. With the TR12 oil a more active hydrogenation catalyst such as NiMo may be beneficial. Adding a cracking component such as γ -zeolite to the catalyst may also be advantageous with the TR12 oil. Preliminary tests with a NiMoP/ γ -zeolite/ Al_2O_3 catalyst obtained from Amoco are promising in this regard.

Catalyst Deactivation

A 48-hour test run was recently completed with TR12 oil and the Haldor Topsoe catalyst to evaluate catalyst deactivation. Figure 2 shows the trend of deoxygenation and hydrogen consumption at an LHSV of 0.1. Hydrogen consumption and the H/C mole ratio (not shown) fell rapidly in the early stages of the test and then leveled off. Deoxygenation fell throughout the test.

Two causes of deactivation have been postulated. The initial deactivation is likely due to coking of the catalyst which we have shown in earlier tests occurs primarily in the first ten hours (11). The longer term deactivation is probably due to buildup of metals, primarily sodium, from the oil. The TR12 oil contains about 3% ash, mostly residual sodium catalyst from the liquefaction process.

CONCLUSIONS

A variety of biomass-derived oils have been upgraded by catalytic hydrotreating in a 1-liter reactor system. Specific conclusions from our studies are as follows:

- High yields of high quality gasoline (C_5 - 225°C boiling range) can be produced from biomass-derived oils, however, low space velocities (long residence times) are required. At high space velocities a low oxygen, highly aromatic crude oil is produced.
- Cracking and hydrogenation of the higher molecular weight components are the rate limiting steps in upgrading biomass-derived oils. Catalyst development should be directed at these reactions.
- The TR7 oil is superior to TR12 and both are much superior to pyrolysis oils as feedstocks for catalytic hydrotreating to produce hydrocarbon fuels.
- Pyrolysis oils can be upgraded by catalytic hydrotreating, however, a catalytic pretreatment step is required.
- Residual sodium catalyst needs to be removed from liquefaction products to prevent rapid catalyst fouling.

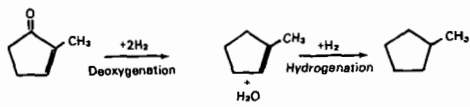
ACKNOWLEDGEMENT

The authors acknowledge the dedicated efforts of W. F. Riemath and G. G. Neuschwander of PNL who assisted in reactor operation and product analysis. The work was funded by the Biomass Thermochemical Conversion Program office at PNL under the direction of G. F. Schiefelbein, D. J. Stevens, and M. A. Gerber. We would also like to acknowledge the support of S. Friedrich of the Biofuels and Municipal Waste Technology Division of the U. S. Department of Energy.

REFERENCES

1. Davis, H., G. et al. 1985. "The Products of Direct Liquefaction of Biomass," in Fundamentals of Thermochemical Biomass Conversion, R. P. Overend, T. A. Milne, and L. K. Mudge, eds. Elsevier Applied Science Publishers.
2. Elliott, D. C. 1985. "Analysis and Comparison of Products from Wood Liquefaction," in Fundamentals of Thermochemical Biomass Conversion, R. P. Overend, T. A. Milne, and L. K. Mudge, eds. Elsevier Applied Science Publishers.
3. Boocock, D. G. B., R. K. M. R. Kallury, and T. T. Tidwell. 1983. Anal. Chem. **55**; 1689.
4. Beckman, D. and D. C. Elliott. 1985. Can. J. Chem. Eng. **63**, 99.
5. Li, C. L., Z. R. Yu, and B. C. Gates. 1985. Ind. Eng. Chem. Proc. Des. Dev. **24**, 92.
6. Elliott, D. C. 1983. Amer. Chem. Soc. Div. Petr. Chem. Prepts. **28**, 3, 667.
7. Elliott, D. C. and E. G. Baker. 1984. "Upgrading Biomass Liquefaction Products Through Hydrodeoxygenation," in Biotechnology and Bioengineering, Symposium No. 14, John Wiley and Sons.
8. Soltes, E. J. and S. C. K. Lin. 1984. "Hydroprocessing of Biomass Tars for Liquid Fuel Engines," in Progress in Biomass Conversion, Academic Press.
9. Furimsky, E. 1983. Catal. Rev-Sci. Eng. **25**, 3, 421.
10. Elliott, D. C. and E. G. Baker. 1986. "Hydrotreating Biomass Liquids to Produce Hydrocarbon Fuels." Presented at Energy from Biomass and Wastes X, Washington, D.C.
11. Elliott, D. C. and E. G. Baker. 1985. "Hydrodeoxygenation of Wood-Derived Liquids to Produce Hydrocarbon Fuels." Presented at the 20th IECEC, Miami, Beach. SAE Paper No. 859096.
12. Noel, F. 1984. Fuel **63**, 931.

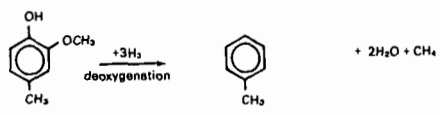
2 - Methyl - 2 - Cyclopentene - One Methyl Cyclopentene Methyl Cyclopentane



4 - Methyl Guaiacol

Toluene

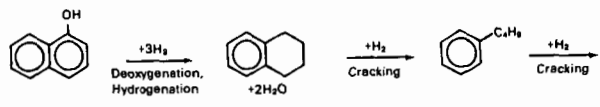
Methane



Naphthol

Tetralin

Butyl Benzene



Benzene

Butene



C₄H₁₀

FIGURE 1. Some Reactions in Catalytic Hydrotreating Biomass-Derived Oils

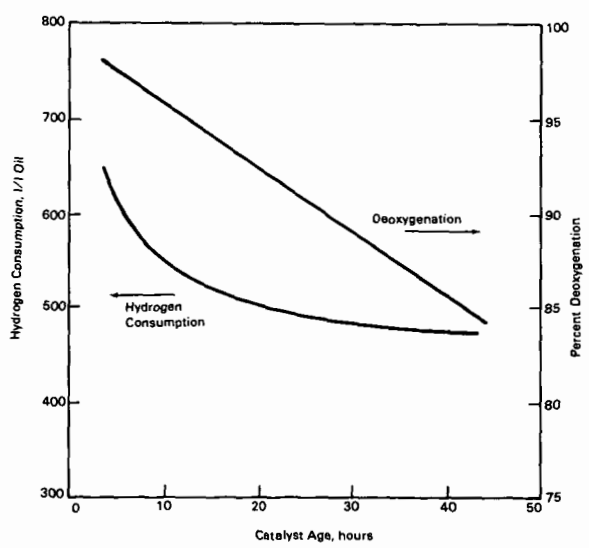


FIGURE 2. Effect of Catalyst Age on Deoxygenation and Hydrogenation, 400°C, 2,000 psig, LHSV = 0.1

FLUIDIZED BED UPGRADING OF WOOD
PYROLYSIS LIQUIDS AND RELATED COMPOUNDS

N. Y. Chen, D. E. Walsh and L. R. Koenig
Mobil Research and Development Corporation
Central Research Laboratory
P. O. Box 1025
Princeton, New Jersey 08540

Abstract

The effective hydrogen index (EHI) is a calculated indicator of the "net" hydrogen/carbon ratio of a pure or mixed heteroatom-containing feed, after debiting the feed's hydrogen content for complete conversion of heteroatoms to NH_3 , H_2S , and H_2O . Compounds with EHI's < 1 are difficult to upgrade to premium products over ZSM-5 catalyst due to rapid catalyst aging in continuous fixed bed processing. However, high conversions of such feeds (acetic acid, methyl acetate, and wood pyrolysis liquids) can be maintained in a fluidized bed system operating under methanol-to-gasoline conditions and employing frequent catalyst regeneration. Synergisms observed when coprocessing blends of low and high EHI model compounds also exist for a wood pyrolysis liquid. Thus, when coprocessed with sufficient methanol, the conversion and hydrocarbon yield from wood pyrolysis liquid increased by 19 and 64%, respectively, while coke yield decreased by 40%. A possible processing scheme is described in which the char penalty associated with wood pyrolysis is diminished by gasifying the carbonaceous residue and producing methanol as a cofeed for the synergistic upgrading of the pyrolysis liquids over ZSM-5.

Introduction

Zeolite ZSM-5 is particularly effective for the conversion of methanol to gasoline range hydrocarbons (1). In addition to methanol, other oxygenate feeds, including complex mixtures, can be converted as well (see, for example, references 2-7).

The effective hydrogen index is defined as:

$$(H/C)_{\text{effective}} \text{ or EHI} = \frac{H-2O-3N-2S}{C}$$

where H, C, O, N, and S are atoms per unit weight of sample of hydrogen, carbon, oxygen, nitrogen and sulfur, respectively. Model oxygenate compounds having EHI's <1 produce a poor product slate and cause rapid zeolite catalyst aging in continuous fixed bed MTG processing (3,8) using ZSM-5. Thus, after 2 hours on stream, acetic acid conversion declines from estimated high initial values to <30%. Hydrocarbons account for <10 wt.% of the products from the aged catalyst and, of the hydrocarbon portion, >70% is C₄⁻ (overwhelmingly butenes) and <25% C₅⁺ gasoline.

Cellulosic biomass is a potential source of liquid hydrocarbon fuels. Wood pyrolysis yields carbon-containing liquid products but suffers from two disadvantages. First, a large percentage of the original wood carbon is lost to a low value char by-product. Second, like the model oxygenates described above, the EHI of the liquid products is substantially less than 1.0.

The present study was undertaken to examine the potential of short contact time regenerative fluid bed processing to obviate the problems associated in extended non-regenerative fixed bed operation with such low EHI feeds.

In addition, Chang, Lang, and Silvestri (8) disclosed that reductions in zeolite catalyst aging rate and synergistic yield benefits could be realized in fixed bed operation if the low EHI (<1) feed were co-processed with a sufficient amount of high EHI (>1) constituent. In fixed bed studies, Chantal et al (9) coprocessed up to 10% methanol with an oil derived from supercritical extraction of wood chips. Although some benefits from methanol were evident, the amounts of methanol used were less than those recommended by Chang et al (8), and run durations did not exceed one hour. Consequently, it was not clear if the amount of methanol was sufficient to maximize product yield benefits and to maintain the catalyst's performance in extended continuous processing. It was of interest to us, therefore, to further examine the potential benefits of methanol co-processing for both model compound feeds and wood pyrolysis liquids in short contact time regenerative fluid bed processing.

Experimental

a) Catalyst

The catalyst used was HZSM-5 in a $\text{SiO}_2/\text{Al}_2\text{O}_3$ binder.

b) Production of Wood Pyrolysis Liquids

Sawdust (primarily pine and fir) pyrolysis was carried out at atmospheric pressure and $\sim 520^\circ\text{C}$ in flowing He. The wood charge had the following elemental analysis (dry basis):

C - 49.20%, H - 6.80%, O - 43.40%, ash - 0.60%.

c) Reactor and Run Procedures

All model compound and wood pyrolysis liquid upgrading runs were performed in a computer controlled fluidized bed apparatus (10) (Figure 1) operating cyclically to effect successive and repeated reaction/regeneration intervals. Approximately 35 cc of catalyst was charged to the vycor reactor along with 15 cc of meshed vycor. He fluidizing gas enters through a frit at the base of the tapered section of the reactor bottom. A small flow of He also sweeps through the feed oil sidearm inlet line. The total He flow (850 cc/min.) plus the vapor phase reactant and products maintain the bed in vigorous motion which, in turn, insures good temperature control. Runs were carried out at 1 WHSV based on the low EHI feed component, 410°C and atmospheric pressure. The catalyst was automatically oxidatively regenerated after each 10-20 min. reaction interval.

The product water phase was separated and gc analyzed for oxygenates from which conversion could be calculated. The hydrocarbon product layer contained only a very small amount of oxygen (<1%). Liquid hydrocarbon product was also subjected to gc analysis as were gaseous products, the latter being checked for their hydrocarbon and CO_x contents. Coke was calculated by the computer from on line CO and CO_2 IR data collected during each catalyst regeneration. Elemental and total material balances were generally >95%. Results presented were normalized to a no loss basis.

Results and Discussion

A) Model Compound Conversions

Experimental data are presented in Table 1. Two conversions are presented for each run. "Total conversion" represents the conversion to all products, while "conversion to non-oxygenates" represents conversion to all hydrocarbon, CO_x and H_2O products. The overall yields from the methanol experiment (EHI = 2.0) are in reasonable agreement with data obtained in the fluid bed MTG process (11). The hydrocarbon gas products, however, are higher in propene and lower in isobutane, probably due to the lower reaction pressure used in this study.

A-1) Conversion of Acetic Acid and Methylacetate

The data obtained for acetic acid illustrate several interesting points which can be contrasted with the fixed bed operation cited above. First, total conversions >90% may be maintained indefinitely provided periodic catalyst regeneration is employed. In spite of its having an EHI of 0, which assumes that oxygen is rejected as water, our experimental data show that decarboxylation takes place to a large extent. As a result, by rejecting oxygen as CO_x , substantial production of hydrocarbons is possible. Hydrocarbon liquid product yield is ~60% larger than that obtained at 2 hours processing time in the non-regenerative fixed bed operation (18.3% vs <10%) and ~65% of the hydrocarbon product is C_5^+ gasoline with a predominantly aromatic character. This high selectivity toward aromatics formation is consistent with the low effective hydrogen content of the "hydrocarbon" fraction of acetic acid.

On a weight basis, acetic acid yields only 40% as much hydrocarbon as methanol. The lower yield is primarily due to decarboxylation, and to a small extent, to coke and CO production.

Methyl acetate has an EHI of 0.67 and thus, ordinarily, would also be considered difficult to process. Its net hydrogen content, however, is substantially higher than acetic acid's. Because of its higher carbon content (48.6% C) and despite decarboxylation and coking reactions, the observed hydrocarbon yield remains comparable to that of methanol. Moreover, hydrocarbon selectivity for direct conversion to C_5^+ gasoline is higher than acetic acid or methanol (79.5%). Thus, the direct yield of C_5^+ gasoline is 32.1% on charge vs 23.3% for methanol.

From a hydrogen balance standpoint, both acetic acid and methyl acetate reject less H_2O and more CO_x than methanol, with resultant C_5^+ liquids having effective H/C^+ s of ~1.3 vs ~1.7-2 for methanol processing.

A-2) Conversion of Mixtures of Acetic Acid and Methanol

Processing a 1.9/1 or a 3.8/1 molar mixture of CH_3OH and acetic acid provided observations similar to those already disclosed by Chang, Lang and Silvestri (7), viz, an enhancement in C_5^+ liquid yield at the expense of C_4^- vs what might be expected if the mixture behaved as the average of its two components, the calculated values for which are shown in parentheses in Table 1. The selectivities of the hydrocarbon products amplify the observed synergism with respect to C_5^+ liquids. Furthermore, there is an enhancement in total hydrocarbon yield vs linear combination expectations.

The means by which this is accomplished is illustrated in Figure 2, which shows the effect of increasing mole percent methanol in the $\text{MeOH}/\text{acetic acid}$ charge and attendant decrease in

oxygen rejection as CO_2 and increase in oxygen removal as H_2O . Thus, more carbon remains available to form hydrocarbon products, much of it becoming C_5^+ liquids.

The above findings demonstrate that short contact time fluid bed reactor operating in a cyclic mode can be used to process low EHI compounds to yield substantial amounts of C_5^+ liquid hydrocarbon products.

By co-processing a low EHI material with a high EHI compound such as methanol, a shift in oxygen rejection from decarboxylation to dehydration takes place. The shift results in an increased yield of hydrocarbons.

The reaction of acetic acid may have potential application in converting fermentation products to hydrocarbons. Acetic acid is a major by-product in bacterial fermentation of biomass to ethanol (12). Mixtures of acetic acid and ethanol may also be processed to hydrocarbons (13).

B) Wood Pyrolysis Liquid Upgrading

The products from sawdust pyrolysis at 520°C in flowing He at atmospheric pressure produced the yields shown in Table 2. Because the object of these experiments was to track the amount of wood carbon which could be converted to hydrocarbons by pyrolysis/ZSM-5 upgrading schemes, the amount of water produced by pyrolysis was not measured, and water in the pyrolysis liquids was fed along with the oxygenate products in subsequent ZSM-5 processing. Elemental analyses and the apparent EHI's (including any water) are presented in Table 3. Inspection of these data indicate that the liquid products contain about 31% of the original wood carbon. The char product accounts for another 49 wt% of the original wood carbon and is available for indirect liquefaction by methanol synthesis. The remaining 20% of the wood carbon becomes CO , CO_2 and methane, about half of which (as CH_4 and CO) is also potentially available for conversion to methanol.

The two pyrolysis liquid layers were homogenized (EHI of the blend was 0.34) by high speed mixing en route to the fluid bed catalytic reactor. The oxygenate conversion obtained at 410°C and 1 LHSV was 87.9% with the product selectivity distribution shown in Table 4A.

Next, the two pyrolysis liquid layers were dissolved in methanol at a 1:1 weight ratio. The solution had an apparent EHI of ~ 1.3 which meets the recommendations set forth by Chang et al (8). The solution was fed to the reactor at 2 WHSV so that the WHSV based on the pyrolysis liquid feed would be identical to that employed when processing was performed without methanol. In this case, the overall conversion, including methanol, was 90.3 wt%. Under these conditions, methanol alone converts completely and produces ~ 56 wt% H_2O and 44 wt% hydrocarbon products (11).

Conversion of the pyrolysis liquids (after subtracting the products from methanol) therefore was 80.6 wt%. The selectivity distribution of the net converted products from the pyrolysis liquid is shown in Table 4B.

The results from methanol co-processing are summarized in Table 5. They show diminished decarboxylation, greatly enhanced hydrocarbon yields, greatly reduced coke yields, and improved overall conversion. Thus, with low EHI wood pyrolysis liquids, methanol co-processing has effects similar to those observed for model compounds. In comparison, in fixed bed processing at low methanol concentrations, Chantal (9) also observed conversion enhancements and diminished decarboxylation. Although it was suggested that the presence of methanol may lead to reduced coke yields, the data were variable with increased coke accompanying increased methanol in the feed in several instances. This was likely due to inadequate amounts of methanol co-feed as discussed above. Also, coke yields were fairly high suggesting that the amount of methanol employed would have been insufficient to sustain catalyst performance over extended operating times.

C) Potential Processing Scheme

The advantages of co-processing methanol and pyrolysis liquids are further illustrated by a comparison of two potential process arrangements shown in Figures 3 and 4. A major feature common to both is the use of the pyrolysis char as a cheap source of methanol.

Figure 3 shows the products obtained in a scheme in which direct upgrading of the wood pyrolysis liquids over ZSM-5 occurs in parallel with upgrading of methanol obtained from synthesis gas derived from gasification of the pyrolysis char. In Figure 4, the methanol is mixed with the pyrolysis liquids prior to co-processing over ZSM-5. Approximately 40 lbs. of methanol is potentially available from the char and pyrolysis gas products. This amount would provide a weight ratio of methanol/pyrolysis liquids of 0.73. Since the EHI for this mixture (~1.2) exceeds 1 and is quite similar to that of the 1/1 mixture described above, comparable product distributions should result.

In the parallel processing scheme, a total of 20.6 lbs. of hydrocarbon (~85% C₅⁺ gasoline, including alkylate) per 100 lbs. of total feed (pyrolysis liquid and methanol) is obtained. In the co-processing mode, ~3 lbs. of additional hydrocarbon result concomitant with reduced oxygenates and coke.

Stated differently, without char gasification recycle of pyrolysis liquid oxygenates to extinction over ZSM-5 yields <10% of the original wood carbon as hydrocarbon products. Parallel upgrading of methanol derived from char gasification can increase this value to ~36%, while methanol co-processing boosts the percent of wood carbon transformed into hydrocarbon products to ~42%.

References

1. C. D. Chang, and W. H. Lang, U. S. Patent 3,894,103 (1975).
2. C. D. Chang and A. J. Silvestri, "The Conversion of Methanol and Other O-Compounds to Hydrocarbons Over Zeolite Catalysts," J. Cat. **47**, 249-259 (1977).
3. W. O. Haag, P. G. Rodewald and P. B. Weisz, U. S. Patent 4,300,009 (1981).
4. J. A. Brennan, P. D. Caesar, J. Ciric and W. E. Garwood, U. S. Patent 4,304,871 (1981).
5. J. C. Kuo, C. D. Prater and J. J. Wise, U. S. Patent 4,041,094 (1977).
6. H. R. Ireland, A. W. Peters and T. R. Stein, U.S. Patent 4,045,505 (1977).
7. P. B. Weisz, W. O. Haag and P. G. Rodewald, Science, **206**, 57 (1979).
8. C. D. Chang, W. H. Lang and A. J. Silvestri, U.S. Patent 3,998,898 (1976).
9. P. Chantal, S. Kaliaguine, J. L. Grandmaison and A. Mahay, "Production of Hydrocarbons from Aspen Poplar Pyrolytic Oils over H-ZSM5", Applied Catalysis **10**, 317-332, Elsevier Science Publishers, Amsterdam, The Netherlands (1984).
10. D. E. Walsh, U. S. Patent 4,419,328 (1983).
11. W. Lee, J. Maziuk, V. W. Weekman, Jr. and S. Yurchak, "Mobil Methanol-to-Gasoline Process," Large Chemical Plants, Elsevier Scientific Publishing Co., Amsterdam, The Netherlands (1979).
12. C. L. Cooney, D. I. C. Wang, S. D. Wang, J. Gordon and M. Jimenez, Biotech. Bioeng. Symp. **8**, 103 (1978).
13. N. Y. Chen, T. F. Degnan and L. R. Koenig, Chemtech, 508-511, August 1986.

TABLE 1
410°C, 1 atm., 1.0-1.1 WHSV, 20 min. reaction intervals
HZSM-5 in SiO₂/Al₂O₃

	Methanol <u>CH₃OH</u>	Acetic Acid <u>CH₃COOH</u>	Methyl Acetate <u>CH₃CO₂CH₃</u>	1.9/1 (molar) MeOH/ Acetic Acid	3.8/1 (molar) MeOH/ Acetic Acid
EHI of Charge	2.0	0.0	0.67	1.0 (1.0)	1.3
Total Conversion	98.6	91.2	89.4	>91 (94.9)	95
Conversion to Non-Oxygenates	98.6	79.8	86.1	90.4 (89.2)	--
<u>Products (Wt. % of Charge)</u>					
CO	0.0	3.7	6.2	2.1 (1.8)	1.1 (1.2)
CO ₂	0.2	31.4	17.6	9.4 (15.8)	5.2 (10.6)
H ₂ O	55.8	28.4	21.5	45.3 (42.1)	48.8 (46.7)
Oxygenates	1.4	20.2	13.9	9.6 (10.8)	5.2 (7.7)
C ₁ Hydro- carbon gas	19.0	3.8	6.0	7.9 (11.4)	9.9 (13.9)
C ₂ Liquid Hydrocarbon	23.3	10.6	32.1	24.9 (17.0)	28.7 (19.1)
Total Hydro- carbons	42.3	14.4	38.1	32.8 (28.4)	38.6 (33.0)
Coke	0.3	1.9	2.7	0.8 (1.1)	1.1 (0.8)
<u>Wt. %'s of Hydrocarbon</u>					
C ₁ + C ₂	5.4	1.5	5.6	7.2	7.6
C ₃ ^o	1.6	0.1	0.7	0.4	0.6
C ₃ ^a	25.9	5.2	6.7	13.8	14.2
iC ₄ ^o	5.5	0.5	0.3	0.4	0.5
nC ₄ ^o	0.4	0.3	0.0	0.1	0.1
C ₄ ^a	5.8	15.7	1.4	1.6	1.9
Total C ₄ ⁻	44.6	23.3	14.7	23.5 (34.0)	24.9 (37.5)
C ₅ ⁺ (gasoline)	54.7	65.0	78.7	74.1 (59.8)	72.3 (58.1)
Coke	0.7	11.7	6.6	2.4 (6.2)	2.8 (4.4)
H/C (effective)* of C ₅	1.7	1.3	1.3	~1.4	~1.4

*Small amounts of oxygen were observed in the C₅⁺ liquid. The use of the effective hydrogen index corrects for this.

Table 2
Wood Pyrolysis at 520°C and 1 atm.

<u>Product</u>	<u>Wt. %</u>
CH ₄	1.4
CO	7.1
CO ₂	8.5
Liquid Oxygenates	55.0
Char	28.0

Table 3
Elemental Analysis, wt%

	<u>Sawdust</u>	<u>Liquid Layer 1 (51%)</u>	<u>Liquid Layer 2 (4%)</u>	<u>Char</u>
C	49.2	25.9	55.0	87.3
H	6.8	8.8	7.5	3.9
O	43.4	65.3	37.5	8.0
Ash	0.6	-	-	No Data
EHI	0.3	0.3	0.6	-

Table 4A
Product Distribution from Conversion
of Wood Pyrolysis Liquids

	wt. %
CO	0.7
CO ₂	10.5
Water	70.7
C ₁ -C ₄	2.5
C ₅ ⁺ Hydrocarbons	8.0
Coke	9.6

Table 4B
Product Distribution from Conversion of Pyrolysis
Liquid When Processed in Conjunction with Methanol

	Wt. %
CO	-
CO ₂	-
Water	82.1
C ₁ -C ₄	2.7
C ₅ ⁺ Hydrocarbons	11.2
Coke	4.0

Table 5
Advantages Resulting from Methanol Co-Processing

	Pyrolysis Liquids	Pyrolysis Liquids + Methanol (1:1 wt/wt)	% Change
Net Conversion, wt. %	87.9	80.6	+18.7
Hydrocarbons, wt. %	8.5	13.9	+63.5
Coke, wt. %	9.6	4.0	-41.7

FIGURE 1: CYCLIC FIXED FLUID BED APPARATUS

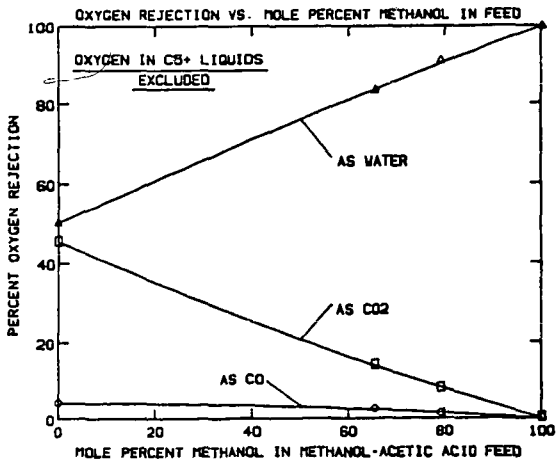
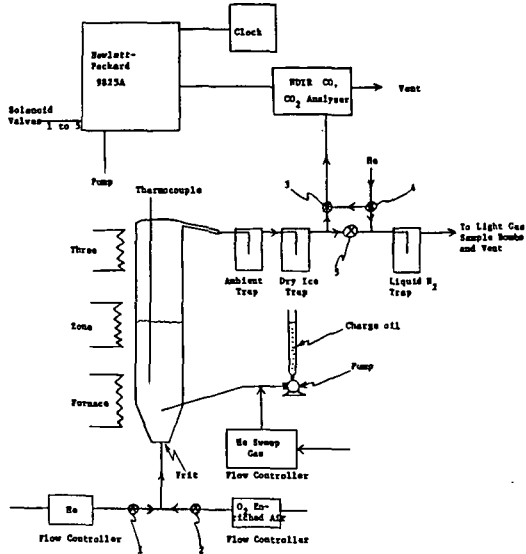


FIGURE 2

FIGURE 3

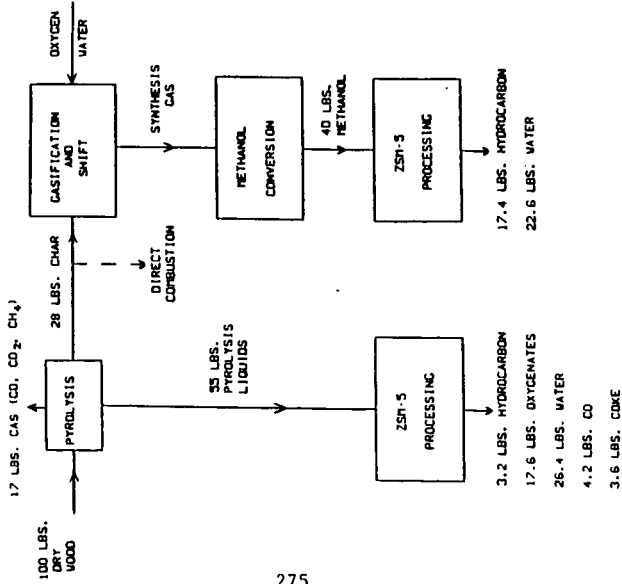
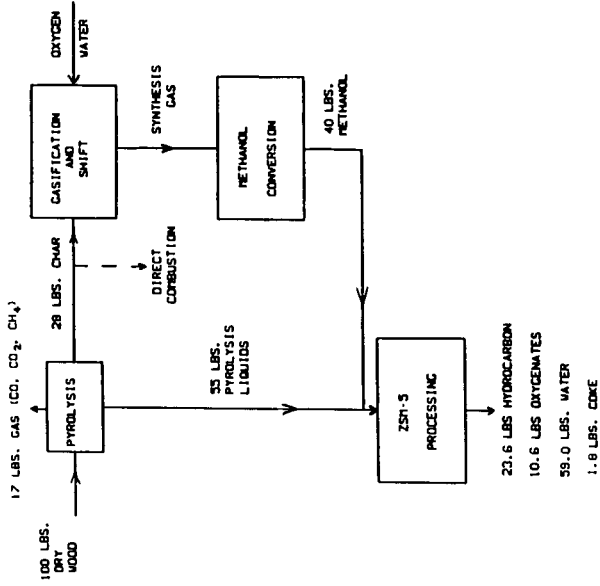


FIGURE 4



CONVERSION OF VACUUM PYROLYTIC OILS FROM
POPULUS DELTOIDES OVER H-ZSM-5

M. Renaud, J.L. Grandmaison, Ch. Roy and S. Kaliaguine
Department of Chemical Engineering
Université Laval, Ste-Foy, Qué., CANADA

INTRODUCTION

As biomaterials are structurally and chemically complex, biomass thermochemical conversion processes^(1,2) produce complex fractions including a liquid fraction which, depending on the process, can be obtained in large (liquefaction, pyrolysis) or small yields (gasification). These liquids have found little utility because of their large contents in oxygen which implies low heat values, instability and corrosive properties. Two routes have been tested^(3,4) in order to produce hydrocarbons from these liquids. The first one involves hydrotreatment with either H₂ or H₂ + CO over classical hydrotreatment catalysts. The second route is the simultaneous dehydration and decarboxylation over HZSM-5 zeolite catalyst in the absence of any reducing gas.

Soltes and Lin⁽⁵⁾ achieved significant deoxygenation of various biomass tars from gasification/pyrolysis processes, in the presence of hydrogen-donor solvents (cyclohexane, tetralin, decalin) and various silica-alumina supported metals catalysts. Elliot and Baker⁽⁶⁾ performed hydrodeoxygenation of the products of a process of liquefaction in the presence of CO at high pressure, using NiS, CoS and MoS₂ catalysts. Hydrodeoxygenation of a biomass tar can be achieved when phenolic compounds are in high concentrations. In wood pyrolysis however, the liquid products contain large amounts of low molecular weight organic acids, ketones, aldehydes and furans as well as phenolic compounds in the methoxy- or dimethoxy⁽⁶⁻⁸⁾ substituted forms. These mixtures are thermally instable in typical hydrotreating conditions.

The second route however seems more appropriate for the conversion of pyrolytic oils. It was indeed shown that a large variety of oxygenated compounds can be converted into hydrocarbons over H-ZSM-5⁽⁹⁻²⁰⁾. In all cases hydrocarbons in the gasoline range are obtained due to the shape selective properties of this zeolite catalyst⁽²¹⁾. Moreover a remarkable resistance to coking is observed due to the sterically restricted transition state selectivity effects, and these properties are also of considerable interest in the context of pyrolytic oils upgrading. Works along this line have been performed by Chantal et al.^(22,25) working with oils derived from Aspen Poplar by dense gas extraction, Frankiewicz⁽²³⁾ who used a dual process combining pyrolysis of solid wastes with a catalytic converter and Mathews et al⁽²⁴⁾ who treated small fractions of the oils produced from wood by their thermochemical process.

In the present paper we report a study of the conversion over H-ZSM-5 catalysts, of the fractionated oil produced by vacuum pyrolysis of Populus Deltoides wood in a process demonstration unit⁽²⁶⁾.

EXPERIMENTAL

Pyrolytic oil

The oil under study was produced by the vacuum pyrolysis process, currently under development at LAVAL University and CRIQ⁽²⁶⁾. The PDU is a six-hearth furnace, 2m high and 0.7 m in diameter. In this unit, the organic vapours and gaseous products are rapidly removed from the reactor through a series of outlet manifolds. Then the

vapours are condensed in a primary cooling unit, and recovered as a liquid fraction for each hearth. As shown in Figure 1 four additional liquid fractions are collected in the secondary cooling unit. In this work only the fractions from the primary cooling unit have been studied and designated as oils #1 to #6 corresponding to the six hearthes from top to bottom.

In standard pyrolysis experiments using *Populus Deltoides* chips, the pressure in the reactor was lower than 80 Torr and the hearth temperatures were 215, 275, 325, 370, 415 and 465°C from top to bottom respectively. Table 1 gives some analytical results for these six oils. The low water contents are due to the separation effect of the primary cooling unit. Formic and acetic acids are considered the most abundant single organic compounds in these oils.

Conversion Reactor

The experimental set-up is a slightly modified version of a reactor described previously⁽²²⁾. As heating the pyrolytic oils to the reaction temperature is believed to induce thermal polymerisation/condensation reactions, a device was designed in order to preheat the vaporized feed and condense at an appropriate temperature the heavier products. This device is described in Figure 2. Using a syringe pump (SAGE 220) the liquid oil is injected in a controlled flow of helium (= 6.0 SCC/min) and first fed to an empty pyrex tube maintained at the same temperature than the tubular reactor. At the outlet of this tube the gas passes through a hot trap (150°C) where a heavy fraction is condensed. The gas flow then enters the microcatalytic pyrex tubular reactor and it is led to the heated (200°C) automatic sampling valve of a Gas Chromatograph (Perkin Elmer, Sigma 115) through a heated line (160°C). After the valve the products are collected as three fractions in three successive traps maintained at 4, -76 and -196°C respectively.

After a test the tubular reactors can be transported to another set-up where they can be regenerated in a controlled flow of dry air at 500°C. The CO₂ and H₂O produced are adsorbed over ascarite and drierite respectively and weighed. The sum of the masses of carbon in CO₂ and hydrogen in H₂O was determined and compared to the measured mass of the coke deposited in each of the two pyrex tubes.

Each experiment was performed using 1.0 ± 0.2 g of one of the three catalysts designated as H-22, H120 and H-450 undiluted. These are the H forms of ZSM-5 samples prepared by the procedure described as method B' by GABELICA et al⁽²⁸⁾. They have Si/Al ratios of 22, 119 and 452, and sodium contents less than 220 ppm as determined by PIXGE⁽²⁹⁾.

The GC on line with the reactor was equipped with TC and FID detectors and a Porapak-Q column (6 ft, 1/8" OD, 80-100 mesh). In instances were peak identification was in doubt, the fraction in the 4°C trap was further analyzed using another GC (Perkin Elmer Sigma 3) equipped with a FID detector and a capillary column DB-1 (30 m).

In typical runs, oil was injected for about 3 000 s but chromatographic analysis was started at 2 000 s for all experiments.

Experimental design

A statistical experimental design was employed to study the effect of the process parameters, namely, temperature (350-450°C), space velocity CLHSV = 0.5-2.5 h⁻¹) and oil fraction, on various response variables. In order to reduce the number of experiments, a Box-Behnken experimental design⁽³⁰⁾ was selected. This design is visualized as a cube in Figure 3. Since 6 oil fractions were studied two Box-Behnken cubes were used in order to minimize the number of experiments by studying three oils

at a time. Eventhough a discrete variable is employed to represent the oil, in reality the hearth number (1 to 6) follows the reaction temperature on the hearth which is continuous. The experiments were performed in a random manner.

RESULTS AND DISCUSSION

Table 2 shows the experimental results and conditions for the catalytic upgrading tests of the six pyrolytic oils. It gives the weight percents of the various fractions of products collected. Coke #1 corresponds for example to the total weight of the material deposited on the wall of the empty pyrex tube whereas coke #2 is the one left in the tubular reactor (on the catalyst) at the end of a test. The tar collected in the hot trap is designated as the residuum, whereas the cumulative mass recovered in all three cold traps is indicated as "traps".

The composition of the "traps" fraction is the one of the stream leaving the reactor. It is given in Table 2 in a condensed manner as weight percents of various components including C_5 - C_{10} hydrocarbons, C_{10}^+ hydrocarbons and oxygenates. These oxygenates are mostly comprising phenolic and furanic compounds. Figure 4 shows some of the characteristics of the six pyrolytic oils. The average molecular weight varies in a continuous manner with the hearth number, showing a maximum value for the oil produced on the 3rd hearth and a minimum value for the one from hearth No 6.

It must be noted that the sum of weight fractions of acetic and formic acids is following a similar pattern except for the oil No 5 which contains much formic acid and is therefore much more acidic. The low content in formic acid of oil No 6 is a clear indication that the solid residue leaving hearth No 5 is very different in nature from the one from hearth No 4 bearing much less intact or slightly degraded cellulose (the main source of formic acid) and much more recondensed material. Figure 5 shows for each oil the average values of the weight percents of coke #1, residuum and the yield in C_5 - C_{10} hydrocarbons. It is interesting to note that at least for the first four oils these values are obviously correlated with both oil average molecular weight and acidity (Figure 4). As expected, coke #1 is higher when the oil is heavier, but the residuum is much smaller. This last result can only be understood if the residuum is seen as an intermediate product of gas phase depolymerization which would be faster for the most acidic mixtures. Indeed for example the low residuum value obtained with oil No 5 would then be the result of this oil being much more acidic than the others.

The C_5 - C_{10} yield is also correlated with \bar{M}_w (up to oil No 5) but this correlation is the result of a more intricate interaction of various factors. C_5 - C_{10} yield does not depend only on molecular size or acidity of the oil but also on its chemical nature. Oil No 3 which contains more lignin fragments is liable to yield small phenolics which are volatile enough to reach the catalyts but which are not converted to hydrocarbons. Similarly oil No 6 which is believed to contain less polysaccharides pyrolysis products shows a very low C_5 - C_{10} yield.

The effect of the various parameters on the "traps" weight percent is reported in Figure 6. This term represents roughly the fraction of the oil reaching the catalyst and must therefore be considered as a yield for the preliminary thermal processing. The curves are drawn not taking into account the results for oil No 5. Comparing the curves obtained at 350 and 450°C (both at 1.2 LHSV) shows that increasing the temperature increases the depolymerisation of the oils components. The two curves at 400°C and 0.5 and 2.5 LHSV show that increasing the residence time in the empty tube and the hot trap increases also the depolymerisation yield.

These results show the interest of the experimental procedure adopted in this work as this gas phase thermal depolymerisation which happens at the same temperature than

the catalytic process can be studied separately. This is not the case when the vaporized oil is directly injected onto the catalyst and both processes happen simultaneously.

Figure 7 gives the yield in C₅-C₁₀ obtained for the various oils as a function of temperature and LHSV. Comparing the curves at 350 and 450°C shows that a rise in temperature increases this yield in proportions roughly similar to the increase of the "traps" fraction (see Figure 6). This suggests that the most important effect of temperature is to increase the yield of thermal depolymerization. This is confirmed by the fact that the oil No 5 which is the most acidic and is more thoroughly depolymerized (yielding a higher "traps" fraction) is also showing the highest C₅-C₁₀ yield. Similar observations can be made for the effect of contact time at 400°C.

It is interesting to note that for several oils (No 1, 2, 4 and 5) yields close to 30% have been reached. This is to be compared with the results of Chantal et al⁽²²⁾ who obtained maximum yields of 15-17% from SCE oils converted on ZSM-5 in a one step process. Figure 8 shows the variations of the percents of oxygenates in the traps. In line with previous discussion, maximum oxygenates are obtained from oils No 3 and 6 which contain respectively more lignin fragments and more product of high temperature decomposition of recondensed material and which therefore both contain more phenolic compounds.

Time on stream data

Figure 9 reports the results of a set of experiments (not shown in Table 2) designed to assess the deactivation behaviour of the catalyst. In these experiments the feed was a mixture of the six oils. It was injected for a fixed time in the reactor assembly maintained at 400°C. Then the gases leaving the reactor were analyzed and the injection of oil was stopped until the chromatographic analysis was completed, at which time the injection was restarted for another fixed time and this operation was repeated three times.

Figure 9 shows that the composition of the product changes with time on stream, with deactivation appearing after 250-500 s. The decrease in deoxygenation activity is seen from the decrease in H₂O, CO, CO₂ and the increase in oxygenates. The appearance of C₁₀⁺ aromatics in the products is of special interest. Since such large compounds cannot be generated within the pores of the ZSM-5 zeolite⁽²¹⁾, they can only be generated either on the external acid sites or from the coke deposit as postulated recently⁽¹³⁾. This would also explain the evolution of the C₅-C₁₀ aromatics distribution with time on stream, showing a relative increase in C₁₀ as well as C₁₀⁺.

The time scale for catalyst deactivation is showing the great resistance of the ZSM-5 catalyst to coking. At similar temperatures for example a pellet of H-Y cracking catalyst is deactivated within 2-3 seconds in the FCC process.

CONCLUSIONS

The experimental set-up used in this work allowed to decouple the gas phase thermal conversion of the pyrolytic oils from the catalytic upgrading. These two sets of reactions happen in the same temperature range and are therefore simultaneous when the oil is directly fed to the catalyst. Preliminary thermal conversions include some coking and an important thermal depolymerization. Both reactions are accelerated in the presence of volatile acids in the gas phase. Moreover performing both reactions in a preheater is beneficial to the catalytic conversion first because the deactivation of the catalyst is less important and secondly because depolymerized fragments yield higher conversions to hydrocarbons. C₅-C₁₀ hydrocarbon yields as high as 30 wt% have been consistently obtained for reaction times of 2000 s.

1. SIMONS RESOURCE CONSULTANTS & B.H. Levelton, "A Comparative Assessment of Forest Biomass Conversion to Energy Forms" Phase I-Proven and Near-Proven Technology Vol I-IX - Phase II - Further development, ENFOR PROJECT C-258, Canada, 1983.
- 2A. E. Chornet & R.P. Overend, "Biomass Liquefaction: An Overview" in "Fundamentals of Thermochemical Biomass Conversion" ed. R.P. Overend, T.A. Milne & L.K. Mudge, Elsevier 1985 p. 967-1002 - 2-B K.L. Tuttle, "Review of Biomass Gasification Technology" in "Progress in Biomass Conversion Vol. 5" ed. D.A. Tillman & E.C. John, Academic Press, 1984, p. 263-279.
3. S. Kaliaguine, "Upgrading pyrolytic oils from wood and other biomasses". Energy Project Office, NRCC, Ottawa, 1981.
4. S. Kaliaguine, Proc. Specialists Meeting on Biomass Liquefaction, Saskatoon, 1982, p. 75-125.
5. E.J. Soltes & S.C.K. Lin, "Hydroprocessing of Biomass Tars for Liquid Engine Fuels" in "Progress in Biomass Conversion" Vol. 5, Ed. D.A. Tillman & E.C. John, AC Press 1984, p. 1-68.
6. D.C. Elliot & E.G. Baker, "Upgrading Biomass Liquefaction Products through Hydrodeoxygenation", Biotechnology & Bioengineering Symp. 14, 159-174 (1984).
7. H. Ménard, C. Roy, A. Gaboury, D. Bélanger & G. Chauvette, "Analyse totale du pyrolytique provenant du Populus Tremuloides par HPLC", Compte-rendu du 4^e Séminaire R & D Bioénergétique, Winnipeg, Manitoba 29-31 mars 1982.
8. C. Roy, B. de Caumia, D. Brouillard & H. Ménard, "The Pyrolysis under Vacuum of Aspen Poplar" in "Fundamentals of Thermochemical Biomass Conversion", ed. R.P. Overend, T.A. Milne & L.K. Mudge Elsevier, N.Y. 1985, p. 237-256.
9. C.D. Chang & A.J. Silvestri, "The Conversion of Methanol and other O-compounds to Hydrocarbons over Zeolite Catalysts", J. Catal., 47, 249-259 (1977).
10. B.L. Maiorella, "Fermentation Alcohol: better to convert to fuel", Hydrocarbon Processing, August 1982, p. 95-97.
11. P.D. Chantal, S. Kaliaguine & J.L. Grandmison, "Reactions of Phenolic Compounds on H-ZSM5", Catalysis on the Energy Scene, Elsevier, 93-100, 1984.
12. P.D. Chantal, S. Kaliaguine & J.L. Grandmison, "Reactions of Phenolic Compounds over H-ZSM5", Appl. Catal., 18, 133-145 (1985).
13. M. Renaud, P.D. Chantal & S. Kaliaguine, "Anisole Production by Alkylation of Phenol over HSM-5", Can. J. Chem. Eng., 64, 787-791 (1986).
14. C.D. Chang, W.H. Lang, A.J. Silvestri, "Manufacture of Gasoline", U.S. Patent #3, 998-898 (1976).
15. W.O. Haag, D.G. Rodewald, P.B. Weisz, "Conversion of Biological Materials to liquid fuels", U.S. Patent #4,300,009, 1981.
16. P.B. Weisz, W.O. Haag, D.G. Rodewald, "Catalytic Production of High Grade Fuel (Gasoline) from Biomass Compounds by Shape-Selective Catalysis", Science, 206, 57-58 (1979).

17. Y.S. Prasad, N.N. Bakhshi, J.F. Mathews & R.L. Eager, "Catalytic Conversion of Canola Oil to Fuels and Chemical Feedstocks Part I Effect of Process Conditions on the Performance of HZSM-5 Catalyst", *Can. J. Chem. Eng.*, 64, 278-293 (1986).
18. N.Y. Chen & L.R. Koenig, "Process for converting carbohydrates to Hydrocarbons", U.S. Patent #4,503,278 (1985).
19. P.A. Pesa, M.W. Blaskie & D.R. Fox, "Decarbonylation of N.-Butyraldehyde using Zeolite Catalysts. "U.S. Patents #4,517,400, (1985).
20. R.M. Gould & S.A. Tabak, "Multistage Process for Converting Oxygenates to Liquid Hydrocarbons with Ethene recycle", U.S. Patents #4,543,435, (1985).
21. E.G. Derouane, "Molecular Shape-Selective Catalysis in Zeolites - Selected Topics", *Catalysis on the Energy Scene*, Elsevier, p. 1-17 (1984).
22. P.D. Chantal, S. Kaliaguine, J.L. Grandmaison and A. Mahay, "Production of Hydrocarbons from Aspen Poplar Pyrolytic oils over H-ZSM5", *Appl. Catal.*, 10, 317-332 (1984).
23. T.C. Frankiewicz, "Process for Converting Oxygenated Hydrocarbons into Hydrocarbons", U.S. Patents #4,308,411 (1981).
24. J.F. Mathews, M.G. Tepylo, R.L. Eager & J.M. Pepper, "Upgrading of Aspen Poplar Wood Oil Over HZSM5 Zeolite Catalyst", *Can. J. Chem. Eng.*, 63, 686-689, (1985).
25. R. Labrecque, S. Kaliaguine & J.L. Grandmaison, "Supercritical Gas extraction of Wood with Methanol", *Ind. Eng. Chem. Prod. Res. Dev.*, 23, (1), 177-182 (1984).
26. C. Roy, R. Lemieux, B. de Caumia & H. Pakdel, "Vacuum Pyrolysis of Biomass in a Multiple-Hearth Furnace", *Biotechn. & Bioeng. Symp.* 15, 107-113 (1985).
27. C. Roy, A. Lalancette, B. de Caumia, D. Blanchette et B. Côté, "Design et construction d'un réacteur de pyrolyse sous vide fonctionnant en mode semi-continu et basé sur le concept du four à soles multiples", in *Third Biomass Liquefaction Specialists Meeting Sherbrooke 29-30 Sept 1983*.
28. Z. Gabelica, N. Blom & E.G. Derouane, "Synthesis and Characterization of ZSM5 type zeolites III. A critical evaluation of the role of alkali and ammonium cations", *Appl. Catal.* 5, 227-248 (1983).
29. I.M. Szogyi, A. Mahay & S. Kaliaguine, "Elemental analysis of zeolites by PIXGE". *Zeolites* 6, 39-46 (1986).
30. G.P.E. Box & D.W. Benhken, "Some new three level designs for the study of quantitative variables", *Technometrics*, 2, (4), 455-475 (1960).
31. P.B. Weisz, "The remarkable active sites: Al in SiO₂", *Ind. Eng. Chem. Fundam.*, 25, 58-62 (1986).

OIL #	% WATER*	FORMIC ACID WT %	ACETIC ACID WT %	\bar{M}_w^{**} Mean-Molecular Weight
1	7.8	2.64	3.63	342
2	5.4	2.34	4.13	528
3	4.4	3.73	5.18	572
4	3.9	4.40	3.26	393
5	7.0	7.25	3.16	233
6	3.8	2.60	2.26	123

* determined by Karl-Fisher
 ** determined by GPC

TABLE 2 Experimental Conditions and Results of Catalytic Upgrading of Pyrolytic Oils.

OIL #	TEMP. °C	LHSV h ⁻¹	COKE wt %		RESIDUUM wt %	TRAPS wt %	PRODUCT DISTRIBUTION, wt %								YIELD C ₅ - C ₁₀
			#1	#2			CO	CO ₂	H ₂ O	C ₁ -L ₄	C ₅ -C ₁₀	OVYD.	BYX	C ₅ -C ₁₀	
1	350	1.2	15.2	2.3	50.8	31.6	1.2	1.7	5.6	1.2	61.9	26.0	23.5	3.3	19.3
1	400	0.5	21.7	6.5	10.9	60.9	0.7	0.8	3.7	2.2	48.7	25.7	21.1	18.4	29.7
1	400	2.5	17.4	2.8	54.8	24.9	1.0	2.0	6.2	4.3	57.6	23.9	19.7	4.9	14.3
1	450	1.2	18.7	2.3	40.9	38.1	0.9	1.1	3.2	1.4	76.8	12.0	18.0	4.6	29.3
2	350	0.5	10.0	4.3	62.9	22.9	0.9	1.2	4.5	1.8	52.2	33.7	18.8	5.4	12.0
2	350	2.5	30.5	3.9	31.2	34.4	1.3	2.7	5.5	1.4	51.4	29.5	13.1	8.1	17.7
2	400	1.2	20.6	5.9	26.5	47.1	0.8	1.0	3.4	2.0	45.8	32.5	17.2	14.6	21.6
2	400	1.2	22.9	5.1	28.8	43.2	0.9	1.2	3.8	2.5	44.4	34.1	18.8	13.1	19.2
2	400	1.2	21.3	5.6	24.0	49.1	1.0	1.2	3.1	1.3	45.4	29.9	17.4	17.1	22.3
2	450	0.5	30.9	3.6	9.1	56.4	0.8	1.2	3.1	2.0	48.3	36.3	18.4	8.5	27.2
2	450	2.5	36.6	2.8	22.5	38.0	2.6	4.6	7.2	4.6	54.7	23.3	22.0	2.8	20.8
3	350	1.2	33.1	4.3	30.7	31.9	0.6	0.7	3.2	0.6	47.0	34.0	10.7	13.9	15.0
3	400	0.5	25.4	3.4	25.4	45.8	1.3	1.9	4.5	4.0	42.6	34.6	28.1	11.1	19.5
3	400	2.5	19.2	3.1	46.9	30.8	0.6	0.9	2.4	1.1	34.9	48.8	8.8	11.3	10.7
3	450	1.2	22.3	5.9	29.4	42.3	0.8	0.9	2.3	1.8	68.6	39.0	17.8	16.5	16.3

TABLE 2 Continued...

DIL #	TEMP °C	LHSV h ⁻¹	COKE wt %		RESIDUUM wt %	TRAPS wt %	PRODUCT DISTRIBUTION, wt %										YIELD C ₅ -C ₁₀	
			#1	#2			CO	CO ₂	H ₂ O	C ₁ -C ₄	C ₅ -C ₁₀	UNYG.	BTX	C ₄ ⁺	C ₅ -C ₁₀			
4	350	1.2	20.1	2.4	52.4	25.0	1.3	1.7	5.1	1.1	58.1	24.6	22.4	8.2	14.5			
4	400	0.5	23.0	2.7	32.4	41.9	1.7	2.2	6.5	2.2	52.6	25.1	27.7	9.8	22.0			
4	400	2.5	11.7	2.6	56.3	27.4	1.3	1.8	8.4	1.9	51.3	27.6	20.0	9.7	14.1			
4	450	1.2	26.3	3.5	17.5	52.6	0.9	1.3	7.1	4.2	48.0	21.9	16.7	16.5	25.2			
5	350	0.5	27.1	3.4	16.9	52.4	1.6	1.9	6.7	1.3	52.2	29.7	26.0	6.6	27.4			
5	350	2.5	21.4	8.6	28.6	41.4	0.9	0.6	8.0	1.5	54.3	31.1	22.1	3.5	22.5			
5	400	1.2	25.5	3.9	24.5	46.1	0.4	0.5	2.9	1.1	53.1	28.5	19.0	13.6	24.5			
5	400	1.2	22.1	4.1	27.9	45.9	0.6	0.9	2.1	1.2	47.9	34.3	17.2	13.0	22.0			
5	400	1.2	29.6	3.2	20.3	46.9	0.3	0.5	4.0	1.4	56.9	24.9	20.4	12.0	26.7			
5	450	0.5	30.6	5.6	9.7	54.2	0.7	0.9	2.3	3.3	52.9	36.8	22.0	2.6	28.7			
5	450	2.5	31.8	1.3	25.2	41.7	2.5	4.7	8.8	12.1	37.1	30.5	30.6	4.1	15.5			
6	350	1.2	18.7	2.9	56.7	21.6	0.2	0.3	1.7	0.2	25.1	71.0	6.9	1.5	5.4			
6	400	0.5	30.3	12.1	3.0	54.5	0.3	0.3	1.0	0.9	30.7	47.2	11.2	19.9	16.7			
6	400	2.5	10.7	2.1	68.2	19.0	1.4	1.9	7.4	2.5	30.7	21.5	19.3	11.7	10.2			
6	450	1.2	20.4	2.4	47.9	29.3	1.3	1.2	3.9	5.9	46.1	23.9	15.6	17.5	13.5			

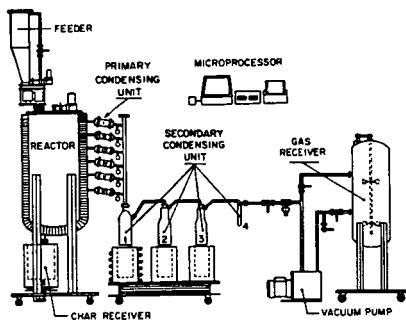


Fig. 1 - Scheme of the vacuum pyrolysis process development unit.

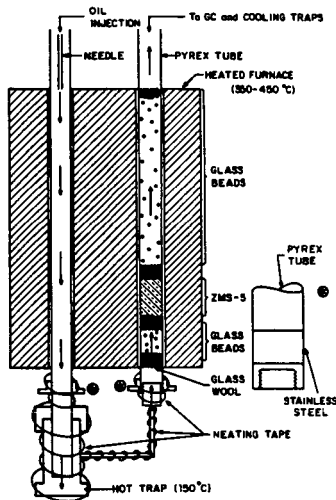


Fig. 2 - Scheme of the oil pretreatment device and reactor.

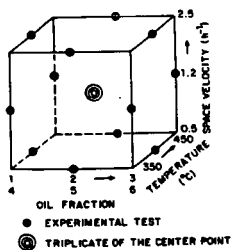


Fig. 3 - Box Behken Experimental Design

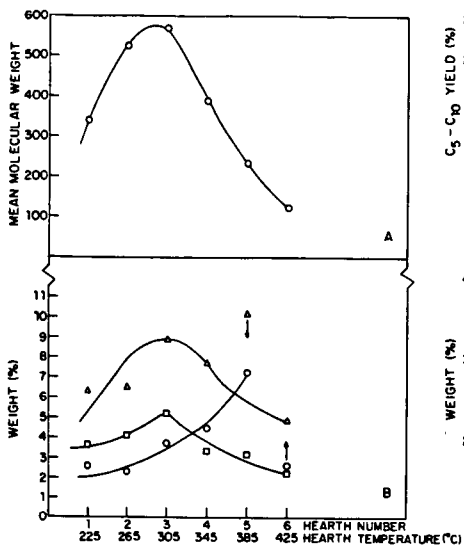


Fig. 4 - Characteristics of the pyrolytic oils. A - average molecular weight. B - Wt % of acetic acid (□), formic acid (○) and sum of acetic + formic acids (Δ).

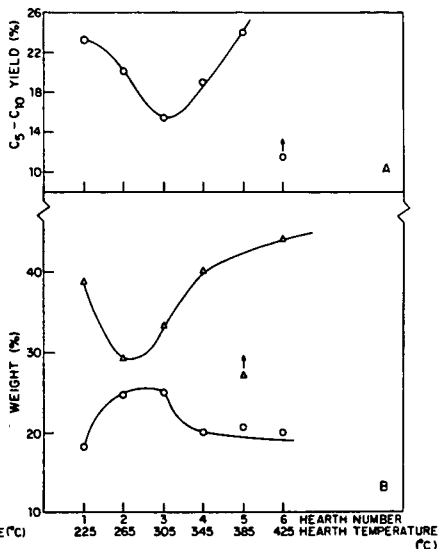


Fig. 5 - Average values for C₅-C₁₀ yields (A) and coke (B ○) and residuum (B Δ).

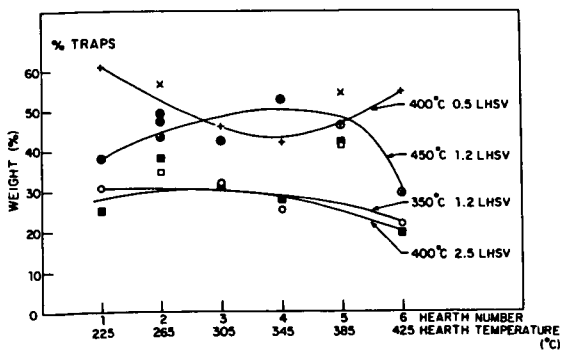


Fig. 6 - Weight % of the products collected in the traps.

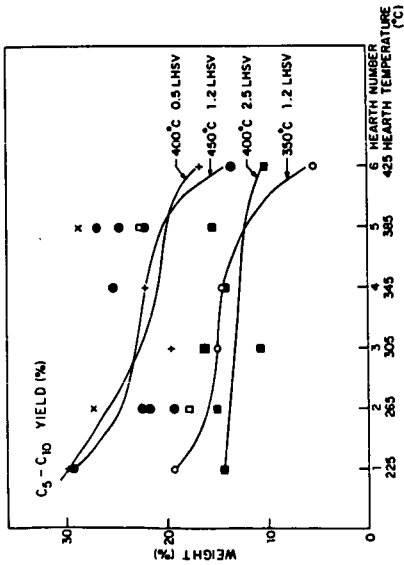


Fig. 7 - C₅-C₁₀ yields

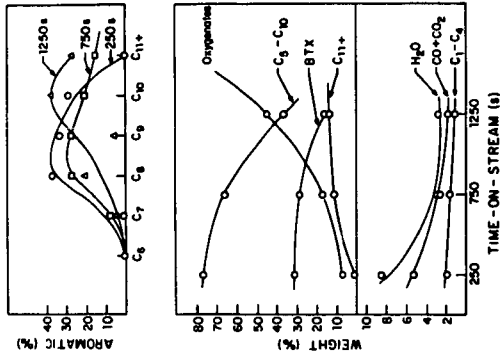


Fig. 9 - Product distribution as a function of time-on-stream

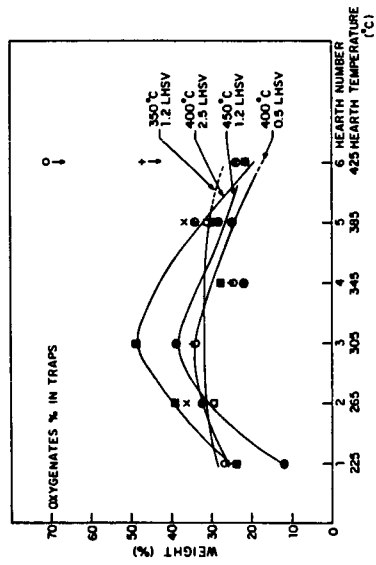


Fig. 8 - Weight % of oxygenates in the traps.

Molecular-Beam, Mass-Spectrometric Studies of Wood Vapor and Model Compounds over HZSM-5 Catalyst

Robert J. Evans and Thomas A. Milne

Chemical Conversion Research Branch
Solar Energy Research Institute
1617 Cole Blvd., Golden, Colorado 80401

INTRODUCTION

Following research and development successes in the gasification of biomass (1), the biomass component of DOE's Biofuels and Municipal Waste Technology Division program is emphasizing direct liquefaction processes to premium hydrocarbon fuels (2). The approach being explored at SERI involves an integrated, ambient-pressure process in which primary wood pyrolysis vapor is formed by fast pyrolysis and immediately passed over a shape-selective catalyst to remove oxygen as H₂O, CO, and CO₂. A leading vapor production method and the engineering aspects of this process are discussed by Diebold in two companion papers in this symposium (3, 4).

We report here preliminary screening results on the behavior of wood pyrolysis vapor and model compounds when passed, at high dilution, over a sample of HZSM-5 supplied by the Mobil Corporation (5).

EXPERIMENTAL

The screening is carried out using a simple, quartz, two-stage reactor coupled to a free-jet, molecular-beam, mass-spectrometer sampling system. This system and typical results for primary and secondary vapors from wood and its constituents are described in a recent publication (6). Carrier gas (He for the results shown below) is preheated in a 30 cm lower section of 2 cm ID quartz. A side arm allows introduction of solid samples to the hot gas or injection of liquids or gases through syringes. The upper 30 cm long section contains the catalyst, placed at the center of the upper section for temperature uniformity.

The catalysts used in this work are: (1) medium pore sized H-ZSM5 provided by Mobil (MCSG-2, extrudate with an unspecified amount of alumina binder); (2) medium pore sized Silicalite provided by Union Carbide (S-115, extrudate with 20% alumina); (3) large pore sized type Y Molecular Sieve provided by Union Carbide (SK-500, extrudate) and (4) silica/alumina obtained from Davidson (980-13, extrudate).

Gases and vapors emerging from the quartz reactor are immediately extracted by a sonic orifice and converted by a second orifice to a molecular beam. Expansion to molecular flow ensures rapid quenching and presents a sample to the ion source of the mass spectrometer that has not suffered wall collisions. In this way, highly condensible species can be sampled in real time. The data shown below are positive ion mass spectra using low energy (22.5 eV) electrons to minimize fragmentation.

This system has the advantage of allowing observation of the actual vapor species that enter the catalyst space and the easy observation of the breakthrough of reactant species. All product species but H₂ can be followed, but fragmentation occasionally interferes and isomers cannot be separately detected. At the moment, the technique is semi-quantitative and is viewed as a supplement to bench-scale systems with product collection for GC analysis, mass balances, and coke determinations (4).

RESULTS AND DISCUSSION

The goals of this catalyst screening project are to gain insight into the conversion of biomass pyrolysis products with a variety of catalysts and under a range of conditions. The screening results allow an assessment of several important aspects of the conversion process: the identification of promising catalysts; the determination of the critical variables in yield optimization; the effect of catalyst composition, structural properties, and physical form on product formation; the behavior of model compounds that represent the range of functionality and structure found in biomass pyrolysis vapors; the determination of relative coking rates for various catalysts and feedstocks; and the regenerability of catalysts. This experimental system was designed to study biomass pyrolysis vapors and has been used to study the fundamentals of biomass pyrolysis, both the initial condensed phase pyrolysis and the subsequent vapor phase pyrolysis (6).

This screening approach is not a stand-alone technique, however, and hence scale experimentation is needed to provide data for parameters which the screening approach does not adequately address: confirmed product identification, product mass balance, long-term studies in assessing catalyst life, and the variation of certain reactor operating conditions which have limited ranges at this scale, such as feed partial pressure or carrier gas flow rate. Initial results are reported here for the effect of the type of catalyst, the effect of weight hourly space velocity (WHSV) and temperature, the estimation of product yields, and the effect of cofeeding methanol for wood vapor conversion to organic products. The relative performance of several model compounds over H-ZSM5 has also been examined and preliminary results are presented.

The relative activities and behavior of four catalysts are shown in Figure 1 which compares the mass spectra of the products. The low-molecular-weight products (m/z 's 18-44) are under-represented in the spectra due to discrimination of the detection system against low masses in these particular experiments. Nevertheless, the uncorrected spectra are sufficient for comparing different catalysts. The H-ZSM5 zeolite was the catalyst used for most of the work in this paper. The Silicalite is also a shape selective catalyst with the ZSM-5 structure, but with nearly zero aluminum in the crystal lattice. The Silicalite gave the same type of products as H-ZSM5, but with differences in the proportions. The formation of light aromatics [benzene (m/z 78), toluene (m/z 92), xylene (m/z 106)], furans [furan (m/z 68) and methyl furan (m/z 82)], alkenes [propylene (m/z 42) and butene (m/z 56)], and naphthalenes [naphthalene (m/z 128) and methyl-naphthalene (m/z 142)] are the major classes of products from wood pyrolysis product conversion over zeolite catalysts. The furans are intermediates that can be subsequently converted to other products with higher reaction severity (i.e., lower WHSV or higher temperatures). The naphthalenes are formed under higher reaction severity and are most likely undesirable products for most applications. The shape-selective nature of these two catalysts is apparent. There is no selectivity observed in the destruction of the wood pyrolysis vapors, as all pyrolysis products are destroyed. However, the higher molecular weight primary products may be converted to coke on the macrosurface of the catalyst, as will be discussed below. The Silicalite appears to be less reactive than the H-ZSM5 since fewer aromatics are formed relative to CO_2 (m/z 44) for the Silicalite, more furan is formed relative to the aromatics, more high-molecular-weight material survives (that is probably associated with the wood primary pyrolysis products), and less of the heavier alkylnaphthalenes are formed relative to the light aromatics.

The third catalyst shown in Figure 1 is a crystalline aluminosilicate derived from a wide bore, type Y molecular sieve that shows significantly less activity than the

H-ZSM5 and silicalite. The intermediate furans are comparable to the light aromatics and unreacted wood pyrolysis products (m/z 's 60, 98, 124, 150 and 164) are present in the spectrum. Olefin yields appear higher than for the first two catalysts, however.

The fourth catalyst in Figure 1 is a silica/alumina catalyst which also shows the intermediate conversion slate (i.e., furans and unreacted pyrolysis products), indicating low activity. The peaks at m/z 's 134, 148, and 162 have higher relative abundance than in the spectra from the other three catalysts and are likely due to tetra-, penta-, and hexamethylbenzene which form in higher amounts than toluene, xylene, and trimethylbenzene because of the lack of shape selectivity, which limits the product size with the zeolite catalysts.

The proportions of organic products that form from wood vapor over H-ZSM5 vary systematically with WHSV and temperature. The effects of these two parameters on the relative abundance of selected products from the conversion of pine pyrolysis products over H-ZSM5 are shown in Figure 2. The temperature was varied from 300° to 550°C and the WHSV from 0.7 to 2.0 hr⁻¹. These are compositional plots and do not directly show the yield of these components since coke will vary with these parameters and is not reflected in the product distribution. The plots of trimethylbenzene, toluene, and benzene show a trend for dealkylation with increased temperature. Trimethylbenzene decreases with temperature, while toluene increases to a maximum at 500°C and then decreases at higher temperatures. A possible explanation is that the dealkylation of trimethylbenzene and xylene lead to increased abundances of toluene, reaching a maximum at 500°C where the depletion of these heavier species and the dealkylation of toluene leads to a decrease in its relative abundance. Benzene increased throughout the temperature range studied. At higher temperatures, benzene relative abundance also increased with lower WHSV's.

The few intermediates from wood vapor are represented in Figure 2 by m/z 118 (probably benzofuran), which shows a maxima at 400°C for all three WHSV's, although the relative abundance increases with WHSV. The alkenes show a steady increase with temperature and a dependence on WHSV at the higher temperatures. The generation of alkenes under extreme reaction conditions possibly indicates that the mechanism of aromatic formation from the alkenes in methanol conversion is not followed in wood pyrolysis product conversion. The aromatics formed from wood are possibly formed more directly by the dehydration and aromatization of the primary pyrolysis products rather than from the polymerization of alkenes as in methanol conversion. The formation of condensed aromatics is also enhanced at higher temperatures, as demonstrated by naphthalene in Figure 2. The trend of lower yields of naphthalenes with lower WHSV's is surprising since these are the final products to form. The dealkylation of the naphthalenes followed the same trend as the alkylbenzenes--methyl-naphthalene went through a maximum and then decreased at higher temperatures.

In methanol conversion, the partial pressure of the feed has a major effect on the product distribution with low partial pressures leading to lower yields of aromatics since they are formed by the polymerization of the alkenes (7). The effect of increasing the partial pressure of feed on the product distribution from the conversion of biomass pyrolysis products may not be the same as with methanol since the aromatics possibly form in a different mechanism. The work reported in this paper is at low partial pressure of wood pyrolysis vapor in helium (1% by volume, assuming a vapor molecular weight of 100). Variation of this parameter remains to be studied and could provide crucial insight as to the mechanisms of both olefin and aromatic production in wood pyrolysis product conversion.

This screening technique is not the optimum method of addressing yields of hydrocarbons based on the initial weight of wood, but an experiment was performed to estimate the yield of organic products, to put the screening results in perspective. Table 1 shows estimates of the wt % of products based on the relative sensitivities of the major products in this mass spectrometric detection method. The vapors analyzed include the moisture in the feed and the water, CO, and CO₂ generated in the primary pyrolysis of the wood. Yields were estimated by correcting the composition of the vapor for coke deposition on the catalyst and the char from the initial pyrolysis. The coke was determined by weighing the catalyst before and after a known amount of wood was pyrolyzed and passed over the catalyst. The resulting estimates of the yield of organics varied from 8% to 11%, depending on the temperature and WHSV. Since the stoichiometry of wood can allow a potential yield of 30% light aromatics from wood due to the removal of oxygen as H₂O and CO (4), the 11% hydrocarbon yield represents 30% of the theoretical yield of hydrocarbons from wood. For additional stoichiometric constraints on aromatic yields, see Diebold and Scahill (4) in this symposium.

The relatively low levels of hydrogen in biomass, coupled with the high amount of oxygen to be rejected, are the reason for the 30% theoretical yield of hydrocarbons. This has led Chen et al. (8) to propose the cofeeding of methanol with carbohydrates to enrich the feedstock in hydrogen and increase the potential hydrocarbon yield. This idea was briefly explored with wood, and the product distributions are shown in Figure 3 for methanol, wood, wood-plus-methanol, and wood-plus-methanol with the methanol contribution subtracted. As in Figure 1, the peaks for water (m/z 18), CO (m/z 28 [also in part due to ethylene]) and CO₂ (m/z 44) are under-represented in these spectra due to the tuning of the mass spectrometer. The product distribution for methanol conversion at 500°C and WHSV = 2.8 (Figure 3A) shows the major classes of products: dimethyl ether (m/z's 45 and 46); the alkenes (m/z's 28 [also in part due to CO], 42, 56, 70, and 84); and the methylated benzenes (m/z's 92, 106, and 120). Alkanes are also a major product from methanol conversion but are not prominent in the runs spectra due to lower ionization sensitivity and increased ionization fragmentation. The peaks at m/z's 147 and 162 are due to penta and hexamethylbenzene, which form in high abundance when methanol is run immediately after wood, possibly due to alkylation of coke precursors and stripping from the catalyst surface. The aspen product distribution at 500°C and WHSV = 1 (Figure 3B) has similarities to the methanol, including the presence of the olefins (m/z's 28, 42, and 56) and the light aromatics. When the

Table 1. Estimated Product Yields from MBMS Data

Temp, °C WHSV, hr ⁻¹	450	450	510	500	495
	2.4	4.2	2.7	3.6	4.0
Water, wt % of Vapors	63.8	50.6	45.3	49.5	50.7
CO, wt % of Vapors	10.7	19.1	23.8	19.8	18.7
CO ₂ , wt % of Vapors	14.5	18.4	16.4	17.0	15.6
Olefins, wt % of Vapors	6.9	6.3	10.3	8.8	9.7
BTX, wt % of Vapors	3.0	4.0	3.3	3.9	4.2
Sum of Organics, wt % of Vapors	11.0	11.9	14.6	13.6	15.0
Sum of Inorganics, wt % of Vapors	89.0	88.1	85.4	86.4	85.0
Yield of Organics, wt % of Wood	8.0	8.7	10.7	9.9	11.0

two are run together, the spectrum looks fairly additive with lesser amounts of olefins than in the pure methanol (Figure 3C). When the methanol contribution is subtracted from the combined run (Figure 3D), it is apparent that the yield of aromatics from the biomass components is increased due to the presence of methanol, and the distribution of products has changed with more xylene and trimethylbenzene, relative to benzene and very little alkenes. The methylation of the biomass-derived aromatics is not only increasing the yield beyond the addition of the two contributions, but is also changing the products toward higher value components. Based upon the GC analysis of the noncondensable gases (4), this increase in methylated benzenes would be expected to occur at the expense of the gaseous alkanes formed from pure methanol.

The behavior of model compounds, in a very preliminary screening, has given some insight toward potential yields. The product spectra of four model compounds are shown in Figure 4. These spectra were collected under different tuning conditions than previous results to bring up the low masses. As with Figures 1 and 2, however, these results have not been calibrated, so peak heights are not directly interpretable as yields. The best use of these model compound screening results is for product slate comparisons. The two major trends are summarized here: (1) the carbohydrate-derived ring compounds such as α -angelicalactone (Figure 4B) and furfuryl alcohol gave the greatest yields of aromatics, while lower yields were obtained from the light oxygenates, such as hydroxyacetaldehyde (Figure 4D); and (2) lignin-derived products, from catechol and guaiacol to isoeugenol (Figure 4A) and coniferyl alcohol, gave very low yields of light aromatics and total organics but were completely destroyed, indicating a high coking potential for the lignin-derived methoxyphenols and phenols.

The formation of furan from cellulose was previously reported (9). Furfural formed furan as shown in Figure 4C; methyl furfural formed mostly methyl furan with minor amounts of furan; and hydroxymethyl furan formed more furan than methyl furan.

The yield of water was always greater than the sum of CO and CO₂ for both the lignin and the carbohydrate products that were studied except for the carbohydrate ring compounds such as α -angelicalactone and furfural. Several compounds gave high yields of particular products that were more related to the functionality than the elemental composition: (1) compounds containing aldehyde groups, such as hydroxyacetaldehyde (Figure 4D) and the furfurals (Figure 4C), gave higher yields of CO (Angelicalactone also gave high yields of CO), (2) acetic acid gave a relatively high abundance of CO₂ as might be expected due to decarboxylation, (3) acetic acid and acetol gave high relative yields of alkenes relative to the heavier compounds, perhaps due to the formation of C₂ and C₃ hydrocarbons after the loss of oxygen as H₂O or CO₂, and (4) hydroxymethylfurfural gave less than half the yields of all organic products than did methyl furfural.

In addition to selected model compounds, three carbohydrates were pyrolyzed and passed over the catalyst. Levoglucosan, glucose, and sucrose gave the same distribution of product classes.

SUMMARY

The results obtained so far with wood vapor over Mobil's sample of HZSM-5 can be summarized as follows:

- Yields of total organics up to 30% of a postulated theoretical maximum yield of 30 wt % have been obtained.

- H₂O always exceeds the sum of CO and CO₂ for wood vapor products.
- Yields of olefins exceed those of aromatics, quite probably due to the low partial pressure of wood vapor in He (typically 1 vol % assuming a wood vapor average molecular weight of 100).
- Fresh catalyst is extremely active, converting all wood-derived species, even heavy lignin species, although coke is a likely major product.
- Methanol (approximately 1.5:1 methanol/wood pyrolysis vapor by weight) increased the hydrocarbon yield, mainly as xylene and trimethylbenzene.
- Product slates can be manipulated by temperature and WHSV.
- There are virtually no intermediates observed from wood vapors (as with dimethyl ether from methanol), except furan species from the carbohydrates.

It is apparent that in future work, catalyst characteristics and variations such as surface acidity, crystallite size, and Si/Al ratio should be explored. In addition, model compounds should be studied to explore the mode of oxygen removal and coking in functionalities present in wood vapor. The synergistic benefits of methanol as a hydrogen carrier should be quantified.

ACKNOWLEDGEMENTS

The support of the Biofuels and Municipal Waste Technology Division of DOE, through Si Friedrich, Gary Schiefelbein, and Don Stevens, is gratefully acknowledged (FTP 646).

REFERENCES

- (1) Pacific Northwest Laboratory, Battelle, "Proceedings of the 1985 Biomass Thermochemical Conversion Contractors' Meeting," October 15-16, 1985, Minneapolis, PNL-SA-13571, CONF-8510167, February 1986.
- (2) Pacific Northwest Laboratory, Battelle, "Biomass Thermochemical Conversion Program Review," 2nd Quarter, FY 85, DOE/BETD, Washington, D.C. (1985).
- (3) Diebold, J. P.; and Scahill, J. W., "Production of Primary Pyrolysis Oils in a Vortex Reactor." See paper in this symposium.
- (4) Diebold, J. P.; and Scahill, J. W., "Biomass-to-Gasoline (BTG): Upgrading Pyrolysis Vapors to Aromatic Gasoline with Zeolite Catalysts at Atmospheric Pressure." See paper in this symposium.
- (5) Samples of ZSM-5 kindly supplied through Gus Weiss, Mobil Research and Development Corporation, Princeton, New Jersey (catalyst designated MCSG-2) (1986).
- (6) Evans, R. J.; and Milne, T. A., "Molecular Characterization of the Pyrolysis of Biomass. I. Fundamentals," to appear in *Energy and Fuels*, 1987.
- (7) Chang, C. D., "Hydrocarbons from Methanol," 1983, Marcel Dekker, Inc.: New York.
- (8) Chen, N. Y.; Degman, T. F.; and Koenig, L. R., "Liquid Fuel from Carbohydrates," *Chemtech*, 1986, pp. 506-511.
- (9) Diebold, J. P.; Chum, H. L.; Evans, R. J.; Milne, T. A.; Reed, T. B.; and Scahill, J. W., "Low Pressure Upgrading of Primary Pyrolysis Oils from Biomass and Organic Wastes," IGT/CBETS Conference on Energy from Biomass and Wastes, X, Washington, D.C., April 7-10, 1986.

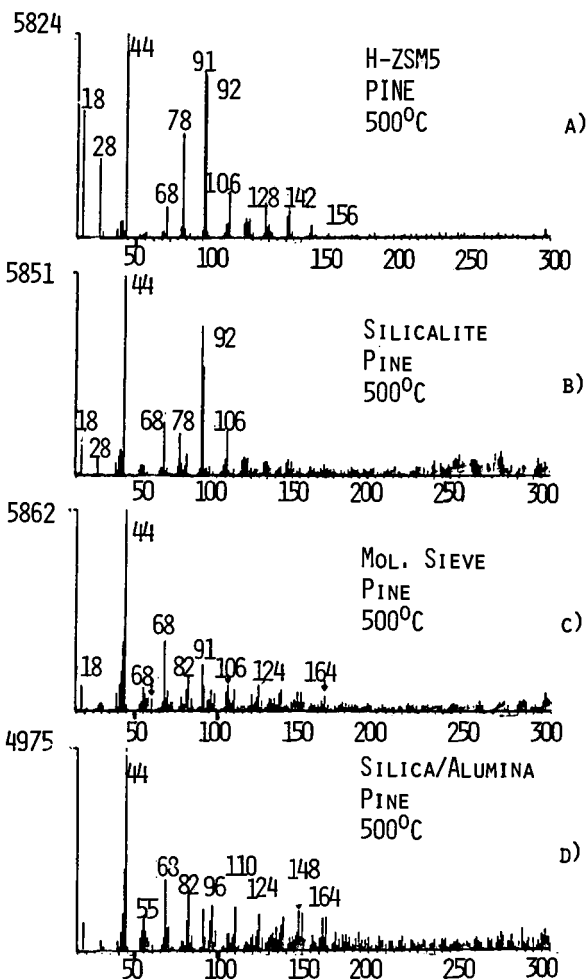


FIGURE 1. MASS SPECTRA OF THE PRODUCTS OF THE CONVERSION OF PINE WOOD PYROLYSIS VAPOR OVER VARIOUS CATALYSTS AT 500°C AND WHSV OF 1: A) MOBIL'S HZSM-5; B) UNION CARBIDE'S SILICALITE; C) UNION CARBIDE'S MOLECULAR SIEVE; AND D) DAVIDSON'S SILICA/ALUMINA.

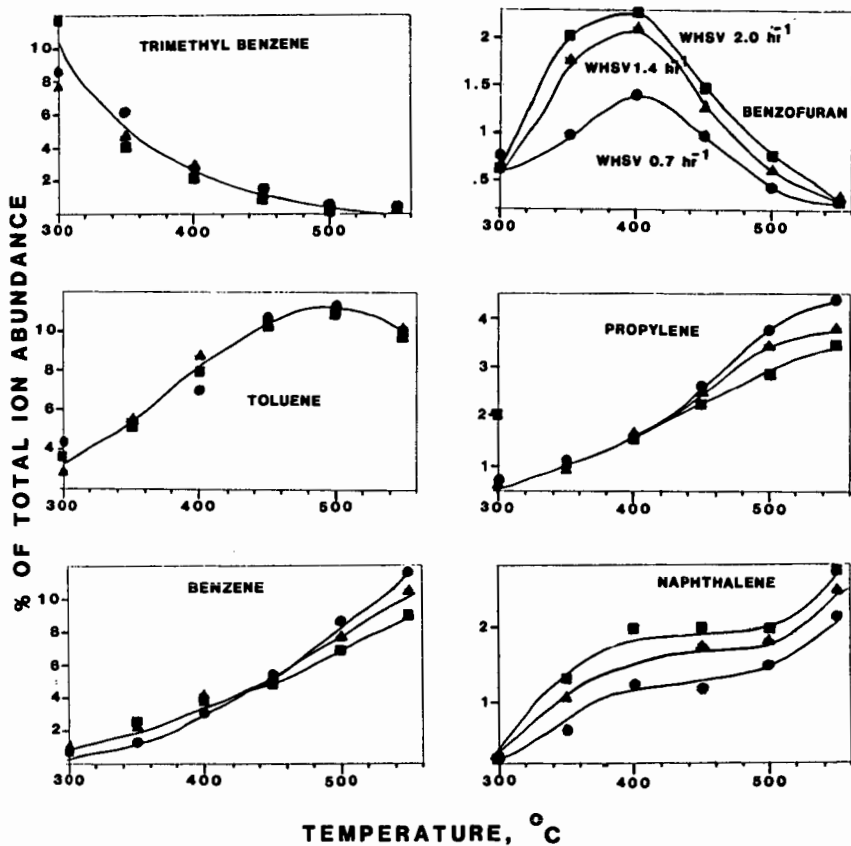


FIGURE 2. THE EFFECT OF TEMPERATURE AND WHSV ON THE DISTRIBUTION OF PRODUCTS FROM THE CONVERSION OF PINE WOOD PYROLYSIS VAPORS OVER H-ZSM5 CATALYST. NOTE: % OF ION ABUNDANCE SHOULD NOT BE EQUATED WITH % OF NEUTRAL PRODUCTS SINCE MASS SPECTROMETER TUNING AND CROSS SECTIONS FAVOR AROMATICS.

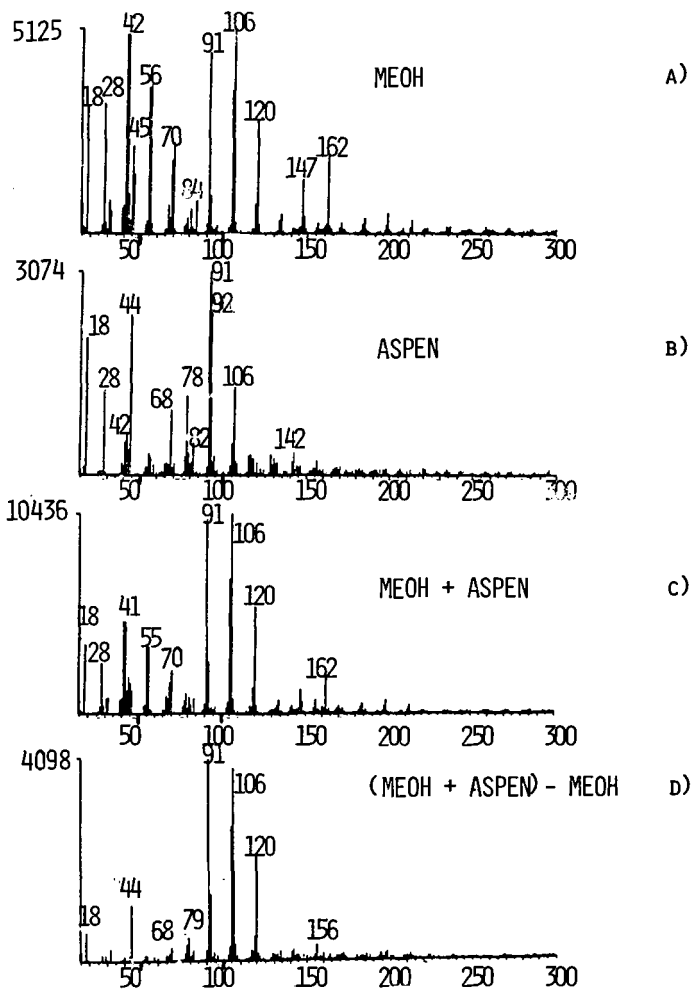


FIGURE 3. MASS SPECTRA OF THE PRODUCTS OF THE CONVERSION OF METHANOL AND ASPEN PYROLYSIS VAPORS OVER HZSM-5: A) METHANOL ALONE, 500°C, WHSV = 2.8; B) ASPEN PYROLYSIS PRODUCTS ALONE, 500°C, WHSV = 1.9; C) COFEEDING METHANOL AND WOOD USING THE CONDITIONS IN A) AND B); D) THE RESULTS IN C) WITH THE METHANOL ALONE RESULTS A) SUBTRACTED SHOWING THE ENHANCEMENT TO THE ASPEN PRODUCT DISTRIBUTION.

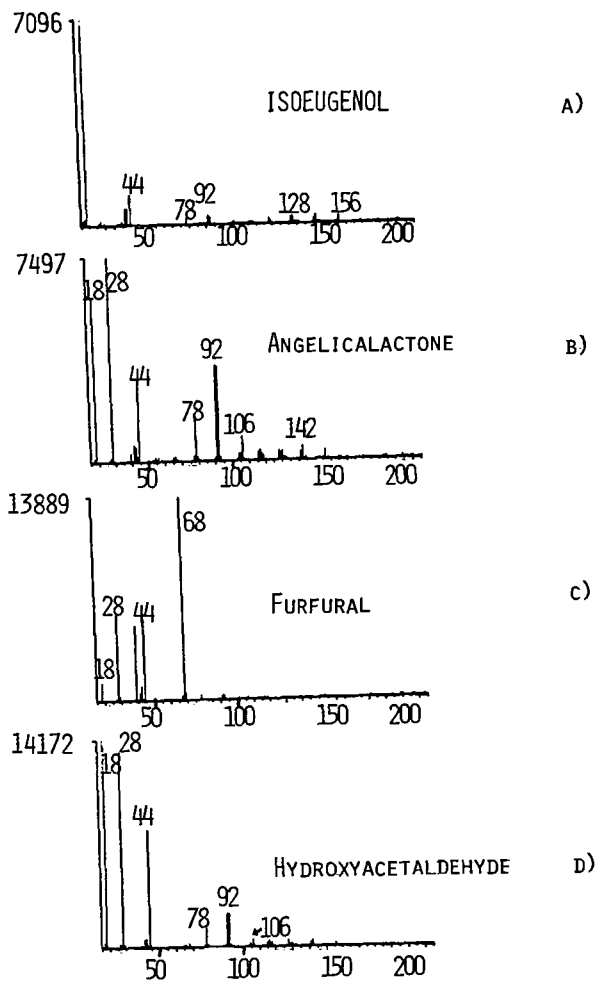


FIGURE 4. MASS SPECTRA OF THE PRODUCTS OF THE CONVERSION OF MODEL COMPOUNDS OVER HZSM-5: A) ISOEUGENOL, 500°C, WHSV = 2.4; B) α -ANGELICALACTONE, 500°C, WHSV = 2.0; C) FURFURAL, 500°C, WHSV = 1.5; AND D) HYDROXYACETALDEHYDE, 500°C, WHSV = 6.1.

**Biomass to Gasoline (BTG): Upgrading Pyrolysis Vapors
to Aromatic Gasoline with Zeolite Catalysis at Atmospheric Pressure**

James Diebold and John Scahill

Chemical Conversion Research Branch
Solar Energy Research Institute
1617 Cole Blvd., Golden, Colorado 80401

ABSTRACT

The primary pyrolysis vapors generated by the fast pyrolysis of biomass at atmospheric pressures consist initially of low-molecular-weight compounds, but which polymerize readily upon condensation. Prior to condensation, these primary vapors have been found to be very reactive with ZSM-5 catalyst to produce methyl benzenes boiling in the gasoline range. This gasoline is predicted to have very high blending octane numbers. By-products are coke, carbon oxides, water, naphthalenes, ethylene, propylene, and some phenols. The effect of different by-products on the theoretical gasoline yield is examined. Preliminary results, generated with a reactor having a fixed bed of 100 g of catalyst, are examined for the continuous feeding of never-condensed primary vapors and compared to feeding methanol in the same reactor.

INTRODUCTION

The conversion of biomass materials to high octane gasoline has been actively pursued for many years. Historically, methanol was made in very low yields by the destructive distillation of hardwoods. More recently, the manufacture of methanol has been by the reaction of synthesis gas over catalysts at high pressures. In theory, any carbon source can be used for this catalytic generation of methanol, but in practice, biomass has not been advantageous relative to coal or natural gas. Other approaches to making liquid fuel from biomass have involved the fermentation of biomass to ethanol in a rather slow process, which produces a substantial amount of by-product solids and liquid wastes. The conversion of biomass to alcohols is technically feasible, but the utilization of the alcohols as transportation fuels will require modifications to the distribution systems and to the individual automobiles. The high-pressure liquefaction of biomass to oxygenated liquids followed by high-pressure catalytic hydrogenation to form hydrocarbons is one approach to convert biomass to liquid fuels (1). However, in the last decade, Mobil has developed the use of a zeolite catalyst for the conversion of methanol to gasoline (2). This process has recently been commercialized and is now in operation in New Zealand (3). The zeolite catalyst used in the Mobil process is a medium pore zeolite, which has shape selectivity to restrict the products to methylated benzenes, isoparaffins, and olefins, while preventing the formation of coke in the catalyst pores (4). This catalyst is known as ZSM-5, and its commercial use is controlled by Mobil.

The reactivity of high-molecular-weight vegetable oils with ZSM-5 was reported in 1979 (5) and, in fact, ZSM-5 catalyst is very reactive toward most small oxygenated species to convert them to methylated benzenes and other products (6, 7). Although alcohols appear to be some of the best feedstocks for ZSM-5 catalysis due to their low coking tendencies, the petroleum industry has long made use of zeolite catalysts for the cracking of very heavy hydrocarbons to produce gasoline and about 5 to 15 weight percent coke. This suggests that the formation of coke and the need for frequent catalyst regeneration will heavily impact the reactor design, but that significant coke formation can be part of a viable commercial process. The thrust

of this paper is to examine possible stoichiometries and preliminary experimental results from using primary pyrolysis vapors made by the fast pyrolysis of sawdust at atmospheric pressure in a vortex reactor. The production of these oxygenate vapors is addressed in a companion paper (8).

STOICHIOMETRY

Although the hydrocarbon products have an unusual feedstock independence, the chemistry involved with different feedstocks over the ZSM-5 catalyst varies considerably with the functionality of the oxygen in the feedstock. As seen in Table 1, the hydroxy and methoxy groups in general have a very strong tendency to reject oxygen in the form of water, as seen for the case of methanol, dimethyl ether (9), glycerol (10), and phenols (11). Rejection of the oxygen as carbon monoxide occurs preferentially to water in a 4:1 ratio with furfural (7, 10). The reaction of n-butyl formate over ZSM-5 produces equal molar amounts of water and carbon monoxide (9). Acetic acid reacts to produce acetone, water, and carbon dioxide with only small amounts of carbon monoxide. The reaction of acetone produces largely water as the oxygen-containing by-product. The acetate group appears to decompose in such a way as to reject four times as much oxygen as carbon dioxide than as carbon monoxide, but with over 50% of the oxygen rejected in the form of water (12). Glucose and starch were reported to reject oxygen preferentially as water rather than as carbon monoxide in a 3-1/2 to 1 ratio with very little formation of carbon dioxide. Sucrose and xylose also produced very little carbon dioxide, but favored the formation of water over carbon monoxide by only 1-1/2 to 1 (7), perhaps due to the formation of some furfural as part of the intermediates. In summary, hydroxyl and methoxy groups tend to reject oxygen in the form of water; aryl ethers reject a nearly equal amount of oxygen in water and carbon monoxide; carbonyl and formate groups reject oxygen largely as carbon monoxide, and carboxyl groups reject oxygen mostly as carbon dioxide and water. With the model compounds listed in Table 1, many of these trends may also be a function of reaction conditions as well as reactants. A model compound study coupled with a process variable study is in progress at SERI with the free-jet, molecular beam/mass spectrometer (FJMBMS) (13).

The method of oxygen rejection which occurs over the catalyst has a very important impact on the potential yield of hydrocarbons, especially for a feedstock like biomass which has a relatively low hydrogen content. Although the products formed from a few compounds reacted with ZSM-5 are known for certain conditions, methods to manipulate the by-product slate are essentially unexplored. However, the desirability to reject oxygen as carbon oxides becomes quite obvious by examining potential product slates which are possible from the stoichiometry of the reacting primary pyrolysis vapors, $\text{CH}_{1.2}\text{O}_{0.49}$. Based on the assumption of a 70 wt % yield of primary vapors, Table 2 shows that of the product slates considered, the best hydrocarbon yields would be attained with oxygen rejection as carbon dioxide, and the excess hydrogen used to also reject oxygen as water. Note that the liquid hydrocarbon product assumed corresponds to xylene, C_8H_{10} , rather than to more hydrogen-rich hydrocarbons such as olefins, C_nH_{2n} (as will be discussed, the liquid hydrocarbon products actually made from these pyrolysis vapors are aromatic in nature). If carbon monoxide is the assumed carbon oxide, more carbon is needed to reject the oxygen, which decreases the potential hydrocarbon yields, as shown by reaction (2) of Table 2. If the by-product gases are a mixture of carbon oxides, methane, olefins, etc., as shown empirically in reaction (3) as $\text{CH}_{0.65}\text{O}_{0.82}$, then the gasoline yields would be lowered due to the noncondensable hydrocarbons. The formation of pure carbon could still result in considerable gasoline yields as shown by reaction (4). However, since coke formation is typically an aromatization reaction to produce polycyclic aromatic hydrocarbons containing residual hydrogen, reaction (5) is probably the more reasonable coking reaction to expect, which

produces water and coke but no gasoline at all. In summary, the more desired reactions produce carbon oxides and water as by-products. Undesired reactions produce noncondensable hydrocarbons and/or coke and water.

EXPERIMENTAL

The primary pyrolysis vapors, used as feedstock, were produced by fast pyrolysis in a vortex reactor from coarse softwood sawdust, as discussed in reference (8). After the vapors left the vortex reactor system, they were allowed to cool to the desired catalytic reaction temperature, as they passed through a tubular transfer line to the catalytic reactor. The transfer line was located inside of a series of six tubular furnaces, which allowed the vapor stream to equilibrate to the desired temperature. The residence time of the vapor in the transfer line was about one-half second prior to reaching the 2.5-cm diameter catalytic reactor shown in Figure 1. The catalytic reactor had a 30-cm-long fixed bed of 100 g of ZSM-5 containing catalyst (MCSG-2), which was located in the middle of the sixth furnace section. The catalyst was in the form of 1.4-mm diameter extrudate and supplied by Mobil Research and Development Corp. in a cooperative agreement with the Solar Energy Research Institute. The temperature of the catalyst bed was measured with an axial thermocouple inside a 6-mm thermowell. The temperature profile of the bed was determined by moving the axial thermocouple within the thermowell. A sintered stainless steel filter rated at 5 micrometers was used to remove char fines from the pyrolysis vapors. The products were collected in water-cooled condensers. The pressure in the reactor was slightly above the local atmospheric pressure at about 95 kPa. Analysis of the organic condensates was with a 5-micrometer wide bore capillary column having a length of 60 m. The capillary column was coated with one micrometer of cross-linked methyl silicones. With helium as the carrier gas, the temperature profile started at 0°C for 4 minutes, followed by a temperature ramp of 8°C/min until a temperature of 260°C was reached. Detection of the eluted organics was by flame ionization detection (FID). Identification of the major peaks was by reference materials, whereas the minor peaks were identified by a combination of the FJMBMS at SERI and a GC/MS located in the Department of Chemical and Petroleum Refining Engineering of the Colorado School of Mines. The noncondensable gases were analyzed with a Carle GC designed for refinery gas analysis, which used thermal conductivity detection (TCD) and was calibrated with a gravimetrically prepared reference mixture. Electronic grade methanol (99.9% pure) was used for comparison to the softwood feedstock.

EXPERIMENTAL RESULTS

Methanol. To verify the activity of the catalyst and to gain experience in the operation of the catalyst system, methanol was metered into a preheater tube located inside of the transfer line heated to 500°C. This preheating proved to be too severe and the products which emerged from the catalytic reactor were dominated by hydrogen and carbon monoxide in a 2:1 ratio, as shown in Table 3. This would be expected from thermal decomposition of the methanol prior to reaching the catalyst. This experiment was repeated using a preheating temperature ramp to just reach 400°C at the entrance to the catalytic reactor. The catalytic reactor was held at a nominal 400°C prior to the addition of the methanol at a space velocity (WHSV) of 0.9 g methanol per gram of catalyst. The noncondensable gas composition is shown in Table 3 and was rich in hydrogen and alkanes (methane, propane, and isobutane). The gaseous olefins would be used to alkylate the reactive isobutane to result in a highly branched-chain gasoline fraction (14). The GC for the hydrocarbon liquid is shown in Figure 2a; the liquid product contained relatively little alkanes or olefins and was dominated by methylated benzenes, such as toluene, xylenes, and trimethyl benzenes. Relatively very small amounts of naphthalenes were

seen. The temperature profile of the catalytic reactor immediately prior to and also during this experiment is shown in Figure 3. The location of the temperature-profile maxima was quite stable, which indicates that the catalyst was not significantly deactivating during the short time of the experiment. This low rate of catalyst deactivation is consistent with data published by Mobil personnel (15). The ratio of gasoline to water in the condensates suggests that the gasoline yield was only about one-third of the potential due to the formation of the noncondensable hydrocarbons. This product slate is in general agreement with data reported by Mobil for the reaction conditions (15).

Primary Pyrolysis Vapors. After a catalyst regeneration cycle to remove residue from the methanol experiments, a slipstream of the primary pyrolysis vapors were passed over the ZSM-5 catalyst using steam as the carrier gas at a weight ratio of two parts of steam to one part of wood feed. The pyrolysis vapors were cooled from 510°C at the exit of the vortex reactor to 400°C at the entrance of the catalytic reactor. Figure 4 shows the temperature profile immediately prior to feeding the biomass, as well as 5-10 minutes later. The temperature profile with pyrolysis vapors as feed was not as large in magnitude as that seen with methanol and it had a very broad maximum. The heat of reaction of the pyrolysis vapors is less exothermic than for methanol and the steam carrier gas also has a moderating effect on the temperature rise. The broadness of the temperature profile reflects that the pyrolysis vapors are a complex mixture of compounds, which are probably reacting at different rates. The broader and lower temperature profile would make temperature control easier in a biomass-to-gasoline (BTG) reactor than in a methanol-to-gasoline (MTG) reactor. The location of the temperature maximum was monitored during the run, as shown in Figure 5. During the fairly short experiment, the temperature maximum was observed to move to the end of the reactor, indicating a fairly rapid deactivation of the catalyst had occurred. During this time, the composition of the hydrocarbon products appeared to be relatively constant. The GC chromatogram of the liquid hydrocarbons is shown in Figure 2b for comparison to the products made from methanol. As can be seen by inspection of the two gas chromatograms, the gasoline fraction (eluting before naphthalene) made from wood is very similar to that made from methanol. The composition of the gas formed over the catalyst from the pyrolysis vapors is shown in Table 3, as calculated from tracer gas concentrations before and after the reactor, along with the gas composition formed by the thermal decomposition of the pyrolysis vapors as determined previously (16); the catalytically formed gases had significantly less hydrogen and methane, but more carbon dioxide and propylene than the thermally formed gases. In comparing the composition of the gases formed by the catalytic conversion of the pyrolysis vapors to the catalytic conversion of the methanol, the relative hydrogen richness of the methanol becomes apparent in the relatively high hydrogen, methane, propane, and isobutane yields. The relative hydrogen richness is summarized by the empirical formulas for the two gas streams, in which the hydrogen-to-carbon ratio for the wood-derived gases is one-fourth that for the methanol-derived gases. This excessive amount of hydrogen in the methanol-derived gases suggests that methanol could be used as a hydrogen donor to hydrogen-poor feedstocks and this has been explored by several researchers (7, 10-12). The very low yield of isobutane from pyrolysis vapors would preclude the use of alkylation to incorporate the ethylene, propylene, and butenes into the gasoline product with a standalone process. Adsorption of the gaseous olefins onto cold ZSM-5 at low pressures may be a viable method to recycle them into the catalytic reactor. A comparison of Tables 2 and 3 reveals that the empirical gas composition calculated to have been made catalytically from the pyrolysis vapors corresponds to reaction (3), which has a thermal efficiency of 57%. However, the laydown of coke on the catalyst would serve to compete for the pyrolysis vapor feedstock and reduce the gasoline yields by reaction (5) as previously discussed. The quantitation of the coke is in progress.

DISCUSSION

Pyrolysis vapors made by the fast pyrolysis of softwood are very reactive with ZSM-5 catalyst to form a liquid hydrocarbon product, which is very similar to that formed from methanol. Although the catalyst is deactivated relatively quickly with pyrolysis vapors compared to methanol, other experimentation we have performed indicates that the catalyst can be oxidatively regenerated. This suggests that a catalytic reactor, which can maintain a high level of catalytic activity in spite of high coking rates, would be desired. This problem has been addressed and resolved by the petroleum refining industry which utilizes an entrained-bed reactor (riser-cracker), to crack heavy hydrocarbons to gasoline and about 5% to 15% coke, coupled with a fluidized-bed oxidative regenerator for the relatively slow, controlled oxidative coke combustion and catalyst regeneration (17). For the conversion of biomass to gasoline, these preliminary data are quite encouraging that a nearly direct conversion of biomass to gasoline can be accomplished at atmospheric pressures in one very rapid thermal cycle without the cost of hydrogen manufacture. With the calculated thermal efficiencies, it appears that there will be sufficient energy in the by-products to operate the process, even including the drying of a rather wet biomass feedstock prior to pyrolysis.

The gasoline product is almost entirely methylated benzenes with only a small amount of benzene. This gasoline would be expected to have octane ratings in excess of 100 and to have blending octane numbers between 115 and 135 based on reported blending octane values for the various methylated benzenes (18). Due to the expected continued demand for unleaded gasoline having higher octane numbers, the gasoline made from biomass by this process would be expected to command premium prices if sold to a petroleum refinery for blending purposes. The naphthalenic fraction of the organic products could easily be hydrocracked to increase the gasoline yields in a modern refinery (19). At this time, the phenolic by-products appear to be present in minor amounts and probably will not warrant recovery.

SUMMARY

The conversion of primary pyrolysis vapors made from biomass is a relatively new research and development area which is showing early promise. The extent to which the product slate can be manipulated by process variables will impact heavily on the viability of this process.

ACKNOWLEDGEMENTS

The financial support of the Biofuels and Municipal Waste Technology Division of the Department of Energy, FTP 619, with Mr. Simon Friedrich as DOE Program Manager and the technical direction of the Program Monitor, Dr. Don J. Stevens, of PNL, are gratefully acknowledged. Mr. M. Maholland of the Colorado School of Mines and Drs. T. A. Milne and R. J. Evans contributed product identification of many of the hydrocarbon products.

REFERENCES

- (1) Baker, E. G. (1987), ACS Symposium on Production, Analysis, and Upgrading of Pyrolysis Oils from Biomass, Denver, CO, April 5-10.
- (2) Meisel, S. L.; McCullough, J. P.; Lechthaler, C. H.; Weiz, P. B. (1976), CHEMTECH, February, 86-89.
- (3) Anon, 1986, Chemical Engineering, March 3, p. 10.

- (4) Dejaive, P.; Auroux, A.; Gravelle, P. C.; Vedrine, J. C. (1981), *J. Cat.*, 70, 123-136.
- (5) Weisz, P. B.; Haag, W. O., and Rodewald, P. G (1979), *Science*, 206, 5 October, 57-58.
- (6) Diebold, J. P.; Chum, H. L.; Evans, R. J.; Milne, T. A.; Reed, T. B.; Scahill, J. W. (1986), *Proceedings of Energy from Biomass and Wastes X, IGT/CBETS*, Washington, D.C., April 7-10.
- (7) Chen, N. Y.; Degnan, T. F., Jr.; Koenig, L. R. (1986), *CHEMTECH*, August, 506-511.
- (8) Diebold, J. P.; and Scahill, J. W. (1987), *ACS symposium on Production, Analysis, and Upgrading of Pyrolysis Oils from Biomass*, Denver, CO, April 5-10.
- (9) Chang, C. D.; and Silvestri, A. J. (1977), *J. Cat.* 47, 249-259.
- (10) Hanniff, M. I.; and Dao, L. H. (1986), *Proceedings of Energy from Biomass and Wastes X, IGT/CBETS*, Washington, D.C., April 7-10.
- (11) Chantal, P. D.; Kaliaguine, S.; and Grandmaison, J. L. (1985), *Appl. Cat.*, 18, 133-145.
- (12) Chang, C. D.; Chen, N. Y.; Koenig, L. R.; and Walsh, D. E. (1983), preprints of 185th ACS Meeting, Div. of Fuel Chem., Seattle, WA, March 20-25, 146-152.
- (13) Evans, R. J.; and Milne, T. A. (1986), private communication, October.
- (14) Kam, A. Y.; and Lee, W. (1978), Fluid Bed Process Studies on Selective Conversion of Methanol to High-Octane Gasoline, Mobil Research and Development Corp., U.S. DOE Contract No. EX-76-C-01-2490 FE-2490-15.
- (15) Chang, C. D. (1983), Hydrocarbons from Methanol, Marcel Dekker, NY.
- (16) Yurchak, S.; Voltz, S. E.; and Warner, J. P. (1979), *Ind. Eng. Chem. Process. Des. Dev.*, 18, No. 3, 527-534.
- (17) Diebold, J. P. (1985), Thesis T-3007, Colorado School of Mines, Golden, CO 80401.
- (18) Decroocq, D. (1984), Catalytic Cracking of Heavy Petroleum Fractions, Gulf Publishing Company, Houston, TX.
- (19) Lovell, W. G. (1948), *Ind. Eng. Chem.*, 40, No. 12, 2388-2438.
- (20) Gary, J. H.; and Handwerk, G. E. (1975), Petroleum Refining, Technology, and Economics, Marcel Dekker, NY, pp. 121-141.

Table 1. Reported Distribution of Oxygen in Inorganic By-Products with Various Feedstocks over ZSM-5 Catalyst

Compound	Oxygen Radical in Reactant*	% of Oxygen in By-Products			Reference
		H ₂ O	CO	CO ₂	
methanol	H, M	100	--	--	(8)
dimethyl ether	E, M	100	--	--	(8)
guaiacol	H, M	96	3	1	(10)
glycerol	H	92	7.5	0.5	(9)
xyleneol	H	93	6	1	(10)
eugenol	H, M	89	9	2	(10)
anisole	M	88	12	tr	(10)
2,4 dimethyl phenol	H	87	12	1	(10)
o-cresol	H	80	17	3	(10)
starch	H, E	78	20	2	(7)
isoeugenol	H, M	77	19	4	(10)
glucose	C1, H, E	75	20	5	(6)
dimethoxymethane	M, E	73	6	21	(8)
xylose	C1, H, E	60	35	5	(6)
sucrose	H, E	56	36	8	(6)
n-butyl formate	C2	54	46	0	(8)
diphenyl ether	E	46	46	8	(10)
furfural	C1, E	14-22	75-84	2.5-3.0	(6, 9)
methyl acetate	C2	54	10	36	(11)
acetic acid	C2	50	4	46	(11)

*H = hydroxy; M = methoxy; E = C-O-C; C1 = carbonyl; C2 = carboxy

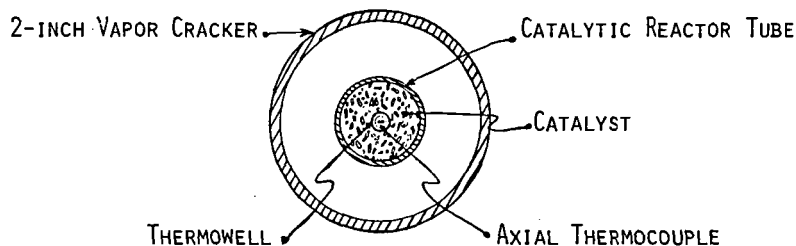


FIGURE 1. CROSS SECTIONAL VIEW OF THE FIXED-BED CATALYTIC REACTOR.

Table 2. Stoichiometric Relationships of By-Products to Gasoline Yields using Primary Softwood Pyrolysis Vapors as the Feedstock

Assumed Reaction	U.S. Gal Gasoline*		Energy in Gasoline*	
	Ton Dry Wood	Wt Wood	Energy in Wood	Energy in Wood
1) $\text{CH}_{1.2}\text{O}_{0.49} + 0.100 \text{C}_8\text{H}_{10} + 0.20 \text{CO}_2 + 0.10 \text{H}_2\text{O}$	99	0.35		0.75
2) $\text{CH}_{1.2}\text{O}_{0.49} + 0.085 \text{C}_8\text{H}_{10} + 0.32 \text{CO} + 0.23 \text{H}_2\text{O}$	84	0.30		0.64
3) $\text{CH}_{1.2}\text{O}_{0.49} + 0.073 \text{C}_8\text{H}_{10} + 0.42 \text{CH}_0.65\text{O}_{0.82} + 0.10 \text{H}_2\text{O}$	75	0.27		0.57
4) $\text{CH}_{1.2}\text{O}_{0.49} + 0.022 \text{C}_8\text{H}_{10} + 0.824 \text{C} + 0.49 \text{H}_2\text{O}$	22	0.08		0.17
5) $\text{CH}_{1.2}\text{O}_{0.49} + \text{CH}_0.22 + 0.49 \text{H}_2\text{O}$ ("coke")	0	0		0

*Yields reflect an assumed 70 wt % conversion of softwood to primary pyrolysis vapors.

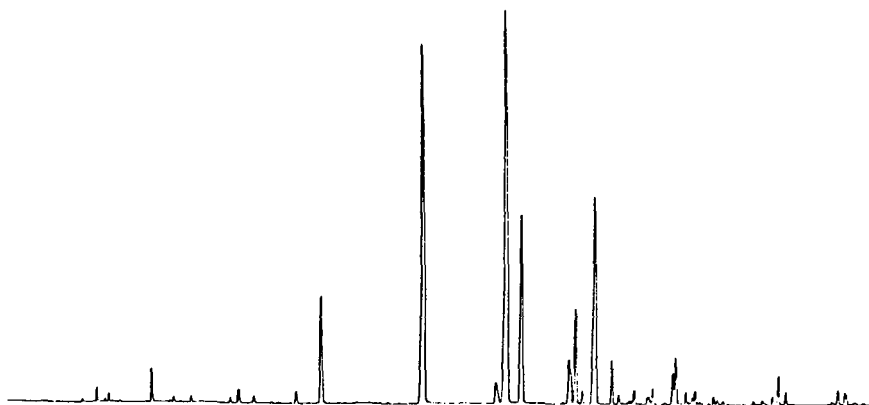


FIGURE 2A. GC OF HYDROCARBON PRODUCTS MADE FROM METHANOL AT 400°C WITH ZSM-5 CATALYST

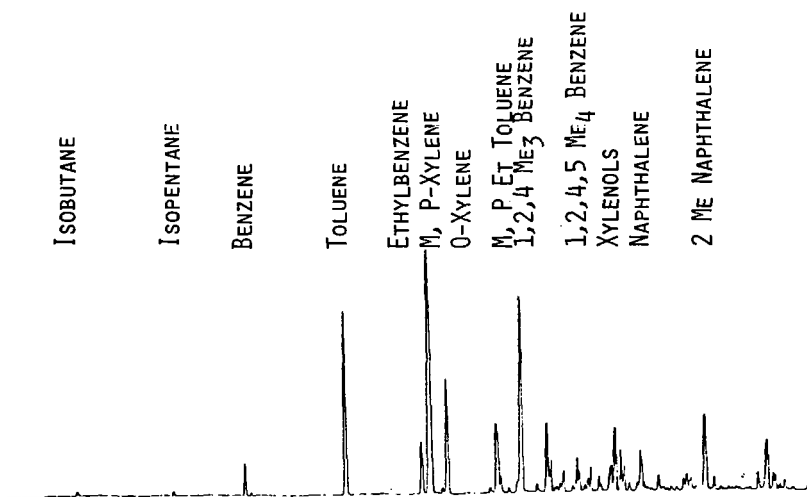


FIGURE 2B. GC OF HYDROCARBON PRODUCTS MADE FROM SOFTWOOD PRIMARY PYROLYSIS OIL VAPORS AT 400°C WITH ZSM-5 CATALYST

Table 3. Calculated Molar Compositions of Net Product Gases
(ZSM-5 containing catalyst - Mobil's MCSG-2)

Reactor	Softwood Pyrolysis Vapor (CH _{1.2} O _{0.49})		(CH ₄ O) Methanol	
	Thermal (Run 55)	Catalytic (Run 76-C)	Thermal (Run 74-C)*	Catalytic (Run 75-C)
H ₂	10.6	-0.6	62.8	18.4
CO	59.4	69.8	31.1	4.4
CO ₂	5.6	15.2	1.4	2.8
CH ₄	12.2	1.4	2.1	16.2
C ₂ H ₂	0.5	--	--	--
C ₂ H ₄	5.3	5.0	1.6	5.3
C ₂ H ₆	1.1	0.3	0.3	4.1
C ₃ H ₆	1.9	6.0	0.7	5.3
C ₃ H ₈	--	0.5	0.4	17.8
C ₄ H ₈	1.1	1.2	--	2.3
iso-C ₄ H ₁₀	--	0.2	0.1	14.4
n-C ₄ H ₁₀	--	--	--	5.3
C ₅ ⁺	2.4	--	--	3.6
Empirical Formula	CH _{1.3} O _{0.65}	CH _{0.65} O _{0.82}	CH _{3.6} O _{0.8}	CH _{2.7} O _{0.05}

*In this run, the methanol is thought to have thermally decomposed for the most part prior to reaching the catalyst.

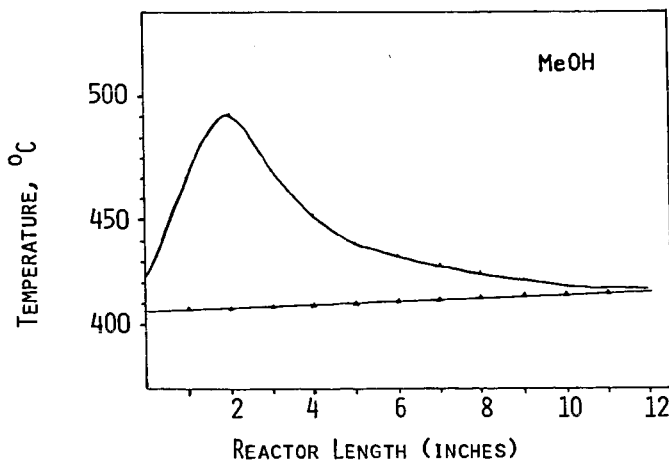


FIGURE 3. TEMPERATURE PROFILE FOR METHANOL REACTANT

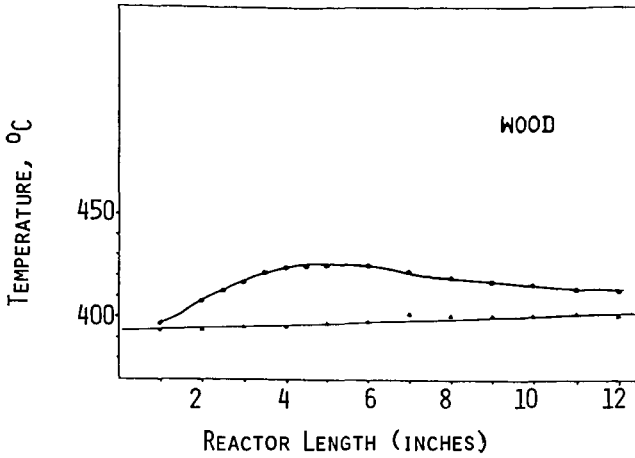


FIGURE 4. TEMPERATURE PROFILE FOR SOFTWOOD PYROLYSIS VAPORS AS THE REACTANTS

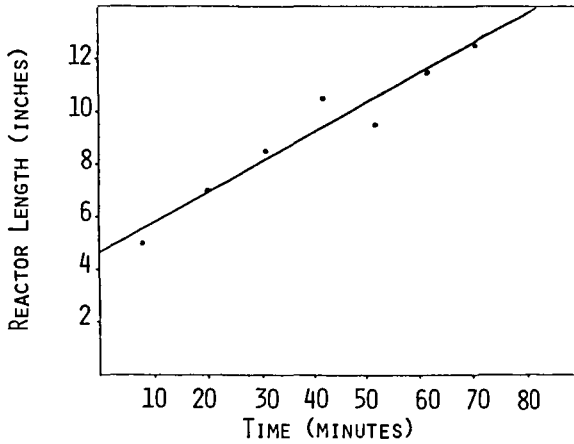


FIGURE 5. LOCATION OF THE MAXIMUM CATALYST BED TEMPERATURE, SHOWING CATALYST DEACTIVATION

REACTIONS OF BIOMASS PYROLYSIS OILS OVER ZSM-5 ZEOLITE CATALYSTS

L.H. Dao*, M. Haniff, A. Houle and D. Lamothe

INRS-Energie, Institut National de la Recherche Scientifique
C.P. 1020, Varennes, Québec, Canada J0L 2P0

INTRODUCTION

It has been shown that synthetic zeolites such as ZSM-5 can be used to convert oxygenated compounds derived from biomass materials into hydrocarbon compounds which can be used as fuels and chemical feedstocks (1,2,3,4).

However, the pyrolysis oils obtained from woods by different thermoliquefaction processes (5,6), show poor hydrocarbon yield and high tar content when contacted over ZSM-5 zeolite catalysts at high temperature (7,8). Since the pyrolysis oils are composed of a wide variety of oxygenated compounds such as cyclopentanone, furfural, phenol, acid and carbohydrate derivatives (9,10), it is difficult to point out exactly which family of compounds is contributing more to the observed tar content and to the deactivation of the catalysts. Catalytic studies on model compounds which are generally found in the pyrolysis oils are therefore primordial in order to determine the best catalytic system. The reactions of phenolic compounds over ZSM-5 catalysts are already reported (8). The present paper thus reports the results for the conversion of cyclopentanone, furfural, glucose and its isopropylidene derivative over H-ZSM-5, Zn-ZSM-5 and Mn-ZSM-5 zeolite catalysts at temperatures ranging from 400°C to 500°C. Some reactions are supplemented with methanol in their feeds so as to determine the effect of increased hydrogen to carbon effective ratio on the deoxygenated hydrocarbon yields.

EXPERIMENTAL

Preparation and characterization of catalysts

The ammonium form of ZSM-5 was prepared according to a published procedure (11). The H-form of the catalyst was obtained by calcination at 500°C for 10 hours. The zinc and manganese loaded catalysts were prepared by ion exchange in a 10% aqueous solution of $Zn(NO_3)_2$ and $Mn(NO_3)_2$ at ~ 80°C. After washing and drying at 160°C over night, the solid was calcined for 10 hours at 520°C. The X-ray diffraction pattern of the three synthetic ZSM-5 are similar to those reported in the literature. The chemical composition of ZSM-5 samples are shown in table 1.

Apparatus

The catalytic conversion were studied in a continuous flow quartz reactor with a fixed bed of diluted catalysts. The reaction conditions are reported in table 1. After an experimental run (about 3 hours), the tar on the catalytic bed was determined by taking the difference in weight of the reactor before and after placing it in a furnace set at 500°C on the presence of air. The reaction products were analyzed by GC and GC/MS (table 1).

RESULTS AND DISCUSSION

Figure 1 shows the yield of conversion, $C_1 - C_6$ aliphatics, aromatics, polyaromatics and tar as a function of reactor temperature for pure cyclopentanone over H-ZSM-5/bentonite (80/20) catalyst. The conversion is completed at 350°C. The

main reaction is thermal decarbonylation giving C_n hydrocarbons that react further on the catalytic bed to produce aliphatic aromatic and polyaromatic hydrocarbons.

Table 2 shows the reaction of pure furfural ($H/C_{eff} = 0$) over various cation exchanged ZSM-5 catalysts at 400°C. The deoxygenated hydrocarbon yields range from 6.6 to 9.4% and the oxygenated hydrocarbon yields range from 25.6 to 50.0%. These values reflect the poor performance of all three catalysts in deoxygenating furfural. The large quantities of furan and CO observed is due to thermal decarboxylation of furfural. Higher tar contents were observed for the metal exchanged catalysts (21.2 and 25.9%) than the hydrogen exchanged catalyst (14.2%). The low water contents (range of 2.7 to 7.0) produced from these reactions indicate poor catalytic deoxygenation of furfural. CO_2 , which is produced from pyrolytic reactions, is obtained in low yields. The yields for the aliphatics ($9.0 \pm 1.4\%$) and olefins ($8.5 \pm 2.1\%$) are comparatively smaller than those for the aromatics ($47.7 \pm 3.5\%$) and polyaromatics ($34.7 \pm 3.8\%$). Polyaromatics are usually produced on the surface of the zeolite because they are too large to enter or leave the channels of the zeolite; high values for these compounds are undesirable because they are not useful as chemical feedstocks.

Figure 2 shows the product distributions for the reaction of various furfural/methanol mixtures over H-ZSM-5/bentonite (80/20) at a reactor temperature of 450°C; only the major components in the products are shown. The abscissa in figure 2 is given in both increasing percentage of methanol and increasing $(H/C)_{eff}$ for the feed. As methanol increases the yields for deoxygenated hydrocarbons and water increase while those for tar, furan and CO decrease. The drastic increase of deoxygenated compounds and water and decrease of furan with increasing methanol concentration indicate that significant catalytic deoxygenation is taking place. At about 55% methanol/45% furfural ($(H/C)_{eff}$ of 0.85, there is complete removal of furan from the reaction products; only small quantities of other oxygenated hydrocarbons were present ($< 0.26\%$). The yields for the other products were similar to those observed previously for furfural. Only at 70% methanol/30% furfural there was a significant reduction in the tar content, i.e. 6.7% (14.1% on carbon basis). The average CO_2 present was $0.3 \pm 0.1\%$.

Table 3 shows the product distribution for reactions of furfural/methanol (30/70) over various concentrations of H-ZSM-5 at 450°C. By diluting the catalyst with bentonite from 80 to 18%, the deoxygenated hydrocarbon yield increased from 30.6 to 41.4%. Changing the support material from bentonite to Al_2O_3/SiO_2 caused a small reduction in the deoxygenated hydrocarbon yield (36.3%); there was, however, less coke formed when compared to the other two cases. The product selectivities were similar to those of previous cases.

Table 4 shows results for reactions of glucose and glucose derivative done over 80% H-ZSM-5 and 20% bentonite at 450°C. With an increased $(H/C)_{eff}$, there were increased deoxygenated hydrocarbon yields for the glucose/methanol/water (20.0/30.0/50.0) and glucose derivative/methanol/water (27.6/60.2/12.2) cases when compared to that of the glucose/water (20.3/79.7) case. Also, there was a simultaneous decrease in tar content with an increase in $(H/C)_{eff}$. However, in all cases the hydrocarbon yields are poor and the tar contents are too high. The high water content observed in all experiments (29.2 to 66.1%) is not only due to catalytic deoxygenation through loss of water but also due to polycondensation reactions of glucose and its derivative. These condensation reactions produce polymeric oxygenated compounds which are responsible for the high tar content observed. Oxygenated hydrocarbons, CO and CO_2 , are minor products which are normally obtained from thermal decomposition of biomass materials (12). The product selectivity indicates a high percentage of aliphatics (23.6 to 50.5%) and aromatics (34.2 to 53.2%).

Except for the reaction with glucose/water, the olefin contents are low for the other two reactions. The production of polyaromatics (mainly indene and naphthalene derivatives) is rather high (2.56 and 7.24%) considering that they are produced from the surface of the zeolite rather than in the channels of the zeolite.

To test the efficiency of the catalyst, experiments were done with 18% H-ZSM-5 (instead of 80%) dispersed in 82% bentonite. Also, the catalytic bed would have less acidic sites (Brönsted sites) which are known to promote polymerization of the carbohydrates and hence reduce the deoxygenated hydrocarbon yield. Table 5 shows the results for experiments done on the diluted catalytic bed. Only in the glucose/methanol/water (20.0/30.0/50.0) case there was a significant increase in the deoxygenated hydrocarbon yield and a decrease in tar content. Hence, reducing the number acidic sites does not reduce the extent of the polymerization of the carbohydrates. However, there was an increase in the polyaromatic content in table 5 compared to that in table 4 indicating that there is more surface reaction in the dilute catalyst case.

When the catalytic support material was changed from bentonite to a mixture of Al_2O_3 and SiO_2 , the yield of deoxygenated hydrocarbon increased for both cases as showed in table 6 when compared for similar cases in tables 4 and 5. There were also a comparable decrease in tar content for these reactions.

Deoxygenation of glucose/water (20.3/79.7) with manganese and zinc exchanged ZSM-5 are reported in table 7. There are a reduction in the deoxygenated hydrocarbon yields when compared to similar reactions in tables 4 and 5. The tar contents were just as high as the reactions before. The product selectivity which is normally influenced by these metal exchanged zeolites were not very different from those reported before.

CONCLUSION

Cyclopentanone is deoxygenated with high yield to hydrocarbons over H-ZSM-5 at 400°C. The reaction of furfural over ZSM-5 catalysts at 400°C and higher temperatures produce pyrolytic products which are volatile and non-volatile. The volatile fraction are deoxygenated to produce hydrocarbon products while the non-volatile fraction remain on the catalytic bed causing desactivation of the zeolite and enhancement of the tar content. Glucose and its isopropylidene derivative undergo thermal reactions which produce a significant amount of tar and a small amount of volatile products. The volatile fraction are deoxygenated by ZSM-5 catalysts to produce hydrocarbon products.

ACKNOWLEDGEMENT

This work was supported by grants from the Natural Sciences and Engineering Research Council of Canada and from the Quebec Ministry of Science and Technology (Transfert of Technology University-Industry).

REFERENCES

1. P.B. Weiz, W.O. Haag and P.G. Rodewald, *Science*, **206**, 57 (1979).
2. T.C. Frankiewicz, U.S. Patent 4 308 411 (1981).
3. L.H. Dao, M. Haniff, "Tenth Canadian Symposium on Catalysis", Kingston, Ontario, Preprint, CIC, 278 (1986).
4. N.Y. Chen and L.R. Koenig, U.S. Patent 4 503 278 (1985).

5. S. Hasnain, Ed. "Fifth Canadian Bioenergy R&D Seminar", Elsevier Applied Sciences, London, 1984.
6. E. Chornet, R.P. Overend, Ed. "Compte-rendu de l'atelier de travail sur la liquéfaction de la biomasse", Sherbrooke, 1983.
7. P.D. Chantal, S. Kaliaguine, J.L. Grandmison, Applied Catalysis, 7, 317 (1984).
8. P.D. Chantal, S. Kaliaguine, J.L. Grandmison, Applied Catalysis, 8, 133 (1985).
9. R.E. Schirmer, T.R. Pahl, D.C. Elliott, Fuel, 368 (1984).
10. L.H. Dao, P. Hébert, A. Houle, M. Haniff, Proceeding of the Ninth Biennial Congress of the International Solar Energy Society, Pergamon Press, Vol. 3, 1812 (1986).
11. E.G. Derouane and E.W. Valyacsik, European Patent 157521 (1985).
12. F. Shafizadek and Y.J. Fu, Carbohydr. Res. 29, 113 (1973).

TABLE 1
Chemical composition of ZSM-5 samples

Component (WT%)	H-ZSM-5	Mn-ZSM-5	Zn-ZSM-5
Na ₂ O	0.55	0.69	0.49
Al ₂ O ₃	2.25	2.33	2.10
SiO ₂	86.86	91.05	87.62
MnO ₂	---	0.78	---
ZnO	---	---	0.26
TiO ₂	0.59	0.64	0.38
L.O.I.*	7.62	3.26	6.68
<u>Molar Ratio</u>			
SiO ₂ /Al ₂ O ₃	65.47	66.32	70.80
Na ₂ O/Al ₂ O ₃	0.40	0.49	0.38

* L.O.I. means loss on ignition of sample weight.

REACTION CONDITIONS

Catalyst weight : 10 g (80% ZSM-5 + 20% bentonite)
 Temperature : 350-560°C
 Pressure : atmospheric pressure
 Inert gas : helium (~ 3 ml/min)
 WHSV ** : variable
 Reaction time : 3 hours

** The weight hourly space velocity (WHSV) is defined as:

$$\text{WHSV} = \frac{\text{g of injected feed per hour}}{\text{g of catalyst}}$$

ANALYTICAL CONDITIONS

- Gas chromatography : HP 5890 GC with DB-5 (SE-54) column (30 m x 0.25 mm, 1.0 μ)
- For liquid : 70°C (4 min), then 4°C/min to 160°C then 20 min at 160°C
- Gas : 33°C (isothermal)
- GC/MS : HP 5890 GC and MS detector
 Pona column and DB-5 column

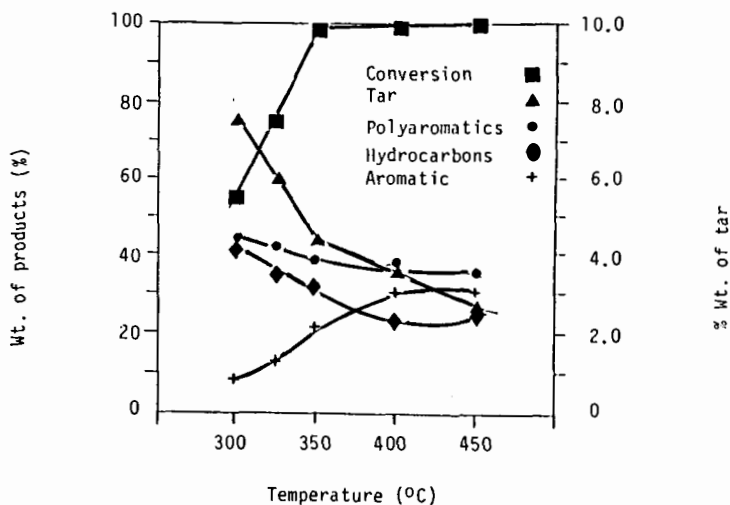


Figure 1: Reaction of cyclopentanone over H-ZSM-5/bentonite (80/20) at different reactor temperature

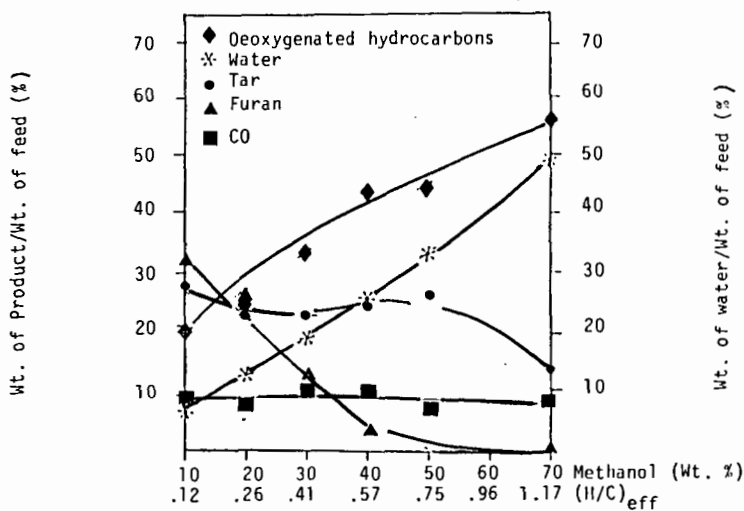


Figure 2: Reaction of furfural/methanol mixtures over H-ZSM-5/bentonite (80/20) at a reactor temperature of 400°C and a WHSV of $.238 \pm .018 \text{ hr}^{-1}$.

TABLE 2

Reaction of furfural over cation exchanges ZSM-5 at 400°C and WHSV of 0.281 hr⁻¹

Experimental conditions:

Catalyst composition:	80% H-ZSM-5 20% bentonite	80% Zn-ZSM-5 20% bentonite	80% Mn-ZSM-5 20% bentonite
Total product distribution (WT%)			
Furan	47.0	23.8	27.8
Oxygenated hydrocarbons	50.0	25.6	40.7
Tar	14.2	21.2	25.9
CO	22.8	36.3	17.9
CO ₂	0.56	4.84	1.89
H ₂ O	4.39	2.69	6.97
Deoxygenated hydrocarbons	8.00	9.42	6.64
Product selectivity (WT%)			
Aliphatics, C ₁ - C ₈	8.84	7.62	10.5
Olefins, C ₂ - C ₆	8.46	10.6	6.48
Aromatics	50.6	48.8	43.9
Polyaromatics	32.1	32.9	39.1

TABLE 3

Reaction of furfural/methanol (30/70) feed ((H/C)_{eff} of 1.17) over H-ZSM-5 at 450°C

Experimental conditions:

Catalyst composition:	80% H-ZSM-5 20% bentonite	18% H-ZSM-5 82% bentonite	18% H-ZSM-5 48% Al ₂ O ₃ 34% SiO ₂
WHSV (Hr ⁻¹)	0.029	1.26	1.26
Total product distribution (WT%)			
Oxygenated hydrocarbons*	---	1.36	0.83
Tar	6.74	7.60	4.90
CO	9.44	7.84	7.25
CO ₂	0.48	0.58	0.30
H ₂ O	52.7	41.6	50.4
Deoxygenated hydrocarbons	30.6	41.1	36.3
Product selectivity (WT%)			
Aliphatics, C ₁ - C ₈	1.82	11.6	20.7
Olefins, C ₂ - C ₆	2.90	3.01	3.63
Aromatics	83.5	72.8	60.8
Polyaromatics	11.9	12.6	14.8

* Mainly furan and benzofuran, derivatives and dimethylether.

TABLE 4

Reaction of glucose and glucose derivative over 80% H-ZSM-5
and 20% bentonite at 450°C

Experimental conditions:

Reactant composition:	20.3 glucose 79.7% water	20.0 glucose 30.0% methanol 50.0% water	27.6 glucose derivative 60.2% methanol 12.2% water
WHSV (Hr ⁻¹)	0.062	0.195	0.313
(H/C) _{eff}	0.0	1.59	1.36
Total product distribution (WT%)			
Oxygenated hydrocarbons	---	0.70*	3.87**
Tar	65.1	33.3	14.1
CO	2.14	0.46	0.23
CO ₂	1.48	1.41	0.92
H ₂ O	29.1	59.7	66.1
Deoxygenated hydrocarbons	2.18	4.43	14.8
Product selectivity (WT%)			
Aliphatics, C ₁ - C ₈	23.6	35.7	50.5
Olefins, C ₂ - C ₆	41.6	3.81	2.74
Aromatics	34.8	53.3	43.2
Polyaromatics***	---	7.24	3.56

TABLE 5

Reaction of glucose and glucose derivative over 18% H-ZSM-5
and 82% bentonite at 450°C

Experimental conditions:

Reactant composition:	20.3% glucose 79.7% water	20.0% glucose 30.0% methanol 50.0% water	27.6% glucose derivative 60.2% methanol 12.2% water
WHSV (Hr ⁻¹)	0.862	1.195	1.12
(H/C) _{eff}	0.0	1.59	1.46
Total product distribution (WT%)			
Oxygenated hydrocarbons	0.58*	0.96*	4.20**
Tar	51.3	21.0	11.1
CO	3.79	1.76	0.84
CO ₂	2.82	0.29	0.79
H ₂ O	39.4	57.9	64.3
Deoxygenated hydrocarbons	2.15	18.1	18.8
Product selectivity (WT%)			
Aliphatics, C ₁ - C ₈	29.0	43.6	17.5
Olefins, C ₂ - C ₆	7.33	1.18	14.0
Aromatics	45.2	45.3	55.8
Polyaromatics***	18.3	9.99	12.7

* Mainly furan and benzofuran derivatives; ** Mainly acetone and furan derivatives; *** Mainly indene and naphthalene derivatives

TABLE 6

Reaction of glucose and glucose derivative over 18% H-ZSM-5
and 48% Al₂O₃ and 34% SiO₂

Experimental conditions:

Reactant composition:	20.0 glucose 30.0% methanol 50.0% water	27.6 glucose derivative 60.2% methanol 12.2% water
WHSV (Hr ⁻¹)	1.18	1.11
(H/C) _{eff}	1.59	1.46
<u>Total product distribution (WT%)</u>		
Oxygenated hydrocarbons	0.12	0.24
Tar	14.3	6.86
CO	1.59	1.76
CO ₂	0.44	0.47
H ₂ O	62.4	53.5
Deoxygenated hydrocarbons	21.2	37.2
<u>Product selectivity (WT%)</u>		
Aliphatics, C ₁ - C ₈	19.0	21.0
Olefins, C ₂ - C ₆	12.0	8.32
Aromatics	65.6	62.0
Polyaromatics	3.42	8.66

TABLE 7

Reaction of 20.3% glucose and 79.7% water over manganese
and zinc exchanged ZSM-5

Experimental conditions:

Catalysis composition	80% Mn-ZSM-5 20% bentonite	80% Zn-ZSM-5 20% bentonite
WHSV (Hr ⁻¹)	0.046	0.055
(H/C) _{eff}	0.0	0.0
<u>Total product distribution (WT%)</u>		
Oxygenated hydrocarbons	---	---
Tar	72.3	53.1
CO	2.60	2.23
CO ₂	1.91	4.19
H ₂ O	22.3	39.8
Deoxygenated hydrocarbons	0.89	0.68
<u>Product selectivity (WT%)</u>		
Aliphatics, C ₁ - C ₈	26.0	35.4
Olefins, C ₂ - C ₆	42.8	2.60
Aromatics	31.0	62.0
Polyaromatics	---	---